Ph.D. Thesis

Composite Higgs, Top Partners and the LHC

Candidate:
Oleksii Matsedonskyi

Università degli Studi di Padova
Dipartimento di Fisica e Astronomia "G. Galilei"
Scuola di Dottorato di Ricerca in Fisica
Via Marzolo 8, I-35131 Padua, Italy
Ciclo XXVI

Advisor: Dr. Andrea Wulzer

Co-Advisor: Prof. Fabio Zwirner

Director of Ph.D. School: Prof. Andrea Vitturi

January 2014

Abstract

The models with a Higgs boson realized as a bound state of new strongly coupled dynamics and featuring the Goldstone symmetry protection mechanism, ensuring its lightness, represent a motivated scenario of New Physics at the TeV scale. We summarize the main ideas behind the formulation of these Composite Higgs (CH) models, focusing on the scenarios invoking the paradigm of Partial Compositeness, the mechanism of Standard Model fermion mass generation by mixing with composite resonances. After reviewing the theoretical tools for the description of the CH setup, we derive structural phenomenological features, and in particular a general relation, valid for a broad class of models, between the Higgs mass and masses of the top partners, i.e. the composite resonances responsible for giving a mass to the top quark through Partial Compositeness. This relation implies that, for a "natural" theory, the top partners are restricted to have a mass below around 1.5 TeV, significantly below the other resonances, and they play a primary role for phenomenology. First of all, their direct observation at the Large Hadron Collider (LHC) seems unavoidable if the considered scenarios are indeed realized in Nature without accidental per-cent tuning. We develop a general minimally model-dependent framework, accounting for the Goldstone nature of the Higgs, in order to identify the best strategies for top partners searches at the LHC. Using current data we exclude a considerable part of the natural parameter space of the CH models. We present an estimate of the future LHC reach for two interesting channels. The light top partners could also manifest themselves in indirect way, contributing to the low-energy observables of the ElectroWeak Precision Tests. Our analysis shows that in this case top partners play an important role for compatibility of CH scenarios with experimental data, in particular we identify a new, potentially large, logarithmically divergent contribution to the S parameter. At the same time we show that the effects dependent on the details of the UV dynamics are important and can give contributions comparable with IR effects, and thus must be taken into account, as for instance the four-fermion operators contributing to Zbb coupling.

Abstract

I modelli con un Higgs Composto, realizzato come un bosone di Goldstone e dunque naturalmente leggero, costituiscono uno scenario ben motivato di nuova fisica alla scala del TeV. Discuteremo la formulazione di tali modelli, seguendo il paradigma della "Partial Compositeness" per la generazione delle masse dei fermioni del Modello Standard tramite il mescolamento con delle risonanze del nuovo settore forte. Dopo aver introdotto gli strumenti tecnici necessari, deriveremo alcune caratteristiche fenomenologiche strutturali, ed in particolare una relazione generale, valida in un'ampia classe di modelli, che lega la massa del bosone di Higgs a quella dei "Top Partners", ovvero le risonanze fermioniche responsabili per la generazione della massa del quark top attraverso il meccanismo di Partial Compositeness sopra descritto. Questa relazione implica che in una teoria "Naturale" i Top Partners sono necessariamente leggeri, con massa al di sotto di circa 1.5 TeV, significativamente pi leggeri delle altre risonanze. Dunque, essi giocano un ruolo fondamentale nella fenomenologia di questi modelli. Prima di tutto, questi stati sono potenzialmente osservabili con relativa facilit al Large Hadron Collider (LHC) del CERN. Svilupperemo uno descrizione semplificata dei Top Partners, adatta per studiarne la fenomenologia al collider, che tuttavia mantenga le caratteristiche teoriche pi importanti dei modelli espliciti, in particolare il fatto che l'Higgs sia un bosone di Goldstone. Confronteremo il modello semplificato con i dati attuali, identificando le regioni escluse del suo spazio dei parametri, e discuteremo le prospettive del futuro run dell'LHC per lo studio di questo tipo di segnali. I Top Partners hanno anche effetti indiretti, contribuendo alle osservabili di bassa energia che sono alla base dei Test di Precisione del Modello Standard. Analizzeremo questi effetti in dettaglio, identificando nuovi contributi, potenzialmente rilevanti, al parametro S. Discuteremo anche altri possibili contributi alle osservabili di precisione, non legati ai Top Partner leggeri ma ai dettagli della fisica microscopica del modello completo da cui i Top Partners emergono. In alcuni casi, per esempio per quanto riguarda il coupling della Z al quark bottom, questi contributi sono comparabili o dominanti rispetto a quelli dovuti ai Top Partners e devono essere tenuti in considerazione.

Contents

Invitation

The recent discovery at the Large Hadron Collider (LHC) [1, 2] of a Higgs-like boson [3] concludes the long-lasting experimental and theoretical effort for detecting the last missing ingredient of the Standard Model of particle physics (SM). Even if the Higgs couplings to vector bosons and SM fermions are not measured very precisely, one obvious fact can not be denied – there exists a light scalar state charged under the SM group and coupled to the top quark. This fact is difficult to accommodate within a modern view on the Standard Model as an effective description of a more fundamental theory, possessing new degrees of freedom at energies above the masses of SM states[1]. The need for such a theory is motivated by many questions which the SM is unable to answer, related for instance to the dark matter problem, possible gauge couplings unification, flavour problem, stability of the electroweak vacuum and, above all, the quantum gravity issue. As will be explained in the next chapter, the elementary weakly coupled SM Higgs boson interacting with a physics at a scale Λ will generically have a mass (and also a vacuum expectation value, which defines the SM mass scale) at least of the same order of Λ, possibly up to a loop factor suppression. This suggests that Λ should be low, in contradiction with the non-observation of any new physics around the SM mass scale. This issue was already emphasized at a time of the LEP experiments [4] and became more striking after the first phase of the LHC data taking.

A large amount of theoretical effort was therefore directed at explaining (**I**) why the Higgs mass is not sensitive to the highest physical energy scale of the fundamental theory of particle physics and which kind of physics cancels this dependence, and (**II**) why the physics responsible for the cancellation was not observed so far. There are several ways to systematically solve the first problem by imposing new symmetries and adding new degrees of freedom into the theory which result in the sensitivity of the Higgs mass only to some intermediate energy scale Λ' not far above the electroweak scale. The second problem instead typically can not be completely solved structurally and requires a certain amount of a fine tuning on the parameters of the theory since the Higgs mass will generically tend to get too close to the new physics scale Λ'. In this thesis we will focus on the new physics scenarios in which the Higgs boson arises as a bound state of a new strongly coupled dynamics [5]. As we will show in the following, this framework allows for answering the two questions posed above with a need of only a moderate tuning of the theory parameters.

The structure of the thesis is as follows. Chapter 1.1 is a review devoted to a detailed analysis of the Higgs mass problem and its possible solution by compositeness. We will give a general sketch of the composite Higgs scenarios, its paradigms and the related field-theoretical techniques, and conclude with an overview of possible experimental confirmations of the composite Higgs hypothesis. In

[1] There could be as well modifications at the same or lower energies, but they are less relevant for the present discussion.

Chapter 2 we consider more closely the generation of the Higgs potential and find a relation between the Higgs mass and a mass of certain colored fermionic composite resonances. By virtue of this relation the fermionic resonances, the "top partners", are restricted to have a mass within 1.5 TeV. Therefore these particles, if they exist, are likely to be the first composite resonances (after the Higgs boson) which will be observed directly at the LHC. In the absence of the corresponding signal, on the contrary, the viability of composite Higgs models, as they are formulated now, will be undermined. The possible production of the top partners at the LHC will be analysed in the Chapter 3. We will use the existing experimental analyses to bound the parameter space of composite Higgs models and discuss the most promising channels for the future searches. The indirect influence of the (light) fermionic composite resonances on the parameters of the ElectroWeak Precision Tests (EWPT) will be evaluated in Chapter 4. Finally, we will summarize our discussion in the Conclusions. Chapters 2-4 are based on publications [6–9], with the results updated to account for the latest experimental data.

Chapter 1

Introduction

1.1 The Standard Model and the Gauge Hierarchy Problem

The Standard Model (SM) of particle physics is a quantum field theory describing all known elementary particles and built upon principles of gauge invariance and renormalizability. The SM is based on the $SU(2)_L$ weak isospin times $U(1)_Y$ hypercharge times $SU(3)_c$ color internal local symmetry group. In order to realize the gauge symmetry one needs to introduce the massless spin-1 gauge bosons corresponding to each generator of the gauge symmetries: three W and one B bosons and eight gluons G [1] with coupling constants g, g' and g_s respectively. Apart from the vectorial gauge bosons, the SM contains "matter" fields – spin-1/2 fermions. Their symmetry properties are

- q_L – $(2,3)_{1/6}$
- u_R – $(1,3)_{2/3}$
- d_R – $(1,3)_{-1/3}$
- l_L – $(2,1)_{-1/2}$
- e_R – $(1,1)_{-1}$

where the numbers in brackets correspond to the dimension of the multiplets under $SU(2)_L \times SU(3)_c$ while the subscript corresponds to their hypercharge. Each of the above fermions comes in three replicas, the three SM fermionic families. Right-handed neutrinos could be added to the picture, but since their existence is not confirmed experimentally, we will stick to the minimal SM field content.

The full renormalizable Lagrangian for the above fields can be schematically written as

$$\mathcal{L}_{f,V} = i\bar{f}(\partial_\mu - igV_\mu)\gamma^\mu f - \frac{1}{4}F_{\mu\nu}F^{\mu\nu}, \tag{1.1.1}$$

where V_μ stands for gauge bosons, g for corresponding gauge couplings, f for fermions and the field strength is defined as $F_{\mu\nu} = \partial_\mu V_\nu - \partial_\nu V_\mu - ig\,[V_\mu, V_\nu]$. In the last expression we omitted CP-violating term with a dual field-strength tensor since it enters with coefficient which is restricted experimentally to a very small value.

[1] The converse is also true: the requirement to have the listed massless bosons forming multiplets in the adjoint representation of the mentioned symmetry group would force us to make a gauge-invariant theory.

The last ingredient is an elementary scalar Higgs doublet neutral under $SU(3)_c$ with a hypercharge 1/2, with a Lagrangian

$$\mathcal{L}_H = \frac{1}{2}|(\partial_\mu - igV_\mu)H|^2 - V(H), \tag{1.1.2}$$

where $V(H)$ is the scalar potential. The Higgs field couples to the fermions by means of Yukawa interactions

$$\mathcal{L}_{\text{Yuk}} = y_u^{ij}\,\bar{q}_L^i\,H^c\,u_R^j + y_d^{ij}\,\bar{q}_L^i\,H\,d_R^j + y_e^{ij}\,\bar{l}_L^i\,H\,e_R^j + h.c., \tag{1.1.3}$$

where $H_\alpha^c = \epsilon_{\alpha\beta}H_\beta^*$ with ϵ – antisymmetric tensor, α and β – $SU(2)_L$ indices and i, j – family indices.

The SM incorporates the minimal mechanism for the spontaneous breaking of the electroweak symmetry ($SU(2)_L \times U(1)_Y$). The breaking is triggered by the Higgs field which acquires a non-zero vacuum expectation value (VEV) v. The $SU(2)_L \times U(1)_Y$-invariant potential of the Higgs field H has the form:

$$V = -\mu^2|H|^2 + \frac{\lambda}{2}|H|^4. \tag{1.1.4}$$

The minimum of the potential corresponds to $\langle|H|\rangle = v/\sqrt{2} = \mu/\sqrt{\lambda}$. This means that the true vacuum state is not invariant under the electroweak symmetry and the latter is broken to the electromagnetic $U(1)_Q$. The symmetry breaking results in masses for vector fields $m_W = g\,v/2$, $m_Z = \sqrt{g^2 + g'^2}\,v/2$ and for the fermions $m_f = y_f\,v/\sqrt{2}$. The masses of neutrinos can take a different form, since their main contribution may come from the operators not included in our description, such as the dimension-5 Weinberg operator, or operators with a right-handed neutrino. From the measured value of the Fermi constant $G_{\text{F}} = g^2/4\sqrt{2}m_W^2$ one can extract $v \simeq 246\,GeV$.

The scalar Lagrangian expanded around a new minimum describes three massless Goldstone bosons and one massive mode with a mass $m_h = 2\mu$. The three Goldstone bosons together with initially massless gauge vector bosons then form massive W and Z bosons, while the fourth scalar, the Higgs boson, remains physical. The existence of a good candidate for the Higgs boson with a mass $m_h \simeq 125\,GeV$ was recently confirmed experimentally [1, 2]. Given that λ is not very different from one, the value of the parameter μ or, interchangeably, the Higgs mass determines the overall scale of masses of the SM particles. The theoretical problem which arises at this point is related to the fact that this scale is very sensitive to quantum corrections. The loops of SM particles induce quadratically divergent correction to the Higgs mass, which is given by:

$$\delta m_h^2 = \frac{3G_{\text{F}}}{4\sqrt{2}\pi^2}(4m_t^2 - 2m_W^2 - m_Z^2 - m_h^2)\Lambda^2. \tag{1.1.5}$$

Taking the effective field theory (EFT) approach, one can treat the regulator Λ as a physical cutoff of the Standard Model, and the whole expression (1.1.5) as an estimate of the contribution of the new physics at the scale Λ to the Higgs mass. Given that the Higgs mass results from the bare one and a correction (1.1.5), one can estimate the degree of cancellation between the two, needed to reproduce the experimentally measured value:

$$\Delta = \frac{\delta m_h^2}{m_h^2} \simeq \left(\frac{\Lambda}{500\,GeV}\right)^2. \tag{1.1.6}$$

The bigger is Δ, the more precise cancellation is needed to accommodate the observed Higgs mass and the less "natural" the theory is [2]. If nothing non-trivial (e.g. supersymmetry, strongly coupled physics, additional space dimensions) appears at the SM cutoff, the Higgs mass will be sensitive to the highest mass scale at which new physics coupled to the Higgs appears. The additional corrections to the m_h due to the new states in general have no reason to cancel against each other or with the SM corrections. Therefore the plausible value of Λ for the tuning estimate can be as large as the Planck mass. In the latter case the tuning defined by Eq. (1.1.6) is 10^{32} and becomes very difficult to tolerate. This fine tuning problem, also called the hierarchy problem, drives the attempts to complete the Standard Model in such a way that some new physics screens the sensitivity of the Higgs mass term to the arbitrarily high energy scales. A general feature of known such theories is that the Higgs mass always receives contribution at least from the energies at which the new physics enters the game, from which, using the formula (1.1.6), one can expect that in the natural case the new physics must show up at energies close to 1 TeV.

The most popular concrete solution to the stated above naturalness problem is a low-energy supersymmetry (SUSY) (for a recent review see for instance [11]). In this scenario the quadratic divergence of the Higgs mass would be cancelled at energies above the SUSY breaking scale $\Lambda_{\rm SUSY}$ due to the enhanced symmetry of a theory, and therefore the Higgs mass itself will be sensitive to $\Lambda_{\rm SUSY}$ and not to possible higher energy scales. One of the main advantages of the most SUSY theories is a calculability provided by their weakly coupled nature.

One of the alternative solutions is instead related to a presence of a hypothetical new strong dynamics. If the Higgs was a bound state originating from this dynamics it would not be sensitive to the quantum corrections coming from the energies above its compositeness scale. The properties of this scenario will be discussed in details in the following sections.

One should however also mention the possibility that $M_{\rm Planck}$ does not introduce quadratic dependence in the m_h, even without some special low-energy screening mechanism, which is not ruled out, though lacks of concrete implementations. If this is true and no other physics capable to contribute to δm_h is present at the intermediate scales between m_h and $M_{\rm Planck}$ or above $M_{\rm Planck}$, the question about the tuning posed above is technically not a good question since there is no physical meaning for Λ [12] [3].

The last thing to mention here is that the apparently unnatural value of the μ parameter in the Higgs potential can be motivated by the anthropic argument. According to it a significant fine tuning in certain fundamental parameters is indeed present. Though the measured values are unlikely in general, they are necessary for the creation of intelligent life. There is no surprise that humans live on the Earth and not any other planet of the Solar system where life can not emerge. Similarly, the parameters of our Universe may be restricted to particular intervals. The analysis [14] showed that indeed the value of the Higgs VEV is typical for the anthropically allowed range. This kind of reasoning would look more plausible if the fundamental theory was allowing for multiple different realisations, as happens in the multi-verse scenarios.

The discussed above Hierarchy problem is not the only one theoretical problem related to the Standard Model. But it is the only one which, if taken seriously, requires a presence of the new

[2] For a detailed recent review of the subject see [10].

[3] See also [13] for the analysis of some new physics scenarios with new degrees of freedom above m_h, allowing for naturally light Higgs, under assumption of the absence of quadratic sensitivity to $M_{\rm Planck}$ without any screening mechanism at low energies.

physics at the TeV energy scales.

1.2 Composite Higgs: General Idea

We have seen in the previous chapter that the coefficient of the quadratic term in the Higgs potential is generically sensitive to the energy scale of any new physics which interacts with a Higgs boson and thus in the absence of cancellations is expected to be of the same size as the highest scale in the underlying theory. One of the possibilities which could potentially answer to the question of why the Higgs mass is not for example of the order of the Planck mass, is that the Higgs field is not elementary but composite. The mass of the composite Higgs would not receive correction from the energies which are higher than the inverse physical size of the Higgs (Fig. 1.1). The quanta of the fields at arbitrarily high energies will not "see" the Higgs, and thus will not generate a mass for it, instead they will interact with its constituents directly. An analogous mechanism is already known in Nature - the typical mass scale of QCD bound states is set, through a mechanism of dimensional transmutation, by the energy at which the coupling between quarks and gluons becomes strong enough to confine them together.

The QCD analogy also provides a hint of why we could already observe one composite state, the Higgs, but no other composite resonances of the new strong dynamics. The mass gap between the lightest QCD states, the pions, and other composites, for example the ρ-mesons [4], is explained by the fact that the pions are Goldstone bosons to a very good approximation. The QCD Lagrangian possesses an approximate chiral symmetry $SU(2)_L \times SU(2)_R$ acting on the chiral up and down quark doublets. This symmetry is spontaneously broken to the vector combination $SU(2)_V$, under which both left and right chiralities transform in the same way, by a quark-antiquark condensate in the QCD vacuum. Then three QCD pions emerge as Goldstone bosons associated to this symmetry breaking. The pions are not massless because the $SU(2)_L \times SU(2)_R$ symmetry is not exact, and the leading breaking effect comes from the small quark masses which mix left and right chiral states, providing the pions with masses $m_\pi^2 \sim m_q$. The next breaking effect comes from the QED interactions which can distinguish between the up and down quarks and generate a small splitting between the masses of the neutral and charged pions $\delta m_\pi^2 \sim \alpha_{\rm EM}$ [5].

The Composite Higgs (CH) scenarios postulate a similar mechanism: the new strong sector, symmetric under a compact Lie group G, confines at energy Λ, which breaks the G to its subgroup H [6]. The Higgs arises as one of the Goldstone bosons associated to this breaking and is naturally light. The explicit Goldstone symmetry breaking can come from the different sources, for example the masses of the techniquarks (constituents of the composite Higgs), interactions with gauge fields, in particular the ones of the SM, couplings to the SM fermions.

From the theoretical point of view, the complete solution of the naturalness problem with the help of compositeness would require finding a confining theory with an appropriate global symmetry breaking structure, solving it and confirming an agreement with all the experimental data. This task

[4] We don't compare with the kaons because they are protected by a similar symmetry as pions.

[5] A pedagogical derivation of these relations can be found for example in a monograph *Weak Interactions* by H. Georgi.

[6] There exist claims for phenomenologically acceptable scenarios in which the Higgs boson, being a composite particle, does not possess the Goldstone symmetry protection mechanism (see for example [18]), in this work we will not consider this class of scenarios.

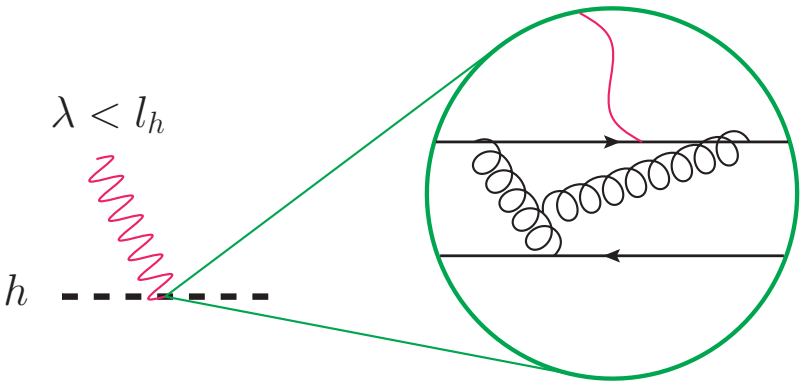

Figure 1.1: *Quanta with a wavelength smaller that the physical size of the composite Higgs boson interact directly with its constituents.*

is difficult to achieve first of all because of computational difficulties related to a strong coupling regime, and the first Composite Higgs models in their modern incarnation were formulated in a dual five-dimensional picture [15] dealing with weakly interacting states. Though the original idea of composite Higgs was formulated in terms of pure four-dimensional strongly coupled theories [5], it did not combine together all the features of the modern formulation. Interesting attempts to construct a realistic four-dimensional UV completion for CH models were recently made in Ref.s [16, 17]. An alternative and most often used approach is not to try to build a relatively complete and consistent UV description, but to describe the resulting effective theory below the confinement scale based on the plausible and minimal assumptions about its behaviour.

The first assumption concerns the spectrum of the effective theory, which should include at least four Nambu-Goldstone bosons (NGb) – the Higgs and three bosons to be "eaten" by three $G_{\rm SM}$ vectors, hence there must be at least four broken symmetry generators ($\dim[G/H] \geq 4$). Evidently, the NGb should transform non-trivially under the SM product group $G_{\rm SM} \equiv SU(2)_L \times U(1)_Y$, therefore the two groups must intersect $G \cap G_{\rm SM} \neq 0$, but the strong sector can not break explicitly $G_{\rm SM}$, hence $G_{\rm SM} \subset G$.

Let us make some simple estimate of the dimensionality of the group G following from the requirement $\dim[G/H] \geq 4$. Taking for the G/H the simplest examples – $SU(N)/SU(N-1) \times U(1)$ and $SO(N)/SO(N-1)$ [7], we find that the minimal N must be 3 and 5 respectively, which corresponds to the unbroken H being $SU(2) \times U(1)$ and $SO(4)$. In both minimal cases (and consequently also for N larger than the minimal one) $G_{\rm SM}$ is entirely embeddable into H [8] which has important consequences for the phenomenology of the models built upon these symmetry breaking patterns. Namely, there exists a limit when $G_{\rm SM}$ is aligned with H ($G_{\rm SM} \subseteq H$) and remains unbroken, and consequently there is a possibility that $G_{\rm SM}$ is just slightly misaligned with respect to the unbroken H, therefore the effects of the $G_{\rm SM}$ breaking are weaker than those of the G breaking, allowing for a separation of the mass scales of the SM particles and the new strong sector. Though this feature came for granted in the considered types of groups, in general it can be singled out as a

[7] For $N > 2$ such breakings can be triggered by a VEV of some field respectively in the adjoint and fundamental representations of the G.

[8] For the $SU(2) \times U(1)$ the embedding of the $G_{\rm SM}$ is evident, for the $SO(4)$ we can use the fact that it is isomorphic to $SU(2)_1 \times SU(2)_2$ and embed the $U(1)_Y$ as one of the generators of the second $SU(2)$.

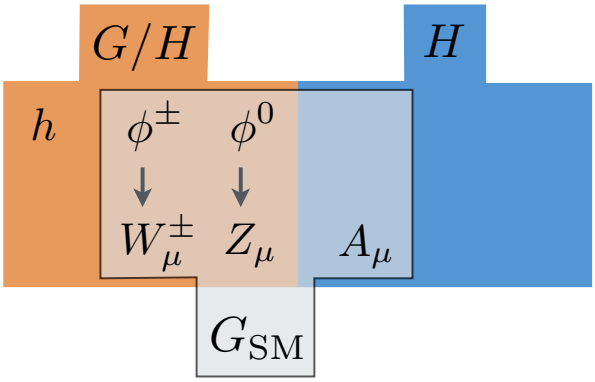

Figure 1.2: *Simplified schematic representation of the typical symmetry breaking pattern in the CH models. The group G is spontaneously broken to the H subgroup, giving rise to Goldstone bosons h, $\phi^\pm$ and ϕ^0, associated to the broken generators of the G/H coset. G_{SM} gauges three broken symmetries belonging to G/H and corresponding vector bosons become massive, absorbing the goldstones. The remaining fourth gauge field A_μ, gauging unbroken generator in H, remains massless and the fourth goldstone h remains a physical scalar.*

second necessary ingredient of the CH models. Apart from the scale separation, the existance of the limit $G_{\rm SM} \subseteq H$ allows the composite Higgs field to transform under $G_{\rm SM}$ similarly to the SM Higgs doublet, since the Goldstone bosons, as any members of the strong sector, are H-multiplets. The schematic pictorial representation of the CH models symmetry structure following from the above requirements is shown in Fig. 1.2.

The third condition is that, even after the $G \to H$ breaking, there must be a residual unbroken by a strong condensate global symmetry $[SU(2)_L \times SU(2)_R]_V$, under which the self-energies of the SM $SU(2)_L$ gauge bosons can only receive equal contributions [9]. Its breaking by strong interactions would introduce large disagreement with the actual value of the Peskin-Takeuchi T-parameter.

The above requirements lead to a formulation of the Minimal CH, based on a global symmetry breaking pattern $SO(5) \to SO(4)$, giving rise to exactly four goldstones. One could easily imagine less minimal cases, in particular those with more Goldstone bosons, for example two Higgs doublets [19], but this goes beyond the scope of our discussion.

Up to now we discussed the global symmetries of the composite sector alone, now we turn on their perturbations. Without them the Higgs is an exact Goldstone boson and can not have any potential, therefore its mass is zero and the VEV is not fixed. In the CH models the SM fields, apart from the Higgs, are typically considered as mostly elementary and not belonging to the new strong sector. The observed properties of the gauge bosons well agree with their elementary nature, therefore, as in the SM, we will assume an existence of the four elementary $G_{\rm SM}$ gauge bosons, which however will be able to mix with composite resonances. Therefore the SM gauge fields should act as external sources with respect to the strong sector, which break the G symmetry since they do not fill complete multiplets of the G group. As we will see in the next section, the misalignment of the external $G_{\rm SM}$ with respect to H can be directly related to the value of the Higgs VEV. It turns out

[9] The second factor $SU(2)_R$ is not necessarily related to an approximate SM symmetry under which the right-handed up- and down-type quarks transform as components of a doublet.

however that the loops of gauge fields can not generate a scalar potential which breaks this same gauge symmetry [21] if $G_{\rm SM} \subseteq H$, therefore additional breaking sources are necessary. The other possible source of the goldstone symmetry breaking can be the SM fermions. We postpone a detailed analysis of the SM fermions to the Section 1.4.1.

The discussion above was purely qualitative, in the three following sections we will review some of the standard tools which can be used to quantitatively describe the composite Higgs models.

1.3 CH Toolkit

1.3.1 CCWZ

Trying to describe a strong dynamics we unavoidably encounter computational difficulties. Nevertheless there are methods allowing to understand some properties of the confined theory without solving exactly the underlying dynamics and even without knowing its details. One of these approaches, the Callan-Coleman-Wess-Zumino (CCWZ) formalism [22], can be used to explore the consequences of the Goldstone nature of the Higgs field allowing to impose non-trivial constraints on the interactions of the low-energy theory. Technically, the CCWZ construction allows to obtain the building blocks of any theory with a spontaneous symmetry breaking. A detailed rigorous description of the formalism can be found for example in the original papers [22], while here we only discuss its central points and their consequences for the CH models.

Let us consider a generic, weakly or strongly coupled theory with a Lagrangian invariant under linearly realized transformations of the compact Lie group G and a vacuum state $\vec{f}$ which is only invariant under a certain subgroup $H \subset G$. Given that the vacuum state is just a certain combination of the fields – G-multiplets, which took a VEV, there in general must be n_ξ distinct dynamical fields ξ which can be obtained by the G acting on $\vec{f}$. Since the unbroken generators T^a annihilate $\vec{f}$ ($T^a \vec{f} = 0$), only the generators $T^{\hat{a}}$ corresponding to the broken symmetries of G ($T^{\hat{a}} \vec{f} \neq 0$) can excite such fields, therefore $n_\xi = \dim(G/H)$. Each $\xi^{\hat{a}}$ then can be seen as an angular real-valued variable corresponding to a rotation with respect to the $\vec{f}$ by a generator $T^{\hat{a}}$. As follows from the above description it is convenient to collect the ξ fields into the unitary matrix U, an element of G

$$U = e^{i\,\xi}, \tag{1.3.1}$$

where $\xi = \xi^{\hat{a}}\, T^{\hat{a}}$. The fields ξ are called Goldstone bosons and accordingly we will call U the Goldstone matrix. Let us understand how they transform under the symmetries of our theory. We know that since the H is unbroken, the U field as any object in the theory must linearly transform as an H multiplet [10]. But in fact there exists a larger, and therefore more constraining, symmetry containing the linearly realized H transformations as a subset. The presence of a larger symmetry is related to the fact that despite $\vec{f}$ breaks the symmetries corresponding to its rotations, the direction of $\vec{f}$ can not have any influence on the observable physical quantities. Therefore there must exist a transformation rule for the H-multiplets which includes all G group transformations and we will show it in the following.

Given that a general transformation belonging to G can be uniquely decomposed as $g = e^{iA} e^{iV}$, where $A = A^{\hat{a}} T^{\hat{a}}$ and $V = V^a T^a$, with $T^{\hat{a}}$ and T^a – broken and unbroken generators respectively,

[10] If the broken generators $T^{\hat{a}}$ form a reducible representation of the group H, the ξ fields form several H-multiplets. In the following, for simplicity, we will assume that $T^{\hat{a}}$ form an irreducible representation.

by acting with g on the U matrix from the left we obtain:

$$g\,U = e^{i\,A^{\hat{a}}\,T^{\hat{a}}}\,e^{i\,V^a\,T^a}\,e^{i\,\xi^{\hat{a}}\,T^{\hat{a}}} \equiv e^{i\,\xi'^{\hat{a}}T^{\hat{a}}}\,e^{iV'^a(\xi)\,T^a} = U'\,h(g,\xi), \tag{1.3.2}$$

where h is a transformation belonging to H. In the second equality of the above equation we defined a transformation rule for the goldstone fields: U acts as a link between the broken group G and unbroken H and the goldstones transform non-linearly and non-homogeneously

$$U \to U' = g\,U h^{-1} \quad \Rightarrow \quad \xi'^{\,i} = \xi^i + A^i + \ldots, \tag{1.3.3}$$

where dots stand for terms containing more than one power of goldstons or transformation parameters $A^{\hat{a}}$ and V^a. As we see, the invariance under the G-transformations implies an invariance under the shift of the Goldstone fields by a constant vector A^i. This symmetry forbids the Goldstone fields to have any potential and consequently allows for any VEV, which can be seen as a manifestation of the arbitrariness of the choice of the vacuum state direction:

$$\vec{f}' = e^{i\langle\xi'\rangle}\,\vec{f}, \tag{1.3.4}$$

where the new vacuum state $\vec{f}'$ differs from the old one by a rotation $e^{i\langle\xi'\rangle}$ with a non-zero goldstones VEV $\langle\xi'\rangle$. Notice that we started our discussion assuming that the Goldstone fields ξ are excitations around the true vacuum, which is invariant under H, with $\langle\xi\rangle = 0$. But by the G-transformation we can switch to the description with non-zero VEVs of the goldstones, $\langle\xi'\rangle \neq 0$, with a vacuum not annihilated by the initially chosen H generators, but without a need to redefine the transformations of the group H. Indeed, from the eq. (1.3.3) we get

$$\begin{cases} \langle\xi^i\rangle = 0 \\ h\,\vec{f} = 0 \\ U \to g\,U\,h^{-1} \end{cases} \quad \Rightarrow \quad \begin{cases} \langle\xi'^{\,i}\rangle = A^i + \ldots \\ h\,\vec{f}' \neq 0 \\ U' \to g\,U'\,h^{-1} \end{cases} \tag{1.3.5}$$

This leads to an ambiguity in how we choose the H generators and the ξ fields, which of course does not affect the physics: a symmetry of any external source will be broken if it doesn't leave unchanged the true vacuum and this can not be cured by a G rotation because it will transform both the vacuum vector and the external source. In the following we will call the group H some reference subgroup inside G which we will choose at our convenience, and the Goldstone fields VEV will parametrize a rotation $e^{i\langle\xi'\rangle}$ of the true vacuum $\vec{f}'$ with respect to the reference direction $\vec{f}$, such that $T^a\vec{f} = 0$ while in general $T^a\vec{f}' \neq 0$. As follows from the latter, our H is not literally an unbroken group, the transformations which leave the vacuum unchanged can be defined as $\tilde{h} = e^{i\langle\xi'\rangle}\,h\,e^{-i\langle\xi'\rangle}$.

The theory under consideration is by construction invariant under the linearly realized group H, therefore besides the goldstones it can contain any H-multiplets, which we collectively denote ψ. We can write down the transformations of the goldstones and ψ fields, forming a non-linear realization of the group G:

$$\begin{cases} g\,U\,h^{-1}(g,U) = U' \\ D(h(g,U))\,\psi = \psi' \end{cases},$$

where D is a linear (in ψ) transformation corresponding to the ψ's representation. The important property of the transformations (1.3.6) is their locality: even though the H is a global symmetry, the

theory must be invariant under local transformations $h(U(x_\mu))$. If we restrict the transformations of G to its unbroken part $g = h$, the ξ fields transform linearly and h becomes independent of ξ.

The ξ fields ("pions") will play a role of the Higgs field in our description, while the ψ will describe other fermionic and bosonic composite resonances.

Now that we have identified the fundamental fields and their transformation properties we can start constructing the Lagrangian. Given that U transforms as $U_{Ii} \to g_{IJ}\, U_{Jj}\, h^{-1}_{ji}$, its first index can only be contracted with the one from another U matrix since there is no other objects with G indices. The first such a combination $U^\dagger U$ is trivial because of unitarity. The next possible object one can construct is $i\, U^\dagger \partial_\mu U$, which is called Maurer-Cartan form and belongs to the Lie algebra of the G group. Therefore one can decompose it by H and G/H generators:

$$i\, U^\dagger \partial_\mu U \equiv -\, d^{\hat{a}}_\mu T^{\hat{a}} - \, e^a_\mu T^a \,. \tag{1.3.6}$$

Applying to it a general G transformation we get

$$i\, U^\dagger \partial_\mu U \to i \left[h\, U^\dagger\, g^\dagger\right] \partial_\mu \left[g\, U h^\dagger\right] = i\, h \left[U^\dagger \partial_\mu U\right] h^\dagger + i\, h\, \partial_\mu h^\dagger, \tag{1.3.7}$$

therefore using the fact that $ih\, \partial_\mu h^\dagger$ belongs to the H algebra we obtain the transformation rules

$$d^i_\mu \;\to (h)^i{}_j\, d^j_\mu \qquad \text{and} \qquad e_\mu \equiv e^a_\mu T^a \;\to\; h\, [e_\mu - i\partial_\mu]\, h^\dagger \,. \tag{1.3.8}$$

We see that the d-symbol transforms homogeneously under H and the e-symbol transforms as a gauge field. Hence the latter can be used to construct covariant derivatives of the ψ fields:

$$\nabla_\mu \psi \;=\; \partial_\mu \psi + i\, e^a_\mu T^a \psi \,. \tag{1.3.9}$$

We recall that the H transformations are effectively local. Another possible covariant combination is an analog of the usual field strength tensor $f_{\mu\nu} \sim [\nabla_\mu, \nabla_\nu]$.

The d-symbol can be used to write a kinetic term of the Goldstone fields. Before doing this let us trade the dimensionless fields ξ by the dimension 1, Π, with a substitution $\xi \to \sqrt{2}\,\Pi/f$. The relevant lagrangian is then

$$\mathcal{L}_\pi = \frac{f^2}{4} d^i_\mu d^{i\,\mu} \;= \frac{1}{2}\, \partial_\mu \Pi^{\hat{a}}\, \partial^\mu \Pi^{\hat{a}} + \frac{c^{\hat{a}\hat{b}\hat{c}\hat{d}}}{f^2}\, \Pi^{\hat{a}}\, \Pi^{\hat{b}}\, \partial_\mu \Pi^{\hat{c}}\, \partial^\mu \Pi^{\hat{d}} + \mathcal{O}(\Pi^6), \tag{1.3.10}$$

where the $c^{\hat{a}\hat{b}\hat{c}\hat{d}}$ are order one coefficients which are completely fixed for a given choice of the G/H coset. With the chosen prefactor of the d^2 term and the above field redefinition the goldstone fields became canonically normalized. In the Eq. (1.3.10) the parameter f acquires a practical meaning – it controls the strength of goldstones interactions. These interactions grow with the external momenta and become non-perturbative at energies $\Lambda_\sigma \simeq 4\pi f$, when for instance the 1-loop correction to the pion-pion scattering amplitude becomes comparable with the tree-level effect. The Λ_σ is therefore an upper bound for a cutoff of our effective description.

We see that inside the composite sector the U matrix only enters with the derivatives and no scalar potential can appear. Derivative couplings of goldstones among themselves and with other composite states, being potentially strong, do not modify the mass spectrum and don't contribute to the generation of the Higgs mass.

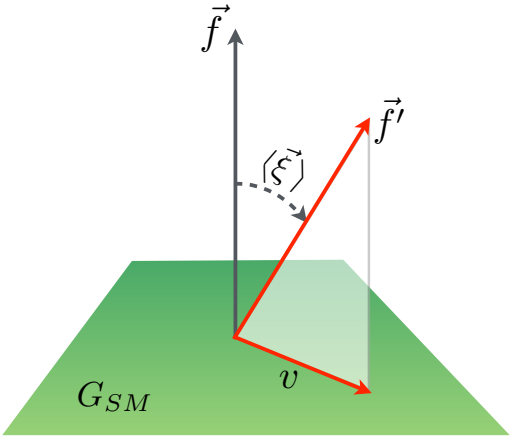

Figure 1.3: *Schematic representation of the typical symmetry breaking pattern in the CH models. The external source symmetric under G_{SM} breaks G explicitly and fixes a non-zero VEV of the goldstones; the projection of the strong sector condensate $\vec{f}'$ on G_{SM} breaks the latter.*

But the U matrix can be used as a link between the states transforming linearly in the representations of the G (which don't participate directly in the spontaneous symmetry breaking and are external to the strong sector) with the composites invariant under H. This kind of interactions with G-breaking external sources is necessary to generate the Higgs mass. To guarantee the smallness of the latter the perturbation of the G symmetry must be weak, therefore we can develop a perturbative expansion in the small G-breaking.

As was argued in the previous section, the gauge fields of the SM should be described as external sources with respect to the strong sector and $G_{\rm SM}$ must be embeddable into H. The situation with SM fermions is more complicated and will be discussed in a dedicated Section 1.4.1. To introduce the gauge fields A_μ consistently we first promote them to the full multiplet in the adjoint representation of G, couple it to the strong sector, and in the end set the unnecessary fields to zero. At the same time a part of G-transformations, corresponding to $G_{\rm SM}$, becomes local, with a transformation law for the gauge fields

$$A_\mu \to A'_\mu = g\,[A_\mu + i\partial_\mu]\,g^t\,. \tag{1.3.11}$$

The G-multiplets can only interact with the Goldstone matrix and according to the transformation law (1.3.3), the gauge fields should act on the U matrix from the left. Therefore introduction of massless gauge fields amounts for replacing the usual derivatives with covariant ones in the *lhs* of Eq. (1.3.6). Definitions of the d and e change correspondingly:

$$U^t\,[A_\mu + i\partial_\mu]\,U \equiv -\,d^{\hat{a}}_\mu T^{\hat{a}} - \,e^a_\mu T^a\,, \tag{1.3.12}$$

With a new definition the leading terms of d and e symbols are

$$d^{\hat{a}}_\mu = \frac{\sqrt{2}}{f}(D_\mu\Pi)^{\hat{a}} + \mathcal{O}(\Pi^3) \quad \text{and} \quad e^a_\mu = -gA^a_\mu - \frac{i}{f^2}(\Pi\overleftrightarrow{D}_\mu\Pi)^a + \mathcal{O}(\Pi^4). \tag{1.3.13}$$

where $D_\mu = \partial_\mu - iA_\mu$ and $\Pi\overleftrightarrow{D}_\mu\Pi = \Pi(D_\mu\Pi) - (D_\mu\Pi)\Pi$.

Let us now focus on a minimal coset $G/H = SO(5)/SO(4)$. In this case we can choose the H such that $G_{\rm SM} \subset H$ using the fact that $SO(4)$ is locally equivalent to $SU(2)_L \times SU(2)_R$. The hypercharge then can be associated with T^3_R. The explicit form of the $SO(5)$ and $SO(4)$ generators can be found in the Appendix 1.7. Explicitly, the A_μ will be

$$A_\mu = \frac{g}{\sqrt{2}} W^+_\mu \left(T^1_L + iT^2_L\right) + \frac{g}{\sqrt{2}} W^-_\mu \left(T^1_L - iT^2_L\right) + g\left(c_{\rm w} Z_\mu + s_{\rm w} A_\mu\right) T^3_L + g'\left(c_{\rm w} A_\mu - s_{\rm w} Z_\mu\right) T^3_R \,, \tag{1.3.14}$$

where $c_{\rm w}$ and $s_{\rm w}$ denote respectively the cosine and the sine of the weak mixing angle and g, g' are the SM couplings of $\mathrm{SU}(2)_L$ and $\mathrm{U}(1)_Y$.

Given this embedding of the $G_{\rm SM}$, the physical Higgs boson h in the unitary gauge corresponds to the fourth component of the Π field. The unbroken group $e^{i\sqrt{2}\langle h\rangle/f}\, H\, e^{-i\sqrt{2}\langle h\rangle/f}$ for the non-zero Higgs VEV will be misaligned with gauged $G_{\rm SM}$, meaning that the latter will be spontaneously broken. This can be seen by expanding the kinetic term of the Higgs field in the Unitary gauge:

$$\mathcal{L}_\pi \;=\; \frac{f^2}{4} d^i_\mu d^{i\,\mu} \;=\; \frac{1}{2}(\partial_\mu h)^2 + \frac{g^2}{4} f^2 \sin^2\frac{h}{f}\left(|W_\mu|^2 + \frac{1}{2c_w^2} Z_\mu^2\right) \,, \tag{1.3.15}$$

from which we can read the W and Z masses $m_W = g/2\, f\, \sin\frac{\langle h\rangle}{f}$, $m_Z = m_W/c_w$. This fixes the relation among the Higgs VEV $\langle h\rangle$ and the EW scale $v_{\rm SM} = 246$ GeV

$$v_{\rm SM} \;=\; f\, \sin\frac{\langle h\rangle}{f} \,. \tag{1.3.16}$$

At the same time it is easy to verify that the couplings of the Higgs with gauge bosons are weaker than in the SM by a factor $\cos\frac{\langle h\rangle}{f}$. The suppression of the couplings of the gauge bosons to the Higgs is a general feature of CH models with compact global groups and a Higgs transforming as an $SU(2)_L$ doublet [23].

The relation (1.3.16) means that the SM gauge group "feels" just a part of the strong sector condensate, which defines the scale of the new strongly coupled dynamics. This fact allows for a limit in which all the effects of compositeness decouple: $f \to \infty$, $v_{\rm SM}$ fixed. This limit however also corresponds to an infinite tuning. Indeed, since the ξ is an angular variable, both the quadratic and quartic terms of its effective potential will obtain contributions originating from an expansion of the same trigonometric function and therefore will generically have coefficients of the same order, giving a minimum for $\langle\vec{\xi}\rangle \sim 1$ and hence $v_{\rm SM} \sim f$. It is however clear that in order to successfully pass all the experimental constraints the electroweak and the strong symmetry breaking scales should be separated, requiring some tuning of the parameters of the model. The measure of this tuning for the CH models can be taken as [20]

$$\xi \equiv \left(\frac{v_{\rm SM}}{f}\right)^2 . \tag{1.3.17}$$

In practice the tuning needed to obtain a realistic Higgs VEV could be worse, depending on the structure of the particular models.

1.3.2 Large $\mathbf{N_c}$ Theories and Generalized Dimensional Analysis

Another tool which helps in understanding of the behaviour of strongly coupled theories below the confinement scale is a large N-colors expansion. It turns out that for $SU(N)$ gauge confining

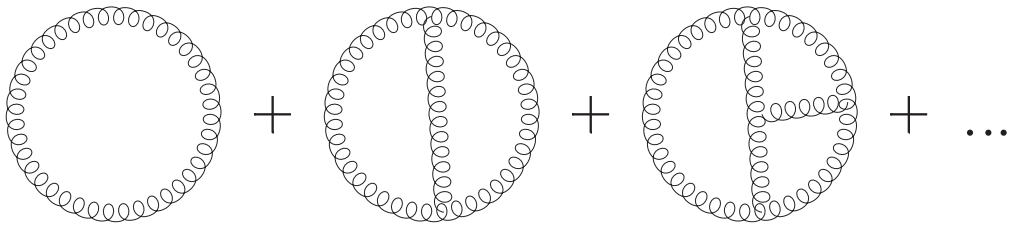

Figure 1.4: *A set of vacuum-vacuum diagrams with gluons.*

theories one can construct a systematic expansion in the small parameter $1/N$ and obtain qualitative information about a theory even in a strongly coupled regime. In this section we show how this can be done and discuss some useful results for the CH phenomenology [11]. We want to consider a gauge $SU(N)$ theory with a coupling constant g_s. We postulate a presence of colored fermionic fields in the fundamental representation of the gauge group, which we call quarks for simplicity. While the corresponding gauge vector fields will be called gluons. We will start with a discussion of connected vacuum-vacuum diagrams containing loops of quarks and gluons, determine their scaling properties with respect to N and in the end will relate these diagrams to the ones describing interactions of composite pions.

To understand the dependence of an amplitude on N one only needs to account for its color structure. The quark and gluon propagators have the following color dependence

$$\begin{aligned} q^a\,\bar{q}_b &\sim \delta^a_b\,, \\ G_{\mu\ b}^{\ a}\,G_{\nu\ d}^{\ c} &\sim (\delta^a_d\delta^c_b - \frac{1}{N}\delta^a_b\delta^c_d)\,, \end{aligned} \tag{1.3.18}$$

where the gluon field is defined as $G_{\mu\ b}^{\ a} = G^A_\mu (T^A)^a_{\ b}$ with T^A – $SU(N)$ generators. The last term in the gluon propagator can be neglected in large N limit, hence we can consider every quark propagator as one color flow and gluon as two oppositely directed flows. In analogy with Feynman diagrams, the color-flow diagrams can be used to simplify the computations. In fig. 1.4 we show a set of vacuum-vacuum diagrams with gluons, and in fig. 1.5 the same set in a color-flow notation. Every closed color line corresponds to a trace $\delta^a_a = N$, therefore, including the $\frac{1}{(4\pi)^2}$ loop factors, we can estimate the vacuum-vacuum diagram as

$$c_1\,N^2\frac{1}{(4\pi)^2} + c_2\,N^3\frac{1}{(4\pi)^2}\frac{g_s^2}{(4\pi)^2} + c_3\,N^4\frac{1}{(4\pi)^2}\frac{g_s^4}{(4\pi)^4} + ... \tag{1.3.19}$$

where c_i – some order-1 coefficients. In the limit $N\to\infty$ and fixed g_s the amplitude (1.3.19) has no definite scaling with N, as the higher order loop contributions come with higher powers of N. However there exists a limit in which a well-defined scaling with N occurs and all the terms have comparable size. This happens if $N\frac{g_s^2}{(4\pi)^2}\sim 1$, which for $N\to\infty$ corresponds to setting $g_s\to 0$ keeping $g_s\sqrt{N}$ fixed. In this case the whole series (1.3.19) scales like N^2 and can be rewritten as

$$\sum_i c_i\,N^2\frac{1}{(4\pi)^2} \sim N^2\frac{1}{(4\pi)^2}. \tag{1.3.20}$$

[11] More comprehensive reviews of the presented here in a short form material can be found in Ref.s [24, 25].

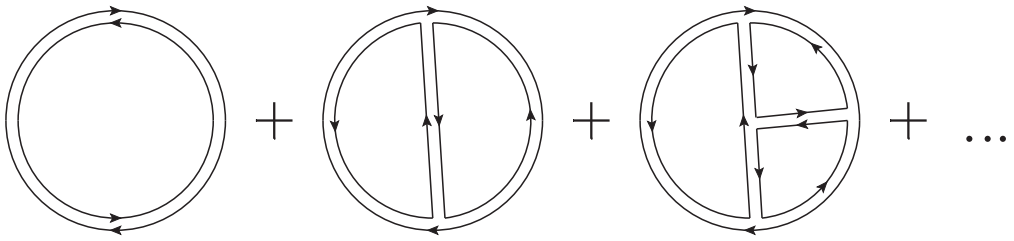

Figure 1.5: *A set of color-flow diagrams corresponding to vacuum-vacuum diagrams with gluons, each gluon is represented as two oppositely-directed color lines.*

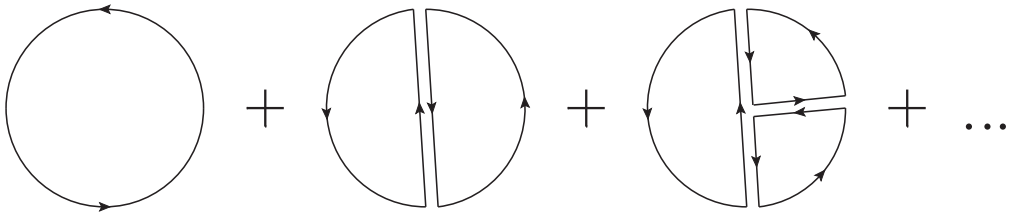

Figure 1.6: *A set of vacuum-vacuum diagrams including gluons and one fermion, each gluon is represented as two color lines and a fermion as one line.*

Each coefficient c_i is expected to be of the order 1, and in the absence of sign correlation between different coefficients one can estimate that the whole sum $\sum_i c_i$ is also of the order 1, such that the relation above holds. The identified limit $N\frac{g_s^2}{(4\pi)^2} \sim 1$ occurs when the so-called 't Hooft coupling

$$g \equiv \sqrt{N} g_s \tag{1.3.21}$$

is of the order 4π. For a smaller value of g our result would be dominated by a leading order term in the expansion (1.3.19), which is a usual perturbative approximation, while for larger g the expansion makes no sense.

After explicit introduction of the 't Hooft coupling we can classify amplitudes according to their scaling with the N, here is the summary of rules to estimate the size of each diagram (see Ref. [24]):

- each interaction vertex brings an additional factor of $g/\sqrt{N}$;
- each closed color line brings a factor of N, every quark carries one color line and every gluon carries two of them;
- every loop brings a factor $1/16\pi^2$.

Therefore the dominant diagrams in this expansion possess the maximal ratio of number of closed color loops to the number of strong couplings. For example the set of diagrams with one fermionic line depicted on the Fig. 1.6 scales like N^1 since every fermion carries just one color index, unlike a gluon which carries two of them. In the limit $g \sim 4\pi$ the overal size of the resummed set of the diagrams with the same N-dependence can be estimated by just considering the leading diagram with the smallest number of loops as we demonstrated for the series (1.3.19).

After this brief description of the large-N limit we are able to estimate some dynamical properties of the theory in the strongly coupled regime. The main physical objects of interest now will be mesons

which can be excited from the vacuum by the quark bilinears of the form $\mathcal{O} = \bar{q}q$. Let us consider a two point function of such bilinears, $\langle \mathcal{O}\mathcal{O} \rangle$, which corresponds to the diagrams shown in Fig. 1.7. The first diagram in Fig. 1.7 corresponds to the third diagram in Fig. 1.6 and thus has the same dependence on N, we can estimate it (together with all the other diagrams with the same scaling, shown in Fig. 1.6, which all contribute to the $\langle \mathcal{O}(k)\mathcal{O}(-k) \rangle$) using given above rules

$$\langle \mathcal{O}(k)\mathcal{O}(-k) \rangle \sim \frac{N}{(4\pi)^2} \tag{1.3.22}$$

The second diagram in Fig. 1.7 instead contains one additional fermionic line, so it gives a contribution suppressed by $1/N$ with respect to the first one. If we cut the leading order diagram in Fig. 1.7, we see that the state appearing in the cut is a quark-antiquark pair forming together with gluons a color singlet, which in a confined theory corresponds to one-meson state [12]. In the case of the subleading diagram (second one in Fig. 1.7), the intermediate state appearing in the cut corresponds to two color-singlet pairs of quarks, corresponding to two mesons. Therefore, $\langle \mathcal{O}\mathcal{O} \rangle$ is mostly determined by one-particle intermediate states, and corresponding two-point function must have poles corresponding to masses of mesons excited by $\mathcal{O}$

$$\langle \mathcal{O}(k)\mathcal{O}(-k) \rangle \simeq \sum_i \frac{Z_i}{k^2 - m_i^2}. \tag{1.3.23}$$

where $\sqrt{Z_i}$ corresponds to the amplitude of creation of the i'th meson from the vacuum by the operator $\mathcal{O}$. From the fact that the two-point function in the *l.h.s.* of Eq. (1.3.23) has a well defined scaling with N, independent on the mesons momentum k, follows that the mesons masses m_i in the *r.h.s.* of Eq. (1.3.23) do not depend on N. Then, according to the estimate (1.3.22), we obtain

$$Z_i \simeq \frac{N}{(4\pi)^2}. \tag{1.3.24}$$

The next object, a four-point function, can be estimated using the same set of rules. From it we obtain the four-meson vertex

$$V_4 = \left(\frac{1}{\sqrt{Z}}\right)^4 \langle \mathcal{O}\mathcal{O}\mathcal{O}\mathcal{O} \rangle\big|_{residue} \simeq \frac{(4\pi)^2}{N} F^{(4)}\left(\frac{E}{m_\rho}\right), \tag{1.3.25}$$

up to some unspecified dimensionless function $F^{(4)}$ dependent on the relevant physical scales in the problem – typical mass of the composite resonances m_ρ and the energy E. Technically, the m_ρ is a dynamically generated confinement scale, hence is should be understood as an inverse physical size of the mesons and not necessarily their mass. In particular if we apply an estimate (1.3.25) to the massless pion-like states, the m_ρ should still be taken as a typical mass of the meson-like resonances not protected by any symmetries.

We see that the effective coupling between the mesons is

$$g_\rho = \frac{4\pi}{\sqrt{N}}, \tag{1.3.26}$$

[12] One can also demonstrate that the additional states consisting of gluons forming a color singlet will not appear in the cut [24].

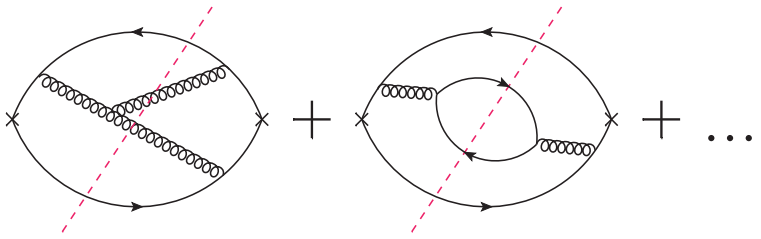

Figure 1.7: *A set of diagrams contributing to the two-point function* $\langle \mathcal{O}\mathcal{O} \rangle$*. Crosses correspond to insertions of the operator* $\mathcal{O}$*. First diagram corresponds to one-meson intermediate state while the second – to two mesons.*

which means that for sufficiently large N they interact weakly despite being formed by strong dynamics, hence one can use a perturbation theory to describe their interactions. One can extend this analysis to the case of an arbitrary number of mesons:

$$V_n \simeq g_\rho^{n-2}\, m_\rho^{4-n}\, F^{(n)}\left(\frac{E}{m_\rho}\right), \tag{1.3.27}$$

where n is a number of external states. We can match this result to the one obtained for the goldstone boson scattering in the CCWZ formalism. Recall that the four-goldstone vertex obtained from Eq. (1.3.10) was proportional to E^2/f^2, where E is a typical energy of the process. Therefore we must single out an E^2/m_ρ^2 term from the expansion of the $F^{(4)}$ function in Eq. (1.3.25). Thus the matching will require

$$E^2/f^2 \simeq g_\rho^2 E^2/m_\rho^2\,, \tag{1.3.28}$$

which relates the mass scale of composite mesons with their coupling and a goldstones decay constant:

$$m_\rho \simeq g_\rho\, f. \tag{1.3.29}$$

We can summarize the results obtained above (Eq.s (1.3.27) and (1.3.29)) in a set of rules for the estimate of the size of the operators generated by the strong dynamics, similar to the ones of Generalized Dimensional Analysis [26], an extension of the Naive Dimensional Analysis [27] (NDA) (see also [20] for the adaptation to known classes of CH models)

- operators should contain a factor m_ρ^4/g_ρ^2;
- each meson comes with a factor $g_\rho/m_\rho \simeq 1/f$;
- each insertion of the external momentum is compensated by one power of the compositeness scale m_ρ;
- gauge fields enter to the theory in a form of covariant derivatives, thus each external gA_μ comes with an inverse power of m_ρ, analogously to external momenta.

These rules are captured by a simple formula

$$\Lambda^2 f^2 \left(\frac{\Pi}{f}\right)^{\#_{\Pi_{ext}}} \left(\frac{\partial}{\Lambda}\right)^{\#_{\partial_{ext}}} \left(\frac{gA}{\Lambda}\right)^{\#_{A_{ext}}}, \tag{1.3.30}$$

where $\#_{\Pi_{ext}}$, $\#_{\partial_{ext}}$ and $\#_{A_{ext}}$ – number of external Goldstone fields, momenta and gauge fields respectively; we took $\Lambda = g_\rho f$ – a typical mass of the composite meson-like states.

1.3.3 Power Counting

All what we typically know about a theory are the light degrees of freedom (described by the IR lagrangian) and a set of symmetries (not necessarily exact) respected by the full theory. Being interested in a particular effective operator, one can reconstruct its necessary ingredients – external fields, powers of external momenta, symmetry breaking spurions and couplings. This structure then can require a multiplication by an additional power of some mass scale Λ in order to match the mass dimension 4 of the whole operator in the Lagrangian. Generically, this mass scale will be determined by the masses of intermediate states which generated a given effective operator. In the following we will write down a rule allowing to reconstruct the needed effective operator, generated by an exchange of weakly coupled states or pure strong dynamics, and its dependence on Λ. But first we want to consider possible types of dependences on the cut-off, and discuss their implications.

- A positive power dependence on Λ means that the operator is dominated by the UV physics contributions and therefore one can only get a very rough estimate of it.

  As an example let us consider a SM Higgs boson mass term. In this case the symmetry structure of the SM doesn't require any additional ingredients for the operator apart from the $|H|^2$. The correct mass dimension of the operator will be restored by multiplying by Λ^2. As a simple check one can consider an additional scalar S with a mass m_S coupled to the Higgs by means of interaction $g_S^2 S^2 |H|^2$ with a coupling constant g_S. In this case the new physics scale m_S corresponds to a cutoff Λ of the effective IR description. The correction to the Higgs mass operator induced by S in the dimensional regularization would look like:

  $$\delta m_h^2 \simeq \frac{g_S^2}{16\pi^2} m_S^2 \log \frac{m_S^2}{\mu^2} \tag{1.3.31}$$

  As we expected, it is quadratically sensitive to the UV physics mass scale and on top of this the operator is suppressed by a loop factor. If this new scalar is present in the UV, neither its mass m_S nor the coupling g_S are known but at the same time its effect can be dominant compared to the known IR contribution (given that by definition all mass parameters in the IR theory are smaller than $\Lambda \sim m_S$), therefore our IR description lacks of predictivity.

- Now let us consider the operators which don't depend on Λ. In this case the minimal ingredients of the operator do not require any additional powers of mass, therefore one can conclude that with any specific UV completion the exact result will be obtained by multiplying the required operator by some dimensionless function of masses of the states present at this scale, therefore this function is expected to be of the order one.

  If the operator is supposed to be generated at one loop and formally needs zero powers of Λ, this would mean that in fact the coefficient must include a $\log \mu^2/\Lambda^2$, where μ is a renormalization scale.

  As an example we can take a fermion mass in a presence of new heavy vectors coupled to the fermion by means of $g_\rho \, \bar{q} \, \rho_\mu \gamma^\mu \, q$. The necessary ingredients of the operator are two fermionic fields $\bar{q}_L q_R$ whose dimension is 3, but the mass of the fermions is protected by a chiral symmetry, i.e. the latter forbids to construct a mass term. Therefore the operator must also contain a chiral symmetry breaking parameter, the bare quark mass m_q^0, which makes it a dimension-4

operator. Given that the correction is generated at one loop, it should also be multiplied by $1/16\pi^2$. The resulting correction to the physical mass is

$$\delta m_q \simeq m_q^0 \frac{g_\rho^2}{16\pi^2} \log \frac{m_\rho^2}{\mu^2} \tag{1.3.32}$$

which is subdominant compared to the bare mass if the coupling g_ρ is weak, while if $g_\rho \lesssim 4\pi$ the UV contribution can become comparable to the IR one. It is also important that the unknown (from the IR point of view) physical scale m_ρ enters in the expression in a logarithm, hence the fact that m_ρ is not known precisely is not crucial. Therefore in the case of the independent on Λ operators (or log-sensitive), one can obtain a relatively precise estimate of the effects of unknown UV physics.

- If computing the coefficient of some operator we find that it contains negative powers of the cutoff this simply means that UV physics contribution is suppressed by its mass scale and the dominant effect will come from the light states. The IR contribution to the considered process, if it is present, is therefore a good quantitative estimate of the operator.

We saw that the cutoff dependence of the operators, which can be inferred from simple arguments without a detailed knowledge of the underlying theory, reflects the dependence on the physical masses of states in a UV theory (m_S and m_ρ), though the latter together with coupling constants (g_S and g_ρ) are not known precisely. It is useful to derive a general expression allowing to estimate a cutoff dependence of the arbitrary operators, taking into account effects of loops and insertions of the symmetry breaking parameters. Such an expression, for the case of the theory described by the goldstones Lagrangian (1.3.15), with addition of fermionic fields, was derived in the Ref. [40] basing on a counting of energy and $\hbar$ powers of the amplitude of a general form. The resulting counting rule is

$$\Lambda^2 f^2 \left(\frac{\Lambda}{4\pi f}\right)^{2\#_{loops}} \left(\frac{\Pi}{f}\right)^{\#_{\Pi_{ext}}} \left(\frac{\partial}{\Lambda}\right)^{\#_{\partial_{ext}}} \left(\frac{gA}{\Lambda}\right)^{\#_{A_{ext}}} \left(\frac{F}{f\sqrt{\Lambda}}\right)^{\#_{F_{ext}}} \left(\frac{m}{\Lambda}\right)^{\#_{mass}} \left(\frac{gf}{\Lambda}\right)^{2\#_{A_{int}}} \tag{1.3.33}$$

where $\#_{\Pi_{ext}}$, $\#_{A_{ext}}$ and $\#_{F_{ext}}$ are numbers of respectively goldstones, gauge bosons and fermions present as external legs in the diagram, $\#_{\partial_{ext}}$ – number of derivatives, $\#_{mass}$ – number of insertions of mass parameters present in the IR Lagrangian, and $\#_{A_{int}}$ – number of insertions of gauge couplings inside the loops (not accounted for by $\#_{A_{ext}}$).

It is easy to verify that the expression (1.3.33) reproduces the effect of heavy states with a mass $\sim \Lambda$ interacting with a strength $g_\rho \simeq \Lambda/f$, in particular one can recover the two results of Eq. (1.3.31) and Eq. (1.3.32). An assignment $g_\rho \simeq \Lambda/f$ is valid for instance for the meson-like resonances discussed in the Section 1.3.2, heavy scalar in the linear sigma-model, and also the n-site models of Composite Higgs discussed in the Section 1.5.1. In addition, in the limit $g_\rho \simeq 4\pi$ the formula converges to a usual NDA estimate of the strong dynamics contribution to the process.

1.4 SM Fermions

1.4.1 Mass Generation

One important ingredient of the composite Higgs scenario described above is the explicit breaking of the Goldstone symmetry (the global group G in notations of the Section 1.2). In the absence of such

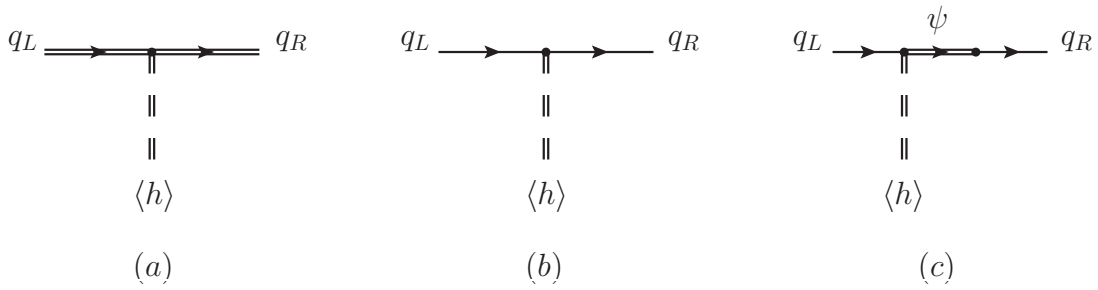

Figure 1.8: *Diagrams responsible for mass generation for the cases of total SM fermion compositeness (a), bilinear interactions with composite sector (b) and linear interactions (c). Single lines correspond to elementary states, double - to composite.*

breaking the position of the unbroken group H inside G would not be fixed (the condensate $\vec{f}$ could have any direction inside the G) and the Higgs boson would be massless. The external breaking source allows for the Higgs potential which fixes the direction of the $\vec{f}$ with respect to the G and the SM gauge symmetry ($G_{\rm SM}$) and hence determines how the latter is broken, the projection of the $\vec{f}$ on the $G_{\rm SM}$ being interpreted as a Higgs VEV.

The EWSB mechanism described above must coexist with a mechanism of the generation of the masses of the elementary states. The generation of the gauge bosons masses is quite straightforward and is unambiguously defined by the choice of the gauging of the group G. The details were discussed in Section 1.3.1. One could imagine three general possibilities of giving a mass to SM fermions:

I All SM fermions are composite objects belonging to the strong sector [28] (Fig. 1.8 (a)). This possibility is disfavoured by precision measurements done at LEP [29]. For example the scale Λ suppressing new flavour-conserving four-fermion interactions of the light SM fermions

$$\frac{1}{\Lambda^2}(\bar{f}f)^2 \tag{1.4.1}$$

which will generically appear due to new vector and scalar composite resonances, must be greater than $\sim$ 5 TeV. In the CH models the four-(composite)fermion operators (see Fig. 1.9) are just suppressed by the strong condensate scale, hence one should take $\Lambda \to f$. This follows from the expression (1.3.33) and can be easily understood as a result of the cancellation of the strong coupling g_ρ, appearing in the numerator of the amplitude corresponding to the diagram 1.9 (a), and a mass of the mediator of the four-fermion interactions, which appears in the denomenator and was estimated in the Eq. (1.3.29) to be $m_\rho \simeq g_\rho f$. From this, one would get $f \gtrsim 5$ TeV which leads to an unacceptable tuning $\xi = (v/f)^2 \lesssim 0.001$.

II SM fermions do not belong to the strong sector and act as an external source for the composite operators (Fig. 1.8 (b)). Since the SM fermions and gauge bosons do not belong to the composite sector, we will call them elementary. In order to couple the SM states q transforming in the G_{SM} it is convenient to formally promote them to multiplets of the G. This can be done by introducing the embeddings $Q_I = \Delta_{I\alpha}\, q_\alpha$, where the index I corresponds to G and α to $G_{\rm SM}$. We further assume that the leading operator involving SM fermions and composites in the UV (at a scale Λ' above the

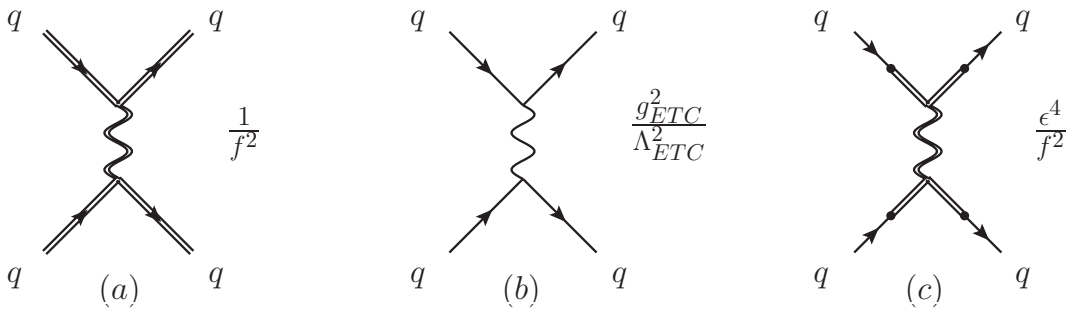

Figure 1.9: *Four fermion operators and their typical strength for the cases of total SM fermion compositeness (a), bilinear interactions with composite sector (b) and linear interactions (c). Single lines correspond to elementary states, double - to composite.*

confinement scale Λ) is *bilinear* in elementary fermions (*à la* extended technicolor [31]):

$$\mathcal{L}_{\text{pert}} = y\,\bar{Q}_L\,\mathcal{O}\,Q_R \tag{1.4.2}$$

where $Q_{L,R}$ denote SM fermions and $\mathcal{O}$ - composite operator, which, for instance, could correspond to a techniquark bilinear $\bar{q}^{tc}q^{tc}$. The dimensionless parameter y defines how strong the external perturbation is.

Given the fact that the scaling dimensions of the elementary fermions Q are close to the canonical one 3/2, at the strong sector confinement scale Λ the strength of the perturbation (1.4.2) will evolve from y to $y\left(\frac{\Lambda}{\Lambda'}\right)^{[\mathcal{O}]-1}$, where $[\mathcal{O}]$ is a scaling dimension of the operator $\mathcal{O}$. The contraction of the VEV of the operator $\mathcal{O}$ with the external source will be proportional to the Higgs VEV, therefore the mass of the quarks can be estimated as:

$$m_q \sim y\,v\left(\frac{\Lambda}{\Lambda'}\right)^{[\mathcal{O}]-1}. \tag{1.4.3}$$

The scaling dimension $[\mathcal{O}]$ can not be smaller than 2. Otherwise the operator $\text{Tr}[\mathcal{O}^\dagger\mathcal{O}]$ would be relevant and hence the scale Λ (which is affected by the VEV of the $\text{Tr}[\mathcal{O}^\dagger\mathcal{O}]$) will tend to get close to the Λ' disallowing for a suppression of the dangerous four-fermion operators. The latter in general case will not respect any flavour symmetry and have a strength

$$\mathcal{L}_{\text{4-q}} = \frac{1}{\Lambda'^2}\,(\bar{Q}Q)(\bar{Q}Q), \tag{1.4.4}$$

generating the flavour-changing and CP-violating processes which are stringently constrained: the scale Λ' must be at least of the order of $10^3 - 10^4$ TeV for CP-conserving process and 10^5 TeV for CP-violating ones [30]. Taking $\Lambda' \sim 10^5$ TeV, we derive from Eq. (1.4.3) that in order to generate the top quark mass one would need the confinement scale Λ to be of the order of 10^4 TeV even for the maximal allowed $y \sim 4\pi$. Given that $f \gtrsim \Lambda/4\pi$, the tuning becomes unacceptable: $\xi < 0.001$. Therefore without additional assumptions about the flavour structure of the theory at the scale Λ' one is not able to proceed.

III The third possibility is that SM fermions are external to the strong sector and the leading elementary-composite operator is *linear* in SM fields [15, 33] (Fig. 1.8 (c)):

$$\mathcal{L}_{\text{pert}} = y\, \bar{Q}_{I_1 I_2 \ldots} \mathcal{O}_{I_1 I_2 \ldots} \tag{1.4.5}$$

where we denoted the G indices as $I_{1,2,\ldots}$ and y is again a dimensionless parameter characterizing the strength of the perturbation. The SM flavour indices are omitted for simplicity, but in general each SM multiplet can couple to its own operator.

Below the confinement energy the operator $\mathcal{O}$ can excite a tower of composite (one- or many-particle) states: $\mathcal{O}|0\rangle = \sum_n f_n |\widetilde{\Psi}_n\rangle$ with $f_n = \langle \widetilde{\Psi}_n | \mathcal{O} \rangle$. Since the composite sector does not respect the symmetry G, the H-invariant states in $\widetilde{\Psi}_n$ will be accompanied by the goldstones living in G/H to restore the invariance under the whole G. Therefore at low energies the perturbation lagrangian can be rewritten as an interaction between the elementary and composite states:

$$\mathcal{L}_{\text{pert}} = y \sum_n f_n\, \bar{Q}_{I_1 I_2 \ldots} \left[U_{I_1 i_1} U_{I_2 i_2} \ldots (\Psi_n)_{i_1 i_2 \ldots} \right] \tag{1.4.6}$$

where the indices i belong to the H. By dimensional analysis one can see that the leading operators will contain a minimal number of generic composites, therefore for the leading terms of (1.4.7) the ψ_n will be just one-particle states and therefore the lagrangian (1.4.7) defines the *mixing* of the elementary and composite particles and their Yukawa interactions. Thus in order to preserve the electroweak symmetry before the confinement occurs, these states must have SM quantum numbers similar to the ones of the elementary fermions they mix with. Moreover, if the state ψ_n is massive, both its chiralities must transform in the same way under G_{SM}, thus the composite fermions are *vector-like*.

To illustrate the implications of the linear mixing of eq. (1.4.7) let us consider a toy model with the third generation quark doublet q_L and a singlet t_R coupled to a composite singlet ψ with a mass $m^\star$. We can write down the first terms of the expansion of the eq. (1.4.7) in fields:

$$\mathcal{L}_{\text{pert}} \supset y_L\, \bar{q}_L\, H^c\, \psi_R + y_R\, f\, \bar{t}_R\, \psi_L + h.c. \tag{1.4.7}$$

After diagonalization of the masses we find that the lightest mass eigenstate t_R is a mixture of the elementary and composite ones, therefore we will call it *partially composite*:

$$t_R^{SM} = \cos\phi_R\, t_R + \sin\phi_R\, \psi_R, \tag{1.4.8}$$

where the ϕ_R is defined by $\tan\phi_R = y_R f / m^\star$ and gives a measure of a degree of compositness of t_R. The mass of the top quark is

$$m_t \simeq \frac{v}{\sqrt{2}} y_L \sin\phi_R = y_L y_R \frac{v}{\sqrt{2}} \frac{f}{m^\star} \tag{1.4.9}$$

This simple model can be straightforwardly extended to include more composite resonances in different representations of the group H and coupled to other SM fermions as well. The masses of the SM fermions will be proportional to the mixing parameters y and inversely proportional to the masses of the resonances they mix with. As we know the ratio of the heaviest SM quark to the lightest one is of the order of 10^5. Trying to generate this spred by simply varying the masses of composites is not promising since they are not expected to be that much separated, hence this will simply change the problem of the SM quark hierarchy to the that of the composite fermions.

Another possibility is to generate a large difference of parameters y. In this case one might hope that the large hierarchy of y in the IR can be generated by the renormalization group evolution from some large scale Λ' above the confinement, where all the y's are of the same order. Assuming that the main effect to the running comes from the renormalization of the composite operator the expression for the quark mass can be written as follows:

$$m_q \sim y_L(\Lambda')\, y_R(\Lambda') \left(\frac{\Lambda}{\Lambda'}\right)^{\gamma_L+\gamma_R} . \tag{1.4.10}$$

By adjusting the anomalous dimensions γ of the composite operators one can reproduce all the masses of the SM fermions. An interesting deviation from the formula (1.4.10) can appear when the anomalous dimensions are negative, in this case the y flows to a fixed value sufficient for the generation of the top mass. At the same time if the smallest scaling dimension of the operators $\mathcal{O}$ is $\sim 5/2$, which is still sufficient to reproduce the top mass, the operator $\mathrm{Tr}[\mathcal{O}^\dagger\mathcal{O}]$ is irrelevant which makes the Higgs mass and the confinement scale insensitive to the UV physics. Given this, even assuming that the large hierarchy of the couplings y is not generated only by the RG running, the explanation to the hierarchy is allowed to reside at any arbitraryly high energy scale. A generic strong sector is however expected to quickly run to a weakly coupled regime at energies above the confinement scale and is therefore unable to generate sufficiently large anomalous dimensions over a large interval of energies. The coupling could remain large if above Λ the theory approaches to the fixed point thus becoming conformal.

In the rest of this work, we will adopt the paradigm of partial compositeness and will explore its implications for the CH phenomenology. In the next section, as a first necessary step, we will consider more closely the flavour physics following from the assumption of partial compositeness. But before doing this let us turn back to the Higgs potential. Given the requirement $G_{\rm SM} \subseteq H \subset G$, the linear couplings with SM fermions will break the goldstone symmetry and play a crucial role in a generation of the Higgs mass together with gauge fields. In fact the loops of gauge fields, if the gauged group is embeddable into H, tend to align the $\vec{f}$ in such a way that it doesn't break the gauge symmetry [21], in other words they fix $v_{\rm SM} = 0$. One of the ways out would be to introduce additional gauge fields in such a way that a new gauge group can not be embedded into H, so the gauge group will be broken in any case [34]. But in fact this is not strictly necessary since the elementary fermions introduce an unavoidable and large source of goldstone symmetry breaking (defined by $y\,\Delta_{I\,\alpha}$) which can easily push the Higgs VEV to a non-zero value. As follows from the eq. (1.4.9), the SM fermions with the highest mass have the largest y and hence introduce the largest source of the Goldstone symmetry breaking. Given this, the top quark and its composite partners will play the main role in EWSB. The implications of this relation will be considered in the Chapter 2.

1.4.2 Partial Compositeness and Flavour

After having discussed the main idea of the partial compositeness we want to consider in details its implications for the flavour structure. We said that one of the ways to generate a large hierarchy in fermionic sector relies on a difference in the anomalous dimensions of the operators coupled to the different SM families. Since the anomalous dimensions are mostly generated by the strong sector itself, it is plausible that one of the the sources of the breaking of the flavour symmetry resides inside

this sector. Therefore in the described picture composite resonances at low energies are not supposed to respect any flavour symmetry. For the phenomenological purposes it turns out that the flavour symmetry in a strong sector might be needed to successfully pass the experimental constraints. In this case one can give up on a described above simple explanation of the hierarchy by the anomalous dimensions, and leave it to some other unknown mechanism. As we have already mentioned, the scale at which this mechanism is at work can be arbitrarily high and corresponding physics can be decoupled from the one responsible for EWSB.

The most general flavour structure of the linear mixing term at high energies (Λ') is

$$\mathcal{L}^{\Lambda'}_{\text{pert}} = \bar{Q}^a \, y^{aA} \, \mathcal{O}^A \,, \tag{1.4.11}$$

where the index a runs over SM flavour eigenstates and A – over the strong sector operators. In general we need at least one strong sector operator for each SM (Dirac) fermion and a non-degenerate mixing matrix y. At least one of the types of SM multiplets (singlets or doublets) must acquire a hierarchical structure of the mixings in the IR. We could either assume that the mixings y^{aA} are already hierarchical at a scale Λ', or assume that they are of the same order and become hierarchical during RG evolution down to confinement scale Λ. For the second case it is easy to see that by a Q and $\mathcal{O}$ rotations the interaction (1.4.12) can be brought to a form in which only one quark species interacts with all the operators of the strong sector (and therefore with the one with a smallest scaling dimension), one quark species interacts with all the operators but one which has the smallest scaling dimension and so on. Hence we will arrive at the low-energy Lagrangian describing interactions between elementary states and composites with a hierarchical structure of mixing strengths y^{aA}

$$\mathcal{L}^{\Lambda}_{\text{pert}} = f \, \bar{Q}^a \, y^{aA} \, \psi^A \,, \tag{1.4.12}$$

where the index A now runs over composite multiplets, Q are now the states arranged according to the redefinition described above. We omitted the G and H indices for simplicity as well as insertions of the Goldstone matrix U.

Another possible leading order "flavour" structure is the mixing between the composite multiplets Y^{AB}. After integrating out heavy composites we can write down the SM fermion Yukawa matrices:

$$y^{ab} = y_L^{aA} f \, \frac{1}{m_\psi^A} \, Y^{AB} \, \frac{1}{m_\psi^B} \, y_R^{Bb} f \equiv \epsilon_L^{aA} \, Y^{AB} \, \epsilon_R^{Bb}, \tag{1.4.13}$$

where m_ψ^A – masses of composite fermions.

These matrices at low energies must reproduce the SM fermion masses as well as the CKM and PMNS mixing matrices. At this point we will summarize the main possibilities considered in the literature allowing to realize this.

Anarchic In this case one assumes that the "proto-Yukawa" matrices Y are non-hierarchical and non-diagonal with all the elements of similar size. The mixings of the left- and right-handed quarks are assumed to be hierarchical, hence:

$$\epsilon_q^3 \gg \epsilon_q^2 \gg \epsilon_q^1 \,, \qquad \epsilon_{u,d}^3 \gg \epsilon_{u,d}^2 \gg \epsilon_{u,d}^1 \,, \tag{1.4.14}$$

where we only put the SM family indices. Each elementary species can mix with all the strong sector flavours with a similar strength. With this assumptions one can easily show that the fermion mass

eigenstates are rotated by matrices of the form

$$L^{ab} \sim \min\left(\frac{\epsilon_q^a}{\epsilon_q^b}, \frac{\epsilon_q^b}{\epsilon_q^a}\right), \qquad R^{ab} \sim \min\left(\frac{\epsilon_{u,d}^a}{\epsilon_{u,d}^b}, \frac{\epsilon_{u,d}^b}{\epsilon_{u,d}^a}\right) \tag{1.4.15}$$

for the left- and right-handed fermions respectively. This is sufficient to reproduce the CKM matrix if one fixes the ratio $\epsilon_q^a/\epsilon_q^{a+1} \simeq s_c^a$ with $s_c = 0.23$ – the sine of the Cabibbo angle. One also has enough free parameters to fix the quark masses.

In order to reproduce the PMNS matrix, which is not hierarchical, and the hierarchy of the charged lepton masses it is sufficient to have a large hierarchy in the mixings of the charged leptons only. In addition the small mixings of the light generations automatically suppress the flavour-changing effects, for example four-fermion operators induced by composite vector resonances.

It turns that the anarchy has difficulties in passing the experimental constraints, in particular the ones coming from the the electron electric dipole moment and $\mu \to e\gamma$ decays [66] or kaon properties [121].

U(3) The suppression of the unwanted flavour-changing and CP-violating effects (especially in the leptonic sector) favours an alternative possibility – the strong sector is invariant under the flavour symmetry $U(3)$ and the only sources of flavour breaking are the mixings with elementary fermions [35]. The quark Yukawas are simply

$$y^{ab} = y_L^{aA} \frac{f}{m_\psi} y_R^{Ab}\,. \tag{1.4.16}$$

This allows to reduce a number of flavour structures in the theory and realize a Minimal Flavour Violation in different ways.

The first minimal option is to assume that only the right-handed mixings $y_R^{(u)}$ and $y_R^{(d)}$ carry the hierarchy and a flavour violation while the left-handed one $y_L^{(q)}$ is proportional to identity. The phenomenological challenge comes from the LEP precision measurements which require the left-handed compositeness of the light families (and hence of all the quarks) to be low. This brings difficulties in generating the large top mass.

The second option would be to make the right-handed mixings proportional to identity and make the left-handed mixings to generate the hierarchies. Clearly one left-handed mixing matrix $y_L^{(q)}$ can not generate six different quark masses and a non-trivial CKM matrix. In fact in some explicit models (for example with the elementary quarks embedded into fundamental of $SO(5)$) it is required that the left-handed quarks have two different embeddings Q_L^u and Q_L^d. Thus they will be accompanied by two independent mixing matrices $y_L^{(u)}$ and $y_L^{(d)}$ which allows to generate a viable mass spectrum. The large right-handed compositness needed to reproduce the top mass is however in some tension with results of the LHC searches for quark compositeness.

U(2) The tensions arising in the $U(3)$-symmetric models are first of all related to the fact that the top quark is in the same flavour multiplet with light generations. Thus they can be relaxed by assuming that flavour structures are at most $U(2)$ - symmetric [36] where the symmetry relates only first two generations of fermions.

In all the listed flavour patterns rather generically the couplings of the top quark to the strong sector are the largest ones. This means that they introduce the largest breaking of the Goldstone symmetry and hence are the most important SM fermions for the generation of the Higgs potential. The fermionic resonances coupled to the top quark by means of interaction (1.4.7), the *top partners*, therefore play a special role in the CH models. As we will show in the Chapter 2 their mass is tightly related to the mass of the Higgs boson and this relation requires them to be anomalously light.

1.5 Modelling Composite Higgs

1.5.1 Deconstructed Models

In the previous sections we discussed some general properties the composite Higgs models should have. These properties however do not define uniquely the theory and many of the important features are left unpredictable. As we will see in this section such important parameters as the Higgs VEV and mass in general case are dominated by divergent contributions which means that they are sensitive to the UV physics and not predictable within a general effective theory in the IR. If we *assume* that the contributions to the desired quantities are defined mostly by a physics below some scale Λ we can *impose* the calculability by requiring the coefficients of the divergent integrals to cancel. This approach though artificial from the first glance allowed to obtain a successful prediction for the QCD [37]. This result hints at a systematic procedure to achieve a calculability: add heavier composite states in the description until the desired quantities become computable and the theoretical predictions become comparable with observations.

An alternative option to achieve a calculability would be not to impose it directly but provide the structure which will automatically make the needed observables predictable. This is what one generically expects from a theory: an exact cancellation of certain combination of parameters must follow from its symmetry properties otherwise being a fine-tuning. Of course in this case one should make a choice of this symmetry structure and this will introduce some model dependence. In the case of the strong dynamics there are not many types of such calculable descriptions. It was first shown in [38] that the models described in the warped 5-dimensional space-time in the IR behave in a very similar way to how we expect the strongly coupled theories to behave. At the same time these 5D dual theories are formulated in purely weakly-coupled way and possess, for example, a computable Higgs potential. Thought this correspondence does not imply that any 5D theory possesses a consistent strongly coupled 4D dual theory, it provides a useful tool for understanding the possible strong dynamics.

As was shown in Ref. [39], the 5D theory can be "deconstructed": the theory with a continuous 5^{th} dimension can be approximated by a 4D theory with the discrete number of "sites". The intuitive understanding of the deconstruction can be given by the following considerations. From the 4D point of view the 5^{th} coordinate is just like an additional "quantum number": as quarks can be enumerated by their flavour, they can in addition be enumerated by the position along the 5^{th} coordinate. Therefore if in 5D we have n_q quarks, $rank[G_{5D}]$ vector bosons etc, from the 4D point of view we will have N copies ("sites") of them. Taking $N \to \infty$ we will approach to a continuous extra dimension while for $N \sim few$ it will look like a discrete approximation for it.

There is still one thing missing in our 4D imitation of a 5D theory. If we have a gauge group G_{5D} in the 5D there should also be an additional 5^{th} component of the 5D gauge vector fields,

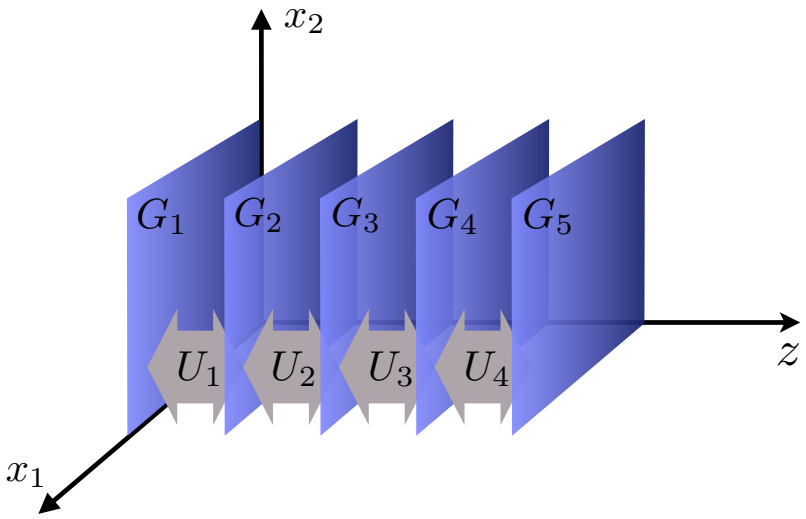

Figure 1.10: *Schematic representation of the structure of N-site models. G_i denote the 4-dimensional gauge groups, goldstone matrices U_i link neighbouring gauge symmetries. The coordinates x_1, x_2 stand for the set of 4D coordinates, while the z coordinate corresponds to a number of a site, or a 5^{th} coordinate in the 5D dual picture.*

which must be a scalar under 4D Lorentz transformations. Now let us remind that the gauge vector fields play a role of a "connection" – they compensate a difference in the gauge transformations between two neighbouring points. Therefore they must enter in a theory as scalar links between neighbouring sites. In addition the 5D gauge invariance forbids to write down a local potential for them (on the very short distances G_{5D} looks as unbroken). The perfect objects to describe these scalars are unitary matrices U_n, transforming from the left under the 4D gauge group of the n-th site and from the right - under the gauge group of the $(n+1)$-th site. This completes the construction schematically described on Fig. 1.10 : N sites, each with its own gauge group and fields transforming accordingly to it, connected to each other by means of unitary matrices $U_n = \exp(iT^a\Pi_n^a)$, where T^a - generators of the G_{5D}. This last ingredient strikingly resembles the composite Higgs which we described above. Indeed, some of these scalars will play a role of the Higgs field in our description, while the others will be "eaten" by the gauge fields to produce a tower of massive composite vector resonances. One can add that the 5D models typically contain some boundary conditions which can be reflected by modifying the particle content of the first and the last sites.

To make this discussion more quantitative, let us consider a 5D action on a flat background, with one compact dimension (with a metric diag$\{1,-1,-1,-1,-1\}$), for a fermionic field ψ coupled to a gauge vector field $A_M = \{A_\mu, A_5\}$, symmetric under some group G and propagating in a bulk:

$$\begin{aligned} S^{(5D)} &= \int d^4x \int \frac{dz}{L}\, i\bar{\psi}(D_M\gamma^M)\psi - \frac{1}{4}\mathrm{Tr}[F_{MN}F^{MN}] \\ &= \int d^4x \int \frac{dz}{L}\, i\bar{\psi}(D_\mu\gamma^\mu + D_5\gamma^5)\psi - \frac{1}{4}\mathrm{Tr}[F_{\mu\nu}F^{\mu\nu}] + \frac{1}{2}\mathrm{Tr}[F_{\mu 5}F^{\mu}{}_{5}] = \int d^4x\, \mathcal{L}^{(4D)}\,, \end{aligned} \tag{1.5.1}$$

where z is a 5^{th} coordinate, $D_N = \partial_N - ig_5A_N$ is a 5D covariant derivative, and the length of the 5^{th} dimension L was introduced explicitly to maintain the canonical 4D energy dimensions of the fields. Our goal is to explicitly discretize the z coordinate; instead of continuum of field variables

we will switch in the end to a discrete set of N sites:

$$z \to \Delta\, n, \quad \psi(x,z) \to \psi_n(x), \quad A_M(x,z) \to A_{M\,n}(x), \quad n \in \mathbb{Z}, \tag{1.5.2}$$

where Δ is a spacing between two neighbouring sites, $\Delta = L/(N-1) \simeq L/N$. First of all we can single out the terms of the 4D Lagrangian density, defined in Eq. (1.5.2), which give the 4D kinetic terms

$$\mathcal{L}^{(4D)} \supset \sum_{n=1}^{N} \frac{\Delta}{L}\, \bar{\psi}_n\, i\, D_\mu \gamma^\mu \psi_n - \frac{1}{4}\frac{\Delta}{L}\, \mathrm{Tr}[F^n_{\mu\nu} F^{n\,\mu\nu}]\,, \tag{1.5.3}$$

which after a fields redefinition $\psi_n \to \sqrt{N}\psi_n$, $A_{M\,n} \to \sqrt{N} A_{M\,n}$ become canonically normalized. With this redefinition the coupling constant appearing in the covariant derivatives is

$$g_4 = g_5 \sqrt{N}\,. \tag{1.5.4}$$

Now let us consider the interactions between different sites. The projection of the fermionic field of the n-th site on the one from the $n+1$-th site, accounting for the change of the field phase, is related with the following object:

$$\begin{aligned} \bar{\psi}(x,z)\, \mathcal{P} \exp\left[i \int_{z+\Delta}^{z} dz' A_5(x,z') \right] \psi(x, z+\Delta) &\simeq \bar{\psi}(x,z)\psi(x,z) + \Delta\, \bar{\psi}(x,z)\, \{\partial_5 - i\, A_5\}\, \psi(x,z) \\ &= \bar{\psi}(x,z)\psi(x,z) + \Delta\, \bar{\psi}(x,z)\, D_5\, \psi(x,z), \end{aligned} \tag{1.5.5}$$

where $\mathcal{P}$ is an ordering operator along the z direction and the coupling constant g_4 was omitted for brevity. The matrix linking two sites is a Wilson line, defined as

$$U(x; z, z+\Delta) = \mathcal{P} \exp\left[i \int_{z+\Delta}^{z} dz' g_5 \sqrt{N} A_5(x,z') \right], \quad U_n(x) = \exp\left[-i\, \Delta g_5 \sqrt{N} A_{5\,n}(x) \right] \tag{1.5.6}$$

in continuous and discrete cases respectively. Applying the equality (1.5.5) to the Lagrangian $\mathcal{L}^{(4)}$ of the Eq. (1.5.2), we obtain for the fermionic part after a chiral rotation [13]

$$\mathcal{L}^{(4D)}_{fermions} = \sum_{n=1}^{N} i\, \bar{\psi}_n D_\mu \gamma^\mu \psi_n + \frac{1}{\Delta} \bar{\psi}_n\, U_n\, \psi_{n+1} - \frac{1}{\Delta} \bar{\psi}_n\, \psi_n\,, \tag{1.5.7}$$

and for the gauge part after a similar substitution we have

$$\mathcal{L}^{(4D)}_{gauge} = \sum_{n=1}^{N} -\frac{1}{4}\mathrm{Tr}[F^n_{\mu\nu} F^{n\,\mu\nu}] + \frac{1}{2\Delta^2 g_4^2}\mathrm{Tr}|\partial_\mu U_n - i g_4\, A_{n\,\mu}\, U_n + i g_4\, U_n\, A_{n+1\,\mu}|^2\,. \tag{1.5.8}$$

This is a Lagrangian of the N-site model. It contains N copies of the fermionic and vector fileds, and is locally (in 4D) invariant under a product group G^N. The G^N is realized non-linearly, corresponding goldstone bosons are contained in the U_n matrices transforming as

$$U_n \to g_n\, U_n\, g^\dagger_{n+1}\,, \tag{1.5.9}$$

[13] In this formula we ignored the fact that Eq. (1.5.5) can not be applied for $n = N$, but in any case the behaviour of the first and the last sites is typically significantly affected by the boundary conditions which we do not discuss for the moment.

where g_n is a transformation belonging to the group G_n of the n-th site. Identifying the links $U_n = \exp\left[-i\,\Delta\, g_4\, A_{5\,n}\right]$ with Goldstone matrices $U_n^G = \exp\left[i\,\Pi_n/f\right]$, introduced in the Section 1.3.1, we can summarize the relation between the parameters of the two dual descriptions:

$$g_4 = \sqrt{N} g_5\,, \qquad f \sim \frac{\sqrt{N}}{g_5 L} = \frac{1}{g_4 \Delta}\,, \qquad m_{\psi,A} \sim \frac{N}{L} = g_4 f\,. \tag{1.5.10}$$

Though the 4D parameters scale with the N, the observed quantities weakly depend on N and have smooth limits for $N \to \infty$. For example the coupling of the gauge bosons corresponding to a diagonal unbroken combination of G^N is defined by g_5 and a mass gap between mass eigenstates – by $1/L$. The mass terms of the fermions can in general also receive contribution from explicitly introduced bulk masses, which we omitted for simplicity. By changing the local density of the discrete points, $\Delta \to \Delta(n)$, we can switch to the description of the 5D models with non-flat backgrounds. Though allowing to mimic the 5D in some specific cases, the deconstructed models are more flexible, allow for a larger number of free parameters to vary and require less particle content. Therefore from the point of view of the CH phenomenology they are very useful. Moreover the structure described by N-site models is not necessarily related to some consistent 5D models and can come as well from some unrelated 4D UV completions.

If in the lagrangian (1.5.7) we replace the fields on a first site with "elementary" SM fields (which can be seen as a boundary condition at $z = 0$), the model will remind a CH with partial compositness and several layers of composite resonances, sitting on the rest of the sites. In the next section, following the Ref. [40] we will introduce the "Discrete Composite Higgs Model" (DCHM), a specific realization of N-site models, and show which are the minimal ingredients needed to achieve the calculability of the Higgs potential.

1.5.2 Higgs Potential

The Higgs boson realized as a fifth component of the gauge fields propagating in the 5-dimensional bulk possesses a calculable potential. Our goal here is to find a minimal number of ingredients needed to reproduce this feature in the N-site models. In order to understand whether the potential is finite (weakly sensitive to UV physics) or not we will use a power counting defined by the Eq. (1.3.33) derived in the Section 1.4.1, where we will take Λ as the scale of the composite resonances which are not accounted for in our description.

Since the Higgs is protected by a Goldstone symmetry, the operator responsible for its mass generation must contain the symmetry breaking parameters. In the CH models with partial compositeness the minimal set of such parameters are the SM gauge couplings and the elementary-composite fermions mixings. Of course since we are talking about a Higgs mass, these parameters can only enter in it via loops involving SM elementary fields and therefore the corresponding operator must contain at least two powers of mixings or gauge couplings.

Let us first do some simple estimates of the Higgs mass using the minimal set of ingredients. From the simplest CCWZ interaction Lagrangian (1.3.15) for the Higgs and gauge bosons we obtain a quadratically divergent contribution to the Higgs mass:

$$\delta m^2_{h\,(gauge)} \sim \frac{g^2}{16\pi^2} m_\rho^2\,, \tag{1.5.11}$$

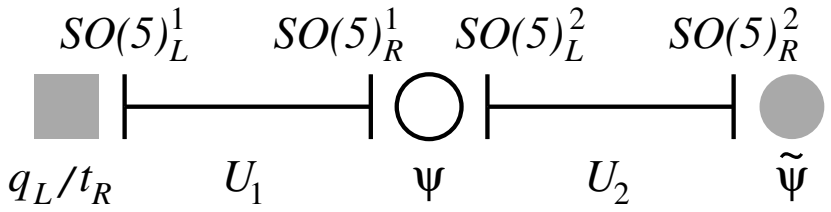

Figure 1.11: *Schematic structure of the three-site DCHM.*

where m_ρ is a characteristic scale of the heavy vector resonances saturating the Higgs potential. Using the simple Yukawa Lagrangian (1.4.7) we can also estimate the size of the fermionic contribution:

$$\delta m^2_{h\,(fermions)} \sim \frac{3y_t}{16\pi^2} m^2_\psi \,, \tag{1.5.12}$$

where m_ψ is a scale of fermionic resonances saturating the Higgs potential. As we see due to the large Yukawa coupling of the top quark and a color factor the fermionic contribution is expected to be dominant if the scales m_ψ and m_ρ are comparable. The power divergence of the Higgs potential means that it must be strongly sensitive to at least the first heavy states, therefore, in order to obtain some reliable predictions about it, we will need to specify the structure of the lowest-level composite resonances.

If we were not required to put SM gauge fields or fermion mixings in a loop (but still somehow being allowed to generate a Higgs mass) the degree of divergence would formally be Λ^4, hence one goldstone symmetry protection lowered the divergence by two powers. The resulting degree of divergence could be even lower if the Higgs mass was protected simultaneously by several symmetries such that only breaking of all of them ("collective breaking") together would allow for a Higgs mass. More precisely, if each symmetry protection lowers the divergence by two as happened now, we would need three symmetries to make the Higgs mass finite (remember that if the formula (1.3.33) gives no dependence on Λ but $\#_{loops} = 1$, the coefficient of the operator is log-divergent).

3-site model

The triple symmetry protection can be naturally realized in a 3-site model. Since it provides a usefull tool for testing the CH idea and will be intensively used in the following chapters, we will provide a detailed description of it. Its structure is summarized on Fig. 1.11. The global symmetry of the 3-site model can be seen as $\mathcal{G}_{3s} = SO(5)_1 \times SO(5)_{2L} \times SO(5)_{2R} \times SO(5)_3$. While the gauged subgroup is $G_{SM} \times [SO(5)_{2L} \times SO(5)_{2R}]_V \times SO(4)$: we gauge a SM subgroup on the first site, the diagonal combination of $SO(5)_{2L} \times SO(5)_{2R}$ on the second site and an $SO(4)$ subgroup on the third site. The SM is embedded into $SU(2)_L \times SU(2)_R \sim SO(4) \subset SO(5)$.

Three sites can only communicate via interactions with link fields U_1 and U_2 defined as

$$U_i = e^{i\sqrt{2}\,\Pi^A_i T^A/f} \,, \tag{1.5.13}$$

where T^A are the $SO(5)$ generators. The transformation properties of goldstone matrices under the global symmetries can be summarized as:

$$\begin{aligned} U_1 &\to g_{SO(5)_1}\; U_1\; g^t_{SO(5)_{2L}} \\ U_2 &\to g_{SO(5)_{2R}}\, U_2\; g^t_{SO(5)_3} \end{aligned} \tag{1.5.14}$$

Each U matrix contains 10 scalar degrees of freedom corresponding to the spontaneous breaking of the pair of $SO(5)$ to their diagonal subgroup.

Apart from the mentioned symmetries the fermions are charged under additional $U(1)_X$ group, for simplicity we don't introduce three copies of it and assume that it acts on all three sites in the same way, and associated gauge vector field is B_μ. The same field gauges the T^3_R generator of the $SU(2)_R$ subgroup on the first site providing that the hypercharge is defined by $T^3_R + X$. The X-charge was introduced in order to be able to reproduce the correct hypercharges of the SM fermions. We will only include the SM quarks of the third generation ($q_L = \{t, b\}_L$ and t_R) and their composite partners since their mixings provide a dominant goldstone symmetry breaking effect. The choice of the representation for the fermionic fields is ambiguous, we will choose the simplest one – a fundamental **5** of $SO(5)$. The **5** decomposes under $SO(4)$ as a bidoublet plus a singlet, and under $SU(2)_L$ as two doublets with $T^3_R = \pm 1/2$ and a singlet. Therefore if we embed q_L into the doublet with $T^3_R = -1/2$, the bottom quark will be invariant under exchange of left and right isospin quantum numbers. This property allows to eliminate large tree-level correction to the Zb_Lb_L vertex [41]. The t_R in this case can only be embedded as a singlet of $SO(4)$.

The $SO(5)$ and $SO(4)$ generators are given in the appendix of this chapter. With these definitions we are now able to discuss the particle content of each site:

- The **first site** (the "UV brane" if we make an analogy with 5d RS models) has a SM gauge symmetry G_{SM} embedded into the $SO(5)\times U(1)_X$ and a set of SM fermions embedded into the fundamental representation of the $SO(5)$. The Lagrangian is just the SM Lagrangian without a Higgs field:
$$\mathcal{L}_1 = i\,\bar{q}_L \not{D}^{(A)} q_L + i\,\bar{t}_R \not{D}^{(A)} t_R - \frac{1}{4}\mathrm{Tr}\left[F^{(A)}_{\mu\nu} F^{(A)\,\mu\nu}\right], \tag{1.5.15}$$
where $D^{(A)}$ and $F^{(A)}$ are a covariant derivative and the field strength for the "elementary" gauge fields A_μ. Embedding of the SM fields q_L and t_R into $SO(5)$ is the following:
$$q^{\mathbf{5}}_L = \frac{1}{\sqrt{2}}\begin{pmatrix} b_L \\ -i\,b_L \\ t_L \\ i\,t_L \\ 0 \end{pmatrix}_{2/3}, \qquad t^{\mathbf{5}}_R = i\begin{pmatrix} 0 \\ 0 \\ 0 \\ 0 \\ t_R \end{pmatrix}_{2/3} \tag{1.5.16}$$
where the subscript denotes the X-charge.

- The **middle site** of the model (the "bulk") possesses a gauged $SO(5)$ symmetry with associated 10 gauge bosons ρ and a fermionic field ψ transforming as a fundamental of the SO(5):
$$\mathcal{L}_2 = i\,\bar{\psi}\not{D}^{(\rho)}\psi - \frac{1}{4}\mathrm{Tr}\left[F^{(\rho)}_{\mu\nu} F^{(\rho)\,\mu\nu}\right] - m\,\bar{\psi}\psi\,, \tag{1.5.17}$$
where $D^{(\rho)}$ and $F^{(\rho)}$ are a covariant derivative and the field strength for the "composite" fields ρ_μ, and the fermionic field ψ can be written in terms of T^3_L and T^3_R eigenstates as
$$\psi = \frac{1}{\sqrt{2}}\begin{pmatrix} B' - {X_{5/3}}' \\ -i\,B' - i\,{X_{5/3}}' \\ T' + {X_{2/3}}' \\ i\,T' - i\,{X_{2/3}}' \\ \sqrt{2}\,i\,\widetilde{T}' \end{pmatrix}_{2/3}, \tag{1.5.18}$$

where the X-charge assignment is dictated by a need to mix this multiplet with the one on the first site. The fundamental representation of SO(5) decomposes as $\mathbf{5} = (\mathbf{2},\mathbf{2}) \oplus (\mathbf{1},\mathbf{1})$ and the bidoublet $(\mathbf{2},\mathbf{2})$ contains, apart from the SM-like massive fermionic doublet $\{T', B'\}$, an $SU(2)_L$ doublet $\{X_{5/3}', X_{2/3}'\}$ with electric charges $\{5/3, 2/3\}$.

- The **third site** (the "IR brane") has a gauged $SO(4)$ symmetry with associated 6 gauge vector bosons $\tilde{\rho}$ and two fermionic multiplets: the four-plet and a singlet of the $SO(4)$ which can be written together in a form of the full five-plet $\tilde{\psi}$ defined analogously to ψ

$$\tilde{\psi} = \frac{1}{\sqrt{2}} \begin{pmatrix} B - X_{5/3} \\ -i\,B - i\,X_{5/3} \\ T + X_{2/3} \\ i\,T - i\,X_{2/3} \\ \sqrt{2}\,i\,\widetilde{T} \end{pmatrix}_{2/3} . \tag{1.5.19}$$

The lagrangian reads

$$\mathcal{L}_3 = i\,\bar{\tilde{\psi}} \not{D}^{(\tilde{\rho})} \tilde{\psi} - \frac{1}{4}\mathrm{Tr}\left[F_{\mu\nu}^{(\tilde{\rho})} F^{(\tilde{\rho})\,\mu\nu}\right] - \bar{\psi}\,\widetilde{m}\,\psi\,, \tag{1.5.20}$$

with an $SO(4)$-symmetric mass matrix $\widetilde{m} = \mathrm{diag}\{m_4, m_4, m_4, m_4, m_1\}$.

The **links** between three sites are realized via interactions with U_i matrices:

$$\begin{aligned} \mathcal{L}_{1\leftrightarrow 2} &= \frac{f^2}{4}\mathrm{Tr}\,|\partial_\mu U_1 - ig\,A_\mu\,U_1 + ig_\rho\,U_1\,\rho_\mu|^2 - \left(y_L\,f\,\bar{q}_L^{\mathbf{5}}\,U_1\,\psi_R + y_R\,f\,\bar{t}_R^{\mathbf{5}}\,U_1\,\psi_L + h.c.\right)\,, \\ \mathcal{L}_{2\leftrightarrow 3} &= \frac{f^2}{4}\mathrm{Tr}\,|\partial_\mu U_2 - ig_\rho\,\rho_\mu\,U_2 + ig_{\tilde{\rho}}\,U_2\,\tilde{\rho}_\mu|^2 - \left(\Delta\,\bar{\psi}\,U_2\,\tilde{\psi} + h.c.\right)\,. \end{aligned} \tag{1.5.21}$$

We will briefly summarize the main properties of the mass spectrum of the theory. The 16 gauge bosons become massive absorbing 16 out of 20 scalars incorporated in the U matrices. Their masses are

$$m_{\rho,\tilde{\rho}} \sim g_{\rho,\tilde{\rho}}\,f. \tag{1.5.22}$$

The 4 remaining scalars play a role of the Higgs doublet. The vectorial combination of the three $SU(2)_L \times U(1)_{T_R^3}$ gauge symmetries remains unbroken if the Higgs VEV is zero and plays a role of the SM gauge group (up to $U(1)_X$). The massless top quark from the first site becomes massive and "partially composite" after EWSB following the mechanism described in Section 1.4.1, with a mass

$$m_t \sim y_L\,y_R\,v, \tag{1.5.23}$$

while the other fermions from the second and the third sites have a mass of the order of their initial masses m, m_4 and m_1.

Higgs potential in the 3-site model

The scalar fields encoded in U_1 are the Nambu-Goldstone bosons associated to the breaking of the product-group $SO(5)_1 \times SO(5)_{2L}$ to its diagonal subgroup, and analogously for U_2 and $SO(5)_{2R} \times SO(5)_3$ group. Therefore the scalar potential must be induced by the explicit breaking of the global symmetry $\mathcal{G}_{3s}$. Let us classify the parameters that break the global symmetries of the model:

- $\{y_L,\, y_R,\, g,\, g'\} \equiv \not{G}_1$ – couplings of the U_1 to the non-$SO(5)_1$ invariant fields. Act on U_1 from the left.
- $\{m,\, g_\rho\} \equiv \mathbb{1}_{\not{G}}$ – break $SO(5)_{2L} \times SO(5)_{2R}$ to its diagonal combination. Can act on both U_1 (from the right) and U_2 (from the left).
- $\{\Delta,\, \widetilde{m},\, g_{\tilde{\rho}}\} \equiv \not{G}_2$ – couplings of the U_2 to the non-$SO(5)_3$ invariant fields. Act on U_2 from the right.

We will now show how the triple protection works. Let us suppose that some combination of the fourth components of the Π_1 and Π_2, which corresponds to a Higgs boson, gets a non-zero VEV. If any of the three breaking sources listed above are taken to zero, by rotations corresponding to exact global symmetries one would be able to rotate away the Higgs VEV in such a way that the theory is equivalent to the one with VEV $= 0$. If the $\not{G}_1 = 0$ one can use the unbroken vector combination of $SO(5)_{2R}$ and $SO(5)_{2L}$ to remove the VEV of Π_2 to the U_1, and then remove all the VEV dependence from the U_1 by the unbroken global $SO(5)_1$. Analogous mechanism will work if the breaking on the third site is absent ($\not{G}_2 = 0$). If we don't gauge the vector combinations of $SO(5)_{2L} \times SO(5)_{2R}$ at the middle site, both $\langle \Pi_1 \rangle$ and $\langle \Pi_2 \rangle$ can be removed by unbroken $SO(5)_{2L}$ and $SO(5)_{2R}$ respectively. It is trivial to show that if more than one breaking sources are absent the Higgs VEV can also be eliminated.

Now to estimate the Higgs potential we just need to write down an operator including the goldstone matrices U_i and containing no other external fields nor derivatives, and all the breaking sources. Given the above list of spurions and the way they interact with goldstone matrices (from the left or from the right) one can easily realize that the shortest chain relevant for the Higgs potential is of the form:

$$\mathcal{O} = \not{G}_1\, U_1\, \mathbb{1}_{\not{G}}\, U_2\, \not{G}_2. \tag{1.5.24}$$

The corresponding contribution to the Higgs potential can be estimated according to the power counting formula (1.3.33)

$$V \supset \frac{1}{16\pi^2 \Lambda^2} \mathrm{Tr}[\mathcal{O}\mathcal{O}^t]. \tag{1.5.25}$$

Any shorter combination than a $\mathrm{Tr}[\mathcal{O}\mathcal{O}^t]$ will lead to a vanishing dependence on U_i.

Therefore three sites provide a sufficient structure to make a Higgs potential calculable at one loop. Adding more sites will provide a finiteness of several-loop correction. In fact, as was demonstrated in Ref. [40] the gauge sector does not bring contributions of the form (1.5.25) and the leading operator is even further suppressed, while the leading fermionic contribution agrees with our formula (1.5.25). If we decrease the number of sites, which is equivalent to sending the masses of one or both layers of the composite states to the cutoff ($m \to \Lambda, g_\rho \to \Lambda/f$), we will recover a logarithmic or quadratic divergence respectively.

1.5.3 Relation with CCWZ

We have just discussed a three-site model in which the the Higgs field arises from two σ-model fields, each corresponding to the breaking $SO(5)_L \times SO(5)_R \to SO(5)_V$. Now we want to show that this model represents a special case of the general $SO(5) \to SO(4)$ CCWZ construction described in the Section 1.2. We will perform the full demonstration with a simpler model – the two-site model

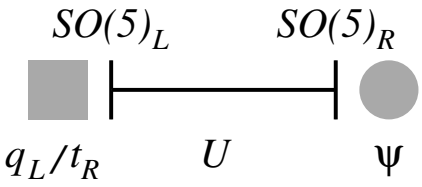

Figure 1.12: *Schematic structure of the two-site DCHM.*

(Fig. 1.12). It can be obtained from the three-site model by taking away the middle site and is described by Lagrangians $\mathcal{L}_1$ and $\mathcal{L}_3$ from the previous section. The elementary-composite mixings are then described by the Lagrangian $\mathcal{L}_{1\leftrightarrow 2}$ in Eq. (1.5.21) after a substitution $\psi \to \tilde{\psi}$. Explicitly the Lagrangian of the two-site model reads:

$$\begin{aligned}
\mathcal{L}_1 &= i\,\bar{q}_L \not{D}^{(A)} q_L + i\,\bar{t}_R \not{D}^{(A)} t_R - \frac{1}{4}\mathrm{Tr}\left[F^{(A)}_{\mu\nu} F^{(A)\,\mu\nu}\right] \\
\mathcal{L}_{1\leftrightarrow 2} &= \frac{f^2}{4}\mathrm{Tr}\left|\partial_\mu U_1 - ig\,A_\mu\,U_1 + ig_\rho\,U_1\,\rho_\mu\right|^2 - \left(y_L\,f\,\bar{q}^{\mathbf{5}}_L\,U_1\,\psi_R + y_R\,f\,\bar{t}^{\mathbf{5}}_R\,U_1\,\psi_L + h.c.\right) \\
\mathcal{L}_2 &= i\,\bar{\psi}\not{D}^{(\rho)}\psi - \frac{1}{4}\mathrm{Tr}\left[F^{(\rho)}_{\mu\nu} F^{(\rho)\,\mu\nu}\right] - \bar{\psi}\,m\,\psi\,,
\end{aligned} \tag{1.5.26}$$

where we omitted all the tilde symbols since now we have only one layer of composite resonances. The global symmetry structure now is $\mathcal{G}_{2s} = SO(5)_1 \times SO(5)_2$ with $G_{SM} \times SO(4)$ subgroup gauged. In contrast to the three-site model, the Higgs field features only a double symmetry protection, therefore the Higgs mass in the two-site model receives logarithmically divergent contribution, but after fixing the VEV with a counterterm becomes calculable.

As a first step it will be convenient to make a preliminary gauge fixing, eliminating the 6 scalar degrees of freedom corresponding to $SO(4)$ generators T^a from the U_1 matrix by a field-dependent $SO(4)$ rotation. As a result the gauge-fixed U_1 becomes equal to the defined in the eq. (1.3.1) Goldstone matrix $U = e^{i\sqrt{2}\,\Pi^{\hat{a}}_i T^{\hat{a}}/f}$, where $T^{\hat{a}}$ are $SO(5)/SO(4)$ generators. Using the definitions of the d and e symbols (1.3.12) we can rewrite the vectorial part of the $\mathcal{L}_{1\leftrightarrow 2}$ as

$$\mathcal{L}_{1\leftrightarrow 2} \supset \frac{f^2}{4}\mathrm{Tr}\left|U^t\partial_\mu U - ig\,U^t\,A_\mu\,U + ig_\rho\,\rho_\mu\right|^2 = \frac{f^2}{4}\left(e_\mu + g_\rho\,\rho_\mu\right)^{a\,2} + \frac{f^2}{4}d^{\hat{a}\,2}_\mu\,, \tag{1.5.27}$$

where a and $\hat{a}$ are $SO(4)$ and $SO(5)/SO(4)$ indices respectively. In the Section 1.3.1 we did not include any composite vector resonances in the CCWZ description, though in principle this is possible. Therefore in order to establish the connection with results of the Section 1.3.1 we will integrate out the vectorial resonances of the second site. At tree level this can be done by substituting their equations of motion to the Lagrangian. The equations of motion for the vectors (neglecting their momentum compared to mass) read:

$$g_\rho\,\rho^a_\mu = -\left(e_\mu + \frac{2}{f^2}J_\mu\right)^a \tag{1.5.28}$$

where J^a_μ is a current of second site fermions $\bar{\psi}\,\gamma_\mu\,T^a\,\psi$. The substitution of the Eq. (1.5.28) does

not modify the first site lagrangian $\mathcal{L}_1$, while for the link and the second site we find

$$\begin{aligned}\mathcal{L}_{1\leftrightarrow 2}+\mathcal{L}_2 \;=\; & \frac{f^2}{4}d_\mu^{\hat{a}\,2}-\frac{c_{4f}}{f^2}J_\mu^{a\,2}-\left(y_L\,f\,\bar{q}_L^{\mathbf{5}}\,U\,\psi_R+y_R\,f\,\bar{t}_R^{\mathbf{5}}\,U\,\psi_L+h.c.\right)\\ & +i\bar{\psi}\left(\partial_\mu+ie_\mu^a T^a\right)\gamma^\mu\psi-\frac{c_f}{4g_\rho^2}\,f^a_{\mu\nu}f^{a\,\mu\nu}\,,\end{aligned}\tag{1.5.29}$$

where we defined $f^a_{\mu\nu}=\partial_\mu e^a_\nu-\partial_\nu e^a_\mu-g_\rho\,f^a_{bc}\,e^b\,e^c$ with f^a_{bc} – $SO(4)$ structure constants, and $c_{4f}=c_f=1$. If we wanted to build a theory with a spontaneous $SO(5)\to SO(4)$ symmetry breaking following the rules of CCWZ and a power counting, assuming partial compositeness and a presence of one composite fermionic four-plet and one singlet we would reconstruct all the terms in the lagrangians (1.5.29). There will be some difference however. First of all, from the power counting one would not be able to fix the coefficients $c_{4f}=c_f=1$ and could only tell that they should be of the order 1 and can have any sign. Second, following the CCWZ we would obtain additional leading-order terms in the composite lagrangian, such as:

$$c_d\,\bar{\psi}^a\,d^a_\mu\,\gamma^\mu\,\psi^5,$$

$$\frac{c'_{4f}}{f^2}\left[\bar{\psi}^5_{c_1}\,\gamma_\mu\,\psi^5_{c_1}\right]\left[\bar{\psi}^5_{c_2}\,\gamma^\mu\,\psi^5_{c_2}\right],\;\frac{c''_{4f}}{f^2}\left[\bar{\psi}^5_{c_1}\,\gamma_\mu\,\psi^5_{c_2}\right]\left[\bar{\psi}^5_{c_2}\,\gamma^\mu\,\psi^5_{c_1}\right],\;\frac{c'''_{4f}}{f^2}\left[\bar{\psi}^i\,\gamma_\mu\,T^a_{ik}\,\psi^l\right]\left[\bar{\psi}^j\,\gamma^\mu\,T^a_{jl}\,\psi^k\right],\;\ldots$$

where a is an $SO(4)$ index and c_i are color indices. Finally, the composite five-plet ψ entering the elementary-composite mixings could be split in a four-plet and a singlet, each with independent coefficient. Therefore we see that a two-site CH model below the mass of the vector resonances corresponds to a CCWZ construction with $c_f=1$, $c_{4f}=1$ and $c_d=c'_{4f}=c''_{4f}=c'''_{4f}=0$.

We would come to a similar result after gauge fixing and integrating out the gauge resonances from the three-site model: it will be a particular case of a CCWZ construction for two layers of composite fermionic resonances ψ and $\tilde{\psi}$. Hence the CCWZ is a useful and a general framework allowing to reproduce different specific models of composite Higgs, which however in the most general case does not provide a calculability of certain observables in contrast to the specific models.

1.6 Confronting Composite Higgs with Experiment

The composite Higgs models provide a large number of new phenomena compared to the SM and predict deviations in the processes existing in the Standard Model. We will provide a brief survey of the possible places to search for the Higgs compositeness. Typically any of this manifestations alone can not unambigously point at the compositeness, but combined together they can provide an evidence for it. All the phenomena listed below are related with the implications of the new strong dynamics below its confinement scale $\Lambda\sim 10$ TeV since it is too large to be reached exprerimentally in the near future.

Higgs partial widths and production cross section

Despite the presence of additional relatively light fermions (as will be explained in the Chapter 2) the Higgs production via gluon-gluon fusion and decay widths to $\gamma\gamma$, ZZ or WW are expected to be only weakly modified compared to the SM [42] and independent on the absolute scale of masses of the composite resonances. As we already mentioned in the section 1.3.1, the interactions of the Higgs

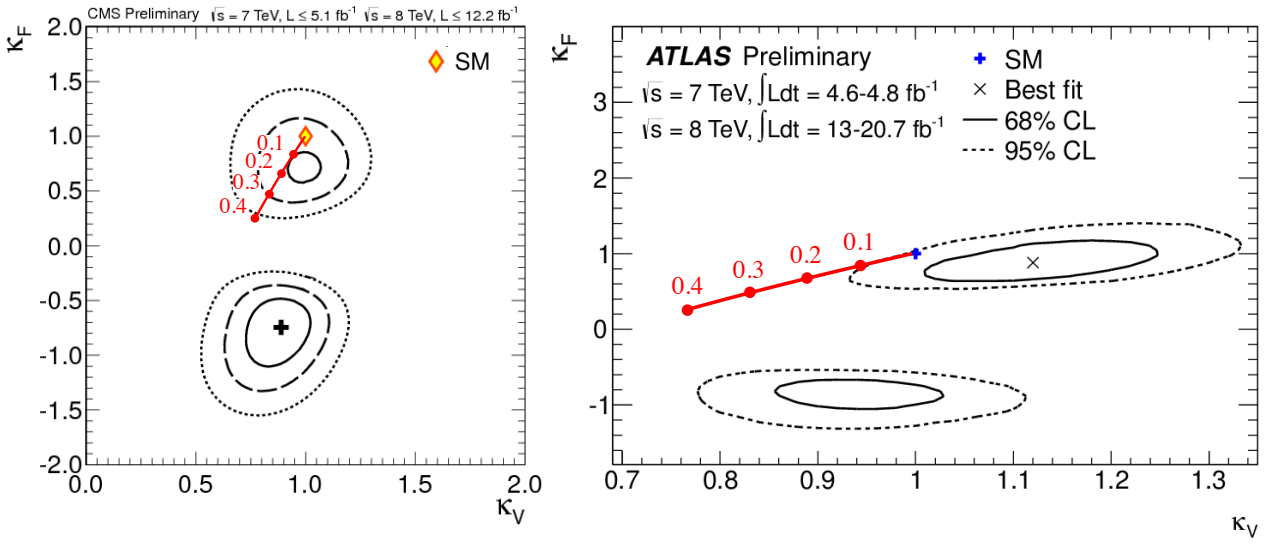

Figure 1.13: *Fits of the modifications of the Higgs couplings based on 7 and 8 TeV data presented by the CMS (left panel) and the ATLAS (right panel) collaborations. For the left plot contours correspond to 68%, 95% and 99% CL. Red trajectories correspond to the CH model with elementary quarks embedded in a* **5** *of* $SO(5)$ *with* ξ *varying from 0 to 0.4.*

and massive gauge bosons in the $SO(5)/SO(4)$ case are all rescaled by the same factor compared to SM values

$$k_V = \cos\frac{\langle h\rangle}{f} = \sqrt{1-\xi}\,. \tag{1.6.1}$$

The rescaling of the SM Yukawa interactions depends on the fermionic embeddings, for the case of **5** of $SO(5)$ we find from the Lagrangian (1.5.26)

$$k_F = \frac{1-2\xi}{\sqrt{1-\xi}} + \mathcal{O}\left(\frac{yv}{m_\psi}\right), \tag{1.6.2}$$

where the mass-dependent correction is typically irrelevant for the states lighter than the top quark. In the SM the effective $H\gamma\gamma$ and Hgg vertices are generated by loops with SM states (mostly the top and the W boson), but in the CH models also the composite resonances will run in loops, in particular the top partners, which are expected to be relatively light. The peculiar structure of Yukawa matrices in the case of partial compositeness can ensure the absence of the dependence of $H\gamma\gamma$ and Hgg couplings on the absolute mass scale of the top partners in the leading order in ξ. For the reference two-site model (1.5.26) the resulting fermionic contribution is rescaled by a factor $k_F^{g,\gamma} = 1 - \frac{3}{2}\xi$ [45], which coincides with k_F up to $\mathcal{O}\left(\frac{y}{m}, \xi\right)$ corrections. This allows us to use the results of the fits (see Fig. 1.13) for k_F and k_V which assume that Hgg and $H\gamma\gamma$ are rescaled respectively as k_F and $\alpha_{SM}k_F - \beta_{SM}k_V$. For the moment the two fits presented by experimental collaborations differ significantly, the CMS results allow for $\xi \lesssim 0.4$ while the ATLAS data point at $\xi \lesssim 0.2$.

Another possible bosonic decay channel, $H \to Z\gamma$, in contrast to the ones discussed above, can receive sizable corrections with respect to the SM predictions without conflicting with other observables [43], like the ones of the EWPT, but the experimental sensitivity in this case is for the moment quite poor [44]. Apart from the standard production channels the CH models allow for

instance for an enhanced double Higgs production [46] or for a Higgs production from composite fermions decays [48].

Longitudinal vector boson scattering at high energies

As was shown in the Section 1.2 the couplings of the composite Higgs to the W and Z boson are generically decreased. Therefore the Higgs will not unitarize the gauge boson scattering which will grow with the energy providing a deviation from the SM predictions [46, 47], though detecting this growth is experimentally challenging given that the deviations of the Higgs couplings with gauge bosons are already strongly constrained from indirect measurements [49, 50].

Multiple Higgs production

Detecting the production of two or three Higgs bosons can give a very important information about the nature of the EWSB sector of a theory, but these processes are very difficult to test and the valuable information might only come with a new particle collider [47].

Direct production of composite resonances

One of the main predictions of Composite Higgs models – new heavy composite resonances interacting with SM fermions and bosons. Vectorial resonances with electroweak quantum numbers are supposed to have a relatively high mass $\gtrsim 2.5$ TeV due to the constraints on S-parameter, and current experimental analyses have already approached this bound [47] (for experimental analyses see for example [51]).

As will be argued in the Chapter 2, probably the most promising new particles for a direct detection are composite fermionic resonances. The 13−14 TeV LHC will be able to probe their masses up to ~ 1.5 TeV [52, 53] and current experimental searches already started squeezing the region of masses preferred by the naturalness considerations. A general framework for the phenomenological studies of the top partners will be discussed in the Chapter 3 as well as implications of the latest LHC results. As we will see, even the region with $\xi = 0.2$ is already significantly constrained by direct searches.

SM fermions production rates

The partially composite fermions will generically interact via four-fermion contact interactions (see Fig. 1.9), therefore one can expect to see some deviations from the SM predictions for example in the searches for the dijets [54, 55]. These searches allow to put some non-trivial constraints on CH models, but typically are not very powerful.

Deviations of the flavour and EWPT observables

The current fits of the ElectroWeak Precision Tests parameters and flavour physics favours the SM, while the CH models generically predict deviations from them but still are capable to pass the constraints with a moderate amount of tuning, $\xi \lesssim 0.2$ (for a detailed discussion of EWPT see Chapter 4). The improvement of the experimental precision in this area could be a competitive

(though indirect) way to constrain the CH models and decrease their viability or, conversely, provide a support for them in a case if some anomalies are observed (see for example [56, 64]).

1.7 Appendix: Explicit CCWZ Construction for $SO(5)/SO(4)$

Generators and Goldstone Matrix

The generators of SO(5) in the fundamental representation are conveniently chosen to be

$$(T^{\alpha}_{L,R})_{IJ} = -\frac{i}{2}\left[\frac{1}{2}\varepsilon^{\alpha\beta\gamma}\left(\delta^{\beta}_{I}\delta^{\gamma}_{J} - \delta^{\beta}_{J}\delta^{\gamma}_{I}\right) \pm \left(\delta^{\alpha}_{I}\delta^{4}_{J} - \delta^{\alpha}_{J}\delta^{4}_{I}\right)\right], \tag{1.7.1}$$

$$T^{i}_{IJ} = -\frac{i}{\sqrt{2}}\left(\delta^{i}_{I}\delta^{5}_{J} - \delta^{i}_{J}\delta^{5}_{I}\right), \tag{1.7.2}$$

where $T^{\alpha}_{L,R}$ ($\alpha = 1,2,3$) are the $\mathrm{SO}(4) \simeq \mathrm{SU}(2)_L \times \mathrm{SU}(2)_R$ unbroken generators, while T^{i} ($i = 1,\dots,4$) are the broken ones and parametrize the coset SO(5)/SO(4). An equivalent notation for unbroken generators which we will use is T^{a} with $a = 1,\dots,6$. The indices IJ take the values $1,\dots,5$. The normalization of the T^{A}'s is chosen as $\mathrm{Tr}[T^{A},T^{B}] = \delta^{AB}$.

The T^{α}_{L} and T^{α}_{R} generators span respectively the $\mathrm{SU}(2)_L$ and $\mathrm{SU}(2)_R$ subgroups, and obey the standard commutation relations

$$\left[T^{\alpha}_{L,R}, T^{\beta}_{L,R}\right] = i\varepsilon^{\alpha\beta\gamma}\, T^{\gamma}_{L,R}\,. \tag{1.7.3}$$

The T_L's are therefore identified as the generators of the SM $\mathrm{SU}(2)_L$. Notice that in our parametrization the unbroken T^{a}'s are block-diagonal

$$T^{a} = \begin{pmatrix} t^{a} & 0 \\ 0 & 0 \end{pmatrix}, \tag{1.7.4}$$

and the generators obey the following commutation relation

$$\left[T^{a}, T^{i}\right] = (t^{a})_{ji}\, T^{j}\,. \tag{1.7.5}$$

With these generators, the parametrization of the Goldstone boson matrix is explicitly given by

$$U = U(\Pi) = \exp\left[i\frac{\sqrt{2}}{f}\Pi_i T^{i}\right] = \begin{pmatrix} \mathbf{1}_{4\times4} - \frac{\vec{\Pi}\vec{\Pi}^{T}}{\Pi^{2}}\left(1-\cos\frac{\Pi}{f}\right) & \frac{\vec{\Pi}}{\Pi}\sin\frac{\Pi}{f} \\ -\frac{\vec{\Pi}^{T}}{\Pi}\sin\frac{\Pi}{f} & \cos\frac{\Pi}{f} \end{pmatrix} \tag{1.7.6}$$

where $\Pi^{2} \equiv \vec{\Pi}^{t}\vec{\Pi}$. Under $g \in \mathrm{SO}(5)$, the Goldstone matrix transforms as

$$U(\Pi) \;\to\; U(\Pi^{(g)}) = g \cdot U(\Pi) \cdot h^{t}(\Pi; g)\,, \tag{1.7.7}$$

where $h(\Pi; g)$ is block-diagonal in our basis

$$h = \begin{pmatrix} h_4 & 0 \\ 0 & 1 \end{pmatrix}, \tag{1.7.8}$$

with $h_4 \in \mathrm{SO}(4)$. Under the unbroken SO(4) the Π's transform *linearly*, using eq. (1.7.5) we get $\Pi^i \to (h_4)^i{}_j \Pi^j$. Given our embedding of the SM group, the Π four-plet can be rewritten as

$$\vec{\Pi} = \begin{pmatrix} \Pi_1 \\ \Pi_2 \\ \Pi_3 \\ \Pi_4 \end{pmatrix} = \frac{1}{\sqrt{2}} \begin{pmatrix} -i\,(h_u - h_u^\dagger) \\ h_u + h_u^\dagger \\ i\,(h_d - h_d^\dagger) \\ h_d + h_d^\dagger \end{pmatrix} , \tag{1.7.9}$$

where

$$H = \begin{pmatrix} h_u \\ h_d \end{pmatrix} , \tag{1.7.10}$$

is the standard Higgs doublet of $+1/2$ Hypercharge.

In the unitary gauge, in which

$$h_u = 0, \qquad h_d \equiv \frac{h}{\sqrt{2}} = \frac{\langle h \rangle + \rho}{\sqrt{2}} , \tag{1.7.11}$$

where ρ is the canonically normalized physical Higgs field, the Goldstone boson matrix of eq. (1.7.8) simplifies and becomes

$$U = \begin{pmatrix} 1 & 0 & 0 & 0 & 0 \\ 0 & 1 & 0 & 0 & 0 \\ 0 & 0 & 1 & 0 & 0 \\ 0 & 0 & 0 & \cos\frac{h}{f} & \sin\frac{h}{f} \\ 0 & 0 & 0 & -\sin\frac{h}{f} & \cos\frac{h}{f} \end{pmatrix} . \tag{1.7.12}$$

The d and e symbols

The general definitions of the d and e symbols were given in Eq. (1.3.12) and their transformation properties in Eq. (1.3.8). Let us now restrict to the case in which A_μ belongs to the SO(4) subalgebra, as for our dynamical fields in eq. (1.3.14). In this case the explicit expressions for d and e are given by

$$\begin{aligned} d_\mu^i &= \sqrt{2}\left(\frac{1}{f} - \frac{\sin\Pi/f}{\Pi}\right)\frac{\vec{\Pi}\cdot\nabla_\mu\vec{\Pi}}{\Pi^2}\Pi^i + \sqrt{2}\frac{\sin\Pi/f}{\Pi}\nabla_\mu\Pi^i \\ e_\mu^a &= -A_\mu^a + 4\,i\,\frac{\sin^2(\Pi/2f)}{\Pi^2}\vec{\Pi}^t t^a \nabla_\mu\vec{\Pi} \end{aligned} \tag{1.7.13}$$

where $\nabla_\mu\Pi$ is the "covariant derivative" of the Π field:

$$\nabla_\mu\Pi^i = \partial_\mu\Pi^i - iA_\mu^a\,(t^a)^i{}_j\,\Pi^j . \tag{1.7.14}$$

Chapter 2

Light Top Partners

The colored femionic composite resonances, top partners, introduced in the Section 1.4.1 is a necessary ingredient of the CH models with partial compositeness. They play an important role in the breaking of the goldstone symmetry and also allow for a generation of the top quark mass. It has been noticed by many authors, and in Ref. [57] for the first time, that in explicit concrete models these particles are anomalously light, much lighter than the other strong sector's resonances. Concretely, one finds that the partners can easily be below 1 TeV, with an upper bound of around 1.5 TeV, while the typical strong sector's scale is above 3 TeV in order to satisfy the EWPT constraints. Moreover, Ref. [57] observed a certain correlation of the mass of the partners with the one of the Higgs boson.

The goal of this chapter which is based on a paper [6] will be to show that the lightness of the top partners has a *structural* origin, rather than being a peculiarity of some explicit model. The point is that in the composite Higgs scenario there is a tight relation among the top partners and the generation of the Higgs potential. This leads to a *parametric* correlation among the mass of the partners and the one of the Higgs boson. In order for the latter to be light as implied by the present data, we find that at least one of the top partners must be anomalously light. In section 2.1 we will describe this mechanism in detail by adopting a general description of the composite Higgs scenario with partial compositeness developed in Ref. [15, 20, 58]. Our results will thus have general validity and they will apply, in particular, to the 5d holographic models of Ref. [15, 57].

For a quantitative confirmation of the effect we need to study a concrete realization of the composite Higgs idea. The simplest possibility is to consider a "Discrete Composite Higgs Model" (DCHM) [40] which is based on the idea of "deconstruction", introduced in the Ref. [39], and described in the Section 1.5.1.

In sections 2.2 and 2.3 we describe in detail the structure of the top partners in the DCHM, and derive analytic explicit formulas that show quantitatively the correlation with the Higgs mass. Section 2.2 is devoted to the study of the 3-site DCHM, which provides a genuinely complete theory of composite Higgs. In this model, two layers of fermionic resonances are introduced and the Higgs potential is completely finite. In section 2.3 we consider instead a simpler but less complete model, the two-site DCHM. In this case one has a single layer of resonances and quite a small number (3, after fixing the top mass) of parameters describing the top partners. However the potential is *not* completely calculable, being affected by a logarithmic divergence at one loop [40]. Nevertheless it turns out that the divergence corresponds to a *unique* operator in the potential and therefore it

can be canceled by renormalizing only one parameter which we can chose to be the Higgs VEV v. Thus, the Higgs mass *is* calculable also in the DCHM$_2$, this model can therefore be considered as the "simplest" composite Higgs model and it can be used to study the phenomenology of the top partners in correlation with the Higgs mass.

The analytic results are further supported by scatter plots, in which we scan all the available parameter space of the model. The results are quite remarkable: in the plane of the masses of the top partners the points with light enough Higgs boson fall very sharply in the region of light partners. Notice that the actual values of the partner's mass is *not* fixed by our argument, it still depends on the overall mass scale of the strong sector. However this scale can only be raised at the price of fine-tuning the parameter $\xi \simeq (v/f_\pi)^2$ to very small values. Reasonable values of ξ, below which the entire scenario starts becoming implausible, are $\xi = 0.2$ or $\xi = 0.1$. For $\xi = 0.2$ we find that the partners are *always* below 1 TeV while for $\xi = 0.1$ the absolute maximum is around 1.5 TeV. We therefore expect that the $13 - 14$-TeV LHC will have enough sensitivity to explore the parameter space of the model completely.

Non-trivial constraints can however already be obtained by the presently available exclusions from the 8-TeV data, as we will briefly discuss in section 2.4. A more detailed phenomenological analysis of the top partners searches will be presented in the Chapter 3.

2.1 Light Higgs Wants Light Partners

If the Higgs is a pNGB its potential, and in particular its mass m_h, can only be generated through the breaking of the Goldstone symmetry. One unavoidable, sizable source of Goldstone symmetry breaking is the top quark Yukawa coupling y_t. Thus it is very reasonable to expect a tight relation among the Higgs mass and the fermionic sector of the theory which is responsible for the generation of y_t. This is particularly true in the canonical scenario of composite Higgs, summarized in the Chapter 1.2, where the *only* sizable contribution to the Higgs potential comes from the top sector. In more general cases there might be additional terms, coming for instance from extra sources of symmetry breaking not associated with the SM fermions and gauge fields [32]. Barring fine-tuning, the latter contributions can however at most *enhance* m_h, the ones from the top therefore provide a robust *lower bound* on the Higgs mass. In order to keep the Higgs mass light, the top sector contribution must therefore be kept small enough by some mechanism. In the minimal scenario, as we will describe below, this is achieved by making anomalously light (and thus more easily detectable) some of the exotic states in the top sector.

In order to understand this mechanism we obviously need to specify in some detail the structure of the theory which controls the generation of m_h and y_t. As anticipated in the Chapter 1.2, the paradigm adopted in the minimal model is the one of partial compositeness, in which the elementary left- and right-handed top fields are mixed with heavy vector-like colored particles, the so-called top partners. After diagonalization the physical top becomes an admixture of elementary and composite states and interacts with the strong sector, and in particular with the Higgs, through its composite component. The Yukawa coupling gets therefore generated and it is proportional to the sine of the mixing angles $\varphi_{L,R}$. The relevant Lagrangian, introduced in ref. [58], has the structure

$$\begin{aligned} \mathcal{L}_{\rm mass} &= -\left(y_L f_\pi\, \bar{t}_L T_R + y_R f_\pi\, \bar{t}_R \widetilde{T}_L + \text{h.c.}\right) - m_T^* \overline{T} T - m_{\widetilde{T}}^* \overline{\widetilde{T}} \widetilde{T}\,, \\ \mathcal{L}_{\rm Yuk} &= Y_* h \overline{T} \widetilde{T} + \text{h.c.}\,, \end{aligned} \tag{2.1.1}$$

where h is the Higgs field (before EWSB, *i.e.* $h = v + \rho$) and we have employed the decay constant f_π of the Goldstone boson Higgs for the normalization of the elementary–composite mixings. After diagonalization, neglecting EWSB, the top Yukawa reads

$$y_t \;=\; Y_* \sin\varphi_L \sin\varphi_R\,, \qquad \text{with} \qquad \begin{cases} \sin\varphi_L = \frac{y_L f_\pi}{m_T} \\ \sin\varphi_R = \frac{y_R f_\pi}{m_{\widetilde{T}}} \end{cases}\,, \tag{2.1.2}$$

where $m_{T,\widetilde{T}} = \sqrt{(m^*_{T,\widetilde{T}})^2 + (y_{L,R} f_\pi)^2}$ are the physical masses of the top partners. [1]

The essential point of making the partners light is that this allows to *decrease* the elementary–composite mixings $y_{L,R}$ while keeping y_t fixed to the experimental value. Let us consider the case of comparable left- and right-handed mixings, $y_L \simeq y_R \equiv y$. This condition, as explained in the following (see also [40]), is enforced in the minimal model by the requirement of a realistic EWSB. We can also assume that m^*_T and $m^*_{\widetilde{T}}$, while potentially small, are still larger than $y_L f_\pi$ and $y_R f_\pi$, the critical value after which eq. (2.1.2) saturates and there is no advantage in further decreasing the masses. Under these conditions eq. (2.1.2) gives

$$y^2 \;=\; \frac{y_t}{Y_*}\frac{m_T m_{\widetilde{T}}}{f_\pi^2}\,, \tag{2.1.3}$$

which shows how y^2 decreases *linearly* with the mass of each partner.

The mixings ensure the communication among the strong sector, which is invariant under the Goldstone symmetry, and the elementary sector which is not. Therefore they break the symmetry and allow for the generation of the Higgs mass. It is thus intuitive that a reduction of their value, as implied by eq. (2.1.3) for light top partners, will lead to a decrease of m_h. To be quantitative, let us anticipate the result of the following section (see also [57] and [40]): m_h can be estimated as

$$m_h \simeq \sqrt{\frac{3}{2}}\frac{y^2 v}{\pi}\,, \tag{2.1.4}$$

where $v \simeq 246$ GeV is the Higgs VEV. This gives, making use of eq. (2.1.3)

$$m_h \simeq 4\sqrt{3} m_t \,\frac{m_T m_{\widetilde{T}}}{4\pi Y_* f_\pi^2}\,. \tag{2.1.5}$$

The above equation already shows the correlation among the Higgs and the top partner mass. Of course we still need to justify eq. (2.1.4) and for this we need the more detailed analysis of the following section.

There is however one important aspect which is *not* captured by this general discussion. We see from eqs. (2.1.3) and (2.1.5) that making both m_T and $m_{\widetilde{T}}$ small at the same time produces a *quadratic* decrease of y^2 and thus of m_h. However this behavior is never found in the explicit models we will investigate in the following sections, the effect is always *linear*. The basic reason is that, due to the Goldstone nature of the Higgs, the coupling Y_* defined in eq. (2.1.1) depends itself on the partners mass. Indeed all the interactions of a pNGB Higgs are controlled by the dimensional coupling f_π and no independent Yukawa-like coupling Y_* can emerge. By dimensional analysis on has $Y_* \simeq m^*_{T,\widetilde{T}}/f_\pi$ or more precisely, as we will also verify below, $Y_* \simeq \max(m^*_T, m^*_{\widetilde{T}})/f_\pi$. Thus if both masses become small one power of $m_{T,\widetilde{T}}$ in eqs. (2.1.3) and (2.1.5) is compensated by Y_* and the effect remains linear.

[1] Actually, the physical masses receive extra tiny corrections due to EWSB.

2.1.1 General Analysis

For a better understanding we need a slightly more careful description of our theory. In particular we must take into account the Goldstone boson nature of the Higgs which is instead hidden in the approach of ref. [58] adopted in the previous discussion. Following ref.s [15, 20] (see also [49]) we describe the Higgs as a pNGB associated with the SO(5) $\to$ SO(4) spontaneous breaking which takes place in the strong sector. We parametrize (see [40] for the conventions) the Goldstone boson matrix as

$$U = e^{i\frac{\sqrt{2}}{f_\pi}\Pi_{\widehat{a}}T^{\widehat{a}}} , \tag{2.1.6}$$

where $T^{\widehat{a}}$ are the broken generators and $\Pi_{\widehat{a}}$ the 4 real Higgs components. The Goldstone matrix transforms under $g \in \mathrm{SO}(5)$ as [22]

$$U \;\to\; g \cdot U \cdot h^t\left(\Pi;\, g\right) , \tag{2.1.7}$$

where h is a non-linear representation of SO(5) which however only lives in SO(4). With our choice of the generators h is block-diagonal

$$h \;=\; \begin{pmatrix} h_4 & 0 \\ 0 & 1 \end{pmatrix} , \tag{2.1.8}$$

with $h_4 \in \mathrm{SO}(4)$

The SM fermions, and in particular the third family quarks $q_L = (t_L\; b_L)$ and t_R, are introduced as elementary fields and they are coupled linearly to the strong sector. In the UV, where SO(5) is restored, we can imagine that the elementary–composite interactions take the form

$$\mathcal{L} \quad = y_L\,(\overline{q}_L)^\alpha\,\Delta^L_{\alpha I}\,(\mathcal{O}_R)^I \;+\; y_R\,(\overline{t}_R)\,\Delta^R_I\,(\mathcal{O}_L)^I \;+\; \text{h.c.}\,, \tag{2.1.9}$$

where the chiral fermionic operators $\mathcal{O}_{L,R}$ transform in a *linear* representation of SO(5). [2] In particular in the minimal model we take both $\mathcal{O}_L$ and $\mathcal{O}_R$ in the fundamental, **5**. The tensors $\Delta^{L,R}$ are uniquely fixed by the need of respecting the SM $\mathrm{SU}(2)\times\mathrm{U}(1)_Y$ group embedded in SO(5) [3]

$$\begin{aligned} \Delta^L_{\alpha I} \;&=\; \frac{1}{\sqrt{2}}\begin{pmatrix} 0 & 0 & 1 & -i & 0 \\ 1 & i & 0 & 0 & 0 \end{pmatrix} , \\ \Delta^R_I \;&=\; -i\,(0\;0\;0\;0\;1)\;. \end{aligned} \tag{2.1.10}$$

Let us also define, for future use, the embedding in the **5** of q_L and of t_R

$$\begin{aligned} \left(q^{\mathbf{5}}_L\right)^I \;&=\; \left(\Delta^{L*}\right)^{\alpha I}\left(q_L\right)_\alpha = \frac{1}{\sqrt{2}}\begin{pmatrix} b_L & -ib_L & t_L & it_L & 0 \end{pmatrix} , \\ \left(t^{\mathbf{5}}_R\right)^I \;&=\; \left(\Delta^{R*}\right)^I t_R = i\begin{pmatrix} 0 & 0 & 0 & 0 & t_R \end{pmatrix} . \end{aligned} \tag{2.1.11}$$

The elementary–composite couplings obviously break the Goldstone symmetry SO(5). However provided the breaking is small we can still obtain valuable information from the SO(5) invariance

[2] We have defined the mixings $y_{L,R}$ as dimensionless couplings, for shortness we have reabsorbed in $\mathcal{O}_{L,R}$ the powers of the UV scale needed to restore the correct energy dimensions.

[3] Actually, one extra $\mathrm{U}(1)_X$ global factor is needed. In order to reproduce the correct SM hypercharges one must indeed define $Y = X + T^3_R$ and assign 2/3 $\mathrm{U}(1)_X$ charge to both $\mathcal{O}_L$ and $\mathcal{O}_R$.

by the method of spurions. The point is that the theory, including the UV mixings in eq. (2.1.9), is perfectly invariant if we transform not just the strong sector fields and operators but also the tensors Δ^L and Δ^R. This invariance survives in the IR description, the effective operators must therefore respect SO(5) if we treat Δ^L and Δ^R as spurions which transform, formally, in the **5** of SO(5). To be precise there are further symmetries one should take into account. These are the "elementary" $\mathrm{U}(2)^0_L$ and $\mathrm{U}(1)^0_R$, under which the strong sector is invariant and only the elementary fermions and the spurions transform. Certain linear combinations of the elementary group generators with the SO(5) (and $\mathrm{U}(1)_X$, see footnote 3) ones correspond to the SM group, these are of course preserved by the mixings.

The Higgs Potential

Let us first discuss the implications of the spurionic analysis on the structure of the Higgs potential. We must classify the non-derivative invariant operators involving the Higgs and the spurions. Notice that the invariance under $\mathrm{U}(2)^0_L \times \mathrm{U}(1)^0_R$ requires that the spurions only appear in the following two combinations

$$\begin{aligned} \Gamma^L_{IJ} &= \left(\Delta^{L*}\right)^\alpha_I \left(\Delta^L\right)_{\alpha J} , \\ \Gamma^R_{IJ} &= \left(\Delta^{R*}\right)_I \left(\Delta^R\right)_J . \end{aligned} \tag{2.1.12}$$

The Higgs enters instead through the Goldstone matrix U. Notice that to build SO(5) invariants we must contract the indices of $\Gamma^{L,R}$ with the *first* index of the matrix U, and not with the second one. Indeed if we rewrite more explicitly equation (2.1.7) as

$$U_{I\bar{\jmath}} \;\to\; g_I{}^{I'} U_{I'\bar{\jmath}'} h_{\bar{\jmath}}{}^{\bar{\jmath}'} , \tag{2.1.13}$$

we see that while the first index transforms with g like the spurion indices do, the second one transforms differently, with h. Remember that h is block-diagonal (see eq. (2.1.8)), thus to respect the symmetry we just need to form SO(4) (rather than SO(5)) invariants with the "barred" indices, in practice we can split them in fourplet and singlet components as $\bar{I} = \{i, 5\}$.

With these tools it is straightforward to classify all the possible invariants at a given order in the spurions. At the quadratic order, up to irrelevant additive constants, only two independent operators exist

$$\begin{aligned} v^L(h) &= \left(U^t \cdot \Gamma^L \cdot U\right)_{55} = \frac{1}{2}\sin^2 h/f_\pi , \\ v^R(h) &= \left(U^t \cdot \Gamma^R \cdot U\right)_{55} = \cos^2 h/f_\pi = 1 - \sin^2 h/f_\pi , \end{aligned} \tag{2.1.14}$$

where we plugged in the explicit value of the spurions in eq. (2.1.10) and of the Goldstone matrix in eq. (2.1.6) taking the Higgs along its VEV $\langle \Pi^{\widehat{a}} \rangle = h\delta^{\widehat{a}4}$. At this order then the potential can only be formed by two operators, with unknown coefficients which would become calculable only within an explicit model. We can nevertheless estimate their expected size. Following [19, 20] we obtain

$$V^{(2)}(h) = \frac{N_c M_*^4}{16\pi^2 g_*^2}\left[c_L y_L^2 v^L(h) + c_R y_R^2 v^R(h)\right] = \frac{N_c M_*^4}{16\pi^2 g_*^2}\left[\frac{1}{2}c_L y_L^2 - c_R y_R^2\right]\sin^2(h/f_\pi) + \text{const.} , \tag{2.1.15}$$

where $c_{L,R}$ are order one parameters and $\{M_*, g_*\}$ are the typical masses and couplings of the strong sector, g_* is defined as $g_* = M_*/f_\pi$. Remember that what we are discussing is the fermionic contribution to the potential, generated by colored fermion loops, this is the origin of the $N_c = 3$ QCD color factor in eq. (2.1.15). Also, this implies that the scale M_* is the one of the fermionic resonances, which could be a priori different from the mass of the vectors m_ρ. [4]

The spurionic analysis has strongly constrained the Higgs potential at the quadratic order. The two independent operators have indeed the same functional dependence on the Higgs and the potential is entirely proportional to $\sin^2(h/f_\pi)$. But then the potential at this order cannot lead to a realistic EWSB, the minimum is either at $h = 0$ or at $h = \pi f_\pi/2$. We would instead need to adjust the minimum in order to have $\xi = \sin^2(v/f_\pi) < 1$, and to achieve this additional contributions are required. In the minimal scenario these are provided by higher order terms in the spurion expansion. The classification of the operators is straightforwardly extended to the quartic order, one finds a second allowed functional dependence [5]

$$V^{(4)}(h) \;=\; \frac{N_c M_*^4}{16\pi^2 g_*^4}\left[c_1^{(4)}\, y^4 \sin^2(h/f_\pi) + c_2^{(4)}\, y^4 \sin^2(h/f_\pi)\cos^2(h/f_\pi)\right] , \tag{2.1.16}$$

where y^4 collectively denotes the quartic terms y_L^4, y_R^4 or $y_L^2 y_R^2$ and $c_{1,2}^{(4)}$ are coefficients of order unity. Notice that, differently from the quadratic one, the quartic potential does not depend strongly on the fermionic scale M_*. Since $M_* = g_* f_\pi$ the prefactor of $V^{(4)}$ can indeed be rewritten as f_π^4.

A priori, $V^{(4)}$ should give a negligible contribution to the potential because it is suppressed with respect to $V^{(2)}$ by a factor $(y_{L,R}/g_*)^2$, which is small in the minimal scenario. To achieve realistic EWSB however we need to tune the coefficients of the $\sin^2(h/f_\pi)$ and $\sin^2(h/f_\pi)\cos^2(h/f_\pi)$ terms in such a way as to cancel the Higgs mass term obtaining $v/f_\pi < 1$. In formulas, we have

$$V \;=\; \alpha \sin^2(h/f_\pi) \;-\; \beta \sin^2(h/f_\pi)\cos^2(h/f_\pi)\,, \qquad \Rightarrow \qquad \sin^2(v/f_\pi) = \frac{\beta-\alpha}{2\beta} \ll 1\,. \tag{2.1.17}$$

But, to make $\alpha \simeq \beta$, we need to cancel $V^{(2)}$, which only contributes to α and not to β, and to make it comparable with $V^{(4)}$. This requires $y_L \simeq y_R \equiv y$ or, more precisely

$$\frac{1}{2} c_L y_L^2 = c_R y_R^2 \left(1 + \mathcal{O}(y^2/g_*^2)\right) . \tag{2.1.18}$$

On top of this preliminary cancellation the tuning of the Higgs VEV in eq. (2.1.17) must be carried on. The total amount of fine-tuning is of order

$$\left(\frac{y}{g_*}\right)^2 \sin^2(v/f_\pi) = \left(\frac{y}{g_*}\right)^2 \xi\,, \tag{2.1.19}$$

and it is worse than the naive estimate by the factor $(y/g_*)^2$. [6] [7]

[4] The mass M_* is the scale at which the potential is saturated and generically it *is not* associated to the masses $m_{T,\tilde{T}}$ of the anomalously light partner. Due to additional structures, and only in the case in which *both* T and $\widetilde{T}$ are anomalously light, one might obtain $M_* \sim m_{T,\tilde{T}}$ in some explicit model because the light degrees of freedom reconstruct the structure of a 2-site DCHM in which the quadratic divergence is canceled.

[5] Actually, also a term proportional to $\cos h/f_\pi$ could appear. This is however forbidden by the parity in $SO(4)$, P_{LR}, for this reason it is not present in the minimal models.

[6] The theory would then be more natural if $y \sim g_*$. For small values of g_*, however, all the fermionic resonaces become lighter and this could give rise to enhanced corrections to the electroweak parameters in contrast with the EWPT. It could however be interesting to study this case explicitly in a concrete model.

[7] We remind the reader that the results of the presence section have general validity, in particular they apply to the

The final outcome of this discussion is that achieving realistic EWSB requires that the quadratic potential is artificially reduced and made comparable with $V^{(4)}$. Therefore we can simply forget about $V^{(2)}$ in eq. (2.1.15) and use instead eq. (2.1.16) as an estimate of the total Higgs potential. In particular we can estimate the physical Higgs mass, which is given by

$$m_h^2 \;=\; \frac{8\beta}{f_\pi^2}\sin^2(v/f_\pi)\cos^2(v/f_\pi) \;\simeq\; \frac{2N_c y^4}{16\pi^2} f_\pi^2 \sin^2(2v/f_\pi)\,, \tag{2.1.20}$$

where we used $g_* = M_*/f_\pi$. Expanding for $v/f_\pi \ll 1$ we recover the result anticipated in eq. (2.1.4).

We would have reached very similar conclusions if we had considered fermionic operators in the **4** of SO(5) rather than in the **5**. As shown in the original paper on the minimal composite Higgs [15], also in that case the potential is the sum of two trigonometric functions with coefficients α and β that scale respectively as $\alpha \sim y^2$ and $\beta \sim y^4$. The condition to obtain a realistic EWSB is again $\alpha \simeq \beta$, *i.e.* eq. (2.1.18), therefore the Higgs mass-term scales like y^4 as in eq. (2.1.20). Since the scaling is the same, all the conclusions drawn in this section, in particular the main result in eq. (2.1.25), will hold in exactly the same way. Moreover it is possible to show that the same structure of the potential emerges in the case of the **10** of SO(5) so that our results will apply also to the latter case. Possible ways to evade the light Higgs-light partner correlation of eq. (2.1.25) will be discussed in the Conclusions.

The Top Mass

For a quantitative estimate of m_h, which will show the correlation with the top partners mass, we need an estimate of y. The mixings $y_{L,R}$ control the generation of the top quark Yukawa, which of course must be fixed to the experimental value. The size of y however is not uniquely fixed because y_t also depends on the masses of the top partners with which the elementary t_L and t_R fields mix. In particular, as explained previously (see eq. (2.1.2)), the top Yukawa would get *enhanced* in the presence of anomalously light partners. To compensate for this, while keeping y_t fixed, one has to *decrease* y, thus lowering the Higgs mass.

We can study this effect in detail by writing down the low energy effective Lagrangian for the top partners. Since the operators $\mathcal{O}_{L,R}$ are in the **5** of SO(5), which decomposes as $\mathbf{5} = \mathbf{4} \oplus \mathbf{1}$ under SO(4), the top partners which appear in the low energy theory will be in the fourplet and in the singlet. [8] We describe these states as CCWZ fields, which transform non-linearly under SO(5) [22]. In particular the fourplet transforms as

$$Q_i \;\to\; (h_4)_i{}^j\, Q_j\,, \tag{2.1.21}$$

with $i = 1, \dots 4$ and h_4 as in eq. (2.1.8). The singlet $\widetilde{T}$ is obviously invariant. For our discussion we will not need to write down the complete Lagrangian, but only the mass terms and mixings. We

5d holographic models studied at length in the literature. In that context the need of an enhanced tuning in order to obtain realistic EWSB has been already pointed out [59] by explicitly computing the logarithmic derivative.

[8] Of course many more states could exist, associated to other UV operators. The presence of the fourplet and the singlet seems however unavoidable.

classify the operators with the spurion method previously outlined and we find, at the leading order

$$\begin{aligned}\mathcal{L} = \quad & -m_T^*\overline{Q}Q - m_{\widetilde{T}}^*\overline{\widetilde{T}}\widetilde{T} \\ & -y_L f_\pi \left(\bar{q}_L^{(5)}\right)^I \left(a_L U_{Ii} Q_R^i + b_L U_{I5}\widetilde{T}_R\right) + \text{h.c.} \\ & -y_R f_\pi \left(\bar{t}_R^{(5)}\right)^I \left(a_R U_{Ii} Q_L^i + b_R U_{I5}\widetilde{T}_L\right) + \text{h.c.}\,, \end{aligned} \tag{2.1.22}$$

where the embeddings $q_L^{\mathbf{5}}$ and $t_R^{\mathbf{5}}$ are defined in eq. (3.1.2).

The one in eq. (2.1.22) is the most general fermion mass Lagrangian allowed by the SO(5) Goldstone symmetry, it is not difficult to see that it leads to a top mass

$$m_t \simeq \frac{|b_L^* b_R m_T^* - a_L^* a_R m_{\widetilde{T}}^*|}{2\sqrt{2}|a_L||b_R|}\sin\varphi_L \sin\varphi_R \sin\left(2v/f_\pi\right)\,, \qquad \text{with} \qquad \begin{cases} \sin\varphi_L = \frac{|a_L| y_L f_\pi}{m_T} \\ \sin\varphi_R = \frac{|b_R| y_R f_\pi}{m_{\widetilde{T}}} \end{cases}\,, \tag{2.1.23}$$

where $m_T^2 = (m_T^*)^2 + |a_L|^2 y_L^2 f_\pi^2$ and $m_{\widetilde{T}}^2 = (m_{\widetilde{T}}^*)^2 + |b_R|^2 y_R^2 f_\pi^2$ are the physical masses of the partners before EWSB. Making contact with eq. (2.1.2) we find, as anticipated, that the Yukawa is controlled by the masses: $Y_* \simeq |b_L^* b_R m_T^* - a_L^* a_R m_{\widetilde{T}}^*|/f_\pi$.

Barring fine-tuning and assuming $m_{T,\widetilde{T}}^* \simeq m_{T,\widetilde{T}}$ we can approximate

$$m_t \simeq \frac{\max(m_T^*, m_{\widetilde{T}}^*)}{2\sqrt{2}}\sin\varphi_L\sin\varphi_R\sin\left(2v/f_\pi\right) = \frac{1}{2\sqrt{2}}\frac{y_L y_R f_\pi^2}{\min(m_T, m_{\widetilde{T}})}\sin\left(2v/f_\pi\right)\,. \tag{2.1.24}$$

Light Partners For a Light Higgs

The equation above, combined with the formula (2.1.20) for m_h finally shows the correlation among the Higgs and the top partners mass:

$$m_h \simeq \frac{\sqrt{N_c}}{\pi}\frac{\min(m_T, m_{\widetilde{T}})}{f_\pi} m_t \simeq 125\,\text{GeV}\frac{\min(m_T, m_{\widetilde{T}})}{1.4 f_\pi}\,. \tag{2.1.25}$$

For $f_\pi \simeq 500$ GeV we see that having a Higgs with a mass $m_h \simeq 125$ GeV requires the presence of at least one state of mass below 700 GeV. For $f_\pi \simeq 750$ GeV, which already corresponds to a significant level of fine-tuning, the partners can reach 1 TeV. This estimate suggests that the requirement of a realistic Higgs mass forces the theory to deliver relatively light top partners, definitely within the reach of the 14 TeV LHC and possibly close to the present bounds from the run at $7-8$ TeV. We will support this claim in the following sections where we will analyze the top partners spectrum within two explicit models.

The existence of an approximate linear correlation among m_h and the mass of the lightest top partner $m_{\text{light}} = \min(m_T, m_{\widetilde{T}})$ was already noticed in ref. [57] in the case of holographic models, however the physical interpretation of the result was not properly understood. To make contact with the argument presented in [57], we notice that from a low-energy perspective the Higgs mass-term arises from a quadratically divergent loop of elementary fermion fields, mixed with strength $y = y_{L,R}$ to the strong sector as in eq. (2.1.9). One can estimate

$$m_h^2 \sim \frac{N_c}{16\pi^2}\xi\frac{y^4}{g_*^2}\Lambda^2\,,$$

where Λ denotes the cutoff scale of the loop integral. To account for the observed linear relation among m_h and $m_{\rm light}$, ref. [57] claims that $\Lambda \simeq m_{\rm light}$, *i.e.* that the propagation of the lightest top partner in the loop is already sufficient to cancel the quadratic divergence. If the pre-factor $(y^2/g_*)^2$ can be estimated with the naive partial-compositeness relation $y_t = y^2/g_*$, irregardless of the presence of the light partner, by assuming $\Lambda \simeq m_{\rm light}$ one recovers eq. (2.1.25). However this argument is incorrect for two reasons. First of all the presence of anomalously light partners modifies the naive relation among y and y_t. This is obvious because the elementary-composite mixing angle, and thus y_t, must be enhanced if the composite particle becomes light. One finds indeed $y_t = y^2 f/m_{\rm light}$ as shown in eq. (2.1.24). Moreover there is no reason why the cutoff scale Λ should be set by $m_{\rm light}$. Indeed there is no known mechanism through which a single multiplet of SO(4) (the four-plet Q or the singlet $\widetilde{T}$) could cancel the quadratic divergence of m_h, and no hint that any such a mechanism should be at work in the composite Higgs framework. The cutoff scale Λ is always given by the strong sector scale m_*, irregardless of the presence of accidentally light partners with mass $m_{\rm light} \ll m_*$. [9] What lowers m_h when the partners are light is not a lower cutoff but, more simply, a smaller elementary/composite coupling. Indeed, by inverting eq. (2.1.24), $y^2 = y_t m_{\rm light}/f$. By setting $\Lambda = m_* = g_* f_\pi$ one obtains again eq. (2.1.25). In conclusion, while the final formula is the same of ref. [57], the derivation of the present section shows that it has a rather different physical origin.

Top Mass in Explicit Models

Before concluding this section we notice that the Lagrangian (2.1.22) is significantly more general than the one we will actually encounter in the specific models. First of all, the concrete models are more restrictive because they enjoy one more symmetry which has not yet been taken into account in the discussion. This is ordinary *parity* invariance of the strong sector, which we always assume for simplicity in our explicit constructions. Parity acts as $\mathcal{O}_L(\vec{x}) \leftrightarrow \mathcal{O}_R^{(P)}(-\vec{x})$ on the operators in eq. (2.1.9), and obviously it is broken by the interaction with the SM particles. [10] However it can be formally restored by the method of spurions, we have to assign transformations $q_L^{\mathbf{5}}(\vec{x}) \leftrightarrow t_R^{\mathbf{5}\,(P)}(-\vec{x})$ to the embeddings, plus of course $y_L \leftrightarrow y_R$. One implication of the parity symmetry is that the two coefficients of the quadratic potential (2.1.15) have to be equal, $c_L = c_R$, and thus the relation among the y_L and y_R mixings (2.1.18) becomes simply $y_L \simeq \sqrt{2} y_R$. For what concerns instead the partners Lagrangian (2.1.22) parity implies $a_L = a_R$ and $b_L = b_R$.

Moreover, the additional symmetry structures which underly the formulation of our models require the relations $a_L = a_R$ and $b_L = b_R$. The reason will become more clear in the following section, the basic point is that in our construction the fourplet and singlet form a fiveplet under an additional SO(5) group which is respected by the mixings.

To make contact with our models, let us then choose $a_L = a_R = b_L = b_R = 1$, the top mass

[9] In the extra-dimensional models m_* is represented by the compactification length, in the deconstructed ones it is provided by the fermonic masses at the internal sites. We have checked explicitly that $\Lambda \simeq m_*$ in the deconstructed models presented in the following section.

[10] The superscript "(P)" denotes the ordinary action of parity on the Dirac spinors, for instance in the Weyl basis $\psi^{(P)} = \gamma^0 \psi$

becomes

$$m_t \simeq \frac{|m_T^* - m_{\widetilde{T}}^*|}{2\sqrt{2}} \sin\varphi_L \sin\varphi_R \sin\left(2v/f_\pi\right) , \qquad \text{with} \qquad \begin{cases} \sin\varphi_L = \frac{y_L f_\pi}{m_T} \\ \sin\varphi_R = \frac{y_R f_\pi}{m_{\widetilde{T}}} \end{cases} , \tag{2.1.26}$$

and it is proportional to the mass-difference $m_T^* - m_{\widetilde{T}}^*$. Indeed for $a_L = a_R = b_L = b_R$ the mixings are proportional to the five-plet Ψ defined as

$$\Psi_I \,=\, U_{Ii} Q^i \,+\, U_{I5}\widetilde{T} \,=\, U_{I\bar{I}} \begin{pmatrix} Q \\ \widetilde{T} \end{pmatrix}_{\bar{I}} , \tag{2.1.27}$$

which is related to the original fields by the orthogonal matrix U. It becomes therefore convenient to perform a field redefinition and to re-express the Lagrangian in terms of Ψ, in this way the mixings become trivial and independent of the Higgs field and the only operators which contain the Higgs boson and no derivatives originate from the rotation of the mass terms. Therefore these operators are proportional to the mass difference $m_T^* - m_{\widetilde{T}}^*$ because for $m_T^* = m_{\widetilde{T}}^*$ also the mass Lagrangian becomes SO(5) invariant and the dependence on the Higgs drops. Explicitly, we have

$$-\,\overline{\Psi}\, U \begin{pmatrix} m_T^* & 0 \\ 0 & m_{\widetilde{T}}^* \end{pmatrix} U^t \Psi \,=\, -m_T^* \overline{T} T - m_{\widetilde{T}}^* \overline{\widetilde{T}} \widetilde{T} - \frac{m_T^* - m_{\widetilde{T}}^*}{2\sqrt{2}} \sin(2h/f_\pi) \overline{T} \widetilde{T} \,+\, \ldots \tag{2.1.28}$$

from which eq. (2.1.26) is immediately rederived.

2.2 Light Partners in the DCHM$_3$

The first explicit model we will consider for our analysis is the 3-site Discrete Composite Higgs Model (DCHM$_3$) [40]. This model provides a simple but complete four-dimensional realization of the composite Higgs paradigm. As we already mentioned in the Chapter 1.2, an important, distinctive property of the DCHM$_3$ model is the finiteness and calculability of the Higgs potential. This feature, together with the *simplicity* of the DCHM approach, will enable us to derive explicit formulas displaying the relation between the Higgs mass and the spectrum of the top partners.

Another important aspect is the fact that the parametrization which we naturally get in the Discrete Composite Higgs framework can be directly mapped onto the general structure of partial compositeness. As we already showed in the previous section partial compositeness plays a crucial role in understanding the relation between the properties of the Higgs boson and the spectum of the fermionic resonances. We will confirm this in the explicit analysis we will present in this section.

The basic structure of the DCHM$_3$ model consists of two replicas of the non-linear σ-model $\mathrm{SO}(5)_L \times \mathrm{SO}(5)_R/\mathrm{SO}(5)_V$ and was described in the Section 1.5.1. For convenience we write down the relevant parts of the lagrangian of the model. The elementary fermions and their mixing with the composites are described by

$$\mathcal{L}^{\mathrm{f}}_{\mathrm{elem}} = i\,\bar{q}_L \not{D} q_L + i\,\bar{t}_R \not{D} t_R - \, y_L f \bar{q}_L^{\mathbf{5}} U \psi_R - y_R\, f \bar{t}_R^{\mathbf{5}} U \psi_L + \mathrm{h.c.}\,, \tag{2.2.1}$$

And the composite resonances are described by the following lagrangian

$$\begin{aligned}\mathcal{L}^{\rm f}_{\rm comp} &= i\,\overline{\psi}\not{D}\psi - m\overline{\psi}\psi \\ &\quad + i\,\overline{\widetilde{\psi}}\not{D}\widetilde{\psi} - \widetilde{m}_{\rm Q}\overline{\widetilde{Q}}\widetilde{Q} - \widetilde{m}_{\rm T}\overline{\widetilde{T}}\widetilde{T} \\ &\quad - \Delta\overline{\psi}\widetilde{\psi} + \text{h.c.}\,. \end{aligned} \tag{2.2.2}$$

Note that the U_2 matrix is substituted by the identity. The Higgs dependence in the U_2 can removed to U_1 by a gauge fixing – a Π_2-dependent $SO(5)$ rotation at the second site. The corresponding gauge is often called holographic.

2.2.1 The Higgs Potential

In this section we will analyze the structure of the Higgs potential deriving an approximate expression for the Higgs mass in terms of the masses of the fermionic resonances.

The most relevant contribution to the Higgs potential comes from the fermionic states. The corrections due to the gauge fields are typically small and we will neglect them altogether in our analysis. The only states which are coupled to the Higgs in our set-up are the top and the resonances of charge 2/3. The contribution of these states to the potential has the form [11]

$$V(h) = -\frac{2N_c}{8\pi^2}\int dp\, p^3 \log\left(1 - \frac{C_1(p^2)\sin^2(h/f_\pi) + C_2(p^2)\sin^2(h/f_\pi)\cos^2(h/f_\pi)}{D(p^2)}\right). \tag{2.2.3}$$

The denominator of the expression in the logarithm is given by

$$D(p^2) = 2p^2 \prod_{I=T,\widetilde{T},T_{2/3}} \left(p^2 + m^2_{I_-}\right)\left(p^2 + m^2_{I_+}\right), \tag{2.2.4}$$

where $m_{I_\pm}$ denote the masses of the charge 2/3 resonances before EWSB. In particular T and $T_{2/3}$ denote the two states in the fourplet, namely T is the state which forms an $SU(2)_L$ doublet with the charge $-1/3$ field (B) and $T_{2/3}$ is the state which appear in the doublet with the exotic state of charge 5/3 ($X_{5/3}$). The $\widetilde{T}$ state denotes instead the singlet. The $\pm$ sign refers to the two levels of composite resonances which are present in the model. Notice that all these masses include the shift due to the mixings with the elementary states. The initial factor p^2 which appears in eq. (2.2.4) is due to the presence of the top which is massless before EWSB. The coefficients appearing in eq. (2.2.4) in the numerator of the expression inside the logarithm are given by

$$\begin{cases} C_1(p^2) = \left(y_L^2 - 2y_R^2\right) f^2 F_1(p^2)F_2(p^2) - (\widetilde{m}_Q - \widetilde{m}_T)\Delta^2 y_L^2 y_R^2 f^4 \left(p^2 + \Delta^2 + \widetilde{m}_Q^2\right) F_1(p^2) \\ C_2(p^2) = -(\widetilde{m}_Q - \widetilde{m}_T)\Delta^2 y_L^2 y_R^2 f^4 F_2(p^2) \end{cases}, \tag{2.2.5}$$

where the functions $F_{1,2}$ are defined as

$$\begin{cases} F_1(p^2) = p^2\Big((m + \widetilde{m}_T)(p^2 + \Delta^2 - m\,\widetilde{m}_Q) + (m + \widetilde{m}_Q)(p^2 + \Delta^2 - m\,\widetilde{m}_T)\Big) \\ F_2(p^2) = (\widetilde{m}_Q - \widetilde{m}_T)\Delta^2\left(p^2 + m^2_{T_{2/3-}}\right)\left(p^2 + m^2_{T_{2/3+}}\right) \end{cases}. \tag{2.2.6}$$

[11] The computation of the Higgs potential can be performed by using the standard textbook formulae for the Coleman–Weinberg potential. Equivalently one can apply the holographic technique as explained in Ref. [62].

The potential can be approximated by expanding at leading order the logarithm in eq. (2.2.3). Although this approximation is formally valid only for small values of h/f_π, [12] it turns out that it is numerically very accurate in a wide range of the parameter space and, in particular, it is valid for all the points we will consider in our numerical analysis.

After the expansion and the integration, the potential takes the general form already considered in eq. (2.1.17)

$$V(h) \simeq \alpha \sin^2(h/f_\pi) - \beta \sin^2(h/f_\pi)\cos^2(h/f_\pi)\,. \tag{2.2.7}$$

Using an expansion in the elementary mixings, the α term is dominated by the leading $\mathcal{O}(y^2)$ contributions, proportional to $y_L^2 - 2y_R^2$. As discussed in section 2.1.1, in order to obtain a realistic value for v/f_π the leading order contributions must be cancelled, such that they can be tuned against the subleading terms. This leads to the condition in eq. (2.1.18) with $c_L = c_R = 1$, namely

$$y_L \simeq \sqrt{2} y_R\,. \tag{2.2.8}$$

This relation is very well verified numerically for realistic points in the parameter space, as shown in [40]. [13]

For realistic configurations, due to the cancellation, the leading term of order $y_{L,R}^2$ becomes of $\mathcal{O}(y_{L,R}^4)$. This means that, if we are interested in an expansion of the potential at quartic order in the elementary–composite mixings, we only need to take the linear term in the expansion of the logarithm in eq. (2.2.3). The value of the coefficient β can be easily found analytically

$$\beta = \frac{N_c}{8\pi^2}(\widetilde{m}_Q - \widetilde{m}_T)^2\,\Delta^4\, y_L^2\, y_R^2\, f^4 \sum_{\substack{I=T_-,T_+,\\ \widetilde{T}_-,\widetilde{T}_+}} \frac{\log(m_I/f)}{\prod_{J\neq I}(m_I^2 - m_J^2)}\,. \tag{2.2.9}$$

In the limit in which the second level of resonances is much heavier than the first one, we can use an expansion in the ratio of the heavy and light states masses and get a simple approximate formula for β:

$$\beta \simeq \frac{N_c}{8\pi^2}(\widetilde{m}_Q - \widetilde{m}_T)^2\,\Delta^4\, y_L^2\, y_R^2\, f^4 \frac{\log\left(m_{T_-}/m_{\widetilde{T}_-}\right)}{\left(m_{T_-}^2 - m_{\widetilde{T}_-}^2\right) m_{T_+}^2\, m_{\widetilde{T}_+}^2}\,. \tag{2.2.10}$$

As can be seen form this formula, when one of the states T_- or $\widetilde{T}_-$ is much lighter than the other, the contribution to β from the first level of resonances is enhanced by the logarithmic factor $\log(m_{T_-}/m_{\widetilde{T}_-})$. In this case the light states contribution completely dominates and the corrections due to the second layer of resonances become negligible. On the other hand, if the two light states have comparable masses, the second level of resonances, in certain regions of the parameter space, can be relatively close in mass to the first one, thus giving sizable corrections to the Higgs mass. The sign of these corrections is fixed, and they always imply a decrease of the Higgs mass. The size of the corrections in the relevant regions of the parameter space is typically below 50%.

[12] This is of course not true in the limit $p^2 \to 0$, in which the argument of the logarithm diverges. However in this case the factor p^3 in front of the logarithm compensate for the divergence and the approximate integrand vanishes for $p \to 0$. The error introduced by this approximation is thus small.

[13] The condition in eq. (2.2.8) differs from the one reported in eq. (57) of [40] by a factor $\sqrt{2}$. This is due to a different choice of the normalization of the y_L mixing (see eq. (2.2.1)).

The expression of the Higgs mass in terms of the β coefficient has already been given in eq. (2.1.20) and reads

$$m_h^2 = \frac{2\beta}{f_\pi^2}\sin^2(2v/f_\pi) \simeq \frac{N_c}{\pi^2}(\widetilde{m}_Q - \widetilde{m}_T)^2\,\Delta^4\,y_L^2\,y_R^2\,f_\pi^3\,\frac{\log\left(m_{T_-}/m_{\widetilde{T}_-}\right)}{\left(m_{T_-}^2 - m_{\widetilde{T}_-}^2\right)m_{T_+}^2 m_{\widetilde{T}_+}^2}\sin^2(2v/f_\pi)\,. \quad (2.2.11)$$

2.2.2 The Higgs Mass and the Top Partners

As shown in the general analysis of section 2.1, it is useful to compare the Higgs mass with the top mass, with the aim of obtaining a relation between m_h and the masses of the top partners.

By performing an expansion in $\sin^2(v/f_\pi)$, we can obtain an approximate expression for the top mass. The result can be recast in the general form of eq. (2.1.26),

$$m_t \simeq \frac{|\widetilde{m}_Q - \widetilde{m}_T|}{2\sqrt{2}}\sin\varphi_L\sin\varphi_R\sin\left(\frac{2v}{f_\pi}\right). \quad (2.2.12)$$

where the mixing angles $\varphi_{L,R}$ are now replaced by some "effective" compositeness angles

$$\begin{aligned}\sin\varphi_L &\equiv \frac{\Delta}{\sqrt{\Delta^2+\widetilde{m}_Q^2}}\frac{y_L f}{\sqrt{\frac{(\Delta^2 - m\,\widetilde{m}_Q)^2}{\Delta^2+\widetilde{m}_Q^2} + (y_L f)^2}}\,,\\ \sin\varphi_R &\equiv \frac{\Delta}{\sqrt{\Delta^2+\widetilde{m}_T^2}}\frac{y_R f}{\sqrt{\frac{(\Delta^2 - m\,\widetilde{m}_T)^2}{\Delta^2+\widetilde{m}_T^2} + (y_R f)^2}}\,.\end{aligned} \quad (2.2.13)$$

There is an equivalent way to rewrite the approximate expression for the top mass in eq. (2.2.12) in terms of the masses of the T and $\widetilde{T}$ resonances:

$$m_t \simeq \frac{|\widetilde{m}_Q - \widetilde{m}_T|}{2\sqrt{2}}\frac{y_L y_R f^2\Delta^2}{m_{T_+}m_{T_-}m_{\widetilde{T}_+}m_{\widetilde{T}_-}}\sin\left(\frac{2v}{f_\pi}\right). \quad (2.2.14)$$

By comparing this expression with the approximate formula for the Higgs mass in eq. (2.2.11) we find a remarkable relation between m_h and the masses of the lightest T and $\widetilde{T}$ resonances:

$$\frac{m_h}{m_t} \simeq \frac{\sqrt{2N_c}}{\pi}\frac{m_{T_-}m_{\widetilde{T}_-}}{f_\pi}\sqrt{\frac{\log\left(m_{T_-}/m_{\widetilde{T}_-}\right)}{m_{T_-}^2 - m_{\widetilde{T}_-}^2}}\,. \quad (2.2.15)$$

As discussed in the previous section, the above expression receives the corrections due to the presence of the second layer of resonances. These corrections are sizable only when the second level of resonances is relatively light. In this case corrections of the order 50% to eq. (2.2.15) can arise.

Let us now compare the expression in eq. (2.2.15) with the general result obtained in section 2.1.1 (eq. (2.1.25)). The two equations show the same qualitative relation between the Higgs mass and the masses of the lightest resonances T and $\widetilde{T}$. In the case $m_T = m_{\widetilde{T}}$ the two expressions exactly coincide, while, when a large hierarchy between the two light states T and $\widetilde{T}$ is present, they differ by a coefficient of $\mathcal{O}(1)$. This shows that the general analysis of section 2.1.1 correctly capture the main connection between the Higgs and the top partners masses, both at a qualitative and a quantitative level. Notice that also the logarithmic term, which originates from the one in the Higgs mass (2.2.11), could have been computed within the general approach of section 2.1.1. It is indeed an IR loop effect associated to the light top partners.

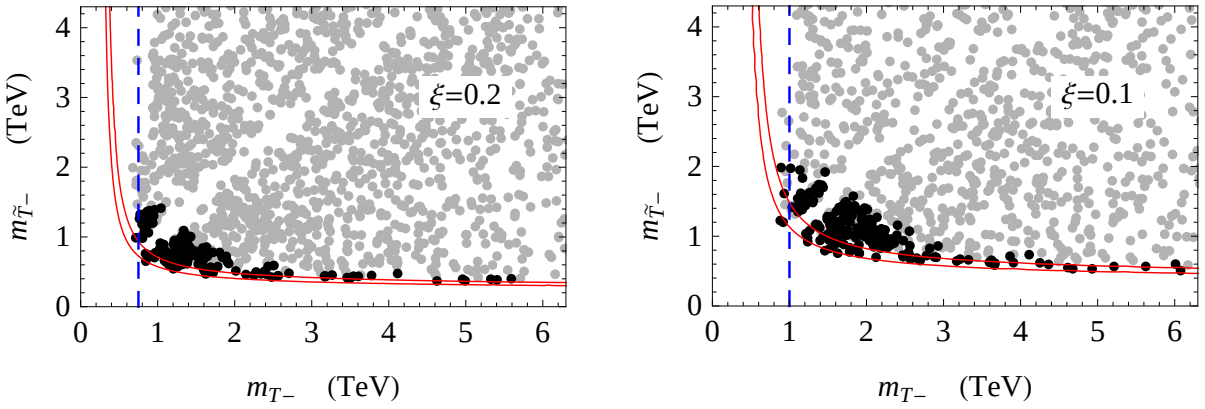

Figure 2.1: *Scatter plots of the masses of the lightest T and $\widetilde{T}$ resonances for $\xi = 0.2$ (left panel) and $\xi = 0.1$ (right panel) in the three-site DCHM model. The black dots denote the points for which* 115 GeV $\leq m_h \leq$ 130 GeV*, while the gray dots have $m_h >$ 130 GeV. The scans have been obtained by varying all the composite sector masses in the range $[-8f, 8f]$ and keeping the top mass fixed at the value $m_t =$ 150 GeV. The area between the solid red lines represents the range obtained by applying the result in eq. (2.2.15) for* 115 GeV $\leq m_h \leq$ 130 GeV*. The dashed blue line corresponds to the estimate of the lower bound on m_{T_-} given in eq. (2.2.19).*

We checked numerically the validity of our results by a scan on the parameter space of the model. In our numerical analysis we take the interval 115 GeV $\leq m_h \leq$ 130 GeV as the range of Higgs masses around the observed one, in order to account for possible subleading corrections from other composite resonances. In our analysis we also fix the top mass to the value $m_t = m_t^{\overline{MS}}(2 \text{ TeV}) = 150$ GeV, which corresponds to $m_t^{pole} = 173$ GeV.

The scatter plots of the masses of the T and $\widetilde{T}$ light resonances are shown in fig. 2.1. One can see that eq. (2.2.15) describes accurately the relation between the Higgs and the resonance masses in the regions in which one state is significantly lighter than the others. For a realistic Higgs mass this happens only when the $\widetilde{T}_-$ is much lighter than the other states. Instead, the situation of a T much lighter than the $\widetilde{T}$ can not happen for a light Higgs due to the presence of a lower bound on the m_{T_-}, which will be discussed in details in the next section. In the region of comparable T_- and $\widetilde{T}_-$ masses sizable deviations from eq. (2.2.15) can occur. These are due to the possible presence of a relatively light second level of resonances, as already discussed.

The numerical results clearly show that resonances with a mass of the order or below 1.5 TeV are needed in order to get a realistic Higgs mass both in the case $\xi = 0.2$ and $\xi = 0.1$. The prediction is even sharper for the cases in which only one state, namely the $\widetilde{T}_-$, is light. In these regions of the parameter space a light Higgs requires states with masses around 400 GeV for the $\xi = 0.2$ case and around 600 GeV for $\xi = 0.1$.

The situation becomes even more interesting if we also consider the masses of the other composite resonances. As we already discussed, the first level of resonances contains, in addition to the T_- and $\widetilde{T}_-$, three other states: a top-like state, the $T_{2/3-}$, a bottom-like state, the B_-, and an exotic state with charge 5/3, the $X_{5/3-}$. These three states together with the T_- form a fourplet of SO(4). Obviously the $X_{5/3-}$ cannot mix with any other state even after EWSB, and therefore it remains always lighter than the other particles in the fourplet. In particular (see fig. 2.7 for a schematic

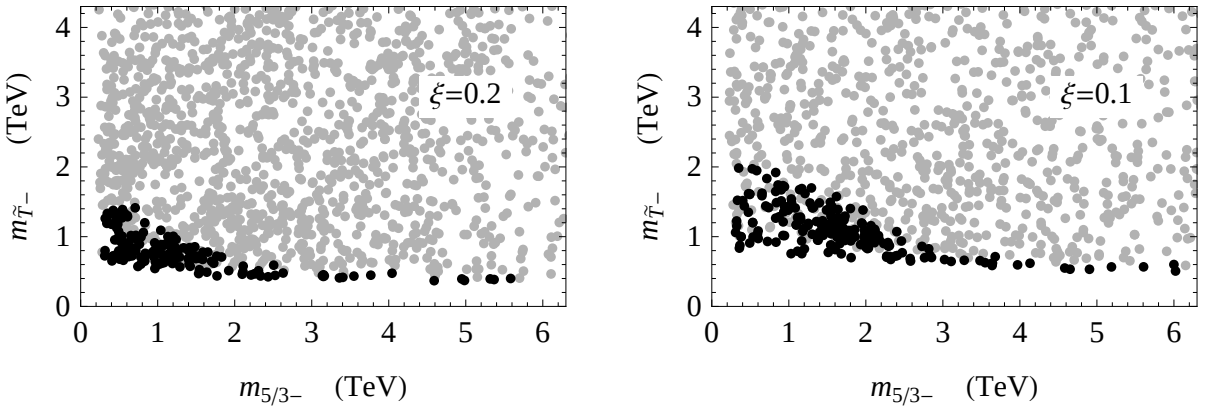

Figure 2.2: *Scatter plots of the masses of the lightest exotic state of charge* 5/3 *and of the lightest* $\widetilde{T}$ *resonance for* $\xi = 0.2$ *(left panel) and* $\xi = 0.1$ *(right panel) in the three-site DCHM model. The black dots denote the points for which* 115 GeV $\leq m_h \leq$ 130 GeV*, while the gray dots have* $m_h >$ 130 GeV*. The scans have been obtained by varying all the composite sector masses in the range* $[-8f, 8f]$ *and keeping the top mass fixed at the value* $m_t = 150$ GeV*.*

picture of the spectrum), it is significantly lighter than the T_- . In fig. 2.2 we show the scatter plots of the masses of the lightest exotic charge 5/3 state and of the $\widetilde{T}$. In the parameter space region in which the Higgs is light the $X_{5/3-}$ resonance can be much lighter than the other resonances, especially in the configurations in which the T_- and $\widetilde{T}_-$ have comparable masses. In these points the mass of the exotic state can be as low as 300 GeV.

Notice that in the plots in fig. 2.1 there are no points in which the masses of the T_- and of the $\widetilde{T}_-$ coincide. This is due to a repulsion of the mass levels induced by the mixings due to EWSB. As expected, this effect is more pronounced for larger values of ξ.

2.2.3 The Top Mass and a Lower Bound on the Higgs Mass

As noticed above, the asymptotic region $m_{T-} \ll m_{\widetilde{T}-}$, which could in principle give rise to configurations with realistic Higgs masses, is not accessible in our model. Indeed in the scatter plots of fig. 2.1 we find a lower bound on m_{T-}. We will show below that this bound comes from the requirement of obtaining a realistic top mass and that an analogous bound, which however is not visible in fig. 2.1, exists for the $\widetilde{T}_-$ mass. From these results we will also derive an absolute lower bound on the Higgs mass.

The starting point of our analysis is the approximate expression for the top mass in eq. (2.2.12). Our aim is to abtain a lower bound on the resonance masses, so we will focus on the configurations in which one of the top partners is much lighter than the others. For definiteness we will consider the case in which the lightest state is the T_- resonance. In a generic situation, all the parameters of the composite sector are of the same order $\Delta \sim m \sim \widetilde{m}_Q \sim \widetilde{m}_T$. The only mass which gets cancelled is m_{T-}, so we can also assume that $m_{T_+} \sim m_{\widetilde{T}_+}$ and that they are of the same order of the composite sector masses. In this regime the effective compositeness angles in eq. (2.2.13) can be approximated as

$$\sin\varphi_L \sim 1\,, \qquad \sin\varphi_R \simeq \frac{y_R f}{m_{\widetilde{T}_-}}\,. \tag{2.2.16}$$

The first equation comes from the fact that we assumed the T_- state to be nearly massless before the mixing with the elementary sector. This condition is equivalent to the relation $\Delta^2 - m\,\widetilde{m}_Q = 0$ (see eq. (80) of [40]).

The expression for the top mass in eq. (2.2.12) now becomes

$$m_t \simeq \frac{y_R f}{2\sqrt{2}} \sin\left(\frac{2v}{f_\pi}\right) \simeq y_R v\,, \tag{2.2.17}$$

and, by using the relation between y_L and y_R in eq (2.2.8), we get

$$y_L \simeq \sqrt{2}\, y_R \simeq \frac{\sqrt{2} m_t}{v}\,. \tag{2.2.18}$$

Given that the mass of the light state predominantly comes from the mixing with the elementary fermions we can use the estimate

$$m_{T_-} \gtrsim y_L f \simeq \frac{2m_t}{v} f_\pi\,. \tag{2.2.19}$$

This inequality implies the lower bounds

$$m_{T_-} \gtrsim 5 m_t \simeq 750\ \text{GeV}\,, \qquad \text{for}\ \ \xi = 0.2\,, \tag{2.2.20}$$

and

$$m_{T_-} \gtrsim 6.7 m_t \simeq 1000\ \text{GeV}\,, \qquad \text{for}\ \ \xi = 0.1\,, \tag{2.2.21}$$

obtained for $m_t = 150$ GeV. In a similar way a lower bound on the mass of the lightest $\widetilde{T}$ state can be found. This bound is a factor 2 weaker than the one on m_{T_-}:

$$m_{\widetilde{T}_-} \gtrsim y_R f \simeq \frac{m_t}{v} f_\pi\,. \tag{2.2.22}$$

The lower bounds on the lightest top partners masses agree with the results of the numerical scans in fig. 2.1. The lower bound on $m_{\widetilde{T}_-}$ is instead below the range of values needed to get a realistic Higgs mass, so it is not visible in the the plot.

The lower bound on the resonance masses can be translated, through eq. (2.2.15) into a lower bound on the Higgs mass. The most favourable configuration is the one in which the lightest mass is $m_{\widetilde{T}_-}$. This leads to the bound

$$m_h \gtrsim \frac{\sqrt{2N_c}}{\pi} \frac{m_t^2}{v} \sqrt{\log\left(\frac{v}{m_t}\frac{m_{T_-}}{f_\pi}\right)}\,. \tag{2.2.23}$$

For $m_{T_-}/f_\pi \sim 4$, which represent a typical point in our parameter space, we get

$$m_h \gtrsim 100\ \text{GeV}\,. \tag{2.2.24}$$

This result is in good agreement with the bound obtained in the scans.

2.3 The Simplest Composite Higgs Model

As shown in Ref. [40], the three-site DCHM we considered in the previous section is the minimal realization of an effective description of a composite Higgs in which all the key observables, and in particular the Higgs potential, are computable at the leading order. This property allowed us to decouple the UV physics and fully characterize the model in terms of the parameters describing the elementary states and two levels of composite resonances.

If we accept to give up a complete predictivity, a much simpler effective model can be employed to describe the low-energy dynamics of a composite Higgs boson and of the top partners. In this model only one layer of composite resonances is introduced, leading to a structure representable with a two-site model (see fig. 1.12). The pattern of divergences in the two-site DCHM has been fully analyzed in Ref. [40]: the electroweak precision parameters remain calculable at leading order, while the Higgs potential becomes logarithmically divergent at one loop.

There is however an interesting property which partially preserves predictivity also for the potential. In the expansion in powers of the elementary–composite mixings, only the leading terms can develop a logarithmic divergence, while the higher order ones are finite at one loop. We have shown in Section 2.1.1 (see eq. (2.1.14)) that at the leading order only two operators exist and that they both give the same contribution, proportional to $\sin^2 h/f_\pi$, to the potential. A single counterterm is therefore enough to regulate the divergence, which corresponds to the renormalization of a single parameter. An interesting possibility is to fix the value of the Higgs VEV, or more precisely of the ratio v/f_π, as renormalization condition obtaining the Higgs mass as a prediction. In this sense, m_h is predictable also in the DCHM$_2$.

Let us briefly summarize the structure of the DCHM$_2$. The model is based on a non-linear σ-model $\mathrm{SO}(5)_L \times \mathrm{SO}(5)_R/\mathrm{SO}(5)_V$ and it is schematically representation in fig. 1.12. As in the three-site DCHM, the first site is associated with the elementary states, while the other is related to the composite resonances. Of course, in this case, only one level of composite resonances is present.

The elementary fermions, *i.e.* the SM chiral states q_L and t_R, are introduced at the first site. Their Lagrangian is

$$\mathcal{L}^{\mathrm{f}}_{\mathrm{elem}} = i\,\bar{q}_L \not{D} q_L + i\,\bar{t}_R \not{D} t_R - y_L f_\pi \bar{q}^{\mathbf{5}}_L U \widetilde{\psi}_R - y_R\, f_\pi \bar{t}^{\mathbf{5}}_R U \widetilde{\psi}_L + \mathrm{h.c.}\,, \tag{2.3.1}$$

where we used the embeddings of the elementary states in the fundamental representation of SO(5) given in eq. (3.1.2).

The Lagrangian for the composite states $\widetilde{\psi}$, in the holographic gauge, is given by

$$\mathcal{L}^{\mathrm{f}}_{\mathrm{comp}} = i\,\overline{\widetilde{\psi}} \not{D} \widetilde{\psi} - \widetilde{m}_{\mathrm{Q}} \overline{\widetilde{Q}} \widetilde{Q} - \widetilde{m}_{\mathrm{T}} \overline{\widetilde{T}} \widetilde{T}\,, \tag{2.3.2}$$

Notice that we have already encountered the fermion Lagrangian of the DCHM$_2$ in the general discussion of section 2.1, and in particular at the end of Section 2.1.1. The DCHM$_2$ can indeed be obtained from the general Lagrangian of eq. (2.1.22) by restricting $a_L = a_R = b_L = b_R$ in order to respect the SO(5) symmetry.

2.3.1 The Higgs Potential

Analogously to the DCHM$_3$ case, the fermionic contribution to the Higgs potential only comes from the charge 2/3 states. Its structure can be put in the same form as eq. (2.2.3)

$$V(h) = -\frac{2N_c}{8\pi^2}\int dp\, p^3 \log\left(1 - \frac{C_1(p^2)\sin^2(h/f_\pi) + C_2(p^2)\sin^2(h/f_\pi)\cos^2(h/f_\pi)}{D(p^2)}\right). \tag{2.3.3}$$

The denominator of the expression in the logarithm now contains only one level of resonances and is given by

$$D(p^2) = 2p^2 \prod_{I=T,\widetilde{T},T_{2/3}} \left(p^2 + m_I^2\right), \tag{2.3.4}$$

where we used a notation similar to the one adopted for the three-site model. For the two-site model the expression for the masses of the top parteners before EWSB are very simple and can be given in closed form

$$m_T^2 = \sqrt{\widetilde{m}_Q^2 + (y_L f_\pi)^2}\,, \qquad m_{T_{2/3}}^2 = \widetilde{m}_Q^2\,, \qquad m_{\widetilde{T}}^2 = \sqrt{\widetilde{m}_T^2 + (y_R f_\pi)^2}\,. \tag{2.3.5}$$

The $C_{1,2}$ coefficients appearing in the expression of the Higgs potential are given by

$$\begin{cases} C_1(p^2) = -\left(\widetilde{m}_Q^2 - \widetilde{m}_T^2\right) p^2 \left(\left(p^2 + m_{T_{2/3}}^2\right)(y_L^2 - 2y_R^2) f_\pi^2 - y_L^2 y_R^2 f_\pi^4\right) \\ C_2(p^2) = -(\widetilde{m}_Q - \widetilde{m}_T)^2 \left(p^2 + m_{T_{2/3}}^2\right) y_L^2 y_R^2 f_\pi^4 \end{cases}. \tag{2.3.6}$$

Similarly to the three-site model, the second term appearing in the logarithm argument in eq. (2.3.3) is typically much smaller than one, so that we can use a series expansion. [14] The potential, taking into account terms up to the quartic order in the elementary–composite mixings, has the usual form

$$V(h) \simeq \alpha \sin^2(h/f_\pi) - \beta \sin^2(h/f_\pi)\cos^2(h/f_\pi)\,. \tag{2.3.7}$$

As we already mentioned, the $\mathcal{O}(y_{L,R}^2)$ terms in the potential are logarithmically divergent, as can be easily checked using the explicit results given above. This implies that the coefficient α in eq. (2.3.7) must be regularized. For this purpose we can add a counterterm of the form given in eq. (2.1.14) with a suitable coefficient. This procedure is equivalent, from a practical point of view, to just consider α as a free parameter. This coefficient can then be fixed by imposing one renormalization condition, for instance by choosing the value of v/f_π.

Notice that, differently from the three-site model, in the two-site case there is no reason to assume that the leading order term in the potential is cancelled by a tuning among y_L and y_R. The tuning of the potential can be totally due to the counterterm which cancels the logarithmic divergence. For this reason, in the following analysis we will not impose any relation between the left and the right elementary–composite mixings.

In order to compute the coefficient β at quartic order in $y_{L,R}$ we need to take into account an expansion of the logarithm in eq. (2.3.3) at the quadratic order. The value of the coefficient β can

[14] For more details see the discussion before eq. (2.2.7).

be easily found analytically and is given by

$$\begin{aligned}\beta &= \frac{N_c}{8\pi^2}\frac{(\widetilde{m}_Q-\widetilde{m}_T)^2 y_L^2 y_R^2 f_\pi^4}{m_T^2-m_{\widetilde{T}}^2}\log\left(\frac{m_T}{m_{\widetilde{T}}}\right)\\ &+\frac{N_c}{8\pi^2}\frac{(\widetilde{m}_Q^2-\widetilde{m}_T^2)^2(y_L^2-2y_R^2)^2 f_\pi^4\left[-(m_T^2-m_{\widetilde{T}}^2)+(m_T^2+m_{\widetilde{T}}^2)\log\left(\frac{m_T}{m_{\widetilde{T}}}\right)\right]}{4(m_T^2-m_{\widetilde{T}}^2)^3}\,. \end{aligned} \tag{2.3.8}$$

The term on the first line of the above expression is analogous to the result found in the three-site case. On the other hand, the second contribution is specific of the two-site model and is there because we did not impose any relation between y_L and y_R. The accidental factor of 4 in the denominator of the second contribution and some cancellations which happen in the expression between square brackets make the second contribution smaller than the first one typically by one order of magnitude. Notice, moreover, that the sign of the two contributions are always the same. Thus the second contribution always determine a small increase of β in absolute size. Neglecting this second term we obtain a Higgs mass

$$m_h^2=\frac{2\beta}{f_\pi^2}\sin^2(2v/f_\pi)\simeq\frac{N_c}{4\pi^2}\frac{(\widetilde{m}_Q-\widetilde{m}_T)^2 y_L^2 y_R^2 f_\pi^2}{m_T^2-m_{\widetilde{T}}^2}\log\left(\frac{m_T}{m_{\widetilde{T}}}\right)\sin^2(2v/f_\pi)\,. \tag{2.3.9}$$

As we did in the three-site model, we can rewrite the Higgs mass in terms of the top mass. The approximate expression for the top mass was already found in section 2.1.1 (eq. (2.1.26)) and is given by

$$m_t\simeq\frac{|\widetilde{m}_Q-\widetilde{m}_T|}{2\sqrt{2}}\frac{y_L y_R f_\pi^2}{m_T m_{\widetilde{T}}}\sin\left(\frac{2v}{f_\pi}\right)\,. \tag{2.3.10}$$

Making use of eq. (2.3.9) we find

$$\frac{m_h}{m_t}\simeq\frac{\sqrt{2N_c}}{\pi}\frac{m_T m_{\widetilde{T}}}{f_\pi}\sqrt{\frac{\log\left(m_T/m_{\widetilde{T}}\right)}{m_T^2-m_{\widetilde{T}}^2}}\,, \tag{2.3.11}$$

which exactly coincides with the expression (2.2.15) obtained in the three-site model when the second level of resonances is heavy.

2.3.2 Numerical Results

We can verify the validity of the relation in eq. (2.3.11) between the Higgs and the top partners masses by performing a numerical scan on the parameter space of the two-site model. However the computation of the Higgs effective potential in the two-site case is not completely straightforward and requires an ad hoc procedure to deal with the logarithmic divergence. In particular, we can not directly integrate eq. (2.3.3) as in the 3-site model. The simplest way to proceed is to notice that eq. (2.3.3) can be rewriten in the standard Coleman–Weinberg form

$$V(h)=-\frac{2N_c}{8\pi^2}\int dp\; p^3\log\left[\prod_i(p^2+m_i^2(h))\right]\,, \tag{2.3.12}$$

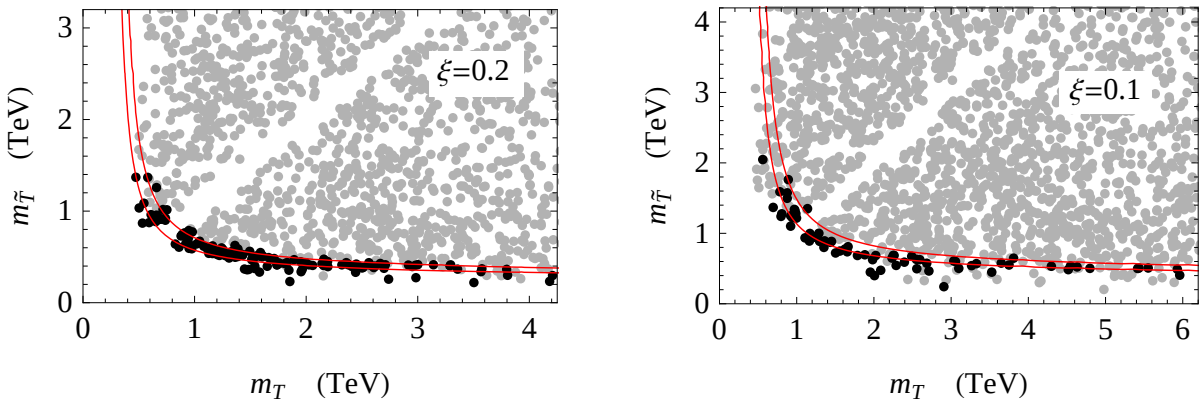

Figure 2.3: *Scatter plots of the masses of the T and $\widetilde{T}$ resonances for $\xi = 0.2$ (left panel) and $\xi = 0.1$ (right panel) in the two-site DCHM model. The black dots denote the points for which* 115 GeV $\leq m_h \leq$ 130 GeV, *while the gray dots have* $m_h >$ 130 GeV. *The scans have been obtained by varying all the composite sector masses in the range* $[-8f_\pi, 8f_\pi]$ *and keeping the top mass fixed at the value* $m_t =$ 150 GeV. *The area between the solid red lines represents the range obtained by applying the result in eq. (2.3.11) for* 115 GeV $\leq m_h \leq$ 130 GeV.

where the product is over all the 2/3-charged fermionic states of our model. Actually, we could have derived eq. (2.3.3) starting from the Coleman–Weinberg expression in eq. (2.3.12). We can now regulate the integral with a hard momentum cutoff Λ and we obtain the standard formula

$$V(h) = -\frac{N_c}{8\pi^2}\Lambda^2 \sum_i m_i^2(h) - \frac{N_c}{16\pi^2}\sum_i m_i^4(h)\left[\log\left(\frac{m_i^2(h)}{\Lambda^2}\right) - \frac{1}{2}\right] . \tag{2.3.13}$$

In the two-site model only a logarithmic divergence can appear in the Higgs potential, and therefore the quadratically divergent term must be independent of the Higgs. This is ensured by the condition

$$\sum_i m_i^2(h) = \sum_i m_i^2(h=0) = \text{const.}\,, \tag{2.3.14}$$

which we can explicitly verify in our model. [15] The logarithmic divergence, as discussed above, must be proportional to $\sin^2 h/f_\pi$ as in eq. (2.1.14). Indeed in our 2-site model one can verify explicitly that

$$\sum_i m_i^4(h) \propto \sin(h/f_\pi^2) + \text{const}\,.$$

We can therefore, as anticipated, cancel the divergence by introducing a single counterterm in the potential, proportional to $\sin^2 h/f_\pi$. This leaves only one free renormalization parameter which we can trade for a scale μ, the renormalized potential takes the form

$$V(h) = -\frac{N_c}{16\pi^2}\sum_i m_i^4(h)\log\left(\frac{m_i^2(h)}{\mu^2}\right) . \tag{2.3.15}$$

We will treat μ as a free parameter, the strategy of our scan will be to choose it, once the other parameters are fixed, in order to fix the minimum of the potential to the required value of v/f_π.

[15] If, as in the 3-site case, the Higgs potential was completely finite at one loop, an analogous condition would hold for the logarithmic term, *i.e.* $\sum_i m_i^4(h) = \sum_i m_i^4(h=0) = \text{const.}$

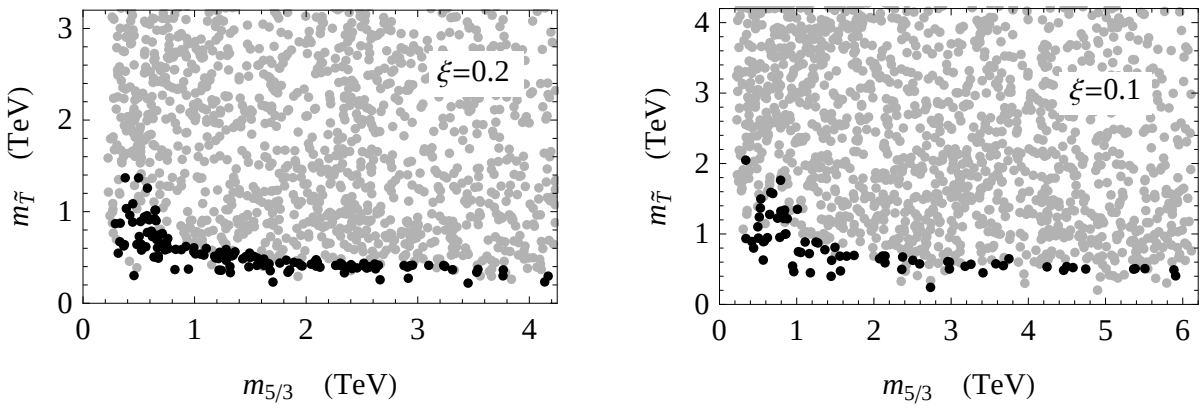

Figure 2.4: *Scatter plots of the masses of the exotic state of charge* 5/3 *and of the* $\widetilde{T}$ *resonance for* $\xi = 0.2$ *(left panel) and* $\xi = 0.1$ *(right panel) in the two-site DCHM model. The black dots denote the points for which* 115 GeV $\leq m_h \leq$ 130 GeV*, while the gray dots have* $m_h >$ 130 GeV*. The scans have been obtained by varying all the composite sector masses in the range* $[-8f_\pi, 8f_\pi]$ *and keeping the top mass fixed at the value* $m_t = 150$ GeV*.*

The result of the numerical scan is shown in fig. 2.3. The black points correspond to configuration with realistic Higgs mass and they lie approximately between the two solid red lines which correspond to the bounds derived from eq. (2.3.11). The small deviations come from the corrections due to the $(y_L^2 - 2y_R^2)$ term in the expression for β in eq. (2.3.8). As discussed before, the effect of these corrections is to increase the Higgs mass, and therefore, keeping the Higgs mass fixed, to make the resonances lighter. In fig. 2.3 we show the scatter plot of masses of the exotic charge 5/3 state and of the $\widetilde{T}$. As in the three-site model the exotic state is lighter than the T, so that, in a large part of the parameter space it is the lightest composite resonance.

2.3.3 Modeling the Effect of the Heavy Resonances

By comparing the scatter plots obtained for the two-site model with the ones for the three-site one, one can see that, although the relation between the Higgs mass and the resonance masses is always reasonably well satisfied, significant deviations can appear. In particular the region in which m_T and $m_{\widetilde{T}}$ are comparable shows larger deviations, while the asympthotic regions in which one of the resonances is much lighter than the others have a smaller spread. The 2-site model is therefore slightly too restrictive, and also too "pessimistic" in that it requires very low resonances. The effect of an additional level of resonances, as the 3-site model results show, can change the 2-site picture significantly.

However, the effect of the heavy resonances on the Higgs potential can be rather simply mimicked in the two-site model by adding to the potential a new contribution to the coefficient β in eq. (2.3.7). The size of the contributions coming from the heavy resonances can be estimated by symmetry considerations and power counting. In our derivation we will respect the general properties which characterize the heavy resonances in the three-site model. First of all we assume that the source of SO(5) breaking is in common with the light states, so that the new operator must contain a factor $(\widetilde{m}_Q - \widetilde{m}_T)^2$. Morever we must introduce four powers of the elementary–composite mixings as dictated by spurion analysis. For simplicity we will write the contribution of the new operator

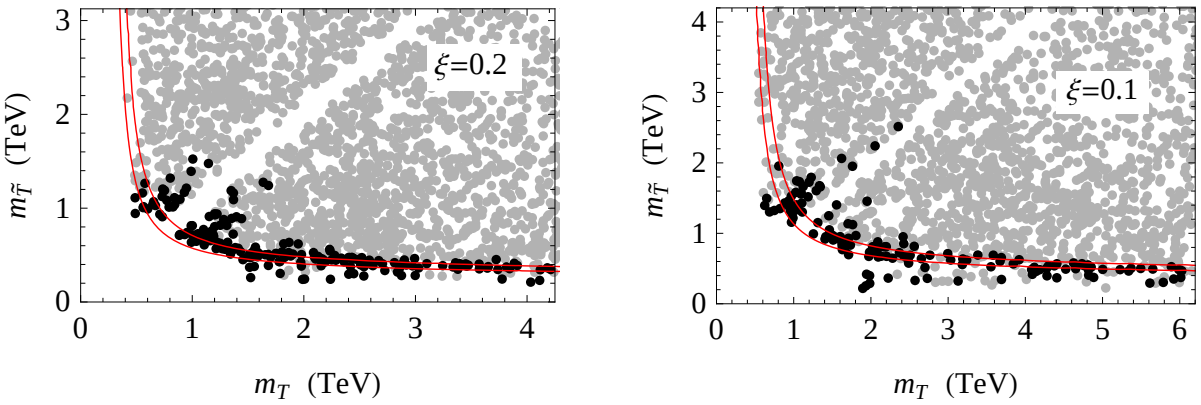

Figure 2.5: *Scatter plots of the masses of the T and $\widetilde{T}$ resonances for $\xi = 0.2$ (left panel) and $\xi = 0.1$ (right panel) in the two-site DCHM model with the addition of the operator in eq. (2.3.16). The black dots denote the points for which* 115 GeV $\leq m_h \leq$ 130 GeV*, while the gray dots have* $m_h >$ 130 GeV*. The scans have been obtained by varying all the composite sector masses in the range* $[-8f_\pi, 8f_\pi]$ *and keeping the top mass fixed at the value* $m_t =$ 150 GeV*. The mass of the heavy resonances has been chosen to be at least* 50% *higher than the one of all the light states. The area between the solid red lines represents the range obtained by applying the result in eq. (2.3.11) for* 115 GeV $\leq m_h \leq$ 130 GeV*.*

to β in the same form of the contribution coming from the light states. In particular we choose the form of the most relevant term, the one on the first line of eq. (2.3.8). Denoting by M the mass of the heavy resonances we write their contribution to the Higgs effective potential as

$$\Delta V(h) = \frac{N_c}{8\pi^2}\frac{(\widetilde{m}_Q - \widetilde{m}_T)^2 y_L^2 y_R^2 f_\pi^4}{M^2}\sin^2(v/f_\pi)\cos^2(v/f_\pi)\,. \tag{2.3.16}$$

Guided by the results of the three-site model, in which the heavy resonances tend to lower the Higgs mass, we fix the sign for the corrections in order to reproduce this effect.

The numerical results of a scan including the effect of the operator in eq. (2.3.16) are shown in fig. 2.5. In the scan we assume that the mass of the heavy resonances is at least 50% higher than the masses of all the light resonances. One can see that the plots show a good qualitative and quantitative agreement with the ones obtained in the three-site model (see fig. 2.1). In particular the plots show an agreement with the relation in eq. (2.3.11) in the asymptotic regions in which one state is much lighter than the others. Larger deviations are present when all the state have comparable masses. This effect can be simply understood by comparing the form of the leading contributions to β in eq. (2.3.8) (the ones on the first line) and the form of the contributions of the operator representing the heavy resonances in eq. (2.3.16). When a high hierarchy between m_T and $m_{\widetilde{T}}$ is present, the logarithm appearing in eq. (2.3.8) enhances the light states contributions to the Higgs mass, thus making the heavy resonances corrections negligible. On the other hand, when $m_T \sim m_{\widetilde{T}}$, the light states contribution are somewhat reduced and the heavy states can give a sizable correction to β.

Finally in fig. 2.6 we show the scatter plot for the masses of the exotic charge 5/3 state and of the $\widetilde{T}$ state. Again a good agreement with the results for the three-site model in fig. 2.2 is found.

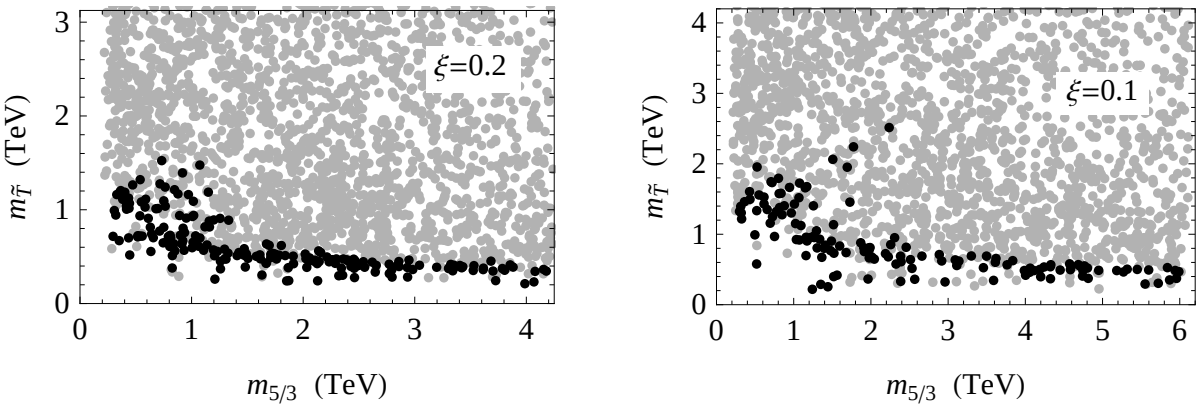

Figure 2.6: *Scatter plots of the masses of the exotic state of charge* 5/3 *and of the* $\widetilde{T}$ *resonance for* $\xi = 0.2$ *(left panel) and* $\xi = 0.1$ *(right panel) in the two-site DCHM model with the addition of the operator in eq. (2.3.16). The black dots denote the points for which* 115 GeV $\leq m_h \leq$ 130 GeV*, while the gray dots have* $m_h >$ 130 GeV*. The scans have been obtained by varying all the composite sector masses in the range* $[-8f_\pi, 8f_\pi]$ *and keeping the top mass fixed at the value* $m_t =$ 150 GeV*. The mass of the heavy resonances has been chosen to be at least* 50% *higher than the one of all the light states.*

2.4 Bounds on the Top Partners

The top partners are generically so light, often below the TeV, that the present experimental results can already place some non-trivial bounds on their mass. In this section we will present a simple discussion of the available constraints; our aim will not be to perform a comprehensive study of all the bound coming from the existing experimental data, but instead to focus on some simple and universal searches whose results are approximately valid independently of the specific model and of the corner of the parameter space we consider.

In particular we will restrict our analysis to the lightest resonance which comes from the composite sector and we will only consider pair production processes in which, due to the universal QCD couplings, the production cross section depends exclusively on the mass of the resonance. The bounds we will derive are thus quite robust and apply to generic composite models. Notice however that, in a large region of the parameter space, single production processes, as well as the presence of other relatively light resonances, can give an enhancement of the signal in the channels considered in the present analysis. In this case the bounds on the masses of the resonances can also become tighter. The next Chapter will be devoted to a more detailed analysis of constraints coming from the direct searches in the scenarios with a totally composite t_R.

Before discussing the details of our analysis, it is useful to briefly describe the general structure of the spectrum of the first level of fermionic resonances. These states, as schematically shown in fig. 2.7, are approximately organized in $SU(2)_L$ multiplets

$$Q = \begin{pmatrix} T \\ B \end{pmatrix}, \qquad X = \begin{pmatrix} X_{5/3} \\ T_{2/3} \end{pmatrix}, \qquad \widetilde{T}\,. \tag{2.4.1}$$

The splitting between the two doublets arises from the mixing of the composite fermions with the elementary states and its size is of order $\Delta m^2 \sim y_L^2 f^2$. Notice that only the Q doublet is mixed

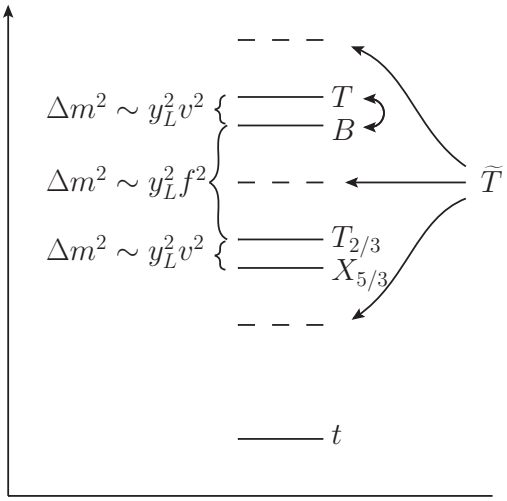

Figure 2.7: *Schematic structure of the spectrum of the lightest multiplet of resonances.*

with the elementary fermions, thus it is always heavier than the X doublet. On the other hand, the mass of the $\widetilde{T}$ singlet has no relation to the ones of the two doublets.

After the breaking of the electroweak symmetry the fermions acquire mass corrections giving rise to a small splitting inside the doublets. Due to the Goldstone nature of the Higgs, the effects of EWSB can only arise if the Goldstone symmetry is broken, that is they must be mediated by the elementary–composite mixings. The mass splitting inside the doublets are thus of order $y_{L,R}^2 v^2$, and are typically suppressed by a factor $(v/f)^2$ with respect to the mass gap between the two doublets. For all the relevant configurations the lightest state of the X doublet is the exotic fermion with charge 5/3, the $X_{5/3}$. The ordering of the states in the Q multiplet instead is not fixed and depends on the specific point in the parameter space we choose.

As we mentioned before, in our analysis we will only consider the lightest fermionic resonance, which is always given by the exotic state $X_{5/3}$ or by the singlet $\widetilde{T}$. We will discuss these two cases separately in the following subsections.

Experimental Bounds on the Charge 5/3 State

As a first case we will consider the configurations in which the exotic state $X_{5/3}$ is the lightest new resonance. The strongest current bound on this type of states comes from the CMS analysis [87], which is designed to be sensitive to the pair produced $X_{5/3}$. Each $X_{5/3}$ is supposed to decay exclusively to a W and a top quark, giving final states with two same sign leptons and jets. Using the data corresponding to 19.6 fb^{-1} of integrated luminosity for 8 TeV collisions, the search [87] with a 95% confidence level excludes the masses of the $X_{5/3}$ lower than 770 GeV.

In contrast with a situation considered in the Ref. [87], in our scenario the singly produced $X_{5/3}$ can also contribute to the considered final states, but we leave a detailed analysis of this effect to the dedicated Chapter 3 while here we will use 770 GeV as a conservative model-independent bound. For the moment we will also neglect the contribution of the B, though the latter can sizably enhance the signal if it is not much heavier than the $X_{5/3}$.

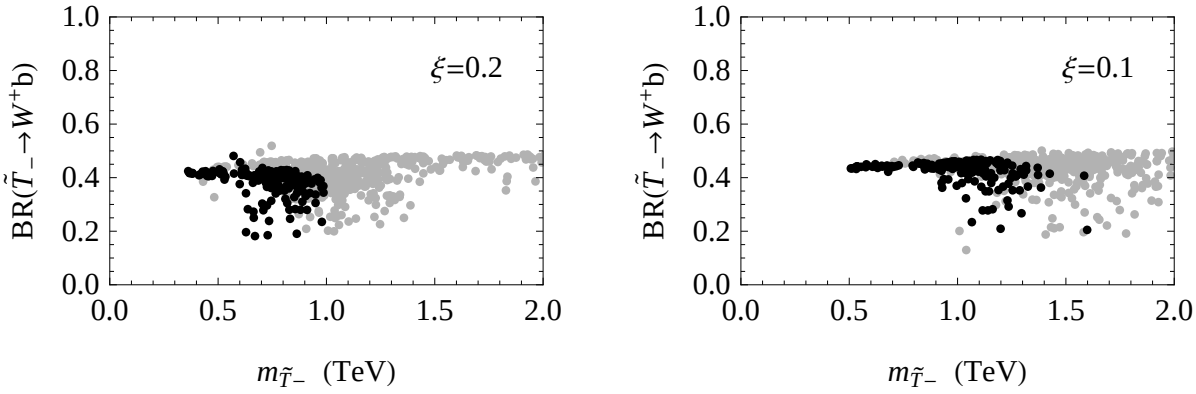

Figure 2.8: *Scatter plot of the branching ratios of the lightest $\widetilde{T}$ resonance into W^+b for the three-site DCHM model with $\xi = 0.2$ (left panel) and $\xi = 0.1$ (right panel). In all the points shown in the plot the $\widetilde{T}$ state has been required to be the lightest composite resonance. The black dots denote the points for which 115 GeV $\leq m_h \leq$ 130 GeV, while the gray dots have $m_h >$ 130 GeV. The scans have been obtained by varying all the composite sector masses in the range $[-8f, 8f]$ ane keeping the top mass fixed to the value $m_t = 150$ GeV.*

Experimental Bounds on $\widetilde{T}$

We now focus on the case in which the lightest resonance is given by the charge 2/3 state $\widetilde{T}$. There exist several LHC analyses searching for pair produced $\widetilde{T}$-like state, performed by the ATLAS [**?**,**?**,**?**] and the CMS [**?**] collaborations which put the limits in a range 600-800 GeV depending on the BR of the $\widetilde{T}$ decays into Ht, Zt and Wb. From a scan of the parameter space of the explicit models, see fig. 2.8, we find that typically the W and Higgs channels dominate, $BR(\widetilde{T} \to bW^+) \sim BR(\widetilde{T} \to th) \sim 0.4$, while the Z channel is slightly suppressed, $BR(\widetilde{T} \to tZ) \sim 0.2$, quite independently of the value of v/f_π. Given these values, the optimal exclusion comes from the CMS search [**?**] which implies $m_{\widetilde{T}} > 693$ GeV at 95% confidence level.

Again, as in the case of the $X_{5/3}$, we will directly adopt the experimental bounds without taking into account the contribution of the single production to the considered signal.

Exclusion Bounds in the DCHM$_3$

To appreciate the impact of the previously derived bounds in the explicit models we show in fig. 2.9 the exclusion regions superimposed on the scatter plots for the masses of the $X_{5/3}$ and $\widetilde{T}$ resonances for the three-site DCHM model.

The bound on the exotic state with charge 5/3 is already quite strong and excludes a sizable portion of the parameter space with realistic Higgs mass. Of course, the bound has a greater impact on the configurations with larger ξ, which predict lighter resonances. Nevertheless even in the case of a relatively small v/f_π, namely $\xi = 0.1$, the exclusion bound on the exotic resonance puts non-trivial constraints.

The situation is slightly different for the cases in which the lightest new state is the singlet $\widetilde{T}$, the bounds are weaker but still sizable at ξ relatively large. On the other hand, for $\xi = 0.1$ the mass of the $\widetilde{T}$ resonances is typically above the current bounds.

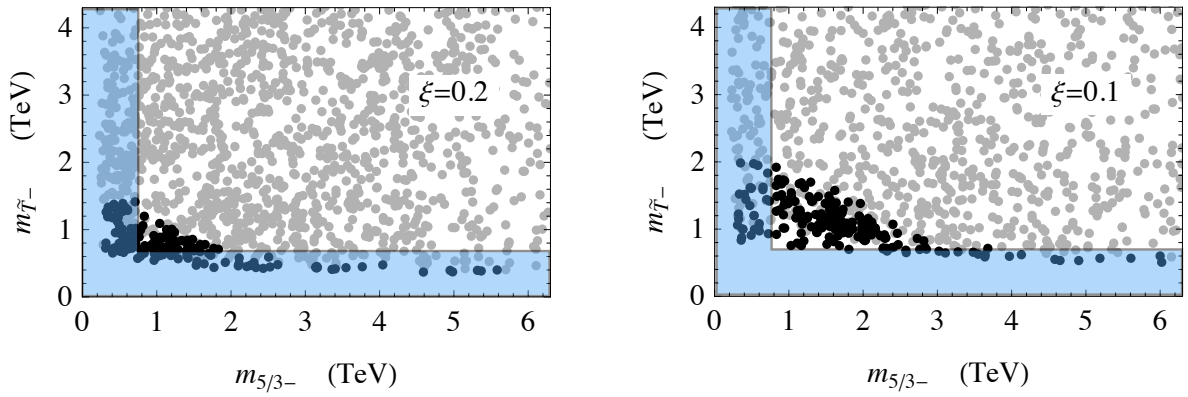

Figure 2.9: *Scatter plot of the masses of the lightest exotic state of charge* $5/3$ *and of the lightest* $\widetilde{T}$ *resonance for the three-site DCHM model with* $\xi = 0.2$ *(left panel) and* $\xi = 0.1$ *(right panel). The shaded region corresponds to the points excluded by our analysis, which gives the bounds* $m_{5/3} > 770$ GeV *and* $m_{\widetilde{T}} > 690$ GeV*. The black dots denote the points for which* $115\ \text{GeV} \leq m_h \leq 130\ \text{GeV}$*, while the gray dots have* $m_h > 130$ GeV*.*

Chapter 3

Direct Top Partners Searches

In the previous Chapter we discussed the relation between the Higgs mass and the masses of the composite fermionic partners of the top quark and found out that in a broad class of CH models this relation implies a presence of relatively light top partners with a mass below 1-1.5 TeV. A more general analysis performed in the Ref. [71] confirms this conclusion and extends it to an even broader range of models. For this reason the searches for the top partners at the LHC become a crucial test of validity of the considered scenarios. In this chapter we want to provide a simplified approach to describe the results of experimental searches for the top partners. Using this approach, we will constrain several types of scenarios basing on the presently available experimental analyses. We will focus on the composite Higgs scenario based on the minimal coset $SO(5)/SO(4)$ and described using a CCWZ construction. The basic simplifying assumption is that the spectrum has the structure depicted in figure 3, where one $SO(4)$ multiplet of colored Dirac fermions Ψ is parametrically lighter than the other states. The model we are going to consider does not possess sufficient structure (states and couplings) to make the Higgs potential calculable (see Section 1.5). But it is very general and from the LHC phenomenology point of view interpolates over a broad class of CH models. It is obviously understood that the limiting situation presented by the simplified model is not expected to be precisely realized in a realistic scenario. However, a realistic situation where the splitting with the next-to-lightest multiplet is of the order M_Ψ is qualitatively already well described by the simplified model. Only if the splitting was parametrically smaller than M_Ψ would there be dramatic changes. There already exists a literature on simplified top partner models in generic composite Higgs scenarios [75], where the role of symmetry is not fully exploited. Focussing on the minimal composite Higgs model based on SO(5)/SO(4) we will develop a systematic approach where all possible top partner models are constructed purely on the basis of symmetry and selection rules.

We shall derive exclusion plots in a reduced parameter space, which in general involves the mass and couplings of the top-partner Ψ. Now, even though these are not the parameters of a fundamental model, given their overall size, we can roughly estimate how natural the Higgs sector is expected to be. The common feature of all scenarios is that the top partners need to be light for a reasonably natural theory, the way the tuning scales with the top-partners' mass is instead different in each case. Here we focus on the possibility that the right handed top quark t_R is a $SO(4)$ singlet belonging to the strong sector, therefore the top Yukawa simply arises from an $SO(5)$ breaking perturbation of the form

$$\lambda_L q_L \mathcal{O}_R + \text{h.c.}\,. \tag{3.0.1}$$

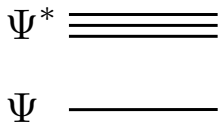

Figure 3.1: Schematic picture of the spectrum.

Here $\mathcal{O}_R$ is a composite operator, which in the low energy theory maps to Ht_R, thus giving rise to a top Yukawa coupling $y_t \sim \lambda_L$. The operator O_R however also interpolates in general for massive states, the top partners. Now, from simple power counting, and also from explicit constructions [40], at leading order in the breaking parameter λ_L we expect the Higgs potential to have the form

$$V(h) = \frac{3y_t^2 m_*^2}{16\pi^2}\left\{ah^2 + \frac{b}{2}\frac{h^4}{f^2} + \frac{c}{3!}\frac{h^6}{f^4} + \dots\right\}. \tag{3.0.2}$$

where $a, b, c, \dots$ are coefficients expected to be $O(1)$, f is the decay constant of the σ-model, while m_* broadly indicates the mass scale of the top partners. Then, since Ψ is, ideally, the lightest top-partner we have $M_\Psi \lesssim m_*$. Given m_* and f, the measured values $v \equiv \langle h\rangle = 246$ GeV and $m_h = 125$ GeV, may require a tuning of a and b below their expected $O(1)$ size. More explicitly one finds

$$a = \frac{m_h^2}{m_*^2}\frac{4\pi^2}{3y_t^2} \simeq \left(\frac{430\,\text{GeV}}{m_*}\right)^2 \tag{3.0.3}$$

and, defining the top-partner coupling as $g_* \equiv m_*/f$ according to Ref. [20],

$$b = \frac{m_h^2}{m_t^2}\frac{2\pi^2}{3g_*^2} \simeq \frac{4}{g_*^2}. \tag{3.0.4}$$

By these equations we deduce that in the most natural scenario the top partners should not only be light (say below a TeV) but also not too strongly coupled. While of course the whole discussion is very qualitative, we still believe eqs. (3.0.3)-(3.0.4) give a valid rule of thumb for where the top partners should best be found. It is with eqs. (3.0.3)-(3.0.4) in mind that one should interpret the results of the searches for top partners. Notice that while naturalness favors sub-TeV fermionic resonances, electroweak precision constraints favor instead bosonic resonances above 2-3 TeV. A technically natural and viable model should therefore be more complex than a generic composite model described by a single scale. This situation closely resembles that of supersymmetric models, where the light squark families and the gluinos are pushed up by direct searches, while technical naturalness demands the stops to be as light as possible.

This Chapter is organized as follows. In Section 3.1 we discuss the structure of the models and their main features such as the mass spectrum and the couplings of the top partners. Then, in Section 3.2 we turn to analyse the phenomenology of the top partners, their production mechanisms and decay channels, highlighting the most relevant channels to focus LHC searches on. The bounds on the model parameters are derived in Section 3.3, using the LHC data available at present. Finally, in the Section 3.4 we present an estimate of the potential reach of the 14 TeV LHC on the top partners masses in two channels, characterized by the presence of two or three same sign leptons.

3.1 The Models

Our first goal is to develop a simplified description of the top partners, suited for studying the phenomenology of their production at the LHC. These simplified models should capture the robust features of more complete explicit constructions[1] or, better, of a putative general class of underlying theories. In particular, robust, and crucial, features are the pNGB nature of the Higgs and the selection rules associated with the small breaking of the corresponding global symmetry. We will see below that these features strongly constrain the structure of the spectrum and of the couplings of the top partners, similarly to what was found in Ref. [40] for the case of partial t_R compositeness.

We thus assume that the Higgs is the pNGB of the minimal coset SO(5)/SO(4) and construct Lagrangians that respect the non-linearly realized SO(5) invariance. We follow the standard CCWZ construction [22], whose detailed formulation for our coset is described in Appendix 1.7. The CCWZ methodology has been first employed to model the top partners in Ref. [95]. The central objects are the Goldstone boson 5×5 matrix U and the d_μ and e_μ symbols constructed out of U and its derivative. The top partner field Ψ has definite transformation properties under the unbroken SO(4) group. We will consider three cases, Ψ transforming in the $r_\Psi = \mathbf{9}$, $r_\Psi = \mathbf{4}$ or $r_\Psi = \mathbf{1}$ of SO(4).

In our construction the right-handed top quark t_R emerges as a chiral bound state of the strong dynamics. t_R must thus belong to a complete multiplet of the unbroken subgroup SO(4), and, given we do not want extra massless states, it must be a singlet. That does not yet fully specify its quantum numbers. This is because, in order to reproduce the correct hypercharge, one must enlarge the global symmetry by including an extra unbroken $\mathrm{U}(1)_X$ factor and define the hypercharge as $Y = T^3_R + X$, where T^3_R is the third $\mathrm{SU}(2)_R$ generator of SO(5).[2] Therefore the coset is actually $\mathrm{SO}(5) \times \mathrm{U}(1)_X / \mathrm{SO}(4) \times \mathrm{U}(1)_X$, t_R has X charge equal to 2/3 while the Higgs is X neutral (its hypercharge coincides with its T^3_R charge).

A second assumption concerns the coupling of the elementary fields, *i.e.* the SM gauge fields W_μ and B_μ and the elementary left-handed doublet $q_L = (t_L, b_L)$, to the strong sector [3]. The EW bosons are coupled by gauging the SM subgroup of $\mathrm{SO}(5) \times \mathrm{U}(1)_X$. The q_L is assumed to be coupled *linearly* to the strong sector, following the hypothesis of partial compositeness (see Section 1.4.1). In the UV Lagrangian this coupling has therefore the form

$$\mathcal{L}^{\rm UV}_{\rm mix} = y\, \overline{q}^\alpha_L \Delta^*_{\alpha\, I_\mathcal{O}} \mathcal{O}^{I_\mathcal{O}} + \text{h.c.} \equiv y \left(\overline{Q}_L\right)_{I_\mathcal{O}} \mathcal{O}^{I_\mathcal{O}} + \text{h.c.}\,, \tag{3.1.1}$$

where $\mathcal{O}$ is an operator of the strong sector that transforms in some representation $r_\mathcal{O}$ of $\mathrm{SO}(5) \times \mathrm{U}(1)_X$. The choice of $r_\mathcal{O}$ is, to some extent, free. Minimality, and the aim of reproducing explicit models considered in the literature, led us to consider two cases: $r_\mathcal{O} = \mathbf{5_{2/3}}$ and $\mathbf{r}_\mathcal{O} = \mathbf{14_{2/3}}$ [4]. Notice that the $\mathrm{U}(1)_X$ charge of the operators must be equal to the one of the t_R in order for the top mass to be generated after EWSB. In total, depending on whether the top partners will be in the $\mathbf{4_{2/3}}$ or in the $\mathbf{1_{2/3}}$ of the unbroken $SO(4)$, we will discuss four models named $\mathbf{M4}_5$, $\mathbf{M4}_{14}$ and

[1] See [71] for a complete calculable model with totally composite t_R, analogous holographic 5d models could be formulated following the approach of Ref. [15].

[2] See Appendix 1.7 for the explicit form of the generators.

[3] The light quark families and the leptons will not be considered here because their couplings are most likely very weak.

[4] Another possible option considered in the literature is $r_\mathcal{O} = \mathbf{4_{1/6}}$. However this option is not available once t_R is chosen to be a $SO(4)$ singlet: the top would not acquire a mass. It should also be remarked that, regardless of the nature of t_R, $r_\mathcal{O} = \mathbf{4_{1/6}}$ is disfavored when considering dangerous tree level corrections to the $Zb\bar{b}$ vertex [19, 41].

	$r_{\mathcal{O}} = \mathbf{5_{2/3}}$	$r_{\mathcal{O}} = \mathbf{14_{2/3}}$
$r_\Psi = \mathbf{9_{2/3}}$	–	$\mathbf{M9}_{14}$
$r_\Psi = \mathbf{4_{2/3}}$	$\mathbf{M4}_5$	$\mathbf{M4}_{14}$
$r_\Psi = \mathbf{1_{2/3}}$	$\mathbf{M1}_5$	$\mathbf{M1}_{14}$

Table 3.1: *The nomenclature of the five models considered in the present Chapter, defined by the choices of the representations* $r_\Psi, r_{\mathcal{O}}$.

$\mathbf{M1}_5$, $\mathbf{M1}_{14}$ respectively. The model with a light $\mathbf{9_{2/3}}$ will be called $\mathbf{M9}_{14}$. The classification of the various models is summarized in Table 3.1.

The explicit breakdown of $SO(5)$ due to y in eq. (3.1.1) gives rise to a leading contribution to the Higgs potential $V(h)$. However, in order to be able to tune the Higgs vacuum expectation value v to be much smaller that its natural scale f, one may need to tune among themselves contributions to $V(h)$ with a different functional dependence on h/f. In the case of $\mathbf{r}_{\mathcal{O}} = \mathbf{14_{2/3}}$, the top Yukawa seed y itself gives rise to two independent structures, whose coefficients can be so tuned that $v/f \ll 1$. On the other hand, in the case of $\mathbf{r}_{\mathcal{O}} = \mathbf{5_{2/3}}$, the leading contribution to the potential consist of just one structure $\propto \sin^2 h/f \cos^2 h/f$, with well defined, non-tunable, minima and maxima. In the latter case then, in order to achieve $v \ll f$, one should assume there exists an additional of $SO(5)$ breaking coupling whose contribution to the potential competes with that of the top. If this additional coupling does not involve the SM fields, which seems reasonable, then its contribution to V will arise at tree level. In order not to outcompete the top contribution, which arises at loop level, then this coupling should be so suppressed that its relative impact on strong sector quantities is of order $O(y^2/16\pi^2)$. The latter should be compared to the effects of relative size $(y/g_\Psi)^2$ induced at tree level by the mixing in eq. (3.1.1). We conclude that, even when an extra $SO(5)$ breaking coupling is needed, it is not likely to affect the phenomenology of top partners in a quantitatively significant way.

Now back to the top partners. Our choices of their quantum numbers correspond to those obtained in explicit constructions. However our choice could also be motivated on general grounds by noticing that the operators $\mathcal{O}$ interpolate for particles with the corresponding quantum numbers. By decomposing $\mathcal{O}$ under the unbroken SO(4) we obtain, respectively, $\mathbf{5_{2/3}} = \mathbf{4_{2/3}} + \mathbf{1_{2/3}}$ and $\mathbf{14_{2/3}} = \mathbf{4_{2/3}} + \mathbf{1_{2/3}} + \mathbf{9_{2/3}}$. In both cases we expect to find a $\mathbf{4_{2/3}}$ and/or a $\mathbf{1_{2/3}}$ in the low-energy spectrum. The top partners in the $\mathbf{9_{2/3}}$ instead appear only in the second case.

The coupling of eq. (3.1.1) breaks the $\mathrm{SO}(5) \times \mathrm{U}(1)_X$ symmetry explicitly, but it must of course respect the SM group. This fixes unambiguously the form of the tensor Δ and thus of the *embeddings*, $(Q_L)_{I_{\mathcal{O}}} = \Delta_{\alpha\, I_{\mathcal{O}}} q_L^\alpha$, of the elementary q_L in $\mathrm{SO}(5) \times \mathrm{U}(1)_X$ multiplets. For the $\mathbf{5}$ and the $\mathbf{14}$, respectively the fundamental and the two-indices symmetric traceless tensor, we have

$$\left(Q_L^{\mathbf{5}}\right)_I = \frac{1}{\sqrt{2}} \begin{pmatrix} ib_L \\ b_L \\ it_L \\ -t_L \\ 0 \end{pmatrix}, \qquad \left(Q_L^{\mathbf{14}}\right)_{I,J} = \frac{1}{\sqrt{2}} \begin{pmatrix} 0 & 0 & 0 & 0 & ib_L \\ 0 & 0 & 0 & 0 & b_L \\ 0 & 0 & 0 & 0 & it_L \\ 0 & 0 & 0 & 0 & -t_L \\ ib_L & b_L & it_L & -t_L & 0 \end{pmatrix}. \tag{3.1.2}$$

Though explicitly broken, the $\mathrm{SO}(5) \times \mathrm{U}(1)_X$ group still gives strong constraints on our theory.

Indeed the elementary-composite interactions of eq. (3.1.1) formally respect the symmetry provided we formally assign suitable transformation properties to the embeddings. Under $g \in \mathrm{SO}(5)$ we have

$$\left(Q_L^{\mathbf{5}}\right)_I \to g_I^{I'} \left(Q_L^{\mathbf{5}}\right)_{I'} , \qquad \left(Q_L^{\mathbf{14}}\right)_{I\,J} \to g_I^{I'} g_J^{J'} \left(Q_L^{\mathbf{14}}\right)_{I'\,J'} , \tag{3.1.3}$$

while the $\mathrm{U}(1)_X$ charge is equal to 2/3 in both cases. We will have to take into account this symmetry in our constructions.

3.1.1 Effective Lagrangians

Based on the symmetry principles specified above we aim at building phenomenological effective Lagrangians for the q_L, the composite t_R and the lightest top partner states Ψ. The basic idea is that our Lagrangians emerge from a "complete" theory by integrating out the heavier resonances in the strong sector. We thus need to rely on some qualitative description of the dynamics in order to estimate the importance of the various effective operators. We follow the "SILH" approach of Ref. [20] and characterize the heavy resonances in terms of a single mass scale m_* and of a single coupling $g_* = m_*/f$. As we already suggested in the introduction, parametrizing the strong sector in terms of a single scale is probably insufficient: a 125 GeV Higgs suggests that the mass scale of the fermionic resonances should be slightly lower than that of the vectors. For our purposes the relevant scale m_* should then be identified with the mass scale of the fermionic sector. We thus adopt the following power-counting rule (simplified compared to a more general expression (1.3.33) derived in the Chapter 1.2)

$$\mathcal{L} = \sum \frac{m_*^4}{g_*^2} \left(\frac{y\, q_L}{m_*^{3/2}}\right)^{n_{\rm el}} \left(\frac{g_* \Psi}{m_*^{3/2}}\right)^{n_{\rm co}} \left(\frac{\partial}{m_*}\right)^{n_\partial} \left(\frac{\Pi}{f}\right)^{n_\pi} , \tag{3.1.4}$$

where $\Pi = \Pi^{1,\dots,4}$ denotes the canonically normalized four real Higgs field components and f is the Goldstone decay constant. Notice the presence of the coupling y that accompanies (due to eq. (3.1.1)) each insertion of the elementary q_L. Analogously the operators involving the SM gauge fields, omitted for shortness from eq. (3.1.4), should be weighted by $g_{\rm SM}/m_*$. The t_R is completely composite and therefore it obeys the same power-counting rule as the top partner field Ψ.

Two terms in our effective Lagrangian will *violate* the power-counting. One is the kinetic term of the elementary fields, which we take to be canonical, while eq. (3.1.4) would assign it a smaller coefficient, $(y/g_*)^2$ in the case of fermions and $(g/g_*)^2$ in the case of gauge fields. This is because the elementary field kinetic term does not emerge from the strong sector, it was already present in the UV Lagrangian with $\mathcal{O}(1)$ coefficient. Indeed it is precisely because their kinetic coefficient is bigger than what established in eq. (3.1.4), that the elementary fields have a coupling weaker than g_*. The other term violating power-counting is the *mass* of the top partners, which we denote by M_Ψ. We assume $M_\Psi < m_*$ in order to justify the construction of an effective theory in which only the top partners are retained while the other resonances are integrated out. The ratio M_Ψ/m_* is our expansion parameter. We will therefore obtain accurate results only in the presence of a large separation, $M_\Psi \ll m_*$, among the lightest state and the other resonances. However already for a moderate separation, $M_\Psi \lesssim m_*$, or even extrapolating towards $M_\Psi \simeq m_*$, our models should provide a valid qualitative description of the relevant physics. Nevertheless for a more careful study of the case of small separation our setup should be generalized by incorporating more resonances in the effective theory.

Top Partners in the Fourplet

First we consider models $\mathbf{M4}_5$ and $\mathbf{M4}_{14}$, in which the top partners are in the $\mathbf{4_{2/3}}$. In this case the top partner field is

$$\Psi = \frac{1}{\sqrt{2}} \begin{pmatrix} iB - iX_{5/3} \\ B + X_{5/3} \\ iT + iX_{2/3} \\ -T + X_{2/3} \end{pmatrix} , \tag{3.1.5}$$

and it transforms, following CCWZ, as

$$\Psi_i \to h(\Pi; g)_i^{\ j} \Psi_j \, , \tag{3.1.6}$$

under a generic element g of SO(5). The 4×4 matrix h is defined by eq.s (1.7.7) and (1.7.8) and provides a non-linear representation of the full SO(5). The four Ψ components decompose into two SM doublets (T, B) and $(X_{5/3}, X_{2/3})$ of hypercharge 1/6 and 7/6 respectively. The first doublet has therefore the same quantum numbers as the (t_L, b_L) doublet while the second one contains a state of exotic charge 5/3 plus another top-like quark $X_{2/3}$.

When the q_L is embedded in the $\mathbf{5_{2/3}}$, *i.e.* in model $\mathbf{M4}_5$, the leading order Lagrangian is

$$\begin{aligned} \mathscr{L}^{\mathbf{M4}_5} \;=\; & i\,\bar{q}_L \not{D}\, q_L + i\,\bar{t}_R \not{D}\, t_R + i\,\bar{\Psi}(\not{D} + i\not{e})\Psi - M_\Psi \bar{\Psi}\Psi \\ & + \left[i\,c_1 \left(\bar{\Psi}_R\right)_i \gamma^\mu d_\mu^i \, t_R + y f \, (\overline{Q}_L^{\mathbf{5}})^I U_{I\,i} \, \Psi_R^i + y\, c_2 f \, (\overline{Q}_L^{\mathbf{5}})^I U_{I\,5} \, t_R + \text{h.c.} \right] , \end{aligned} \tag{3.1.7}$$

where $c_{1,2}$ are coefficients expected to be of order 1. The above Lagrangian with totally composite t_R was first written in Ref. [95]. Notice the presence of the $\not{e} = e_\mu \gamma^\mu$ term which accompanies the derivative of the top partner field: it reconstructs the CCWZ covariant derivative and is essential to respect $SO(5)$ (explicit expression for the d and e symbols are given in the Appendix of the Chapter 1.2). In the second line of the equation above we find, first of all, a *direct* interaction, not mediated by the coupling y, among the composite t_R and the top partners. This term is entirely generated by the strong sector and would have been suppressed in the case of partial t_R compositeness. It delivers, looking at the explicit form of d_μ in eq. (1.7.13), couplings involving the top, the partners and the SM gauge fields. These will play an important role in the single production and in the decay of the top partners. The last two terms give rise, in particular, to the top quark mass but also to trilinear couplings contributing to the single production of top partners. Notice that the indices of the embedding $Q_L^{\mathbf{5}}$ *can not* be contracted directly with those of Ψ because they live in different spaces. The embeddings transform linearly under SO(5) as reported in eq. (3.1.3) while Ψ transforms under the non-linear representation h. For this reason one insertion of the Goldstone matrix, transforming according to eq. (1.7.7), is needed.

For brevity we omitted from eq. (3.1.7) the kinetic term of the gauge fields and of the Goldstone Higgs. Moreover we have not yet specified the covariant derivatives D_μ associated with the SM gauge group, these are obviously given by

$$D_\mu q_L = \left(\partial_\mu - i g W_\mu^i \frac{\sigma^i}{2} - i \frac{1}{6} g' B_\mu - i\, g_S G_\mu \right) q_L \, , \tag{3.1.8}$$

$$D_\mu t_R = \left(\partial_\mu - i \frac{2}{3} g' B_\mu - i\, g_S G_\mu \right) t_R \, , \tag{3.1.9}$$

$$D_\mu \Psi = \left(\partial_\mu - i \frac{2}{3} g' B_\mu - i\, g_S G_\mu \right) \Psi \, . \tag{3.1.10}$$

where g, g' and g_S are the $\mathrm{SU}(2)_L \times \mathrm{U}(1)_Y$ and $\mathrm{SU}(3)_c$ gauge couplings. We remind the reader that the top partners form a color triplet, hence the gluon in the above equation.

The Lagrangian is very similar for model $\mathbf{M4}_{14}$, where the q_L is embedded in the symmetric traceless $Q_L^{\mathbf{14}}$. We have

$$\begin{aligned}\mathscr{L}^{\mathbf{M4}_{14}} &= i\,\bar{q}_L \not{D}\, q_L + i\,\bar{t}_R \not{D}\, t_R + i\,\bar{\Psi}(\not{D} + i\not{e})\Psi - M_\Psi \bar{\Psi}\Psi \\ &+ \Big[i\,c_1 \left(\bar{\Psi}_R\right)_i \gamma^\mu d_\mu^i\, t_R + y f\, (\overline{Q}_L^{\mathbf{14}})^{I\,J} U_{I\,i} U_{J\,5}\, \Psi_R^i + \frac{y c_2}{2} f\, (\overline{Q}_L^{\mathbf{14}})^{I\,J} U_{I\,5} U_{J\,5}\, t_R + \text{h.c.}\Big] \end{aligned} \tag{3.1.11}$$

notice that the two indices of $Q_L^{\mathbf{14}}$ are symmetric and therefore the term that mixes it with Ψ is unique. The factor $\frac{1}{2}$ introduced in the last term is merely conventional.

In both models $\mathbf{M4}_5$ and $\mathbf{M4}_{14}$ the leading order Lagrangian contains four parameters, $\{M_\psi$, y, c_1, $c_2\}$, on top of the Goldstone decay constant f. One parameter will however have to be fixed to reproduce the correct top mass, while the remaining three parameters could be traded for two physical masses, for instance $m_{X_{5/3}}$ and m_B, and the coupling c_1. It will often be convenient to associate the mass M_Ψ with a coupling g_ψ

$$g_\Psi \equiv \frac{M_\Psi}{f}\,.$$

We will see below that $c_1 \times g_\Psi$ controls the strength of the interactions between the top partners and the Goldstone bosons at energy $\sim M_\Psi$. In particular it controls the on-shell couplings relevant for single production and for two body decays. Notice that, as a function of energy, the effective strength of this trilinear interaction is instead $\sim c_1 E/f$. For $c_1 = O(1)$, as suggested by power counting, the effective coupling is of order $g_* \equiv m_*/f$ at the energy scale of the heavier resonances, in accord with the principle of partial UV completion proposed in Ref. [67]. Power counting and partial UV completion then equivalently imply $c_1 = O(1)$ and therefore $c_1 g_\Psi < g_*$. This result obviously follows from the fact that the Higgs is a derivatively coupled pNGB. It would be lost if the Higgs was instead treated as a generic resonance. In the latter case the expected coupling would be independent of the mass and it would be larger, of order g_*. Moreover notice that, although on shell it leads to an effective Yukawa vertex, the interaction associated with c_1 does not affect the spectrum when H acquires a vacuuum expectation value. That again would not be true if we did not account for the pNGB nature of H. The pNGB nature of H is not accounted for in the first thorough work on simplified top partner models [52] and in the following studies (see in particular [53, 74]).

Notice that, a priori, one of the four parameters describing the simplified model could be complex. This is because we have at our disposal only 3 chiral rotations to eliminate the phases from the Lagrangians (3.1.7) and (3.1.11). Nevertheless we are entitled to keep all the parameters real if we demand the strong sector respects a CP symmetry. It is easy to check that CP requires the non-derivative couplings to be real while the coefficient of the term involving to d_μ must be purely imaginary. CP conservations is an additional hypothesis of our construction, however the broad phenomenology does not significantly depend on it.

Top Partners in the Singlet

The Lagrangian is even simpler if the top partners are in the $\mathbf{1}_{\mathbf{2/3}}$. In this case we only have one exotic top-like state which we denote as $\widetilde{T}$. For the two models, $\mathbf{M1}_5$ and $\mathbf{M1}_{14}$ that we aim to

consider the Lagrangian reads, respectively

$$\begin{aligned}
\mathscr{L}^{\mathbf{M1}_5} &= \bar{q}_L\, i\not{D}\, q_L + \bar{t}_R\, i\not{D}\, t_R + i\bar{\Psi} i\not{D}\Psi - M_\Psi \bar{\Psi}\Psi \\
&+ \left[y f\, (\overline{Q}_L^{\mathbf{5}})^I U_{I\,5} \Psi_R + y\, c_2 f\, (\overline{Q}_L^{\mathbf{5}})^I U_{I\,5}\, t_R + \text{h.c.} \right] , \\
\mathscr{L}^{\mathbf{M1}_{14}} &= \bar{q}_L\, i\not{D}\, q_L + \bar{t}_R\, i\not{D}\, t_R + i\bar{\Psi} i\not{D}\Psi - M_\Psi \bar{\Psi}\Psi \\
&+ \left[\frac{y}{2} f\, (\overline{Q}_L^{\mathbf{14}})^{I\,J} U_{I\,5} U_{J\,5} \Psi_R + \frac{y\, c_2}{2} f\, (\overline{Q}_L^{\mathbf{14}})^{I\,J} U_{I\,5} U_{J\,5}\, t_R + \text{h.c.} \right] .
\end{aligned} \tag{3.1.12}$$

Notice that we could have also written a direct mixing among t_R and Ψ because the two fields now have identical quantum numbers. However this mixing can obviously be removed by a field redefinition. Models $\mathbf{M1}_5$ and $\mathbf{M1}_{14}$, apart from f, contain three parameters, $\{M_\psi,\, y,\, c_2\}$, one of which must again be fixed to reproduce the top mass. We are left with two free parameters that correspond to the coupling c_2 and to the mass $m_{\widetilde{T}}$ of the partners. Notice that in this case all the parameters can be made real by chiral rotations without need of imposing the CP symmetry. The latter symmetry is automatically respected in models $\mathbf{M1}_5$ and $\mathbf{M1}_{14}$.

Top Partners in the Nine-plet

The components of the nine-plet can be further divided according to how they transform under the SM gauge group: three triplets of $SU(2)_L$

$$\Psi \supset \{X_{8/3}, X_{5/3}, X_{2/3}\},\ \{Y_{5/3}, Y_{2/3}, Y_{\text{-}1/3}\},\ \{Z_{2/3}, Z_{\text{-}1/3}, Z_{\text{-}4/3}\}, \tag{3.1.13}$$

separated according to their $T^3_R = +1, 0, -1$. The subscript denotes the electric charge of the states. The full SO(4) nine-plet Ψ can be written as a 4×4 block of the full 5×5 matrix (the representation is symmetric and elements in the upper diagonal have been omitted for clarity)

$$\frac{1}{2}\begin{pmatrix}
-X_{8/3} + Y_{2/3} - Z_{\text{-}4/3} & & & \\
i Z_{\text{-}4/3} - i X_{8/3} & X_{8/3} + Y_{2/3} + Z_{\text{-}4/3} & & \\
\frac{X_{5/3}}{\sqrt{2}} - \frac{Y_{\text{-}1/3}}{\sqrt{2}} + \frac{Y_{5/3}}{\sqrt{2}} - \frac{Z_{\text{-}1/3}}{\sqrt{2}} & \frac{iX_{5/3}}{\sqrt{2}} + \frac{iY_{\text{-}1/3}}{\sqrt{2}} + \frac{iY_{5/3}}{\sqrt{2}} + \frac{iZ_{\text{-}1/3}}{\sqrt{2}} & -X_{2/3} - Y_{2/3} - Z_{2/3} & \\
-\frac{iX_{5/3}}{\sqrt{2}} + \frac{iY_{\text{-}1/3}}{\sqrt{2}} + \frac{iY_{5/3}}{\sqrt{2}} - \frac{iZ_{\text{-}1/3}}{\sqrt{2}} & \frac{X_{5/3}}{\sqrt{2}} + \frac{Y_{\text{-}1/3}}{\sqrt{2}} - \frac{Y_{5/3}}{\sqrt{2}} - \frac{Z_{\text{-}1/3}}{\sqrt{2}} & iX_{2/3} - iZ_{2/3} & X_{2/3} - Y_{2/3} + Z_{2/3}
\end{pmatrix} \tag{3.1.14}$$

The Lagrangian of the model reads

$$\begin{aligned}
\mathscr{L}^{\mathbf{M9}_{14}} &= i\,\bar{q}_L\, \not{D}\, q_L + i\,\bar{t}_R\, \not{D}\, t_R + i\,\bar{\Psi}^{i\,j}_L (\not{D} + 2i\not{e}^a T^{j\,k}_a) \Psi^{k\,i}_L - M_\Psi\, \bar{\Psi}\Psi \\
&+ c_1 y f\, (\overline{Q}_L^{\mathbf{14}})^{I\,J} U_{I\,i} U_{J\,j} \Psi^{i\,j}_R + y f\, (\overline{Q}_L^{\mathbf{14}})^{I\,J} U_{I\,5} U_{J\,5} t_R \\
&+ \frac{f^2}{4}\, d^i_\mu d^{\mu\,i} + \frac{c_2}{m_*}\, \Psi^{i\,j}_L d^i_\mu d^{\mu\,j} t_R\,,
\end{aligned} \tag{3.1.15}$$

where i and I are $SO(4)$ and $SO(5)$ indices respectively, and $a = 1...6$ enumerates the $SO(4)$ generators T^a. Here the second line includes the linear mixings between the elementary fermions and the strong sector resonances, as implied by partial compositeness. The last term of the lagrangian, despite being suppressed by a cutoff m_* will play an important role in the top partners decays. As we see from the above lagrangian, the model $\mathbf{M9}_{14}$ contains five free parameters $\{M_\psi,\, y,\, c_1,\, c_2,\, M_*\}$. The y can be used to fix the top mass, the M_ψ controls the mass of the lightest partners, c_1 – their leading couplings to the SM fermions and c_2 – the first subleading coupling between composites and

the t_R. According to adopted power counting, the coefficients c_1 and c_2 are expected to be of the order 1.

In order to complete the definition of our models let us discuss the theoretically expected size of their parameters. From the discussion in the introduction and from experience with concrete models, one can reasonably argue that the favorite range for M_Ψ is between 500 GeV and 1.5 TeV, while g_Ψ is favored in the range $1 \lesssim g_\Psi \lesssim 3$. It is also worth recalling the favorite range of the decay constant $f \equiv M_\Psi/g_\Psi$, which is conveniently traded for the parameter ξ defined in Ref. [15]

$$\xi = \frac{v^2}{f^2}\,, \tag{3.1.16}$$

where $v = 2m_W/g = 246$ GeV is the EWSB scale. Since ξ controls the deviation from the SM at low energies it cannot be too large. Electroweak precision tests suggest $\xi \simeq 0.2$ or $\xi \simeq 0.1$, which corresponds to $f \simeq 500$ GeV or $f \simeq 800$ GeV. Smaller values of ξ would of course require more tuning. Finally, the strength of the elementary-composite coupling y is fixed by the need of reproducing the correct mass of the top quark. We will see in the following section that this implies $y \sim y_t = 1$.

3.1.2 A First Look at the Models

Now that the models are defined let us start discussing their implications. The simplest aspects will be examined in the present section while a more detailed analysis of their phenomenology will be postponed to the following one.

The Spectrum

We start from model $\mathbf{M4}_5$ and we first focus on the fermionic spectrum. The mass-matrix after EWSB is easily computed form eqs. (3.1.7) and (3.1.2) by using the explicit form of U on the Higgs VEV obtained from eq. (1.7.12). By restricting to the sector of 2/3-charged states we find

$$\begin{pmatrix} \bar{t}_L \\ \bar{T}_L \\ \overline{X}_{2/3\,L} \end{pmatrix}^T \begin{pmatrix} -\frac{c_2 y f}{\sqrt{2}} \sin\epsilon & y f \cos^2\frac{\epsilon}{2} & y f \sin^2\frac{\epsilon}{2} \\ 0 & -M_\psi & 0 \\ 0 & 0 & -M_\psi \end{pmatrix} \begin{pmatrix} t_R \\ T_R \\ X_{2/3\,R} \end{pmatrix}\,, \tag{3.1.17}$$

where $\epsilon = \langle h \rangle / f$ is defined as the ratio among the VEV of the Higgs field and the Goldstone decay constant. The relation among $\langle h \rangle$ and the EWSB scale is reported in eq. (1.3.16), from which we derive

$$\xi = \frac{v^2}{f^2} = \sin^2\epsilon\,. \tag{3.1.18}$$

We immediately notice a remarkable feature of the mass-matrix (3.1.17): only the *first line*, *i.e.* the terms which involve the t_L, is sensitive to EWSB while the rest of the matrix remains unperturbed. This is due to the fact that the Higgs is a pNGB and therefore its non-derivative interactions can only originate from the breaking of the Goldstone symmetry SO(5). The SO(5) invariant terms just produce derivative couplings of the Higgs and therefore they cannot contribute to the mass-matrix. Since the Goldstone symmetry is broken exclusively by the terms involving the elementary q_L it is obvious that the mass-matrix must have the form of eq. (3.1.17). Notice that this structure would

have been lost if we had not taken into account the pNGB nature of the Higgs. Indeed if we had treated the Higgs as a generic composite SO(4) fourplet, Yukawa-like couplings of order g_* and involving t_R and Ψ would have been allowed. After EWSB those terms would have given rise to $(2,1)$ and $(3,1)$ mass matrix entries of order $g_* v$.

The peculiar structure of the mass-matrix has an interesting consequence. It implies that only one linear combination of T and $X_{2/3}$, with coefficients proportional to the $(1,2)$ and $(1,3)$ entries, mixes with the q_L, while the orthogonal combination does not mix either with the q_L or with any other state. Explicitly, the two combinations are

$$\begin{aligned} T' = &\quad \frac{1}{\sqrt{\cos^4\frac{\epsilon}{2}+\sin^4\frac{\epsilon}{2}}}\left[\cos^2\frac{\epsilon}{2}T+\sin^2\frac{\epsilon}{2}X_{2/3}\right], \\ {X_{2/3}}' = &\quad \frac{1}{\sqrt{\cos^4\frac{\epsilon}{2}+\sin^4\frac{\epsilon}{2}}}\left[\cos^2\frac{\epsilon}{2}X_{2/3}-\sin^2\frac{\epsilon}{2}T\right]. \end{aligned} \tag{3.1.19}$$

After this field redefinition the mass-matrix becomes block-diagonal

$$\begin{pmatrix} \bar{t}_L \\ \overline{T}'_L \\ \overline{X}'_{2/3\,L} \end{pmatrix}^T \begin{pmatrix} -\frac{c_2 y f}{\sqrt{2}}\sin\epsilon & y f\sqrt{\cos^4\frac{\epsilon}{2}+\sin^4\frac{\epsilon}{2}} & 0 \\ 0 & -M_\psi & 0 \\ 0 & 0 & -M_\psi \end{pmatrix} \begin{pmatrix} t_R \\ T'_R \\ X'_{2/3\,R} \end{pmatrix}, \tag{3.1.20}$$

so that the state $X'_{2/3}$ is already a mass eigenstate with mass $m_{X_{2/3}} = M_\Psi$. But the spectrum also contains a second particle with exactly the same mass. Indeed the $X_{5/3}$ cannot mix because it is the only state with exotic charge and therefore it maintains the mass $m_{X_{5/3}} = M_\Psi$ it had before EWSB. The $X_{2/3}$ and the $X_{5/3}$ are thus *exactly degenerate*. This remarkable property is due to the pNGB nature of the Higgs and it would be generically violated, as previously discussed, if this assumption was relaxed. This result also depends on t_R being a composite singlet. If t_R was instead a partially composite state mixing to a non-trivial representation of $SO(5)$ (for instance a $\mathbf{5}$) there would be additional entries in the mass matrix. [5] In a sense our result depends on y being the only relevant parameter that breaks $SO(5)$ explicitly.

Once the mass-matrix has been put in the block-diagonal form of eq. (3.1.20) it is straightforward to diagonalize it and to obtain exact formulae for the rotation matrices and for the masses of the top and of the T partner. However the resulting expressions are rather involved and we just report here approximate expressions for the masses. We have

$$\begin{aligned} m_t \simeq &\quad \frac{c_2 y f}{\sqrt{2}}\frac{g_\Psi}{\sqrt{g_\Psi^2+y^2}}\sin\epsilon, \\ m_T \simeq &\quad \sqrt{M_\Psi^2+y^2 f^2}\left[1-\frac{y^2\left(g_\Psi^2+(1-c_2^2)y^2\right)}{4\left(g_\Psi^2+y^2\right)^2}\sin^2\epsilon\right]. \end{aligned} \tag{3.1.21}$$

From the above equation we obtain the correct order of magnitude for the top mass if, as anticipated, $y \sim y_t$ and $g_\Psi \gtrsim 1$. In this region of the parameter space the corrections to the approximate formulae are rather small, being suppressed by both a factor y^2/g_Ψ^2 (which is preferentially smaller than one) and by $\xi \ll 1$. However we will consider departures from this theoretically expected region and therefore we will need to use the exact formulae in the following sections.

[5] The top partner's spectrum with partially composite t_R has been worked out in Ref. [6, 40].

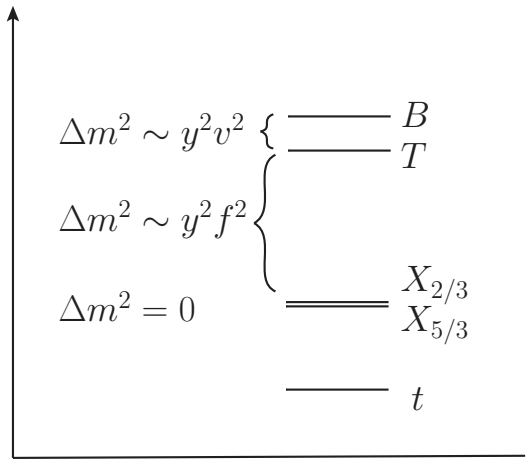

Figure 3.2: *The typical spectrum of the top partners in the four-plet.*

Similarly we can study the sector of $-1/3$ charge states. It contains a massless b_L, because we are not including the b_R in our model, plus the heavy B particle with a mass

$$m_B = \sqrt{M_\Psi^2 + y^2 f^2}\,. \tag{3.1.22}$$

This formula is exact and shows that the bottom sector does not receive, in this model, any contribution from EWSB. By comparing the equation above with the previous one we find that the splitting among T and B is typically small

$$m_B^2 - m_T^2 \simeq y^2 f^2 \frac{g_\Psi^2 + (1-c_2^2)y^2}{2\left(g_\Psi^2 + y^2\right)} \sin^2\epsilon\,, \tag{3.1.23}$$

and positive in the preferred region $g_\Psi > y$, although there are points in the parameter space where the ordering $m_T > m_B$ can occur. The splitting among the two doublets is instead always positive, $m_B^2 - m_{X_{5/3}}^2 = y^2 f^2$. The typical spectrum of the top partners that we have in our model is depicted in figure 3.2.

The situation is not much different in model $\mathbf{M4}_{14}$. The mass-matrix for charge 2/3 states has again the form of eq. (3.1.17) and again it can be put in a block-diagonal form by a rotation among the T and the $X_{2/3}$ similar to the one in eq. (3.1.19). Therefore also in model $\mathbf{M4}_{14}$ the physical $X_{2/3}$ has mass M_Ψ and it is degenerate with the $X_{5/3}$. The approximate top and T mass are given in this case by

$$\begin{aligned} m_t &\simeq \frac{c_2 y\, f}{\sqrt{2}} \frac{g_\Psi}{\sqrt{g_\Psi^2 + y^2}} \frac{\sin 2\epsilon}{2}\,, \\ m_T &\simeq \sqrt{M_\Psi^2 + y^2 f^2}\left[1 - \frac{y^2\left(5g_\Psi^2 + (5-c_2^2)y^2\right)}{4\left(g_\Psi^2 + y^2\right)^2}\sin^2\epsilon\right]. \end{aligned} \tag{3.1.24}$$

Similarly we can compute the mass of the B partner and we find

$$m_B = \sqrt{M_\Psi^2 + y^2 f^2 \cos^2\epsilon} \simeq \sqrt{M_\Psi^2 + y^2 f^2} - \frac{y^2 f^2}{2\sqrt{M_\Psi^2 + y^2 f^2}} \sin^2\epsilon\,. \tag{3.1.25}$$

In this case, differently from model $\mathbf{M4}_5$ (see eq. (3.1.22)), the mass of the B is sensitive to EWSB. Apart from this little difference the spectrum is very similar to the one of model $\mathbf{M4}_{14}$ described in figure 3.2.

The models with the singlet are much simpler because there is only one exotic state. The mass matrices read:

$$\begin{pmatrix} \bar{t}_L \\ \widetilde{\bar{T}}_L \end{pmatrix}^T \begin{pmatrix} -\frac{c_2 y f}{\sqrt{2}} \sin\epsilon & -\frac{y f}{\sqrt{2}} \sin\epsilon \\ 0 & -M_\psi \end{pmatrix} \begin{pmatrix} t_R \\ \widetilde{T}_R \end{pmatrix} , \tag{3.1.26}$$

$$\begin{pmatrix} \bar{t}_L \\ \widetilde{\bar{T}}_L \end{pmatrix}^T \begin{pmatrix} -\frac{c_2 y f}{2\sqrt{2}} \sin 2\epsilon & -\frac{y f}{2\sqrt{2}} \sin 2\epsilon \\ 0 & -M_\psi \end{pmatrix} \begin{pmatrix} t_R \\ \widetilde{T}_R \end{pmatrix} , \tag{3.1.27}$$

for models $\mathbf{M1}_5$ and $\mathbf{M1}_{14}$ respectively. The mass eigenvalues for model $\mathbf{M1}_5$ are

$$\begin{aligned} m_t &\simeq \frac{c_2 y f}{\sqrt{2}} \sin\epsilon \,, \\ m_{\widetilde{T}} &\simeq M_\Psi \left[1 + \frac{y^2}{4 g_\Psi^2} \sin^2\epsilon \right] . \end{aligned} \tag{3.1.28}$$

For model $\mathbf{M1}_{14}$ instead we have

$$\begin{aligned} m_t &\simeq \frac{c_2 y f}{2\sqrt{2}} \sin 2\epsilon \,, \\ m_{\widetilde{T}} &\simeq M_\Psi \left[1 + \frac{y^2}{4 g_\Psi^2} \sin^2\epsilon \right] . \end{aligned} \tag{3.1.29}$$

As one can see from the last expressions the mass of the $\widetilde{T}$ receives positive contributions proportional to y^2 and hence for a fixed mass of the $\widetilde{T}$, y must be limited from above. Unlike the models with fourplet partners, in the singlet case y completely controls the couplings of the $\widetilde{T}$ with the top and bottom quarks (see Sec. 3.2.2). Therefore one can expect that for a given $m_{\widetilde{T}}$ there exists a maximal allowed coupling of the SM particles with the top partner and hence for small masses the single production of $\widetilde{T}$ is suppressed. In addition small values of $m_{\widetilde{T}}$ become unnatural since they require very small y together with a very large c_2 needed to recover correct top mass. By minimizing the largest eigenvalue of the mass matrix with respect to M_Ψ for fixed y and f one can find a minimal allowed mass of the $\widetilde{T}$ which is given by

$$\begin{aligned} m_{\widetilde{T}}^{\text{min, } \mathbf{M1}_5} &= m_t + \frac{1}{\sqrt{2}} y f \sin\epsilon \,, \\ m_{\widetilde{T}}^{\text{min, } \mathbf{M1}_{14}} &= m_t + \frac{1}{2\sqrt{2}} y f \sin 2\epsilon \,, \end{aligned} \tag{3.1.30}$$

for the models $\mathbf{M1}_5$ and $\mathbf{M1}_{14}$ respectively.

The spectrum of the model $\mathbf{M9}_{14}$ is much reacher but at the same time very compressed and the masses are mostly determined by the parameter M_Ψ. The reason is that the only distortion of the $SO(4)$ symmetric spectrum comes from the mixings with the SM states with a half-integer isospin, while the nine-plet members have integer isospin quantum numbers. Hence their mixing necessarily involves the Higgs VEV and is therefore suppressed. We will not report the full mass matrices for the charge 2/3 and -1/3 states and will only mention that they possess a similar form

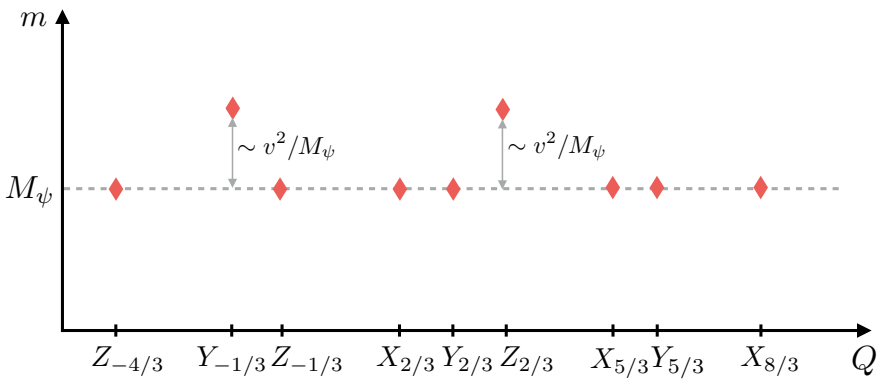

Figure 3.3: *Mass spectrum of the new heavy states present in a model with* $(\mathbf{3},\mathbf{3})_{2/3}$.

to the eq. (3.1.17) and therefore some of the mass eigenvalues are solely defined by M_Ψ. The masses of the charge 2/3 states expanded in ϵ are given by

$$\begin{aligned} m_t &\simeq yv\,, \\ m_{X_{2/3}} &\simeq M_\Psi\left(1+\frac{5c_1^2y^2\epsilon^2}{4g_\Psi^2}\right)\,, \\ m_{Y_{2/3}} &= M_\Psi\,, \\ m_{Z_{2/3}} &= M_\Psi\,. \end{aligned} \tag{3.1.31}$$

For the charge -1/3 we have one massless bottom quark (because we neglected the bottom partners) and two states with masses

$$\begin{aligned} m_{Y_{-1/3}} &\simeq M_\Psi\left(1+\frac{c_1^2y^2\epsilon^2}{g_\Psi^2}\right)\,, \\ m_{Z_{-1/3}} &= M_\Psi. \end{aligned} \tag{3.1.32}$$

The masses of charge -4/3, 5/3 and 8/3 states are all equal to M_Ψ because they don't have the elementary partners to mix with. The schematic representation of the mass spectrum is given on the Fig. 3.3.

3.2 Top Partners Phenomenology

Let us now turn to discuss the main production mechanisms and decay channels of the top partners in the models under consideration. We will first of all, in sect. 3.2.1, describe how the cross-sections of the production processes can be conveniently parametrized analytically in terms of few universal functions, extracted from the Monte Carlo integration. This method, supplemented with tree-level event simulations to compute the acceptances associated with the specific cuts of each experimental search, will allow us to explore efficiently the multi-dimensional parameter space of our model avoiding a time-consuming scan. In sect. 3.2.2 we will present an estimate of the various processes based on the use of the Goldstone boson Equivalence Theorem [77], this will allow us to classify (in sect. 3.2.3) the channels which are more promising for the search of the top partners at the LHC.

M	7 TeV	8 TeV	14 TeV
600	92.3	168.7	1459
700	29.0	56.40	581.4
800	9.88	20.53	254.3
900	3.55	7.943	119.4
1000	1.33	3.213	59.21
1100	0.507	1.341	30.68
1200	0.196	0.573	16.47

M	8 TeV	14 TeV
1300	0.248	9.101
1400	0.108	5.149
1500	0.047	2.971
1600	0.020	1.743
1700	0.009	1.036
1800	0.004	0.623
1900	0.001	0.378

Table 3.2: *NNLO pair production cross-section of heavy colored fermions in fb, at* $\sqrt{s} = 7, 8, 14$ *TeV, calculated using the HATHOR code [81], using MSTW2008 parton distribution functions (PDF) [?].*

3.2.1 Production and Decay

Given that the partners are colored they can be produced in pairs through the QCD interactions. The pair production cross-section is universal for all the partners and it can be parametrized by a function

$$\sigma_{\text{pair}}(m_X)\,, \tag{3.2.1}$$

which depends uniquely on the partner's mass m_X, for which we have analytical formulae. We have constructed σ_{pair} by interpolation using the HATHOR code [81] which incorporates perturbative QCD corrections up to NNLO. The values of the cross-section used in the fit are reported in Table 3.2 for the LHC at 7, 8 and 14 TeV center of mass energy. In this and all the other simulations we adopted the set of parton distribution functions MSTW2008 [82].

The other relevant process is the single production of the top partners in association with either a top or a bottom quark. This originates, as depicted in Figure 3.4, from a virtual EW boson $V = \{W^{\pm}, Z\}$ emitted from a quark line which interacts with a gluon producing the top partner and one third-family anti-quark. The possible relevance of single production was first pointed out in Ref. [78]. The relevant couplings have the form

$$g_{Xt_R}\overline{X}_R \not{V} t_R + g_{Xt_L}\overline{X}_L \not{V} t_L + g_{Xb_L}\overline{X}_L \not{V} b_L\,, \tag{3.2.2}$$

where X denotes generically any of the top partners apart from the $X_{8/3}$, for which this type of interactions is forbidden by a charge conservation [6]. At each vertex the EW boson V is understood to be the one of appropriate electric charge. Notice that there is no vertex with the b_R because the latter state is completely decoupled in our model, we expect this coupling to be negligible even in more complete constructions.

It is important to outline that the couplings g_{Xt_R}, g_{Xt_L} and g_{Xb_L} can be computed analytically in our models. They arise from the interactions reported in the Section 3.1.1 after performing the rotation to the physical basis of mass eigenstates. Since the rotation matrices can be expressed in a closed form, the explicit formulae for the couplings are straightforwardly derived. The result is

[6] The vertex of the type $\bar{t} W_\mu W^\mu X_{8/3}$ can mediate the single production of the $X_{8/3}$ either via $W^+ t \to X_{8/3} W^-$ or via $W^+ W^+ \to X_{8/3}\bar{t}$. However, beside being suppressed by the scale Λ, the corresponding production cross section pays additional weak coupling suppression or a suppression due to more final states compared to the usual single production, therefore we don't expect it to have a comparable rate with a pair production and we will neglect it.

Figure 3.4: *The single-production diagrams.*

rather involved and for this reason it will not be reported here, however it is easily implemented in a *Mathematica* package.

The single production cross-sections are quadratic polynomials in the couplings, with coefficients that encapsulate the effect of the QCD interactions, the integration over the phase-space and the convolution with the parton distribution functions. These coefficients depend uniquely on the mass of the partner and can be computed by Monte Carlo integration. Once the latter are known we obtain semi-analytical formulae for the cross-sections. The production in association with the $\bar{b}$ is simply proportional to $g^2_{Xb_L}$ while the one with $\bar{t}$ would be, a priori, the sum of three terms proportional to $g^2_{Xt_L}$, $g^2_{Xt_R}$ and $g_{Xt_L}\cdot g_{Xt_R}$ which account, respectively, for the effect of the left-handed coupling, of the right-handed one and of the interference among the two. However in the limit of massless top quark, $m_t \ll m_X$, the processes mediated by the left-handed and by the right-handed couplings become physically distinguishable because the anti-top produced in association with X will have opposite chirality in the two cases. Therefore the interference term should be suppressed by m_t divided by a characteristic energy of the process – the mass of the top partner. The coefficients of the ${g_{Xt_L}}^2$ and ${g_{Xt_R}}^2$ terms will be equal because the QCD interactions are invariant under parity. Thus the cross-sections will be very simply parametrized as

$$\begin{aligned}
\sigma_{\rm sing}(X\bar{t}) &= \left[(g_{Xt_L})^2 + (g_{Xt_R})^2\right]\sigma_{Vt}(m_X) + 2\,g_{Xt_L}\,g_{Xt_R}\left(\frac{m_t}{m_X}\right)\sigma'_{Vt}(m_X)\,,\\
\sigma_{\rm sing}(X\bar{b}) &= (g_{Xb_L})^2\,\sigma_{Vb}(m_X)\,,
\end{aligned} \tag{3.2.3}$$

in terms of few functions $\sigma_{Vt}(m_X)$, $\sigma_{Vb}(m_X)$ and $\sigma'_{Vt}(m_X)$. The $\sigma'_{Vt}(m_X)$, controlling the interference, turns out to be somewhat enhanced with respect to $\sigma_{Vb}(m_X)$ and has a negative sign, for the $m_X \sim 1$ TeV and $\sqrt{s} = 8$ TeV we obtained

$$\sigma'_{Vt}(m_X) \simeq -2.2\,\sigma_{Vt}(m_X) \tag{3.2.4}$$

The charge-conjugate processes, in which either $\overline{X}\,t$ or $\overline{X}\,b$ are produced, can be parametrized in terms of a similar set of coefficient functions. The only difference is the charge of the virtual V emitted from the light quark line. We thus have

$$\begin{aligned}
\sigma_{\rm sing}(\overline{X}t) &= \left[(g_{Xt_L})^2 + (g_{Xt_R})^2\right]\sigma_{V^\dagger t}(m_X) + 2\,g_{Xt_L}\,g_{Xt_R}\left(\frac{m_t}{m_X}\right)\sigma'_{V^\dagger t}(m_X)\,,\\
\sigma_{\rm sing}(\overline{X}b) &= (g_{Xb_L})^2\,\sigma_{V^\dagger b}(m_X)\,,
\end{aligned} \tag{3.2.5}$$

where $V^\dagger$ denotes the charge conjugate of the vector boson V. A similar way of computing cross sections of the $W-b$ fusion type of single-production was carried out in Ref. [79] where they adapted the fitting functions of Ref. [80] to non-SM couplings.

	σ [pb] @ NLO single production of $\bar{t}B + t\overline{B}$		σ [pb] @ NLO single production of $\bar{b}\widetilde{T} + b\overline{\widetilde{T}}$	
M [GeV]	$\sqrt{s} = 7$ TeV	$\sqrt{s} = 8$ TeV	$\sqrt{s} = 7$ TeV	$\sqrt{s} = 8$ TeV
400	(2.70) 3.10	(4.32) 4.92	(32.49) 43.47	(47.83) 61.43
500	(1.49) 1.80	(2.50) 2.97	(15.85) 20.44	(24.10) 33.10
600	(0.858) 1.06	(1.49) 1.84	(8.53) 12.89	(13.55) 18.80
700	(0.511) 0.637	(0.928) 1.15	(4.60) 6.70	(7.92) 11.34
800	(0.313) 0.399	(0.590) 0.745	(2.82) 4.01	(4.58) 7.22
900	(0.194) 0.250	(0.377) 0.497	(1.60) 2.50	(2.89) 4.48
1000	(0.121) 0.160	(0.246) 0.325	(0.956) 1.636	(1.81) 2.83
1100	(0.075) 0.103	(0.164) 0.215	(0.604) 0.980	(1.181) 1.72
1200	(0.048) 0.066	(0.107) 0.146	(0.377) 0.586	(0.726) 1.23.
1300	(0.031) 0.043	(0.072) 0.098	(0.234) 0.386	(0.463) 0.731

Table 3.3: *Cross sections for the NLO single production of B and $\tilde{T}$ for a unit coupling, at $\sqrt{s} = 7, 8$ TeV (the LO values are in brackets), with MCFM [83]. The cross sections given for the B partner are expected to be the same for the charge-5/3 exotic state, which single production has the same topology.*

Despite the enhanced interference, we will neglect it when analysing the CH models that we introduced above. In that case the interference is not only suppressed by m_t/m_X, but it is further reduced because the left- and right-handed couplings are never comparable, one of the two always dominates over the other. This enhances the leading term, $g^2_{Xt_L}$ or $g^2_{Xt_R}$, in comparison with the interference $g_{Xt_L} \cdot g_{Xt_R}$. Moreover this implies that eq.s (3.2.3) and (3.2.5) could be further simplified, in the sum it would be enough to retain the term which is dominant in each case. We will show in the following section that the dominant coupling is g_{Xt_R} in the case of the fourplet (models $\mathbf{M4}_5$ and $\mathbf{M4}_{14}$) and g_{Xt_L} in the case of the singlet (models $\mathbf{M1}_5$ and $\mathbf{M1}_{14}$) and the nine-plet (model $\mathbf{M9}_{14}$).

It total, all the single-production processes are parameterized in terms of 6 universal coefficient functions $\sigma_{W^\pm t}$, σ_{Zt}, $\sigma_{W^\pm b}$ and σ_{Zb}. We have computed the coefficient functions $\sigma_{W^\pm t}$ and $\sigma_{W^\pm b}$, including the QCD corrections up to NLO, using the MCFM code [83]. To illustrate the results, we report in Table 3.3 the single production cross-section with coupling set to unity, for different values of the heavy fermion mass, and for the 7 and 8 TeV LHC. The values in the table correspond to the sum of the cross sections for producing the heavy fermion and its antiparticle, on the left side we show the results for $t\,B$ production, on the right one we consider the case of $b\,\widetilde{T}$. In our parametrization of eq.s (3.2.3) and (3.2.5) the cross-sections in the table correspond respectively to $\sigma_{W^+t} + \sigma_{W^-t}$ and to $\sigma_{W^+b} + \sigma_{W^-b}$. We see that the production with the b is one order of magnitude larger than the one with the t, this is not surprising because the t production has a higher kinematical threshold and therefore it is suppressed by the steep fall of the partonic luminosities. The values in the table do not yet correspond to the physical single-production cross-sections, they must still be multiplied by the appropriate couplings with vector bosons. The coefficient functions σ_{Zt} and σ_{Zb} cannot be computed in MCFM, however we do not compute them since they will not be used in the following analysis.

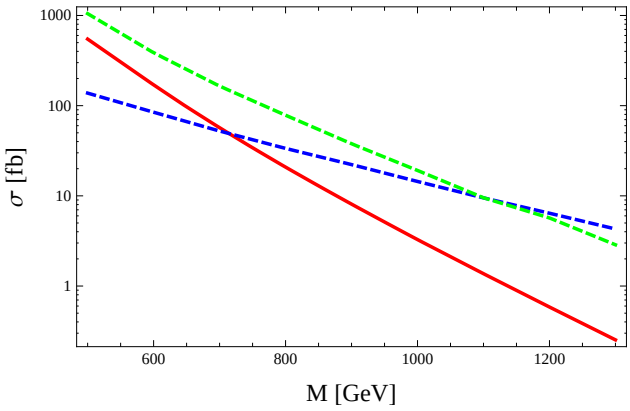

Figure 3.5: *Comparison of the production cross sections for 8 TeV LHC. In red: the cross sections of pair production. In dashed green and blue the single production of the $\widetilde{T}$ (in association with a b) and of the $X_{5/3}$ (in association with a t), respectively in model* $\mathbf{M1}_5$ *and* $\mathbf{M4}_5$*. The point chosen in the parameter space is $\xi = 0.2$, $c_1 = 1$ and $y = 1$. The value of c_2 is fixed, at each value of M_Ψ, in order to reproduce the top quark mass.*

In order to quantify the importance of single production we plot in figure 3.5 the cross-sections for the various production mechanisms in our models as a function of the mass of the partners and for a typical choice of parameters. We see that the single production rate can be very sizeable and that it dominates over the QCD pair production already at moderately high mass. This is again due to the more favorable lower kinematical threshold, as carefully discussed in Ref. [53].

Let us finally discuss the decays of the top partners. The main channels are two-body decays to vector bosons and third-family quarks, mediated by the couplings in eq. (3.2.2). The only exception is $X_{8/3}$ which can only have three-body decays to WWt. For the partners of charge $2/3$ and $-1/3$ also the decay to the Higgs boson is allowed, and competitive with the others in some cases. The relevant couplings can be computed analytically similarly to the $g_{t_{L,R}X}$ and $g_{b_L X}$. Thus we easily obtain analytical tree-level expressions for the partial widths and eventually for the branching fractions. In principle cascade decays $X \to X'V$ or $X'H$ are also allowed, however these are never sizable in our model as we will discuss in sect. 3.2.3.

3.2.2 Couplings to Goldstone Bosons

Let us now turn to classify the relative importance of the various production mechanisms and decay channels described in the previous section. Since the partners are much heavier than the EW bosons, $m_X \gg m_W$, their dynamics is conveniently studied by using the Equivalence Theorem, which applies at energies $E \gg m_W$. To this end, we will momentarily abandon the unitary gauge and describe our model in the R_ξ-gauge where the Goldstone degrees of freedom associated with the unphysical Higgs components are reintroduced. The Higgs field is now parameterized as [7]

$$H = \begin{pmatrix} h_u \\ h_d \end{pmatrix} = \begin{pmatrix} \phi^+ \\ \frac{1}{\sqrt{2}}\left(\langle h \rangle + \rho + i\phi^0\right) \end{pmatrix} . \tag{3.2.6}$$

[7] Notice that the Goldstone fields $\phi^{\pm,0}$ in eq. (3.2.6) are not canonically normalized. Indeed the non-linearities in the Higgs kinetic term lead to a kinetic coefficient equal to $\sin\epsilon/\epsilon$, with $\epsilon = \langle h \rangle / f$. However this is irrelevant for the purpose of the present discussion.

The Equivalence Theorem states that, at high energies, the longitudinal components of the $W^\pm$ and of the Z bosons are described, respectively, by the charged and the neutral Goldstone fields $\phi^\pm$ and ϕ^0. The transverse polarizations are instead well described by vector fields $W^\pm_\mu$ and Z_μ, in the absence of symmetry breaking. However the transverse components give a negligible contribution to our processes, and this is for two reasons. First, their interactions emerge from the SM covariant derivatives and therefore these are proportional to the EW couplings g or g'. We will see below that the couplings of the longitudinal, *i.e.* of the Goldstones, are typically larger than that. Second, the transverse components can not mediate, before EWSB, any transition between particles in different multiplets of the gauge group. Indeed the couplings of the $W^\pm_\mu$ and Z_μ fields are completely fixed by gauge invariance and therefore they are diagonal in flavor space. Only after EWSB do states from different multiplets mix and flavor-changing couplings like in eq. (3.2.2) arise. Therefore these effects must be suppressed by a power of $\epsilon = \langle h \rangle / f$. This means that the transverse gauge bosons basically do not participate to the production and decay of the top partners: the decay will mostly be to longitudinally polarized vectors, while the virtual V exchanged in single production diagram will be dominantly longitudinally polarized. The use of the Equivalence Theorem will allow us to treat the interactions with the Higgs and with the longitudinal vector bosons on the same footing, which will, in particular, simplify the estimate of the branching ratios of the top partners decays.

For our purposes, we can thus simply ignore the vector fields and concentrate on the Goldstones. In the models with the fourplet, $\mathbf{M4}_5$ (3.1.7) and $\mathbf{M4}_{14}$ (3.1.11), the first source of Goldstone couplings is the term $i\, c_1 \left(\bar\Psi_R\right)_i \not{d}^i\, t_R$. One would naively expect this interaction to be the dominant one because it originates entirely from the strong sector without paying any insertion of the elementary-composite coupling y. Before EWSB the couplings are

$$i\,\frac{\sqrt{2}c_1}{f}\left[-\overline{T}\gamma^\mu t_R \partial_\mu\left(\frac{\rho - i\phi^0}{\sqrt{2}}\right) + \overline{B}\gamma^\mu t_R \partial_\mu \phi^- + \overline{X}_{2/3}\gamma^\mu t_R \partial_\mu\left(\frac{\rho + i\phi^0}{\sqrt{2}}\right) + \overline{X}_{5/3}\gamma^\mu t_R \partial_\mu \phi^+\right] + \text{h.c.}\,. \tag{3.2.7}$$

It is not difficult to check that the interactions above respect not only the SM but also the full SO(4) symmetry of the strong sector. Eq. (3.2.7) contains derivative operators, therefore it is not yet suited to read out the actual strength of the interactions. However it can be simplified, provided we work at the tree-level order, by making use of the equations of motion of the fermion fields. [8] After integrating by parts and neglecting the top mass, we find

$$\frac{\sqrt{2}c_1}{f}\left[-m_T\left(\frac{\rho - i\phi^0}{\sqrt{2}}\right)\overline{T}t_R + m_B \phi^- \overline{B} t_R + m_{X_{2/3}}\left(\frac{\rho + i\phi^0}{\sqrt{2}}\right)\overline{X}_{2/3} t_R + m_{X_{5/3}}\phi^+ \overline{X}_{5/3} t_R\right] + \text{h.c.}\,, \tag{3.2.8}$$

showing that the strength of the interaction is controlled by the masses of the heavy fermions. Neglecting the elementary-composite coupling y, the masses all equal M_Ψ, and the coupling, modulo an $O(1)$ coefficient, is given by $g_\Psi = M_\Psi / f$, as anticipated in the previous section. Once again we

[8] When considering a perturbation described by a small parameter η to a Lagrangian, the use of the equations of motion of the unperturbed theory is equivalent to permorming field redefinitions of the form $\Phi \to \Phi + \eta F[\Phi, \partial]$. For example, to deal with the first term of eq. (3.2.7), the relevant redefinition is

$$\begin{aligned} T_R &\to T_R + \tfrac{\sqrt{2}c_1}{f} h_d^\dagger t_R \\ t_R &\to t_R - \tfrac{\sqrt{2}c_1}{f} h_d T_R \end{aligned}\,.$$

This eliminates the derivative interaction and makes the first term of eq. (3.2.8) appear. It also leads to new interactions with more fields that however are irrelevant for our processes at the tree-level.

remark that this feature follows from the Goldstone boson nature of the Higgs. Indeed if the Higgs were a generic resonance, not a Goldstone, then it could more plausibly have a Yukawa $g_*\overline{\Psi}^i\Pi_i t_R$ vertex with strength dictated by the strong sector coupling g_*.

Those of eq. (3.2.8) are the complete Goldstone interactions in the limit of a negligible elementary-composite coupling y. However we can not rely on this approximation because we will often be interested in relatively light top partners, with $g_\Psi \leq y \simeq y_t$. It is straightforward to incorporate the effect of y, due to the mixing terms in eq.s (3.1.7) and (3.1.11) for model $\mathbf{M4}_5$ and $\mathbf{M4}_{14}$, respectively. After diagonalizing the mass-matrix, again neglecting EWSB, the Goldstone interactions for both models become

	$\mathbf{M4}_5$, $\mathbf{M4}_{14}$
$\phi^+\overline{X}_{5/3L}\,t_R$	$\sqrt{2}c_1 g_\psi$
$(\rho+i\phi^0)\overline{X}_{2/3L}\,t_R$	$c_1 g_\psi$
$(\rho-i\phi^0)\overline{T}_L\,t_R$	$-c_1\sqrt{y^2+g_\psi^2}+\frac{c_2 y^2}{\sqrt{2}\sqrt{y^2+g_\psi^2}}$
$\phi^-\overline{B}_L\,t_R$	$c_1\sqrt{2}\sqrt{y^2+g_\psi^2}-\frac{c_2 y^2}{\sqrt{y^2+g_\psi^2}}$

(3.2.9)

which reduces to eq. (3.2.8) for $y \ll g_\Psi$. Notice that eq. (3.2.9) only contains couplings with the right-handed top quark. This is not surprising because the top partners live in SM doublets and therefore their only allowed Yukawa-like interactions are with the t_R singlet. The couplings with the q_L doublet emerge only after EWSB and are suppressed by one power of ϵ. Therefore they typically do not play a mayor role in the phenomenology. Obviously the SM symmetry is respected in eq. (3.2.9), this explains the $\sqrt{2}$ suppression of the $X_{2/3}$ and of the T couplings compared with the ones of the $X_{5/3}$ and of the B.

The situation is different in the models with the singlet, $\mathbf{M1}_5$ and $\mathbf{M1}_{14}$ (3.1.12). In that case there is no direct contribution from the strong sector to the Goldstone coupling and all the interactions are mediated by y. The couplings are

	$\mathbf{M1}_5$, $\mathbf{M1}_{14}$
$(\rho+i\phi^0)\widetilde{\overline{T}}_R\,t_L$	$\frac{y}{\sqrt{2}}$
$\phi^+\widetilde{\overline{T}}_R\,b_L$	y

(3.2.10)

The top partner $\widetilde{T}$ now is in a SM singlet, therefore the interactions allowed before EWSB are the ones with the left-handed doublet. The $\sqrt{2}$ suppression of the coupling with the top is due, once again, to the SM symmetry. One important implication of eq. (3.2.10) is that the $\widetilde{T}$, contrary to the partners in the fourplet, can be copiously produced singly in association with a bottom quark. We will discuss this and other features of our models in the following section.

We conclude with an interaction lagrangian for the model $\mathbf{M9}_{14}$:

$$\begin{aligned}\mathcal{L} \supset\ & -c_1 y\,\bar{t}_L\left[\sqrt{2}\,\phi^- Y_{5/3}+\phi^+ Y_{1/3}+\phi^+ Z_{1/3}+\frac{1}{\sqrt{10}}\left(4i\,\phi^0 Y_{2/3}+(3i\,\phi^0+5\,h)Z_{2/3}\right)\right]\\ & +c_1 y\,\bar{b}_L\left[\frac{2}{\sqrt{5}}\,\phi^- Y_{2/3}-\frac{1}{\sqrt{5}}\,\phi^- Z_{2/3}-2\,\phi^+ Z_{-4/3}+\sqrt{2}\,h Y_{-1/3}+i\sqrt{2}\,\phi^0 Z_{-1/3}\right]\\ & -c_1\xi\frac{y}{\sqrt{2}}\left[(h+i\phi^0)\bar{t}_L X_{2/3}-\sqrt{2}\,\phi^-\bar{b}_L X_{2/3}\right]+\text{h.c.}\,,\end{aligned} \tag{3.2.11}$$

The extra ξ suppression for members of the X group is due to the fact that they mostly consist of states with the right isospin $T^3_R(X)=+1$ and need therefore at least three insertions of the Higgs

(which is a doublet of $SU(2)_R$) to couple with the SM fermions, whose right isospin is $T^3_R(q) = -1/2$. The states $X_{5/3}$ and $Y_{5/3}$ are degenerate at tree level, but split by loop effects. The leading such effects, coming from the Yukawa with the elementary top quark, align the states such that eq. (3.2.11) holds. Nevertheless, interactions with transverse elementary gauge fields, can introduce corrections of order $\mathcal{O}(g^2\xi)$. Similar arguments apply to other degenerate states: true mass eigenstates will differ from the ones used in the eq. (3.2.11) by at most a rotation proportional to ξ; this will not affect the discussion which follows. Couplings of $X_{5/3}$ to the top quark and ϕ^+ are present at subleading orders in $\xi g^2/y^2$, in addition $X_{5/3}$ couples to the transverse components of the W, therefore $X_{5/3}$ is expected to decay with probability ~ 1 into Wt.

For charge conservation, there are no two-body decays of $X_{8/3}$ into SM fields; its dominant interactions come from the covariant derivative (it is now more convenient to use explicitly the couplings with vector bosons)

$$\mathcal{L} \supset g\,\overline{X}_{8/3}\not{W}^+ X_{5/3} + g\,\frac{3\xi}{4}\,\overline{X}_{8/3}\not{W}^+ Y_{5/3} + \text{h.c.} \tag{3.2.12}$$

and from the effective interaction in the last term of the eq. (3.1.16),

$$\mathcal{L} \supset -\xi\,\frac{c_2\,g^2}{2M_*}\,\overline{X}_{8/3}\,W^+W^+\,t_R + \text{h.c.} \tag{3.2.13}$$

3.2.3 The Most Relevant Channels

We discuss here the most relevant production and decay processes of each top partner, identifying the best channels where these particles should be looked for at the LHC. Let us first consider the models $\mathbf{M4}_5$, $\mathbf{M4}_{14}$ and analyze separately each of the new fermions.

- $X_{5/3}$

  $X_{5/3}$, together with $X_{2/3}$, is the lightest top partner, it is therefore the easiest to produce. Production can occur in pair, via QCD interactions, or in association with a top quark through its coupling with a top and a W^+. The coupling, see eq. (3.2.9), is controlled by $g_\psi = m_{X_{5/3}}/f$, which grows with mass at fixed f. We thus expect single production to play an important role at high mass, where it is enhanced with respect to pair production by both kinematics and a larger coupling (at fixed f). This is confirmed, for a particular but typical choice of parameters, by the plot in Figure 3.5.

  Since it is the lightest partner, $X_{5/3}$ decays to W^+t with unit branching ratio. The relevant channel for its observation is $X_{5/3} \to tW$ in association with a second top quark of opposite charge. The latter is present in both single and pair production processes. This results in clean signals consisting of either same-sign dileptons or trileptons plus jets; it also turns out that one lepton plus jets channel can also be relevant and even more useful provided that the boosted techniques are used in the analysis [88]. In the following section we will recast the LHC searches for these signals and obtain a limit on $X_{5/3}$ production. In addition to two top quarks and a W, pair production also leads to a second hard W while single production (see Figure (3.4)) features a light-quark jet associated with virtual W emission.

  Notice that the light-quark jet in single production is typically forward with a $p_T \lesssim m_W$ because the emission of the virtual W is enhanced in this kinematical region [53]. In practice

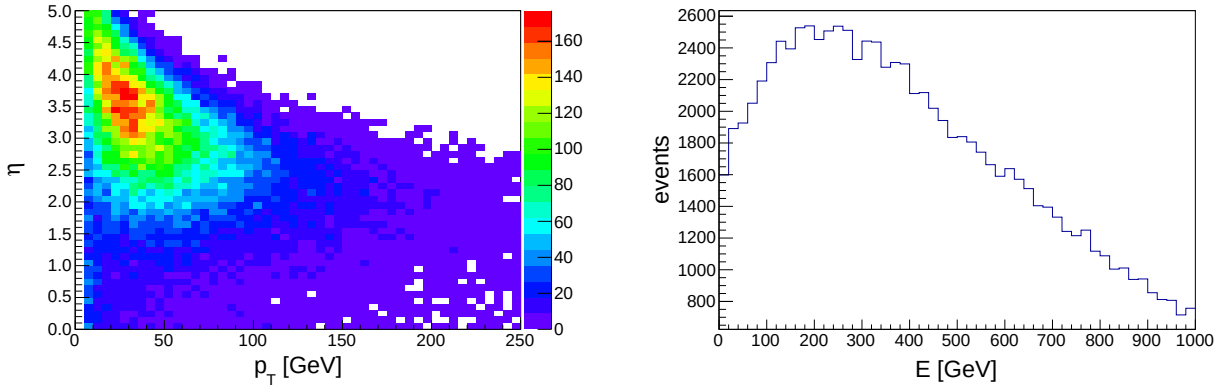

Figure 3.6: $p_T - \eta$ *and energy distributions of the forward jets produced in a single production of the top partner with a mass* 600 GeV *produced in 7 TeV collisions.*

this jet has the same features of the"tag jets" in VBF Higgs production and in WW–scattering. The events are thus characterized by a forward isolated jet in one of the hemispheres. The relevant kinematical distributions are shown in Figure (3.6) for the production of a 600 GeV partner. Like in VBF or WW-scattering, one might hope to employ the forward jet as a tag to discriminate single production form the background. Ref. [53] argued that the main source of forward jets in the background, QCD initial state radiation, tends to produce more central and less energetic jets, however further investigations are needed. Present LHC searches are designed for pair- rather than for single-production. Because of the η^{jet} and p_T^{jet} cuts that they adopt, they are thus weakly sensitivity to forward jets. We believe that it would be worth to explore the possible relevance of forward jets in designing the searches for top partners.

- $X_{2/3}$

  $X_{2/3}$ is also light and therefore easier to produce than the heavier partners. At the leading order, as eq. (3.2.9) shows, it couples with strength $c_1 g_\psi$ to the Higgs and Z bosons. The dominant decay channels are thus $X_{2/3} \to Zt$ and $X_{2/3} \to ht$ and $\mathrm{BR}(X_{2/3} \to Z\,t) \approx \mathrm{BR}(X_{2/3} \to h\,t) \approx 0.5$. In model $\mathbf{M4}_5$ the coupling to Wb vanishes exactly, while in model $\mathbf{M4}_{14}$ the coupling is non-zero but suppressed by $\epsilon \sim v/f$. The decay $X_{2/3} \to Wb$ is therefore typically sub-dominant and can become relevant only in a corner of parameter space characterized by low mass, $y\epsilon = O(1)$ and $c_1 < 1$. Given that $X_{2/3} \to ht$ is probably difficult to detect (see however Ref. [76] for recent analyses), the search for $X_{2/3}$ must rely on the decay mode $X_{2/3} \to Zt$, with Z further decaying to charged leptons. An extra suppression from the small branching ratio must then be payed. This disfavors the $X_{2/3}$ signal compared to that of $X_{5/3}$, for which the branching ratio needed to reach the leptonic final state is close to one.

  $X_{2/3}$ is produced in pairs via QCD interactions and singly via the $ZX_{2/3}t$ coupling. In the latter case a top quark is produced in association. Both production modes lead to a resonant $X_{2/3} \to Zt$ plus one top of opposite charge. In the case of single production there will be a forward jet, as previously discussed in the case of $X_{5/3}$. In the case of pair production there will be either a Higgs or a Z from the other partner. Another possible single production mode, in association with a b quark rather than a t, is strictly forbidden in model $\mathbf{M4}_5$ and is suppressed

by the small coupling to Wb in model $\mathbf{M4}_{14}$. However single production in association with a b is kinematically favored over that with t. Kinematics then compensates the suppressed coupling and makes the two rates typically comparable in model $\mathbf{M4}_{14}$. In the case of $X_{2/3}$, single production in association with a t is suppressed compared to the case of $X_{5/3}$. This is mainly due to the $\sqrt{2}$ factor in charged current versus neutral current vertices, see eq. (3.2.9). Moreover, the difference between the W and Z couplings, taking into account u- and the d-type valence quark content of the proton, further enhances by a ~ 1.2 factor the virtual W emission rate with respect to the Z rate.

- T

  T is systematically heavier than $X_{2/3}$, but the phenomenology is very similar. Therefore it will merely give a subdominant contribution to the $X_{2/3}$ channels described in the previous paragraph. Indeed, by eq. (3.2.9), also T couples at leading order with equal strength to the Higgs and to the Z, leading to $\mathrm{BR}(T \to Z\,t) \approx \mathrm{BR}(T \to h\,t) \approx 0.5$. The coupling to Wb arises at order ϵ, and it can be relevant, as explained for $X_{2/3}$ above, thanks to the favorable kinematics of associated production with a b.

  One may in principle consider chain decays seeded by $T \to X_{2/3}Z$, $T \to X_{2/3}h$ or $T \to X_{5/3}W$, given these channels are normally kinematically open. However the corresponding couplings are generically smaller than those controlling the direct decays to t_R. This is a straightforward consequence of the equivalence theorem and of $SU(2)$ selection rules. The decays to t_R, involve longitudinally polarized vectors and h, living in the linear Higgs doublet H: given the top partners are $SU(2)$ doublets and t_R is a singlet, the coupling respects $SU(2)$ and so it arises at zeroth order in ϵ. On the other hand, the transitions among top partners living in different $SU(2)$ doublets obviously require an extra insertion of the Higgs vacuum expectation value. The resulting amplitudes are therefore suppressed by one power of ϵ and the corresponding branching ratios negligible.

- B

  B is even heavier than T, though the mass difference, $m_B - m_T \sim y^2v^2/4m_B$ (see eq. (3.1.23)), is typically rather small. The most relevant decay mode is $B \to Wt$, mediated by the coupling $\sim c_1 g_\Psi$ in eq. (3.2.9). Like in the case of T, $SU(2)$ selection rules suppress the decay to $WX_{2/3}$. Moreover, the decay $B \to WT$, when kinematically allowed, proceeds either via a transverse W, with SM gauge coupling $g < g_\Psi$, or via a longitudinal W, with effective coupling suppressed by ϵ. Therefore also this decay is significantly suppressed. The decay $B \to Zb$ is forbidden because, flavor-changing neutral couplings are absent in the charge $-1/3$ sector. The $B \to hb$ channel is forbidden in model $\mathbf{M4}_5$ and suppressed by ϵ in model $\mathbf{M4}_{14}$. In the latter model it can play a role, but only in a corner of the parameter space.

  Single production, since the ZBb vertex is absent, is always accompanied by a top quark. The signature of single B production is therefore a resonant $B \to Wt$ plus an opposite charge top, the same final states of single $X_{5/3}$ production. In the end, B production, single and pair, has the same signatures as $X_{5/3}$ production.

Let us now switch to models $\mathbf{M1}_5$ and $\mathbf{M1}_{14}$, where the only new heavy fermion is the $\tilde{T}$.

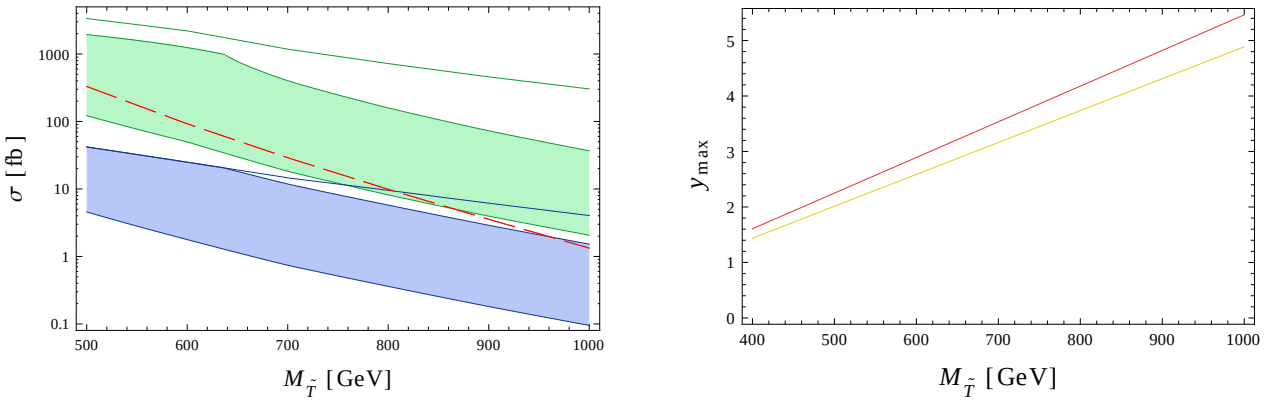

Figure 3.7: *Left panel: cross sections for the different production mechanisms of* $\widetilde{T}$ *for the models* $\mathbf{M1}_5$ *and* $\mathbf{M1}_{14}$ *for* $\xi = 0.2$ *at 7 TeV LHC. Red dashed: pair production; green line:* $\tilde{T}b$ *production with the maximal allowed coupling, green band:* $\tilde{T}b$ *production for* $0.5 < c_2 < 2$*; blue line:* $\tilde{T}t$ *production for the maximal allowed coupling, blue band:* $\tilde{T}t$ *production for* $0.5 < c_2 < 2$*. Right panel: maximal allowed* y *for the models* $\mathbf{M1}_5$ *(in yellow) and* $\mathbf{M1}_{14}$ *(in red).*

- $\widetilde{T}$

  $\widetilde{T}$ has a very rich phenomenology because it can be copiously produced through all the three mechanisms described above. We see in eq. (3.2.10) that $\widetilde{T}$ couples to both Zt and Wb, with a coupling of order $y \sim y_t/c_2$. It can therefore be singly produced either in association with a top or with a bottom quark. Notice that in the range $c_2 \sim 1$ suggested by power counting, the trilinear coupling is of order y_t, which is expected to be generically smaller than the strong sector coupling g_ψ that controls the single production of top partners in a $(2,2)$. The bands in the left panel of Fig. 3.7, indicate the single prooduction cross section[9] for $0.5 < c_2 < 2$: comparing the blue band to the corresponding case of $X_{2/3}t$ and $X_{5/3}t$ production in models $\mathbf{M4}_5$ and $\mathbf{M4}_{14}$, one notices, as expected, a typically smaller rate for models $\mathbf{M1}_5$ and $\mathbf{M1}_{14}$. While $y \sim y_t$ ($c_2 \sim 1$) is favored by naive power counting, one can entertain the possibility of choosing $y > y_t$ ($c_2 < 1$), for which the single production rate can be sizeable. However, for a given value of $m_{\widetilde{T}}$ and f, there is a mathematical upper bound y_{max} on y determined by eqs. (3.1.30). The right plot in Fig. 3.7 shows that y_{max} grows with $m_{\widetilde{T}}$ and that it is comparable in model $\mathbf{M1}_5$ and model $\mathbf{M1}_{14}$. In the left panel of Fig. 3.7, the green line and the blue line shows, respectively for $\tilde{T}b$ and $\tilde{T}t$, the maximal allowed cross section, which almost coincides with the choice $y = y_{max}$. For such maximal values the single production cross section can be quite sizeable.

  Single production of a $\tilde{T}$-like partner was considered in the context of Little Higgs models, and more recently for composite Higgs models in Ref. [75], where it was also considered the possibility of using a forward jet tag as a handle for this kind of searches. The total cross section in this channel is favored over single production with a t by both kinematics and by the $\sqrt{2}$ factor in charged current transitions. Indeed, as shown in Fig. 3.7, associated $\tilde{T}b$ production dominates even over pair production in all the relevant mass-range while single production

[9] By fixing m_t, ξ, c_2 and $m_{\widetilde{T}}$ the result for model $\mathbf{M1}_{14}$ and $\mathbf{M1}_5$ coincide. Indeed, the gauge vertices and the mass spectrum of model $\mathbf{M1}_{14}$ equal those of model $\mathbf{M1}_5$ when the equality $y^{\mathbf{M1}_5} \sin\epsilon = y^{\mathbf{M1}_{14}} \sin 2\epsilon/2$ holds.

with the t is rather small. The role of kinematics is especially important in this result, as the large $\tilde{T}b$ cross section is dominated by the emission of a soft b, with energy in the tens of GeV, a regime obviously unattainable in the similar process wih a t. Indeed by performing a hard cut of order m_t on the p_T of the b, the $\tilde{T}b$ cross section would become comparable to that for $\tilde{T}t$. Unfortunately the current LHC searches do not exploit the large inclusive rate of production with the b quark because they are designed to detect pair production.

Also concerning decays, all the possible channels are important in the case of $\widetilde{T}$. It decays to Wb, Zt and ht at zeroth order in ϵ, with a fixed ratio of couplings. By looking at eq. (3.2.10) we obtain $\mathrm{BR}(\widetilde{T} \to Z\,t) \approx \mathrm{BR}(\widetilde{T} \to h\,t) \approx \frac{1}{2}\,\mathrm{BR}(\widetilde{T} \to W\,b) \approx 0.25$. Actually the branching fraction to Wb is even further enhanced by the larger phase space, though this is only relevant for low values of $m_{\widetilde{T}}$. Given that the branching fraction is larger, ideally the resonant Wb production would be the best channel to detect the $\widetilde{T}$. However one should manage to design a search strategy to reject the background while retaining the signal. In particular one should retain as much as possible the contribution from the large single production in association with the b. A possibly cleaner decay channel could then be $\widetilde{T} \to Z\,t$ with leptonic Z.

The last model we consider is the $\mathbf{M9}_{14}$. We will not consider every state alone but will just mention some exceptional features of the model phenomenology:

- The spectrum contains several groups of particles which could potentially contribute to the same final states enhancing the signal. This kind of enhancement is especially important in the case of $\mathbf{M9}_{14}$ since the masses of the states are almost degenerate. In particular, there are five particles ($X_{8/3}$, $X_{5/3}$, $Y_{5/3}$, $Y_{-1/3}$ and $Z_{-1/3}$) giving two same sign leptons final states.

- The $X_{8/3}$ can decay to three same sign leptons via the decay $X_{8/3} \to WWt \to WWWb$. This signature will practically have no background and therefore can be a smoking gun signature of the nine-plet, supported for example by a signal in the two same sign leptons channel. The $X_{8/3}$ decays can be mediated either by an off-shell charge-5/3 states, or by a contact interaction $X_{8/3}WWt$ coming from a term with $d_\mu d^\mu$ in the lagrangian (3.1.16), in both cases giving two W-bosons and a top quark. The ratio of corresponding branching fractions is approximately given by

$$\frac{\Gamma_{dd}}{\Gamma_{5/3}} \approx \frac{c_2^2}{c_1^2 y_R^2}\,\frac{0.1}{v^2/f^2}\,\frac{M_\Psi^4}{f^2 M_*^2}\,. \tag{3.2.14}$$

  where for definiteness in the following we take $M_* = 3$ TeV. Therefore the two partial widths are comparable, but the differential distributions of the decay products differ substantially, as shown in the Fig. 3.8 for the energies of all three W bosons, including the one from the top quark decay. When the top partners are heavy, and consequently produced almost at rest, both decay modes will produce almost identical decay spectra (Fig. 3.8, dashed lines). The behaviour of E_W significantly changes if the initial $X_{8/3}$ is slightly boosted, which is the case for relatively low $M_{8/3}$ (Fig. 3.8, solid lines): the contact interaction now tends to produce less energetic W's compared to 5/3-mediated decays. The energy distributions of the decay products give an important information about how easily they would be able to pass hard p_t cuts[10] which are typically needed to suppress the backgrounds.

[10] Given that in the pair production process no preferred direction is present, the shapes of p_t distributions will resemble the ones of the energy distributions.

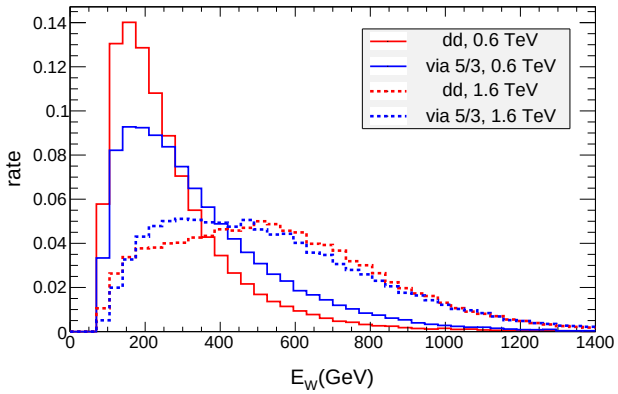

Figure 3.8: *Comparison of energy distributions of W bosons produced in the $X_{8/3} \to WWWb$ decays of the pair produced $X_{8/3}$ with mass 600 GeV (solid lines) and 1600 GeV (dashed lines), at the LHC with 8 TeV center of mass energy, assuming that decays proceed via contact interaction (red lines) or via intermediate charge-5/3 state (blue lines).*

- The states $Y_{2/3}$, $Z_{-4/3}$, $Z_{2/3}$ and $Z_{-1/3}$ are coupled to the bottom quark. As was discussed above, this coupling can significantly enhance the single production with respect to the pair production due to a small mass of the bottom quark.

3.3 Current LHC Bounds

In this section we derive bounds on our models using the presently available LHC searches. For each type of models we will concentrate on one the most constraining search.

For $\mathbf{M4}_5$ $\mathbf{M4}_{14}$ and $\mathbf{M9}_{14}$ this will be the searches for two same sign leptons ($2ssl$) by the ATLAS [86] and CMS [87] collaborations which use 8 TeV data. In the first two models this is motivated by a presence of two particles contributing to the $2ssl$ final state ($X_{5/3}$ and B), one of which ($X_{5/3}$) is the lightest top partner and has a branching fraction 1 for the decay into Wt which subsequently give two same sign leptons. It is nevertheless worth mentioning that with further improvement of the experimental bounds the constraints coming from the searches for final states with just one lepton and reconstructed boosted W bosons and top quarks can become more sensitive to this type of partners [88]. As for the model $\mathbf{M9}_{14}$, it contains two charge 5/3 states and two charge -1/3 states, all with almost degenerate masses, which would significantly enhance a potential $2ssl$ signal compared to models with smaller multiplets. But the main contribution to the signal in this case comes from the exotic charge-8/3 state. Indeed, W's decay leptonically about 2/9 of the times (more if one includes leptonic τ decays) so that $\overline{X}_{8/3}X_{8/3}$ decays produce at least two same-sign leptons approximately 1/4 of the times – almost three times more than charge-5/3 resonances.

The models $\mathbf{M1}_5$ and $\mathbf{M1}_{14}$ can be efficiently constrained from the searches for the pair produced charge 2/3 states decaying to Wb, Zt and Ht [89]. We will concentrate on the search by the CMS collabotation [89], as the most constraining one among presently available analyses. Though the $\widetilde{T}$ can be very efficiently produced in a single production in association with the b-quark, the existing searches would not be sensitive to this type of production because the signal in this case produces

final states with a relatively low number of constituents.

The last search [89] can be easily used to obtain a bound on the models with $\widetilde{T}$, one just needs to compute for each parameter space point the branching ratios of the decays to Wb, Zt and Ht, and compare the $\widetilde{T}$ mass with a bound on it, which is given for all possible combinations of the BR's. Quite independently on the model and a choice of the parameters, we obtain a lower bound on the $\widetilde{T}$ mass ~ 700 GeV.

Using the $2ssl$ searches [86, 87] is slightly more complicated because the benchmark models, used in these analyses, describe only one heavy fermion, which is only produced in pairs via QCD interactions. In what follows, we quantify the impact of these searches on our models, by adopting the following strategy. We compute separately the production cross-sections of the top partners, the branching fractions into the relevant channels and the efficiencies associated with the selection cuts performed in each experimental search. The cross-sections and the branching fractions at each point of the parameter space are encapsulated in semi-analytical formulae as described in section 3.2. The efficiencies must instead be obtained numerically through a Monte Carlo simulation. Not having at our disposal a reliable tool to estimate the response of the detector, a fully realistic simulation of the hadronic final states would not be useful. Therefore we decided not to include hadronization effects in our analysis, but perform showering in the cases where it is crucial. We applied the reconstruction (e.g., of b-jets and leptons) and selection cuts on the partonic events in order to get an estimate of the kinematical acceptance. Moreover, we included the efficiencies for b-tagging, lepton reconstruction and trigger through universal reweighting factors extracted from the experimental papers. Jet clustering, W and top tagging where needed were also performed at a parton level. Afterwords, a requirement that the predicted by a model number of the signal events

$$N_{signal} = \mathcal{L} \sum_n \mathrm{BR}_n \, \epsilon_n \, \sigma_n(M_n) \,, \tag{3.3.1}$$

is greater than the bound on it defines, which regions of the parameter space are excluded. In the last expression $\mathcal{L}$ is an integrated luminosity, the sum runs over all the relevant top partners and their decay channels, BR_n are branching ratios of the considered final states, ϵ_n – cuts acceptances of each production-decay mode and $\sigma_n(M_n)$ – single or pair production cross section of the top partners.

3.3.1 Two Same Sign Leptons Searches

Ref. [87], using $19.6\,\mathrm{fb}^{-1}$ of collected data, puts the strongest limit on pair produced charge 5/3 states that decay exclusively to Wt. This analysis searches for an excess of events containing two same sign leptons (e or μ, including those from τ decays) and at least $N_{con} = 5$ other leptons or jets. A dedicated technique is used to reconstruct top quarks and W-bosons from their decay products if the latter are highly boosted. The candidate leptons and jets are required to satisfy isolation criteria, minimal p_t and η cuts and the invariant mass of the leptons pairs must be away from M_Z to further suppress the WZ and ZZ background. On top of this, the sum of the transverse momenta of the particles in the event must be larger than 900 GeV. The search did not find any significant excess and put a 95% C.L. lower limit of 770 GeV on the mass of charge 5/3 states. This corresponds to an upper limit $N_{95}^{\mathrm{CMS}} \simeq 12$ on signal events passing the selection criteria.

Though the bound on a pair production cross section coming from the described above analysis is stronger than the one of the Ref. [86], the latter search applies a much milder cut on the total number

CMS, s.p.				CMS, p.p.			
M [GeV]	$Q=\frac{5}{3}$ left	$Q=\frac{5}{3}$ right	$Q=\frac{5}{3}$ from [88]	M [GeV]	$Q=\frac{5}{3}$ left	$Q=\frac{5}{3}$ right	$Q=\frac{5}{3}$ from [87]
700	1.65	1.85	2.01	700	16.6	22.7	18.5
800	2.10	2.69	2.66	800	19.5	26.4	23.3
900	2.37	3.08	3.12	900	21.9	28.5	25.7

Table 3.4: *Acceptance of the cuts of the analysis [87] multiplied by BR of W bosons, needed to reach $2ssl$, and by 10^3, for the single- (left panel) and pair- (right panel) produced charge-5/3 top partner for the purely left- and right-handed couplings. Last columns show the values of the acceptances extracted from the Ref.s [87, 88].*

of constituents – at least two jets. This means that the cuts acceptance to the single production of the $X_{5/3}$ and B (which typically produces at most 5 energetic jets, one of which is very forward and has a low p_t) for the search [86] is higher than in the case of the search [87]. Apart from exactly two same sign leptons and two additional jets, the analysis [86] requires the events to contain at least one b-tagged jet, jets and leptons candidates must satisfy isolation criteria, minimal p_t and η cuts, the invariant mass of the pairs of leptons must be away from M_Z; finally, there should be a missing transverse energy $E_{\rm T}^{\rm miss} > 40$ GeV and the scalar sum of the p_t's of all the jets and leptons in the event must be greater than 650 GeV. Resulting bound on mass of the pair-produced fourth generation b' quark, obtained with 14.3 fb^{-1} of integrated luminosity, is 720 GeV, which corresponds to $N_{95}^{\rm ATLAS} \simeq 13$ signal events.

Coming back to our models, the top partners contributing to the $2ssl$ signal are those with charges 8/3, 5/3 and -1/3. To derive the bound we must compute, for each partner and production mode, the efficiency of the signal as a function of the partner's mass. Combining the cross-sections with the efficiencies we obtain the signal yields for both analyses, according to the formula (3.3.1), that must be compared with the bounds on number of events $N_{95}^{\rm ATLAS}$ and $N_{95}^{\rm CMS}$.

Efficiencies

The first step is to simulate the signal processes. Rather than employing our complete models we have used a set of simplified MadGraph models containing the SM fields and interactions plus the relevant new particles – $X_{5/3}$, B and $X_{8/3}$ – with the appropriate couplings, responsible for the pair and single production and the decay. For the $X_{5/3}$ and B we made two sets of simulations – with left- and right-handed vertices. We will see that the chirality of the couplings significantly affects the efficiencies. The efficiency for the decays with both left- and right-handed couplings can be obtained by the interpolation between the purely left- and right-handed cases. Due to a similar topology of the $X_{5/3}$ and B production and decays, corresponding cuts acceptances are very similar, therefore we will use the same values for both particles.

The cuts acceptances times BR's for the analyses of the Ref.s [87] and [86] are given in Tables 3.4 and 3.5 respectively, for different mass points and purely left- or right-handed couplings. In addition, for comparison, we present the efficiencies extracted from the original experimental papers and the Ref. [88], where the efficiencies for the single production were evaluated. As we see, in the case of

ATLAS, s.p.		
M [GeV]	$Q=\frac{5}{3}$ left	$Q=\frac{5}{3}$ right
700	9.52	11.4
800	10.1	12.6
900	11.0	13.1
1000	10.9	12.3
1100	11.3	12.6
1200	11.9	12.5

ATLAS, p.p.			
M [GeV]	$Q=\frac{5}{3}$ left	$Q=\frac{5}{3}$ right	$Q=-\frac{1}{3}(b')$ from [86]
700	18.7	21.7	18.4
800	19.5	22.3	20.3
900	20.0	22.2	20.6
1000	20.3	22.3	–
1100	20.7	22.4	–
1200	20.6	22.3	–

Table 3.5: *Acceptance of the cuts of the analysis [86] multiplied by BR of W bosons, needed to reach* $2ssl$*, and by* 10^3*, for the single- (left panel) and pair- (right panel) produced charge-5/3 top partner for the purely left- and right-handed couplings. The last column of the right plot shows the values of the acceptances extracted from the Ref. [86] for the case of the fourth generation* b' *quark.*

M[GeV]	$Q=8/3$, via dd	$Q=8/3$, via 5/3
600	51	101
800	97	108
1000	124	114
1200	133	119
1400	138	122
1600	139	125

Table 3.6: *Acceptance of the cuts of the analysis [87] multiplied by* $BR\times10^3$ *for the pair-produced charge-8/3 top partner decaying via contact interaction (Eq. 3.2.13) or via intermediate charge-5/3 state.*

the CMS search (Table 3.4), the average of the acceptances for the left and right couplings (which corresponds to the acceptance when left and right couplings are equal) deviates by at most 15% from the reference results given in the last columns. We also find a good agreement for the ATLAS search, when comparing our results for the left coupling with the acceptances extracted from the Ref. [86] which were computed for the case of b', which also has a left-handed coupling with the top quark.

From Tables 3.4 and 3.5 we see that the efficiency for the right-handed coupling is larger than the one for the purely left-handed case. This is because the right-handed top (and the left-handed anti-top), produced in the top partner decay, produce more energetic charged leptons than a left-handed top. The lepton p_T distribution is therefore harder and the p_T cut is more easily satisfied.

The $X_{8/3}$ contributes to the signal in a significantly more efficient way than charge-5/3 states due to a larger combinatoric factor and a larger probability to pass all the cuts given a larger number of final states, as can be seen from the Table 3.6. We only computed the acceptances for the case of the CMS search, since its drawback – a severe cut on the number of constituents – becomes almost harmless for the $X_{8/3}$, which produces a large number of jets and leptons.

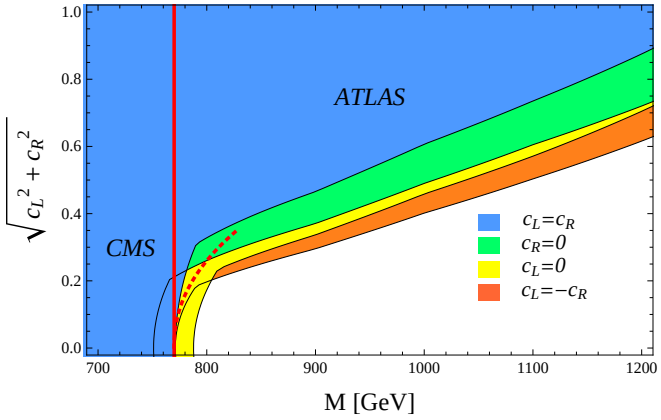

Figure 3.9: *Model-independent exclusions for one charge-5/3 (or -1/3) state for different combinations of the left (c_L) and right (c_R) couplings, as indicated on the plot. The exclusion below ~ 800 GeV is driven by the CMS analysis [87], while above it comes from the ATLAS analysis [86] due to its good sensitivity to the single production. Red solid line is a limit on charge-5/3 state mass, derived in the Ref. [87] by considering the pair production only. Red dashed line corresponds to the exclusion obtained in the Ref. [88] basing on the experimental analysis [87], where the effect of the single production with $c_L = c_R$ was taken into account, but the contribution of the interference term of the Eq. (3.2.3) was not included.*

Implications for the Models $\mathbf{M4}_5$ and $\mathbf{M4}_{14}$

The top partners of the models $\mathbf{M4}_5$ and $\mathbf{M4}_{14}$ dominantly couple to the right-handed top, hence for their analysis we will use corresponding efficiencies. But before presenting the specific results for the considered models, we give a general model-independent exclusion for one charge-5/3 (or -1/3) state (Fig. 3.9), depending only on the coupling to the Wt and the mass. The plot on the Fig. 3.9 shows a remarkably strong dependence of the exclusion on the chirality of the coupling with the top quark, which comes from the interference term of Eq. (3.2.3).

In Fig. 3.10 we show the excluded region for the models $\mathbf{M4}_5$ and $\mathbf{M4}_{14}$ in the (ξ,$M_{X_{5/3}}$) plane, where $\xi = (\frac{v}{f})^2$, depending on whether the single production is suppressed ($c_1 = 0.3$) or enhanced ($c_1 = 3$) and whether also B contributes to the signal ($M_B \gtrsim M_{X_{5/3}}$, $y = 0.3$) or not ($M_B \gg M_{X_{5/3}}$, $y = 3$). Fig. 3.11 shows the exclusion in terms of $M_{X_{5/3}}$ and c_1. Since, as was discussed in sect. 3.2.2, the leading contribution to single production couplings is the same for models $\mathbf{M4}_5$ and $\mathbf{M4}_{14}$, the excluded regions are also similar for both models. A difference shows up when $c_1 \ll 1$ and the $h\bar{B}b$ vertex of model $\mathbf{M4}_{14}$ becomes important thus decreasing BR($B \to Wt$) and also when $\frac{y}{g_\psi}\epsilon = \mathcal{O}(1)$ and higher order effects modify the single production couplings. The excluded regions are almost symmetric with respect to $c_1 \to -c_1$, which can be understood as follows. When only $X_{5/3}$ production matters, the single production rate is proportional to $|c_1|^2$ at lowest order in ϵ. Higher order terms only matter in the region of small $|c_1|$ where the single production rate is anyway negligible and the bound is driven by pair production which is insensitive to c_1. When B production matters, that is because $m_B - m_{X_{5/3}} \ll m_{X_{5/3}}$, corresponding to $y \ll g_\psi$. From eq. (3.2.9) it is then evident that in this regime the couplings of both particles are approximately $\propto c_1$, so that the signal yield is again symmetric under $c_1 \to -c_1$.

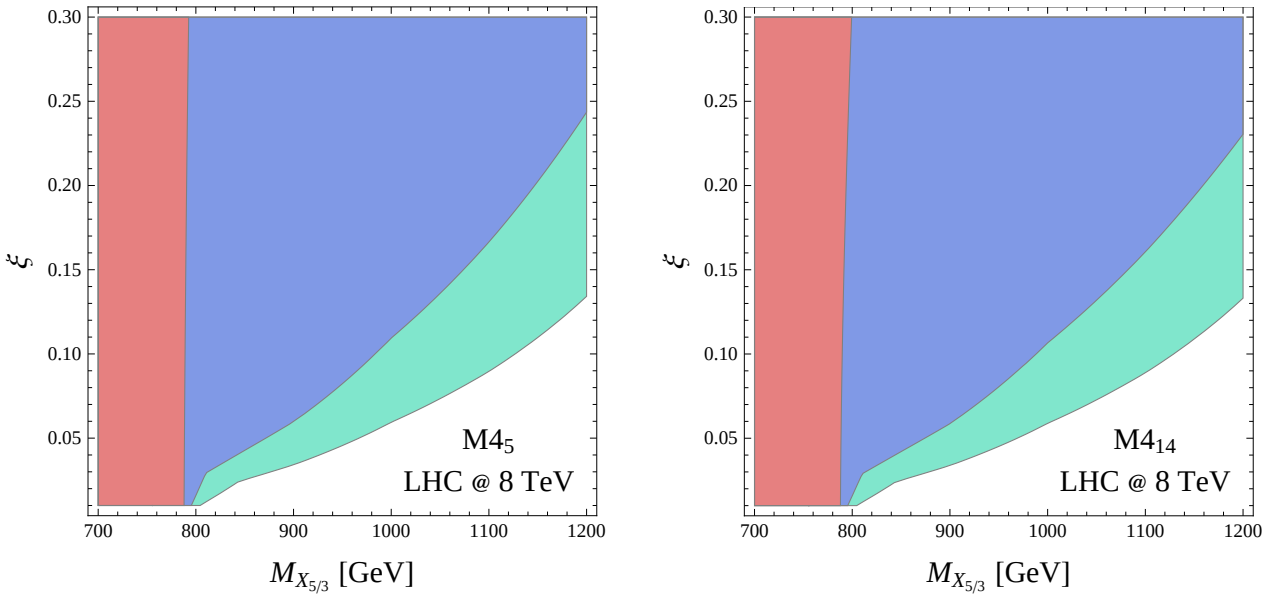

Figure 3.10: *Excluded (95%CL) regions in the* $(M_{X_{5/3}}, \xi)$ *plane for the models* **M4**$_5$ *and* **M4**$_{14}$*, using the searches [86, 87]. In red:* $c_1 = 0.3$ *and* $y = 3$ *(*$M_B \gg M_{X_{5/3}}$*), in blue:* $c_1 = 3$ *and* $y = 3$ *(*$M_B \gg M_{X_{5/3}}$*), in green:* $c_1 = 3$ *and* $y = 0.3$ *(*$M_B \gtrsim M_{X_{5/3}}$ *for* $\xi \gtrsim 0.1$*,* $M_B \gg M_{X_{5/3}}$ *for* $\xi \ll 0.1$*).*

Implications for the Model M9$_{14}$

In the model **M9**$_{14}$ the 5/3 and 8/3 states decay almost exclusively to the Wt while decays of the $-1/3$ states are significantly suppressed by a BR^2. Given this, the signal is mostly determined by the charge 5/3 and 8/3 states and therefore depends on the single parameter M defining their masses. Moreover, given that the signal is mostly determined by the charge-8/3 state due to its large cuts acceptance, we neglect the single production of the charge-5/3 states, which is suppressed for the case of the analysis from the Ref. [87], which is optimal for constraining the signal from the pair-produced $X_{8/3}$. We will also neglect the single production of the $X_{8/3}$ with $W^+t \to X_{8/3}W^-$ or $W^+W^+ \to X_{8/3}\bar{t}$ topologies, which is suppressed with respect to pair production by the scale M_* and by an additional power of the weak coupling [11]. Using current data, we obtain a lower bound for the model **M9**$_{14}$

$$M \geq 990 \text{ GeV} \quad @ \quad 95\% \text{ C.L.}, \tag{3.3.2}$$

which is marginally stronger than the bound obtained assuming that only the $X_{8/3}$ is present: $M \geq 940$ GeV.

3.3.2 Summary of Exclusions

The results of the searches described above can be conveniently summarized by scanning over the values of the model parameters and selecting the most and the least stringent bounds on the top-partners' masses. The highest excluded masses of $X_{5/3}$ and $X_{2/3}$ correspond to the lowest value of y and highest c_1 and ξ, and the opposite for the lowest exclusion. For T and B the highest exclusion

[11] However at very high masses one can expect that the single production can become competitive with the pair production due to the smaller kinematical threshold.

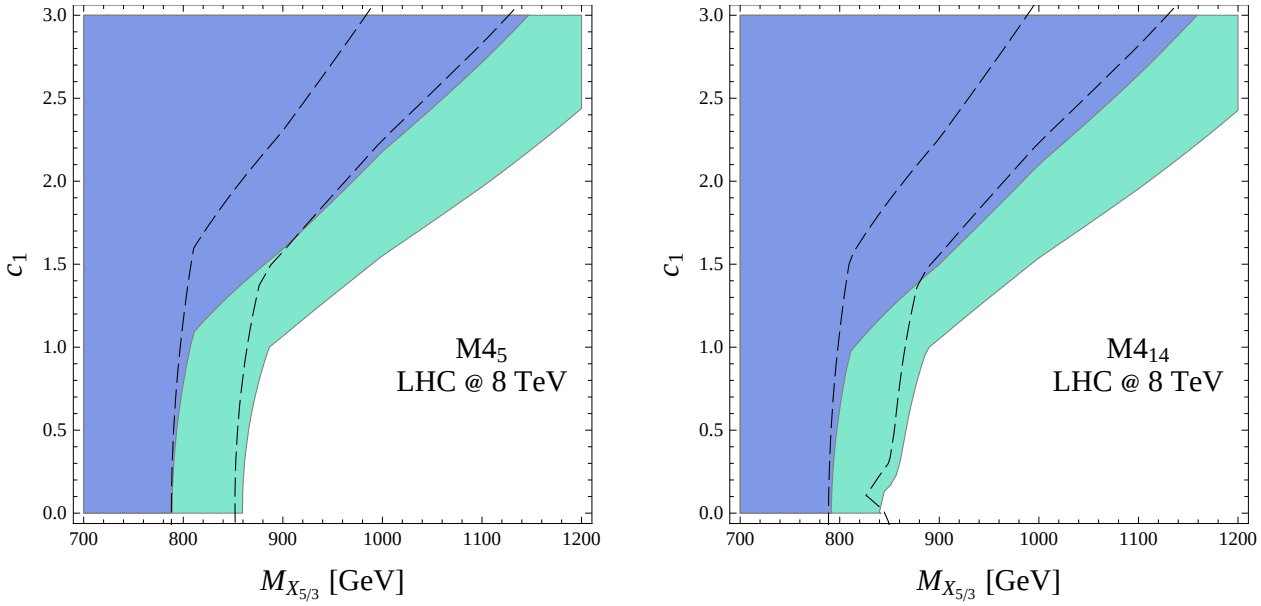

Figure 3.11: Excluded (95%CL) regions in the $(M_{X_{5/3}}, c_1)$ plane for $\xi = 0.2$ for the models $\mathbf{M4}_5$ and $\mathbf{M4}_{14}$, using the searches [86, 87]. In blue: $y = 3$ ($M_B \gg M_{X_{5/3}}$), in green: $y = 0.3$ ($M_B \gtrsim M_{X_{5/3}}$). Black dashed lines correspond to the exclusions with $\xi = 0.1$.

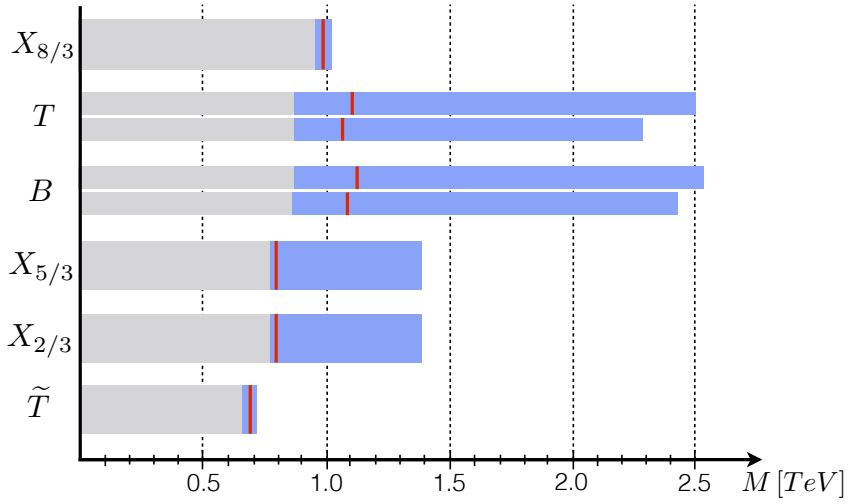

Figure 3.12: *Maxmal and minimal bounds on the masses of top partners for* $y \in [0.3, 3]$, $c_1 \in [0.3, 3]$ *and* $\xi \in [0.1, 0.3]$ *for the models* $\mathbf{M9}_{14}$, $\mathbf{M4}_5$, $\mathbf{M4}_{14}$, $\mathbf{M1}_5$ *and* $\mathbf{M1}_{14}$. *Grey regions are excluded for all the considered range of parameters while blue can be allowed depending on which values are taken by* y, c_1 *and* ξ. *Red lines correspond to the exclusions for the reference values* $\xi = 0.1$, $c_1 = 1$, $y = 1$. *For the states* T *and* B *upper and lower lines correspond to the exclusions obtained in the models* $\mathbf{M4}_5$ *and* $\mathbf{M4}_{14}$ *respectively, while for the* $X_{5/3}$, $X_{2/3}$ *and* $\widetilde{T}$ *the difference between different models is insignificant.*

corresponds to the highest y, c_1 and $1/\xi$ and the opposite for the lowest exclusion. In Fig. 3.12, we show our results for the maximal and minimal exclusions obtained by varying the parameters in the

ranges: $y \in [0.3, 3]$, $c_1 \in [0.3, 3]$ and $\xi \in [0.1, 0.3]$.

3.4 Future LHC bounds on the M9$_{14}$ and a dedicated analysis for the $X_{8/3}$

In this section we will estimate the bounds that could be put on the model **M9**$_{14}$ by the future LHC searches and compare the exclusion reach of the possible search channels, analysing the events with two or three same sign leptons plus jets.

Two Same Sign Leptons

Now, similarly to what we have done in the previous section, we want to estimate the reach of the 14 TeV LHC on the exclusion of the parameter space of the model **M9**$_{14}$ by recasting the exploratory $2ssl$ analysis of Ref. [90], tailored for charge-5/3 states. Its main difference with respect to the 8 TeV analysis of Ref. [87] is harder cuts on the transverse momenta. We report the estimated cuts acceptances for $X_{8/3}$ and $X_{5/3}$ at 14 TeV in the Table 3.7 and the $X_{8/3}$ mass reach is illustrated on the Fig. 3.13 in green.

Again, we can judge the accuracy of our study by comparing our efficiency for charge-5/3 states, with those of Ref. [90] (4^{th} and 5^{th} columns of Table 3.7). The two analyses differ by at most 20% at low masses and by up to 47% at 2 TeV. This means that our analysis, while still providing a good estimate of the experimental sensitivity, misses some effects, likely related to the high boost and the collinearity of the decay products. Nevertheless, in the case of $X_{8/3}$, the energy is distributed among a larger number of particles which are consequently less boosted than for the charge 5/3, implying that the distortion between a realistic analysis and ours will be smaller. Another factor that reduces the sensitivity to high boosts, is the collinearity between the b and the eventual lepton in the top-quark decay, which compromises the ability to single out the lepton. This effect, affects in a bigger proportion searches for charge-5/3 states, which produce at most two leptons (and if one is lost do not pass the $2ssl$ cut), than $X_{8/3}$ searches, which are most likely to produce non-collinear leptons.

Three Same Sign Leptons

Let us now analyze the possibility to construct a different, dedicated, experimental search to test the production of charge 8/3 states: with three same sign leptons ($3ssl$) final states. This analysis would certainly be necessary if a $2ssl$ signal is ever observed, in order to distinguish between the $X_{8/3}$ and other resonances with $2ssl$ decays, but it can also potentially be used to search directly for the $X_{8/3}$. In what follows, we compare the sensitivity of a $3ssl$ search w.r.t. the $2ssl$ one, in order to establish their relative exclusion potential.

The great advantage of the $3ssl$ channel is that the background is practically vanishing. The $3ssl$ events in the SM can originate as genuine $3ssl$ signals or as $2ssl$ events in which the charge of one of the extra leptons has been misidentified, or a jet has been taken for a lepton. The former can be predicted from theory, the dominant contributions coming from ZZZ, WZZ and WWZ events, and their rate is about a factor $\sim \alpha_{\rm em}$ smaller than for the WZ and ZZ backgrounds affecting $2ssl$ searches (see Ref. [87]). The ZZZ and WZZ events, together with contributions from $\bar{t}tZ$,

M [GeV]	$Q=\frac{8}{3}$ (contact)	$Q=\frac{8}{3}$ (via $\frac{5}{3}$)	$Q=\frac{5}{3}$	$Q=\frac{5}{3}$ (from [90])
1000	22.7	76.6	5.53	7.10
1200	51.9	91.9	13.7	12.3
1400	83.1	103	17.6	15.0
1600	114	115	21.5	16.9
1800	128	118	23.7	16.8
2000	136	119	23.6	16.1

Table 3.7: *Acceptance $\epsilon_{2ssl}(M_{8/3})$ for the cuts of the* 2ssl *analysis of Ref. [87] at 8 TeV (left panel) and of Ref. [90] at 14 TeV (right panel), multiplied by BR$\times 10^3$, for top partners of different electric charges Q; numbers include the BR's of the W bosons but assume that all the* 5/3 *states decay exclusively to $t+W$. The acceptance for the $X_{8/3}$ is given separately for two possible decay channels: with intermediate $X_{5/3}$ or $Y_{5/3}$, and via contact interactions with a d-symbol. The last columns corresponds to the original analyses [87,90]. Given that their decays have similar topology, at 14 TeV, efficiencies for the charge -1/3 states are taken equal to the ones of the 5/3.*

are efficiently eliminated with a Z veto, requiring the invariant mass of any two leptons to be off the Z-pole. On the other hand, the part from WWZ, and $\bar{t}tW$, is less sensitive to the Z veto, but is penalized by requiring a large number N_{con} of extra hard constituents in the event, since these events are not typically accompanied by several hard jets.

Leptons with misidentified charge, on the other hand, correspond to a genuine $2ssl$ background (dominantly WZ and ZZ) with extra misidentified leptons. While the probability to misidentify muons is negligible, the electrons/positron misidentification probability is estimated as $P_{misid} = 5.89 \times 10^{-4}$ [109]. The Z veto is also efficient in this case.

Finally, backgrounds due to jet misidentification are typically extracted using data-driven techniques which lie beyond the reach of our analysis. Nevertheless, this source of background is efficiently eliminated by requiring a large number of final states [109].

In order to suppress these background most efficiently, while preserving the signal, we apply the following selection cuts:

- Reconstruction criteria:
  - Leptons (e and μ) are required to have $p_T(l) > 30$ GeV and pseudorapidity $|\eta(l)| < 2.4$. They should also satisfy the following isolation criterium: sum of the p_T of the objects inside a cone with a radius $\Delta R = 0.3$ around a lepton candidate should not exceed 15% (20%) of the electron (muon) p_T.
  - Top jets are reconstructed using the Cambridge-Aachen clustering algorithm [91] with a distance parameter $R = 0.8$, and are required to have a $p_T > 200$ GeV, $|\eta| < 2.4$, invariant mass $m_{inv} \in [140, 250]$ GeV, at least 3 constituent subjets and a minimal pair-wise mass of the constituents of at least 50 GeV.
  - W jet candidates are also reconstructed using the Cambridge-Aachen clustering algorithm with $R = 0.8$ and with requirements $p_T > 200$ GeV, $|\eta| < 2.4$, $m_{inv} \in [60, 130]$ GeV and must

Contact Interaction

Mass, GeV	3ssl	M_{ll}	$N_{con} \geq 3$
1000	11.6	9.98	9.71
1200	12.5	11.0	10.9
1400	13.0	11.8	11.7
1600	13.6	12.6	12.5
1800	13.6	12.7	12.6
2000	12.5	11.9	11.7

Via charge-5/3 states

Mass, GeV	3ssl	M_{ll}	$N_{con} \geq 3$
1000	10.3	8.69	8.56
1200	9.71	8.47	8.39
1400	10.7	9.72	9.62
1600	11.8	10.9	10.8
1800	11.0	10.1	10.1
2000	10.5	9.74	9.56

Table 3.8: *Acceptance of the cuts times BR* $\times 10^3$ *for 3ssl from the* $X_{8/3}$ *for the decays via contact interaction (left panel) and for decays via an off-shell charge-5/3 state (right panels).*

consist of two subjets.

- Jets which are not identified as boosted tops or W's are clustered using anti-k_T algorithm [92] with $R = 0.5$ and are required to have $p_T > 30$ GeV and $|\eta| < 2.4$.
- Any jet must be separated from the reconstructed leptons by at least $\Delta R = 0.3$ and from other jets by $\Delta R = 0.8$.

▶ Event selection:

- 3 same sign leptons (e or μ).
- Z and quarkonia veto: $M(ll) > 20$ GeV for any pair of leptons, $M(\mu^+\mu^-) \notin [76, 106]$ GeV for opposite-sign muons and $M(ee) \notin [76, 106]$ GeV for any pair of electrons.
- A minimal number of constituents $N_{con} = 3$ apart from $3ssl$ (this includes other leptons and jets candidates, with top jets counted as three and W's as two constituents).

We simulated the most relevant backgrounds using MadGraph 5 and compared the efficiency of the cuts described above. For 100 fb^{-1}, at 14 TeV, the number of $3ssl$ background events from WZ and ZZ with a misidentified lepton, is approximately 5; this reduces below sensitivity after the Z veto. This is true also for genuine $3ssl$ contributions from WZZ and ZZZ, which are reduced from about 4 events to ~ 0.3 and are rendered negligible by a further N_{con} cut. The $3ssl$ contribution from $\bar{t}tW$ (and also the one from WWZ) is very small (of order 0.1) and can be neglected.

On the contrary, the signal is almost unaffected by these selection cuts. We summarize the cut acceptances (including branching ratios) $\epsilon_{3ssl}(M_{8/3})\times$BR for different masses at 14 TeV, obtained from the similar simulation as in the previous section, in the Table 3.8.

In order to estimate the excluding power of the $3ssl$ we performed a statistical analysis assuming that the observed signal equals to background, i.e. there is no excess, given that at present no experimental data is available for $3ssl$ channel. Under this assumption, the hypothesis predicting more than $N_{95}^{3ssl} = 3$ events is excluded with a 95% CL. Then, using Eq. (3.3.1), we estimate the bound on the $X_{8/3}$ mass depending on the integrated luminosity, that we report in Fig. 3.13 (in blue).

As we can see from Fig. 3.13, the 3ssl channel would not be able to overpass $2ssl$ for 14 TeV experiments. The smallness of the background can not compensate a great drawback of the $3ssl$

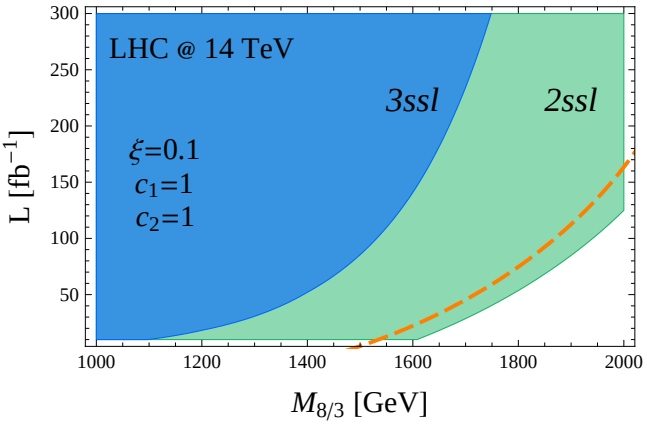

Figure 3.13: *A comparison of expected excluded masses of the charge* $8/3$ *state for the* $2ssl$ *(green) and* $3ssl$ *(blue) search channels in the complete model, with all the states of the nine-plet contributing to the signal, for different integrated luminosities for 14 TeV experiment. Orange dashed lines correspond to the exclusion provided by the 2ssl channel alone, assuming that only* $X_{8/3}$ *is produced.*

search: the small BR$\sim 2\%$ into three same-sign final state leptons reduces the signal acceptance by roughly a factor of 10. We conclude that, although the $3ssl$ search remains an important discriminant for these models in case of discovery, its sensitivity is not competitive with $2ssl$ searches.

Chapter 4

EWPT with Light Top Partners

In Chapter 2 we argued that the light composite fermionic partners of the top quark might be needed in order to allow for an observed small mass of the Higgs boson [1]. In this chapter we are going to consider the effect of the light composite fermionic resonances on the Electro-Weak Precision Tests (EWPT) constraints on CH models. The composite nature of the Higgs is a source of an infrared-saturated contribution to the EW oblique parameters [49] that, taken on its own, sets a stringent bound on the compositeness scale of the Higgs boson and inevitably raises the amount of fine-tuning [112–115]. It is thus clear that a scenario with an acceptable amount of tuning can only be obtained if further corrections to the EW parameters are present.

One possible source of additional contributions are the composite resonances and in particular the fermionic ones. Even if they do not give tree-level corrections to the EW oblique parameters, the top partners do contribute to them at one loop and these contributions can be sizable if the partners are light. In this chapter we concentrate on a model-independent general parametrization of the effect of new composite fermions. This allows us to reproduce different existing models and identify the effects that do not appear in some particular realizations.

In this Chapter (based on the paper [8]) we extend previous analyses [49,68,116–121] and provide the first computation of the fermion one-loop contribution to the $\widehat{S}$ parameter taking into account the Higgs non-linearities associated to its composite nature. The result of this computation is the identification of a new logarithmically enhanced contribution that can be interpreted as a running effect from the mass of the top partners to the scale of the EW vector resonances. We also study the contributions of the top partners to the $\widehat{T}$ parameter which, though finite, can be large and positive, in particular in the presence of a light $SU(2)$ singlet partner, and can compensate the Higgs contribution. We also clarify the structure of the deviations of the $Z\bar{b}_L b_L$ coupling which can become logarithmically divergent when 4-fermion interactions with a chirality structure LLRR are introduced in the composite sector.

This Chapter is organized as follows. In section 4.1 we present the effective Lagrangian describing a composite Higgs as Goldstone boson associated to the coset SO(5)/SO(4) together with the light top partners and their couplings to the SM fermions. In section 4.2 we present a general analysis of the corrections to the EW observables. In particular we estimate the contributions of the top partners to the EW oblique parameters and to the deviations of the couplings of the Z gauge boson to the b quark. Section 4.3 is devoted to the numerical analysis of some explicit models. In section 4.4

[1] This idea was also discussed and further developed in the Refs. [71, 95, 96].

we repeat the previous analysis within an alternative set-up in which the t_R appears as a completely composite state. And finally in section 4.5 we compute the modifications of the couplings of the top quark induced by the mixing with its partners. The appendices collect a few technical details.

4.1 The Effective Lagrangian

We want to construct an effective description of the composite Higgs models in which only the light fermionic states coming from the strong sector are included, while the heavier fermionic states and the bosonic resonances are integrated out. We associate to the heavy resonances a typical mass scale m_*, which can be interpreted as the cut-off of our effective theory. In a generic strongly coupled sector m_* is connected to the coupling of the strong dynamics g_* and to the Goldstone decay constant f by the relation $m_* \simeq g_* f$ [20]. Of course our effective description is valid as far as there is a mass gap between the light and the heavy resonances $m_{light} \ll m_*$.

We will consider a CH model with $SO(5) \to SO(4)$ breaking pattern. We assume the partial compositeness and account for the presence of the light fermionic resonances coupled to the top quark. In our derivation of the effective theory we will follow the standard CCWZ approach, which allows to build all the operators in the effective Lagrangian starting from elements in irreducible representations of the unbroken global group SO(4).

The Higgs doublet is described by the set of 4 Goldstone bosons Π_i encoded in the Goldstone matrix U,

$$U \equiv \exp\left[i\frac{\sqrt{2}}{f}\Pi_i T^i\right] , \tag{4.1.1}$$

where T^i $(i = 1, \dots, 4)$ are the generators of the SO(5)/SO(4) coset. he operators in the effective Lagrangian can be written in terms of the U matrix and of the CCWZ operators e_μ and d_μ, that come from the covariant derivative of the Goldstone matrix. The e_μ symbol is used to build the covariant derivative of the composite fermions. The d_μ symbol transforms as a 4-plet of SO(4) and enters in the kinetic terms for the Goldstones, which read

$$\mathcal{L}_{gold} = \frac{f^2}{4} d^i_\mu d^\mu_i \, . \tag{4.1.2}$$

The fermion sector of the theory depends on the quantum numbers we choose for the composite sector operators $\mathcal{O}_{L,R}$. In the following we will concentrate on the case in which the operators belong to the fundamental representation of SO(5). With this choice we are able to parametrize the low-energy dynamics of several explicit models proposed in the literature (see for example Refs. [40, 57, 60, 69, 122, 123]). The requirement of a mixing with the elementary top quark fixes the $\mathrm{U}(1)_X$ charge of these operators to be 2/3.

As mentioned before, in the effective theory we can describe the low-energy dynamics of the strong sector through a set of fermionic states. For simplicity we include only one level of composite fermions in our effective description and we identify the cut-off with the mass of the lightest of the other resonances. In the CCWZ approach the fields are introduced as irreducible representations of the unbroken group SO(4) and transform non-linearly under the full SO(5) symmetry. The quantum numbers of the $\mathcal{O}_{L,R}$ operators determine the representations of the fields which can be directly coupled to the elementary fermions. The fundamental representation of SO(5) decomposes

under SO(4) as $\mathbf{5} = \mathbf{4}+\mathbf{1}$. For this reason we include in our theory two composite fermion multiplets corresponding to representations $\mathbf{4_{2/3}}$ and $\mathbf{1_{2/3}}$ of $\mathrm{SO}(4) \times \mathrm{U}(1)_X$, which we denote by ψ_4 and ψ_1 respectively.

In order to estimate the size of the coefficients of the various terms in the effective Lagrangian we need to use a suitable power-counting rule. Following the approach of Refs. [7, 20] we adopt the following formula

$$\mathcal{L} = \sum \frac{m_*^4}{g_*^2} \left(\frac{y\,\psi_{el}}{m_*^{3/2}}\right)^{n_{el}} \left(\frac{g_*\Psi}{m_*^{3/2}}\right)^{n_{co}} \left(\frac{\partial}{m_*}\right)^{n_d} \left(\frac{\Pi}{f}\right)^{n_\pi} \left(\frac{gA_\mu}{m_*}\right)^{n_A} , \tag{4.1.3}$$

where ψ_{el} generically denotes the elementary fields q_L or t_R, while Ψ denotes the composite fermions. Notice that each insertion of an elementary fermion is accompanied by a corresponding factor of the elementary-composite mixing y. We assume that the rule in eq. (4.1.3) has only two exceptions [7]. [2] The first one is the kinetic term of the elementary fermions, which we set to be canonical. This is justified by the fact that the elementary fermions are external with respect to the strong dynamics and their kinetic term is set by the UV theory. The second exception is the mass of the fermion resonances included in our low-energy description, which we assume to be smaller than the cut-off m_*. This is needed in order to write an effective theory in which only a few resonances are present, while the other ones, at the scale m_*, are integrated out.

The full effective Lagrangian can be split into three pieces which correspond to the terms containing only composite states, the ones containing only elementary fields and the elementary–composite mixings:

$$\mathcal{L} = \mathcal{L}_{comp} + \mathcal{L}_{elem} + \mathcal{L}_{mixing} . \tag{4.1.4}$$

The leading order Lagrangian for the composite fermions is given by

$$\mathcal{L}_{comp} = i\overline{\psi}_4 \not{D}\psi_4 + i\overline{\psi}_1 \not{D}\psi_1 - m_4\overline{\psi}_4\psi_4 - m_1\overline{\psi}_1\psi_1 + \left(i\,c\,\overline{\psi}_4^i\gamma^\mu d_\mu^i\psi_1 + \text{h.c.}\right) + \frac{1}{f^2}(\overline{\psi}\psi)^2 , \tag{4.1.5}$$

where the index i labels components of the SO(4) 4-plets. Notice that the covariant derivative of the ψ_4 field contains, in addition to the usual derivative and to the coupling to the $\mathrm{U}(1)_X$ gauge boson, the CCWZ e_μ symbol: $D_\mu\psi_4 = (\partial_\mu - 2/3ig'X_\mu + ie_\mu)\psi_4$. The presence of the e_μ term is essential to restore the full SO(5) invariance of the Lagrangian and gives rise to non-linear derivative couplings between the 4-plet components and the Goldstones. In addition to the usual kinetic and mass terms we can also write an additional term using the CCWZ d_μ symbol. This operator induces some interactions between the 4-plet and the singlet mediated by the gauge fields and by the Goldstones. In general two independent terms with the d_μ symbol can be present, one for the left-handed and one for the right-handed composite fermions. For simplicity, however we assumed that the strong sector is invariant under parity, which forces the two operators to have the same coefficient.

Finally we denote collectively by $(\overline{\psi}\psi)^2/f^2$ possible contact interactions with 4 composite fermions. In spite of having dimension 6 these operators are not suppressed by the cut-off m_*, instead, their natural coefficient is of order $1/f^2$. Operators of this kind are typically generated by the exchange of heavy vector or scalar resonances (see diagrams in fig. 4.1). The suppression due to the propagator of the heavy boson is compensated by the large coupling, $g_* \simeq m_*/f$, thus explaining the order $1/f^2$ coefficient.

[2] Notice that the power-counting rule can also be violated in the presence of sum rules which forbid the generation of some operators.

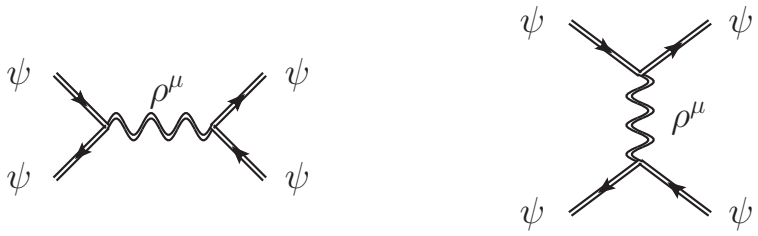

Figure 4.1: *Structure of the Feynman diagrams which generate* 4*-fermions operator through the exchange of heavy gauge resonances. In the diagrams we represent the composite resonances with a double line.*

The Lagrangian involving the elementary fields includes the usual canonical kinetic terms

$$\mathcal{L}_{elem} = i\bar{q}_L \not{D} q_L + i\bar{t}_R \not{D} t_R \,, \tag{4.1.6}$$

and the elementary–composite mixing

$$\begin{aligned} \mathcal{L}_{mixing} \;=\; & y_{L4} f \left(\bar{q}_L^{\mathbf{5}}\right)^I U_{Ii}\, \psi_4^i + y_{L1} f \left(\bar{q}_L^{\mathbf{5}}\right)^I U_{I5}\, \psi_1 + \text{h.c.} \\ & + y_{R4} f \left(\bar{t}_R^{\mathbf{5}}\right)^I U_{Ii}\, \psi_4^i + y_{R1} f \left(\bar{t}_R^{\mathbf{5}}\right)^I U_{I5}\, \psi_1 + \text{h.c.}\,, \end{aligned} \tag{4.1.7}$$

where $q_L^{\mathbf{5}}$ and $t_R^{\mathbf{5}}$ denote the embedding of the elementary fermions in an incomplete **5** of SO(5), namely

$$q_L^{\mathbf{5}} = \frac{1}{\sqrt{2}} \begin{pmatrix} i\, b_L \\ b_L \\ i\, t_L \\ -t_L \\ 0 \end{pmatrix} , \qquad t_R^{\mathbf{5}} = \begin{pmatrix} 0 \\ 0 \\ 0 \\ 0 \\ t_R \end{pmatrix} , \tag{4.1.8}$$

and U is the Goldstone matrix defined in eq. (4.1.1). The form of the elementary–composite mixings is dictated by the SO(5) symmetry. The assumption of partial compositeness tells us that the elementary fields are mixed with operators which transform in a *linear* representation of SO(5). The ψ_4 and ψ_1 CCWZ fields, instead, transform non-linearly under the global symmetry, so they can not be directly mixed with the elementary fields. To write down a mixing term we thus need to compensate for the non-linear transformation and this can be done by multiplying the CCWZ fields by the Goldstone matrix.

Notice that the coefficients which appear in our effective Lagrangian are in general complex. By means of chiral rotations of the elementary and composite fields one can remove only 3 complex phases, thus some parameters are still complex. In order to simplify the analysis we assume that our Lagrangian is invariant under CP [7]. Under this hypothesis all the parameters in the Lagrangian in eqs. (4.1.5) and (4.1.7) are real. [3]

4.2 General Analysis of the EW Parameters

In this section we provide a general analysis of the new physics corrections to the EW observables, in particular we will focus on the oblique parameters, $\widehat{S}$ and $\widehat{T}$, and on the $Z\bar{b}_L b_L$ coupling. As we

[3]The CP invariance fixes the coefficient of the d_μ symbol term to be purely imaginary. Thus our parameter c is real.

will see, several effects can generate distortions of this parameters and it is important to carefully study all of them. The primary aim of this section is to estimate the size of the various corrections and to determine which observables can be reliably computed in our low-energy effective approach.

4.2.1 The Oblique Parameters

We start our analysis by considering the oblique EW parameters, $\widehat{S}$ and $\widehat{T}$, [124, 125] that encode the corrections to the two point functions of the EW gauge bosons. The contributions to the oblique parameters come from three main effects: the Goldstone nature of the Higgs, the presence of vector resonances and the presence of fermionic resonances.

The first effect is related to the non-linear Higgs dynamics which induces a modification of the Higgs couplings with the EW gauge bosons. This distortion is present in any composite-Higgs model and is fully determined by the symmetry breaking pattern which gives rise to the Goldstones, in our case SO(5)/SO(4). In particular the leading logarithmically-enhanced contribution is universal and is completely fixed by the IR dynamics [49]. As we will see, while the contribution to $\widehat{S}$ is small, the effect on $\widehat{T}$ is sizable and, without further corrections, would lead to very stringent bounds on the Higgs compositeness scale f.

The second source of corrections is the presence of EW gauge resonances. In our effective Lagrangian approach the gauge resonances have been integrated out, thus this corrections arise as a purely UV effect. The most important contribution is generated at tree level due to the mixing of the composite resonances with the elementary gauge bosons and it gives a sizable correction to the $\widehat{S}$ parameter.

Finally the third class of contributions comes from loop effects induced by the composite fermions. This is the class of contributions we will be mainly interested in in the present analysis. As we will see, these corrections are typically large and including them is essential in order to obtain a reliable fit of the EW parameters. Although these effects have been already considered in the literature, most of the previous analyses did not take into account the full non-linear structure of the composite Higgs Lagrangian. Our analysis will show that the non-linearities are relevant and their inclusion can significantly affect the result and lead to new important effects.

The $\widehat{S}$ Parameter

At tree level the $\widehat{S}$ parameter receives a correction due to the mixing of the elementary gauge fields with the composite vector bosons. An estimate of this correction is given by [20]

$$\Delta\widehat{S} \simeq \frac{g^2}{g_*^2}\xi \simeq \frac{m_w^2}{m_*^2}\,. \tag{4.2.1}$$

The UV dynamics can lead to deviations with respect to the above formula. However those deviations are typically small and eq. (4.2.1) is usually in good agreement with the predictions of explicit models. Assuming that the correction in eq. (4.2.1) is the dominant contribution to $\widehat{S}$ (or at least that the other contributions to $\widehat{S}$ are positive), a rather strong upper bound on the mass of the EW gauge resonances is found, $m_* \gtrsim 2$ TeV (see the fit of the oblique parameters in fig. 4.2).

The other contributions to the $\widehat{S}$ parameter arise at loop level due to the non-linear Higgs dynamics and to the presence of fermion resonances. The leading contribution due to the non-linear

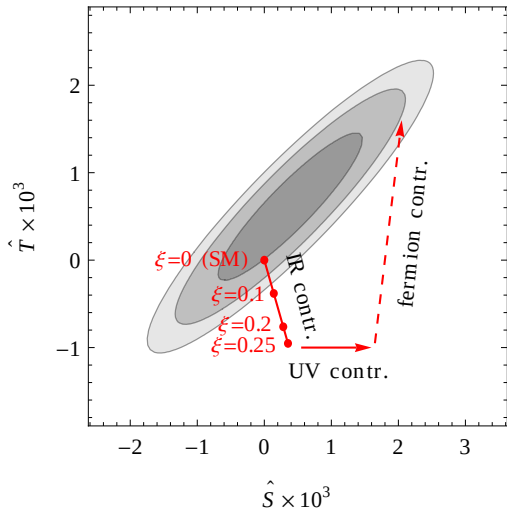

Figure 4.2: *Constraints on the oblique EW parameters $\widehat{S}$ and $\widehat{T}$ [126]. The gray ellipses correspond to the 68%, 95% and 99% confidence level contours for $m_h = 126$ GeV and $m_t = 173$ GeV. The red lines show the contributions which arise in composite Higgs models as explained in the main text. The IR contribution corresponds to the corrections due to non-linear Higgs dynamics, approximately given in eqs. (4.2.2) and (4.2.7), and is obtained fixing $m_* \sim 3$ TeV. The UV contribution is due to the EW gauge resonances (see eq. (4.2.1)).*

Higgs dynamics is given by [49]

$$\Delta\widehat{S} = \frac{g^2}{192\pi^2}\xi \log\left(\frac{m_*^2}{m_h^2}\right) \simeq 1.4\cdot 10^{-3}\,\xi\,. \tag{4.2.2}$$

where g denotes the SM $\mathrm{SU}(2)_L$ gauge coupling. In the above formulae we identified the cut-off with the mass scale of the EW gauge resonances and we chose $m_* \sim 3$ TeV and $m_h = 126$ GeV to derive the numerical estimate.

The contribution in eq. (4.2.2) arises from one-loop diagrams with gauge bosons and Goldstone virtual states. The diagrams contributing to $\widehat{S}$ are superficially logarithmically divergent. However, in the SM the logaritmic divergence exactly cancels due to the physical Higgs contribution. This is no longer true when the Higgs couplings are modified and in composite Higgs models a residual logarithmic dependence on the cut-off scale is present. [4] As can be seen from the numerical estimate the contribution in eq. (4.2.2) is much smaller than the absolute bounds on $\widehat{S}$ (compare fig. 4.2) and is typically negligible.

Let us finally consider the contribution due to loops of fermionic resonances. The general expression for the corrections to $\widehat{S}$ due to an arbitrary set of new vector-like fermion multiplets has been derived in Ref. [128]. The final formula contains a divergent contribution to $\widehat{S}$ given by

$$\Delta\widehat{S}^{div}_{ferm} = \frac{N_c g^2}{96\pi^2}\mathrm{Tr}\left[U_L^\dagger Y_L + U_R^\dagger Y_R\right]\log(m_*^2)\,, \tag{4.2.3}$$

where $U_{L,R}$ and $Y_{L,R}$ are the matrices of the couplings of left- and right-handed fermions to the W^3_μ and to the B_μ gauge bosons respectively and N_c is the number of QCD colors. In a renormalizable

[4] A more detailed analysis of the corrections to the $\widehat{S}$ parameter related to the Goldstone nature of the Higgs has been presented in Ref. [127].

theory in which the couplings of the gauge bosons to the fermions are just given by the usual covariant derivatives it is easy to see that the trace appearing in eq. (4.2.3) vanishes, so that no logarithmically divergent contribution to $\widehat{S}$ is present. [5] This is no longer true when the Higgs is a Goldstone boson. In this case higher order interactions of the gauge bosons mediated by the Higgs are present in the Lagrangian. Interactions of this kind are contained in the e_μ term in the covariant derivative of the composite 4-plet ψ_4 and in the d_μ-symbol term. After EWSB a distortion of the gauge couplings to the fermions is induced by these operators and a logarithmically divergent contribution to $\widehat{S}$ is generated. The presence of a logarithmically enhanced contribution can be also understood in simple terms as a running of the operators related to the $\widehat{S}$ parameter. We postpone a discussion of this aspect to the end of this subsection.

The logarithmically divergent correction can be straightforwardly computed:

$$\Delta\widehat{S}^{div}_{ferm} = \frac{g^2}{8\pi^2}(1-2c^2)\,\xi\log\left(\frac{m_*^2}{m_4^2}\right) . \tag{4.2.4}$$

It is important to notice that this contribution is there only if at least one SO(4) 4-plet is present in the effective theory. In fact, as we said, the only terms in the effective Lagrangian that can lead to relevant distortions of the gauge couplings are the 4-plet kinetic term and the d_μ-symbol term, which are clearly absent if only singlets are present. The connection of the divergence with the 4-plets justifies the identification of the argument of the logarithm in eq. (4.2.4) with the ratio m_*^2/m_4^2. It is also remarkable the fact that the correction in eq. (4.2.4) is independent of the elementary–composite mixings $y_{L,R}$. This implies that any SO(4) 4-plet below the cut-off of the effective theory would contribute to $\widehat{S}$ with a similar shift. [6]

Another interesting property of the divergent contribution to $\widehat{S}$ is the fact that it vanishes if $c^2 = 1/2$. As we will see later on, this choice of the parameter c implies the presence of an extra symmetry in the effective Lagrangian which protects the EW observables.

The logarithmic contribution to $\widehat{S}$ in eq. (4.2.4) is sizable if c^2 is not too close to $1/2$ and is typically much larger than the corresponding effect due to the Higgs non-linearities (eq. (4.2.2)). The correction due to fermion loops can even be comparable with the tree-level contribution estimated in eq. (4.2.1) if the strong coupling g_* is large, $g_* \gtrsim 5$. From the point of view of our effective approach, the coefficient c is just a free parameter, thus in principle the divergent fermion contribution can have an arbitrary sign. In particular for $c^2 > 1/2$ a sizable negative shift in $\widehat{S}$ would be possible, which could improve the agreement with the EW precision measurements (see fig. 4.2).

It is important to notice that in explicit models which provide a partial UV completion of our effective theory the value of c is typically fixed. A possible extension of our effective Lagrangian is given by the 2-site model proposed in Refs. [6, 40]. In this model $c = 0$, so that a sizable positive shift in $\widehat{S}$ seems unavoidable if a relatively light 4-plet is present. For example for $m_4 \simeq 700$ GeV and $m_* \simeq 3$ TeV a tight upper bound, $\xi \lesssim 0.1$, is obtained if we marginalize on $\widehat{T}$. The limits on the compositeness scale as a function of the 4-plet mass taking into account only the constraints on the $\widehat{S}$ parameter are shown in fig. 4.3. Notice that the bounds become typically stronger if the

[5] To prove this one can notice that the sum of the W^3_μ couplings to the fermions in each $SU(2)_L$ multiplet is zero. After EWSB the gauge couplings of the fermion mass eigenstates are obtained by unitary rotations of the initial coupling matrices. These rotation clearly cancel out in the trace in eq. (4.2.3), so that the divergent term vanishes.

[6] Resonances in larger SO(4) multiplets also lead to divergent contributions. For instance, states in the **9** lead to a contribution 6 times larger than the one in eq. (4.2.4).

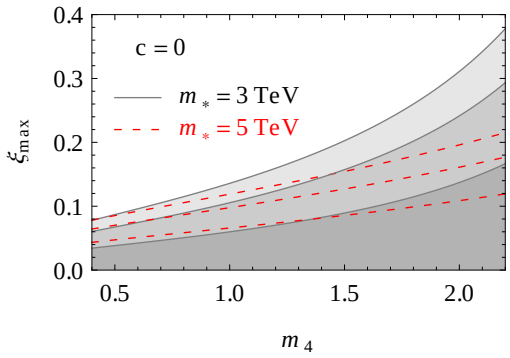

Figure 4.3: *Upper bounds on ξ in the 2-site model ($c = 0$) as a function of the 4-plet mass parameter m_4 for different values of the cut-off m_*. The results have been obtained by considering the shift in $\widehat{S}$ given in eqs. (4.2.1), (4.2.2) and (4.2.4) and by marginalizing on $\widehat{T}$. The shaded regions correspond to the points compatible with the constraints at the 68%, 95% and 99% confidence level for $m_* = 3$ TeV. The dashed red curves show how the bounds are modified for $m_* = 5$ TeV.*

cut-off scale increases. This is due to the fact that the logarithmically enhanced fermion contribution in eq. (4.2.4) grows at larger m_* and dominates over the tree-level correction in eq. (4.2.1) which instead decreases when the gauge resonances become heavier.

The 2-site realization of the composite models allows us also to find a connection between the fermion corrections to $\widehat{S}$ and the dynamics of the gauge resonances. In fact it turns out that the diagrams which give rise to the divergence in $\widehat{S}$ are closely related to the ones which determine the running of the gauge resonance coupling g_*. The divergent contribution to $\widehat{S}$ in this picture arises from the distortion of the mixing between the elementary and the composite gauge fields after EWSB.

A fermion contribution to $\widehat{S}$ similar to the one we found is in principle present also in the extra-dimensional realization of the composite Higgs scenario. The corrections to the oblique EW parameters due to fermion loops in this class of theories have been considered in the literature [123, 129], however no divergent or enhanced contribution was noticed. It is probable however that a contribution of this kind was overlooked because of its peculiar origin. Similarly to what happens in the 2-site model, in extra dimensions the divergence in $\widehat{S}$ derives from the mixing of the gauge zero-modes with the gauge resonances after EWSB. In the literature the computation of $\widehat{S}$ has been made neglecting this mixing, thus the divergent contribution was not found.

Notice that, in addition to the divergent contributions which explicitly depend on the cut-off, large finite contributions can also arise from the UV dynamics of the theory. We can estimate the one-loop UV contributions as

$$\Delta\widehat{S} \sim \frac{g^2}{16\pi^2}\xi \simeq 3 \cdot 10^{-3}\xi\,. \tag{4.2.5}$$

It is easy to see that these effects can in principle be sizable and could significantly change the fit to the EW data. We will see an explicit example of non-decoupling effects in subsection 4.3.1.

The Corrections to $\widehat{S}$ as a Running Effect

We can understand in simple terms the origin of the large logarithmically enhanced contributions to the $\widehat{S}$ parameter with an operator approach. In the effective theory the corrections to the $\widehat{S}$

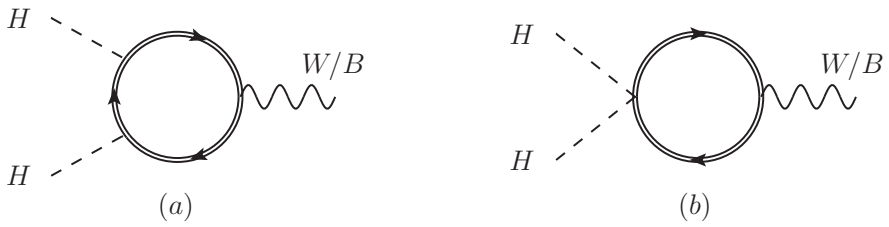

Figure 4.4: *Diagrams with resonance loops which can contribute to the $\mathcal{O}_{W,B}$ operators.*

parameter are induced by two dimension-6 operators [20]:

$$\mathcal{O}_W = i\left(H^\dagger \sigma^i \overleftrightarrow{D^\mu} H\right)(D^\nu W_{\mu\nu})^i \qquad \text{and} \qquad \mathcal{O}_B = i\left(H^\dagger \overleftrightarrow{D^\mu} H\right)(D^\nu B_{\mu\nu})\,, \tag{4.2.6}$$

where H denotes the usual Higgs doublet and $H^\dagger \overleftrightarrow{D_\mu} H$ is the derivative $H^\dagger(D_\mu H) - (D_\mu H)^\dagger H$.

The corrections to the $\mathcal{O}_{W,B}$ operators can be connected to the diagrams with two external Higgs states and one gauge field. In a renormalizable theory with only standard Yukawa Higgs couplings to the fermions the corrections from heavy resonances loops come from the (a) diagrams in fig. 4.4. By noticing that the $\mathcal{O}_{W,B}$ operators contain three powers of the external momenta it is easy to realize that these diagrams are always finite.

In a theory with a non-linear Higgs dynamics the situation is instead drastically different. In this case non-renormalizable contact interactions with two Higgses and two composite fermions are present. In particular the e_μ symbol in the kinetic term of the composite 4-plets induces a non-renormalizable interaction $i(\vec{\Pi}^t t^a \partial_\mu \vec{\Pi})(\overline{\psi}_4 \gamma^\mu \psi_4)$. This non-linear vertex, together with the usual gauge interactions, gives rise to the new class of diagrams denoted by (b) in fig. 4.4. These diagrams are logarithmically divergent and induce a corresponding running of the $\mathcal{O}_{W,B}$ operators leading to an enhanced contribution to $\widehat{S}$. This running effect generates the c-independent term in the correction to $\widehat{S}$ (see eq. (4.2.4)). [7]

Non-renormalizable Higgs interactions are also generated by the d_μ symbol terms. In particular it gives rise to a new vertex of the form $(\partial_\mu \Pi^i)\overline{\psi}_4^i \gamma^\mu \psi_1 + \text{h.c.}$. This vertex induces a logarithmically divergent contribution to $\mathcal{O}_{W,B}$ through diagrams analogous to the type (a) shown in fig. 4.4. The related contribution to the $\widehat{S}$ parameter corresponds to the term proportional to c^2 in eq. (4.2.4).

Before concluding the discussion on $\widehat{S}$ we want to comment on the relation between our results and the ones of Refs. [130, 131]. In Refs. [130, 131] an effective approach was used in which only the SM fields are retained and all the composite resonances are integrated out. In this framework it was shown that two effective operators $\mathcal{O}_{Hq} = i(\overline{q}_L \gamma^\mu q_L)(H^\dagger \overleftrightarrow{D_\mu} H)$ and $\mathcal{O}'_{Hq} = i(\overline{q}_L \gamma^\mu \sigma^i q_L)(H^\dagger \sigma^i \overleftrightarrow{D_\mu} H)$ induce a logarithmic running for $\widehat{S}$ between the top mass, m_t and the energy scale at which the effective operators are generated, m. Differently from Refs. [130, 131], in our approach the resonances are included in the effective theory and the effective operators $\mathcal{O}_{Hq}$ and $\mathcal{O}'_{Hq}$ are not present directly in our Lagrangian. At low energy, however, they are generated through the exchange of resonances of mass m with a coefficient y^2/m^2. From the previous discussion it is easy to understand that in

[7] Notice that the diagrams with the new non-linear Higgs vertex can in principle contribute also to two other dimension-6 operators, $\mathcal{O}_{HW} = i(D^\mu H)^\dagger \sigma^i (D^\nu H) W^i_{\mu\nu}$ and $\mathcal{O}_{HB} = i(D^\mu H)^\dagger (D^\nu H) B_{\mu\nu}$. Differently from $\mathcal{O}_{W,B}$, these two operators do not contribute to $\widehat{S}$ and are not minimally coupled [20]. With an explicit computation we found that the logarithmically divergent diagrams only generate a running of the minimally coupled operators $\mathcal{O}_{W,B}$ and not of $\mathcal{O}_{HW,HB}$.

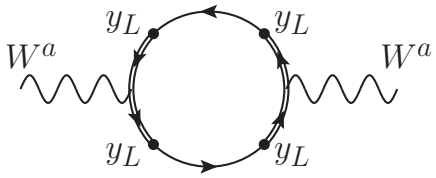

Figure 4.5: *Schematic structure of a fermion loop diagram contributing to the $\widehat{T}$ parameter at leading order in the y expansion.*

our approach the logarithmically divergent corrections to $\widehat{S}$ found in Refs. [130, 131] do not appear as real divergences but rather correspond to corrections which scale as $y^2/m^2 \log(m^2/m_t^2)$. Terms of this form can be recognized, for example, in the explicit analytic result for $\widehat{S}$ given in eq. (4.3.2). [8]

The $\widehat{T}$ Parameter

We can now analyze the corrections to the $\widehat{T}$ parameter. Thanks to the custodial symmetry $\widehat{T}$ does not receive correction at tree level and the only contributions come at loop level from diagrams with insertions of the operators which break the custodial symmetry. In our effective Lagrangian this breaking is induced by the weak gauging of the hypercharge $\mathrm{U}(1)_Y$ with coupling g' and by the mixings $y_{L4,1}$ of the q_L elementary doublet with the composite fermions.

The main correction due to the hypercharge coupling breaking comes from the IR contribution associated to the Goldstone nature of the Higgs. This effect is analogous to the one we already discussed for the $\widehat{S}$ parameter. The leading logarithmically enhanced contribution is given by [49]

$$\Delta\widehat{T} = -\frac{3g'^2}{64\pi^2}\xi \log\left(\frac{m_*^2}{m_h^2}\right) \simeq -3.8\cdot 10^{-3}\,\xi\,. \tag{4.2.7}$$

Differently from the analogous contribution to $\widehat{S}$ which was negligible due to accidental suppression factors, the contribution in eq. (4.2.7) gives a sizable correction to $\widehat{T}$. In particular, if we assume that this is the dominant correction to $\widehat{T}$ and that the shift in $\widehat{S}$ is non negative, a very stringent bound on ξ is obtained, $\xi \lesssim 0.1$ (see fig. 4.2). [9]

The second correction comes from fermion loops. As already noticed, in order to induce a contribution to $\widehat{T}$ the corresponding diagrams must contain some insertions of the symmetry breaking couplings $y_{L4,1}$. Under $\mathrm{SU}(2)_L \times \mathrm{SU}(2)_R$ the $y_{L4,1}$ mixings transform in the $(\mathbf{1},\mathbf{2})$ representation, thus at least 4 insertions are needed to generate a shift in $\widehat{T}$ [20]. This minimal number of insertions guarantees that the fermion one-loop corrections to $\widehat{T}$ are finite. A typical diagram contributing at leading order in the y expansion is shown in fig. 4.5.

It is straightforward to estimate the corrections to $\widehat{T}$ at leading order in the elementary–composite mixing [20]:

$$\Delta\widehat{T} \simeq \frac{N_c}{16\pi^2}\frac{y_L^4 f^2}{m^2}\,\xi\,, \tag{4.2.8}$$

where we denoted by m the mass scale of the lightest top partners in our effective Lagrangian. To get a quantitative estimate we can extract the value of the y_L mixing from the top mass. If we

[8] Notice that other effective operators with the structure $\mathcal{O}_t = H^\dagger H(\bar{q}_L H^c t_R)$ do not generate a running for $\widehat{S}$ [130].

[9] A similar bound has been derived in Ref. [113], where the phenomenological impact of the IR corrections to $\widehat{S}$ and $\widehat{T}$ on the fit of the Higgs couplings has been analyzed.

assume that the elementary–composite mixings have comparable sizes, $y_{L4} \simeq y_{L1} \simeq y_{R4} \simeq y_{R1} \simeq y$, the top Yukawa can be estimated as $y_t \simeq y^2 f/m$. By using this expression we get the estimate

$$\Delta\widehat{T} \simeq \frac{N_c}{16\pi^2} y_t^2\, \xi \simeq 2 \cdot 10^{-2}\, \xi\,. \tag{4.2.9}$$

Notice that this contribution is usually dominant with respect to the one given in eq. (4.2.7). Moreover, as we will see in the next section with an explicit calculation, the sign of the fermion contribution can be positive, so that it can compensate the negative shift in eq. (4.2.7). Notice that, if $\widehat{S}$ is not negative, a positive correction to $\widehat{T}$ from the fermion loops is essential in order to satisfy the EW constraints as can be clearly seen from the bound in fig. 4.2.

Notice that the finiteness of the fermion loop contribution to $\widehat{T}$ implies that the correction coming from the lightest resonances is dominant with respect to the one coming from heavier states. The contribution due to the UV dynamics can be estimated as [20]

$$\Delta\widehat{T} \simeq \frac{N_c}{16\pi^2} \frac{y_L^4}{g_*^2} \xi\,. \tag{4.2.10}$$

This contribution is suppressed with respect to the one in eq. (4.2.8) by a factor m^2/m_*^2. This shows that $\widehat{T}$ can be predicted in a robust way using our effective field theory approach.

4.2.2 The $Z\bar{b}_L b_L$ Vertex

Another observable which can be used to constrain the parameter space of new physics models is the Z boson coupling to the left-handed bottom quark. We define the Z interactions with the bottom by the formula

$$\mathcal{L}^Z = \frac{g}{c_w} Z_\mu \bar{b} \gamma^\mu \left[(g_{b_L}^{SM} + \delta g_{b_L}) P_L + (g_{b_R}^{SM} + \delta g_{b_R}) P_R \right] b\,, \tag{4.2.11}$$

where g^{SM} denotes the SM couplings (including the loop corrections), δg denotes the corrections due to new physics and $P_{L,R}$ are the left and right projectors. In the following we will denote by s_w and c_w the sine and cosine of the weak mixing angle. The SM tree-level values for the couplings are

$$g_{b_L}^{SM,tree} = -\frac{1}{2} + \frac{1}{3} s_w^2\,, \qquad g_{b_R}^{SM,tree} = \frac{1}{3} s_w^2\,, \tag{4.2.12}$$

and the one-loop corrections (computed in the limit $g \to 0$) are

$$g_{b_L}^{SM,loop} = \frac{m_t^2}{16\pi^2 v^2}\,, \qquad g_{b_R}^{SM,loop} = 0\,. \tag{4.2.13}$$

As can be seen from the current bounds shown in fig. 4.6, the deviation of the $Z\bar{b}_L b_L$ coupling are constrained to be at the level $3 \cdot 10^{-3}$, while the bounds on the coupling with the right-handed bottom component are one order of magnitude less stringent. In composite models the corrections to the g_{b_R} coupling are typically small, at most of the same order of the deviations in g_{b_L}. If we impose the constraint $|\delta g_{b_R}| \lesssim few \cdot 10^{-3}$, a negative value for δg_{b_L} of order $-2 \cdot 10^{-3}$ is preferred, while a positive shift worsens the fit with respect to the SM. The region favored by the current fit in the $(\delta g_{b_L}, \delta g_{b_R})$ plane is shown in fig. 4.6 and corresponds to the intersection of the gray ellipses with the vertical band.

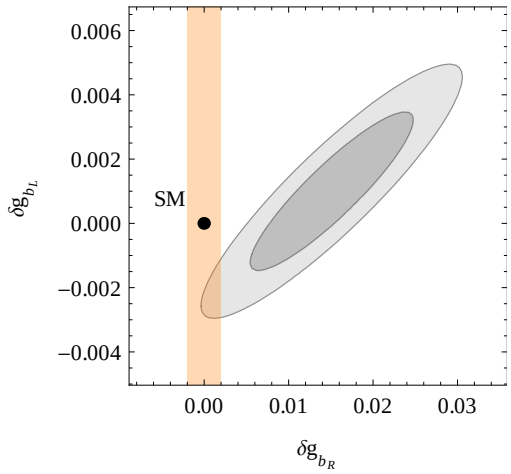

Figure 4.6: *Constraints on the corrections to the Z boson couplings to the bottom quark. The ellipses show the exclusion contours at 68% and 95% confidence level [132]. The vertical band shows the expected size of the corrections to the g_{b_R} coupling.*

Tree-Level Corrections

Let us now analyze the new physics corrections which arise in our scenario. The presence of an automatic P_{LR} symmetry in the composite sector and the fact that the elementary b_L state is invariant under this symmetry implies the absence of tree-level corrections to the $Z\bar{b}_L b_L$ vertex at zero momentum [41]. The tree-level corrections induced at non-zero momentum are related to operators of the form $D_\mu F^{\mu\nu}\bar{q}_L\gamma_\nu q_L$ and their size can be estimated as

$$\frac{\delta g_{b_L}}{g_{b_L}^{SM}} \sim \frac{y_L^2 f^2}{m^2}\frac{m_z^2}{m_*^2} \simeq 8\cdot 10^{-4}\,\frac{f}{m}\left(\frac{4\pi}{g_*}\right)^2 \xi\,, \tag{4.2.14}$$

where m is the mass scale of the composite fields mixed with the bottom, which in our scenario correspond to the charge $-1/3$ state inside the 4-plet ψ_4.

Notice that in our effective Lagrangian we did not include an elementary b_R state. For this reason the bottom is massless in our theory. In a more complete scenario a chiral field corresponding to the b_R will be present together extra composite fermions which are needed to generate the bottom mass. In this case the elementary q_L doublet has additional mixing terms with the new resonances and a tree-level correction to the $Z\bar{b}_L b_L$ vertex could be generated. For instance this happens in the case in which the additional bottom partners are contained in a 5 of SO(5) with $\mathrm{U}(1)_X$ charge $-1/3$. The contribution to the $Z\bar{b}_L b_L$ vertex coming from these states can be estimated as

$$\frac{\delta g_{b_L}}{g_{b_L}^{SM}} \simeq \frac{(y_L^b f)^2}{m_B^2}\xi\,, \tag{4.2.15}$$

where we denoted by y_L^b the mixing of q_L to the new multiplet and by m_B the typical mass scale of the new bottom partners. We can relate y_L^b to the bottom Yukawa by assuming that $y_L^b \simeq y_R^b$, in this case $(y_L^b)^2 \simeq (y_R^b)^2 \simeq y_b m_B/f$. The correction in eq. (4.2.15) becomes

$$\frac{\delta g_{b_L}}{g_{b_L}^{SM}} \simeq y_b\frac{f}{m_B}\xi \simeq 2\cdot 10^{-2}\frac{f}{m_B}\xi\,. \tag{4.2.16}$$

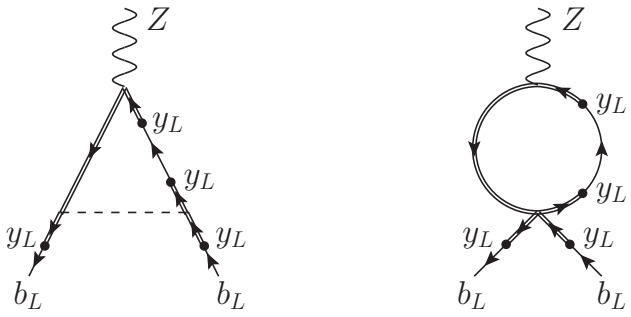

Figure 4.7: *Schematic structure of fermion loop diagrams contributing to the $Z\bar{b}_L b_L$ vertex with insertions of the y_L couplings on the external fermion legs.*

This correction can easily have a size comparable with the current bounds on δg_{b_L} in the case in which the new bottom partners are relatively light. Of course this correction can be suppressed if we relax the assumption $y^b_L \simeq y^b_R$ or if we chose $m_B \gg f$.

Corrections from Fermion Loops

We can now consider the one-loop contributions to the $Z\bar{b}_L b_L$ vertex. As a first step we will analyze the degree of divergence of the diagrams contributing to this effect. The degree of divergence can be easily obtained by using the power-counting method explained in Ref. [40]. It is straightforward to check that the $Z\bar{b}_L b_L$ operator at one loop is naively associated to a quadratic divergence. In our set-up, however, the P_{LR} symmetry implies a reduction of the naive degree of divergence. This is an obvious consequence of the fact that a new physics contribution to the $Z\bar{b}_L b_L$ vertex can be generated only if some powers of the couplings which break the P_{LR} symmetry are inserted in the diagrams. In our Lagrangian only the y_L mixings induce a breaking of this symmetry. These mixings correspond to some mass operators, so that each insertion in loop diagrams lowers the degree of divergence by one. [10] Let us now count how many insertions of the y_L mixing are necessary to generate a distortion of the $Z\bar{b}_L b_L$ vertex. Each external b_L is of course associated to a power of y_L. However, due to the fact that the b_L fields are external legs and they are invariant under P_{LR}, these insertions do not lead to a breaking of the symmetry. As a consequence at least four insertions of y_L are needed to generate a non-vanishing contribution. [11]

If the four y_L insertions are all inside the loop the corresponding contribution to the $Z\bar{b}_L b_L$ vertex is finite. This necessarily happens in the case in which only a singlet is present in the effective theory. Instead, if a 4-plet is also present, two y_L insertions can be on the external legs. In this case the two "external" insertions do not influence the degree of divergence and a logarithmically divergent contribution can be present. Examples of diagrams which could lead to this kind of corrections are shown in fig. 4.7.

In our effective theory a further subtlety is present which partially protects the $Z\bar{b}_L b_L$ vertex.

[10] The y_L mixing could in principle appear also in higher-dimensional operators. These operators, which we did not include in our effective Lagrangian, are suppressed by powers of the UV cut-off m_* as can be inferred from our power-counting rule in eq. (4.1.3). For this reason their insertions also lead to a reduction of the degree of divergence in agreement with the power counting expectation.

[11] A more rigorous proof of this statement can be obtained by using an operator analysis. For simplicity we do not present this analysis in the main text and postpone it to appendix 4.6.A.

The structure of the elementary–composite mixings implies the presence of a selection rule which forbids logarithmically divergent corrections coming from a large class of diagrams. As we will see the only diagrams which can lead to a divergent contribution are a subset of the "bubble"-type diagrams (see the diagram on the right of fig. 4.7), so that this kind of correction is necessarily related to the presence of 4-fermion operators.

To understand the origin of the selection rule we can analyze the "triangle"-type diagrams with y_L insertions on the external legs shown on the left of fig. 4.7. The external b_L's are both mixed with the B_L state coming from ψ_4. In order to generate a divergence the vertices containing a Goldstone boson must also contain a power of the momentum, that is they must be of the type $\partial_\mu \phi \overline{\psi}_L \gamma^\mu \psi_L$, where we generically denote by ϕ the Goldstone field and by ψ the composite fermions. [12] The structure of the vertex implies that the composite fermions which enter in the loop must be necessarily left-handed. But the left-handed composite fermions in the leading order Lagrangian mix with the elementary states only through y_R. As a consequence in order to generate a triangle diagram of this type some y_R or some composite mass insertions are needed in addition to the y_L mixings and this lowers the degree of divergence making the diagrams finite.

The only diagrams which can give rise to a logarithmic divergence are the "bubble" ones shown on the right of fig. 4.7. They of course crucially depend on the presence of 4-fermion operators in the effective Lagrangian. Two types of 4-fermion vertices can generate a diagram which contributes to δg_{b_L}. The first type of vertex has the form

$$\mathcal{O}_L^{4-ferm} = \frac{e_L}{f^2}(\overline{B}_L \gamma^\mu B_L)(\overline{\mathcal{T}}_L \gamma_\mu \mathcal{T}_L)\,, \tag{4.2.17}$$

where by $\mathcal{T}$ we denote any composite state with charge 2/3. For shortness in eq. (4.2.17) we did not specify the color structure which is not relevant for the present discussion. By adapting the previous analysis of the "triangle" diagrams, it is straightforward to show that the "bubble" diagrams with the vertex in eq. (4.2.17) are also protected by the selection rule, so that they are finite. The second type of 4-fermion vertex is of the form

$$\mathcal{O}_R^{4-ferm} = \frac{e_R}{f^2}(\overline{B}_L \gamma^\mu B_L)(\overline{\mathcal{T}}_R \gamma_\mu \mathcal{T}_R)\,. \tag{4.2.18}$$

In this case the selection rule is violated because the $\mathcal{T}_R$ fields can clearly mix with the q_L doublet through y_L. This class of vertices, as we will show with an explicit calculation, gives rise to a logarithmically divergent contribution to the $Z\bar{b}_L b_L$ vertex.

Of course in our effective Lagrangian higher-order mixing terms between the elementary and the composite states can in general be present. An example of such operators is a kinetic mixing between the q_L doublet and the composite 4-plet: $y_L f/m_* \left(\overline{q}_L^{\mathbf{5}}\right)^I U_{Ii} \not{D} \psi_{4L}^i + \text{h.c.}$. A term like this would induce a correction to the $Z\bar{b}_L b_L$ vertex through diagrams analogous to the "triangle" ones we considered before. Such a diagram would be superficially quadratically divergent (the kinetic higher-order mixing gives an extra power of the momentum). However the coefficient of the kinetic mixing, following our power counting in eq. (4.1.3), is suppressed by the UV cut-off, m_*, so that the final contribution is finite. Even though these diagrams can not give a logarithmically divergent contribution, they induce a correction which is not suppressed by powers of the cut-off, thus they can contribute at leading order to the $Z\bar{b}_L b_L$ vertex.

[12] In our effective Lagrangian vertices of this kind are generated by the d_μ symbol term.

Notice that the presence of unsuppressed contributions of this kind also implies a non-decoupling of the fermionic resonances. Even if we send the mass of a resonance to the cut-off, it can generate a higher-order effective operator in the low-energy Lagrangian which breaks the selection rule and gives a sizable contribution to the $Z\bar{b}_L b_L$ vertex. We will discuss an example of this effect in the next section.

The above discussion clearly shows that, even in the absence of logarithmically divergent contributions, the $Z\bar{b}_L b_L$ vertex is highly sensitive to the UV dynamics of the theory and can be reliably computed in a low-energy effective approach only if the logarithmically divergent contributions dominate or if we assume that the contributions coming from the UV dynamics are (accidentally) suppressed.

To conclude the general analysis of the $Z\bar{b}_L b_L$ vertex corrections we derive an estimate of the size of the contribution due to the fermion loops. The logarithmically divergent contribution can be estimated as

$$\frac{\delta g_{b_L}}{g_{b_L}^{SM}} \simeq \frac{y_L^2}{16\pi^2}\frac{y_{L4}^2 f^2}{m_4^2 + y_{L4}^2 f^2}\xi \log\left(\frac{m_*^2}{m_4^2}\right) . \tag{4.2.19}$$

Notice that we explicitly included a factor $y_{L4}^2 f^2/(m_4^2 + y_{L4}^2 f^2)$ which corresponds to the mixings between the b_L and the B_L which appears in the external legs of the logarithmically divergent diagrams. Using the relation between $y_{L,R}$ and the top Yukawa we get

$$\frac{\delta g_{b_L}}{g_{b_L}^{SM}} \simeq \frac{y_t^2}{16\pi^2}\xi \log\left(\frac{m_*^2}{m_4^2}\right) \simeq 2 \cdot 10^{-2}\,\xi\,, \tag{4.2.20}$$

where for the numerical estimate we set $m_* \simeq 3$ TeV and $m_4 \simeq 700$ GeV. In the case in which the logarithmically divergent contribution is not present or is suppressed the estimate becomes

$$\frac{\delta g_{b_L}}{g_{b_L}^{SM}} \simeq \frac{y_L^2}{16\pi^2}\frac{y_L^2 f^2}{m^2}\xi \simeq \frac{y_t^2}{16\pi^2}\xi \simeq 6 \cdot 10^{-3}\,\xi\,, \tag{4.2.21}$$

with m the mass of the lightest top partner.

The corrections in eqs. (4.2.19) and (4.2.21) are typically larger than the tree-level contribution generated at non zero momentum given in eq. (4.2.14). This is especially true if the mass of the resonances is not too small, $m \gtrsim f$, and the strong coupling is large, $g_* \gtrsim 5$. The corrections due to the bottom partners estimated in eq. (4.2.16) can in principle be comparable to the ones coming from fermion loops if the scale of the bottom partner is relatively small $m_B \sim f$. These corrections crucially depend on the quantum numbers of the bottom partners. In minimal scenarios (bottom partners in the fundamental representation of SO(5)) they are positive and some cancellation seems required to pass the present bounds. For simplicity, in our explicit analysis we will neglect both tree-level corrections.

4.2.3 Symmetries in the Effective Lagrangian

As we saw in the analysis of the $\widehat{S}$ parameter the divergent contributions coming from fermion loops are finite if the relation $c^2 = 1/2$ holds. We want now to study our effective Lagrangian in this case and understand the origin of the protection of the EW parameters. For definiteness we will focus on the case $c = 1/\sqrt{2}$ and we will comment at the end on the other possibility $c = -1/\sqrt{2}$.

Let us start with the Lagrangian for the composite fields given in eq. (4.1.5). A straightforward computation shows that the leading order terms in the case $c = 1/\sqrt{2}$ can be simply rewritten as

$$\mathcal{L}_{comp}^{c=1/\sqrt{2}} = i\bar{(}\Psi U^\dagger)\gamma^\mu(\partial_\mu - igA_\mu)(U\Psi) - m_4\overline{\Psi}\Psi - (m_1 - m_4)\overline{\Psi}_5\Psi_5\,, \tag{4.2.22}$$

where we introduced the 5-plet

$$\Psi = \begin{pmatrix} \psi_4 \\ \psi_1 \end{pmatrix} \tag{4.2.23}$$

and we denoted by Ψ_5 the fifth component of Ψ, namely $\Psi_5 = \psi_1$, while A_μ represents the elementary gauge fields in a compact notation. A simple field redefinition, $\Psi \to \Psi' \equiv U^\dagger\Psi$, shows that the only dependence on the Goldstone fields in the composite fermion Lagrangian is associated to the mass term

$$\mathcal{L}_{comp}^{c=1/\sqrt{2}} \supset -(m_1 - m_4)(\overline{\Psi}'U)_5(U^\dagger\Psi')_5\,, \tag{4.2.24}$$

which gives the mass splitting between the 4-plet and the singlet. Notice that this property is a consequence of our choice of c, in the general Lagrangian the dependence on the Goldstones in the kinetic terms of the composite fields can not be removed. It is clear that, if $m_1 = m_4$, in the composite sector Lagrangian an additional SO(5) symmetry is present, which allows us to remove the Higgs VEV.

With the same redefinition of the composite fields the Lagrangian for the elementary states in eq. (4.1.7) becomes

$$\begin{aligned} \mathcal{L}_{elem}^{c=1/\sqrt{2}} \;=\; & i\bar{q}_L \not{D} q_L + i\bar{t}_R \not{D} t_R \\ & + y_{L4} f\, \bar{q}_L^{\mathbf{5}}\Psi' + (y_{L1} - y_{L4}) f \left(\bar{q}_L^{\mathbf{5}} U\right)_5 (U^\dagger\Psi')_5 \\ & + y_{R4} f\, \bar{t}_R^{\mathbf{5}}\Psi' + (y_{R1} - y_{R4}) f \left(\bar{t}_R^{\mathbf{5}} U\right)_5 (U^\dagger\Psi')_5 + \text{h.c.}\,. \end{aligned} \tag{4.2.25}$$

The Goldstones in this case appear only in association with the $(y_{L1} - y_{L4})f$ and $(y_{R1} - y_{R4})f$ mass mixings.

From the structure of the Lagrangian in eqs. (4.2.22) and (4.2.25) we can simply understand why no divergence arises in the fermion contribution to $\widehat{S}$. In order to generate an effect which feels EWSB the corresponding operator must necessarily include some insertions of the Lagrangian terms containing the Goldstones. For our choice of c the Goldstones are always associated to mass operators and any insertion leads to a reduction of the degree of divergence. The $\widehat{S}$ parameter is naively logarithmically divergent at one loop, thus the extra mass insertions make it finite.

A similar protection mechanism is also present for the fermion corrections to the $Z\bar{b}_L b_L$ vertex. In the case in which $y_{L1} = y_{L4}$ the remaining $y_{L4} f \bar{q}_L^{\mathbf{5}}\Psi'$ mixing is independent of the Goldstones. The only operators containing the U matrix are the $(m_1 - m_4)$ mass term and the $(y_{R1} - y_{R4})f$ mixing. In order to generate a correction to g_{b_L} some insertions of these operators are needed in addition to the four insertions of y_{L4}. These extra mass insertions make the corrections to the $Z\bar{b}_L b_L$ vertex finite.

A similar structure of the effective Lagrangian is also present if $c = -1/\sqrt{2}$. This case can be connected to the one we discussed with the redefinitions $\psi_1 \to -\psi_1$, $y_{L,R1} \to -y_{L,R1}$, which just reverse the sign of c.

A particular implementation of our effective Lagrangian with $c = 1/\sqrt{2}$ has been studied in Ref. [69]. In this work the additional relations $y_{L4} = y_{L1}$ and $y_{R4} = y_{R1}$ are assumed. In this

particular case the only dependence on the Goldstones comes from the mass splitting term between the composite 4-plet and the singlet. The explicit computation of the fermion corrections to the $Z\bar{b}_L b_L$ vertex presented in Ref. [69] shows that the new physics contributions are finite, in agreement with the results of our analysis.

4.3 Results in Explicit Models

After the general analysis presented in the previous section, we now focus on a more detailed study of the corrections to the EW precision parameters in some explicit scenarios. First of all we will consider the simplified set-ups in which only one light composite multiplet is present in the effective theory. Afterwards we will study two more complete models containing a composite 4-plet as well as a singlet.

The analysis of explicit scenarios is of course essential to obtain a reliable quantitative determination of the constraints coming from the EW precision data. Moreover it allows to check the validity of the general results derived in the previous section.

In all our numerical results we fix the top mass to the value $m_t = m_t^{\overline{MS}}(2\text{ TeV}) = 150$ GeV, which corresponds to the pole mass $m_t^{pole} = 173$ GeV. Moreover, to estimate the constraints from the oblique parameters, we chose a cut-off scale $m_* = 3$ TeV.

4.3.1 The Case of a Light Singlet

As a first example we consider the case in which only a light composite singlet is present in the effective theory. The effective Lagrangian for this set-up can be easily read from the general one of section 4.1 by removing the terms containing ψ_4. In this configuration the resonance spectrum contains only one composite state, the $\widetilde{T}$, which has the same electric charge as the top and a mass

$$m_{\widetilde{T}}^2 = m_1^2 + y_{R1}^2 f^2 \,. \tag{4.3.1}$$

We start our analysis by considering the corrections to the $\widehat{S}$ parameter. In the general analysis we saw that the fermion contributions to $\widehat{S}$ can diverge only if the spectrum contains a light 4-plet, thus in our present set-up we expect a finite result. In fact at leading order in the v/f expansion we find that the one-loop fermion contribution is given by

$$\Delta\widehat{S}_{ferm} = \frac{g^2}{192\pi^2}\xi\frac{m_1^2 y_{L1}^2 f^2}{(m_1^2+y_{R1}^2 f^2)^2}\left[-5+2\log\left(\frac{2(m_1^2+y_{R1}^2 f^2)^2}{v^2 y_{L1}^2 y_{R1}^2 f^2}\right)\right] . \tag{4.3.2}$$

Notice that the argument of the logarithm can be identified with the ratio between the mass of the heavy fermion resonance $m_{\widetilde{T}}$ and the top mass.

$$m_t^2 \simeq \frac{v^2\, y_{L1}^2 y_{R1}^2 f^2}{2(m_1^2+y_{R1}^2 f^2)} \,. \tag{4.3.3}$$

For typical values of the parameters, $y_{L1} \sim y_{R1} \sim 1$, $m_1 \lesssim 1$ TeV and $\xi \lesssim 0.2$, the contribution in eq. (4.3.2) is positive and small, $\Delta\widehat{S}_{ferm} \lesssim 10^{-4}$.

As we discussed in section 4.2, although the correction to $\widehat{S}$ coming from the low-energy dynamics is calculable, large uncalculable UV contributions can be present. Even if we assume that the tree-level effects given in eq. (4.2.1) are negligible, the loop contributions coming from the UV dynamics

(see the estimate in eq. (4.2.5)) are typically dominant with respect to the corrections in eq. (4.3.2). We can check that the UV effects can be important by slightly modifying our explicit computation. We consider an effective theory in which a composite 4-plet is present as well as a singlet. In order to recover the case with only a light singlet, we then take the limit in which the 4-plet mass is sent to the cut-off m_*. To ensure that $\widehat{S}$ is calculable in the effective theory we set $c^2 = 1/2$. The explicit computation of $\Delta\widehat{S}$ leads to the result in eq. (4.3.2) plus an additional shift which, at the leading order in an expansion in the cut-off, is given by

$$\Delta\widehat{S}^{UV}_{ferm} = -\frac{g^2}{24\pi^2}\xi \simeq -1.8\cdot 10^{-3}\,\xi\,. \tag{4.3.4}$$

As expected, the 4-plet does not decouple in the limit in which it becomes heavy. The UV corrections in eq. (4.3.4) have a size compatible with our estimate in eq. (4.2.5) and are typically larger than the singlet contribution in eq. (4.3.2). Notice that the result in eq. (4.3.4) gives only an example of possible UV effects and should not be thought as a complete determination of the UV contributions. In order to properly compute the total shift in $\widehat{S}$ the whole UV completion of the model should be taken into account.

Let us now consider the $\widehat{T}$ parameter. As shown in the general analysis, the fermion corrections are finite and saturated by the low-energy contributions. The explicit calculation gives the following result at leading order in v/f:

$$\Delta\widehat{T}_{ferm} = \frac{3\,\xi}{64\pi^2}\frac{y_{L1}^4 m_1^2 f^2}{(m_1^2+y_{R1}^2 f^2)^3}\left\{m_1^2+2y_{R1}^2 f^2\left[\log\left(\frac{2(m_1^2+y_{R1}^2 f^2)^2}{v^2 y_{L1}^2 y_{R1}^2 f^2}\right)-1\right]\right\}. \tag{4.3.5}$$

This contribution is positive and, in a large part of the parameter space, can compensate the negative shift which comes from the non-linear Higgs dynamics (see eq. (4.2.7)). In the points in which $y_{L1}\sim y_{R1}\sim 1$, the estimate given in eq. (4.2.8) is approximately valid. The total shift in $\widehat{T}$ is shown in fig. 4.8 for the reference value $\xi = 0.2$, corresponding to $f = 550$ GeV. It can be seen that sizable positive values of $\Delta\widehat{T}$ can easily be obtained for reasonable values of the singlet mass and of the elementary–composite mixings.

Finally we analyze the corrections to the $Z\bar{b}_L b_L$ vertex. We showed in section 4.2 that in the case with only a light singlet the one-loop fermion corrections to this observable are finite. The absence of a 4-plet also implies that additional contributions coming from 4-fermion operators and from the UV dynamics are suppressed by the cut-off scale and can be expected to be negligible. At leading order in v/f we find that the shift in g_{b_L} is given by

$$\delta g_{b_L} = \frac{\xi}{64\pi^2}\frac{y_{L1}^4 m_1^2 f^2}{(m_1^2+y_{R1}^2 f^2)^3}\left\{m_1^2+2y_{R1}^2 f^2\left[\log\left(\frac{2(m_1^2+y_{R1}^2 f^2)^2}{v^2 y_{L1}^2 y_{R1}^2 f^2}\right)-1\right]\right\}. \tag{4.3.6}$$

Comparing this result with the fermion contribution to $\widehat{T}$ in eq. (4.3.5) we can notice that a strict relation exists between the two quantities $\Delta\widehat{T}_{ferm} = 3\delta g_{b_L}$. [13] In particular the positive correction to $\widehat{T}$ is related to a corresponding positive shift in g_{b_L}. For the typical size of the fermion contribution to $\widehat{T}$ needed to satisfy the experimental bounds, $1\cdot 10^{-3} < \Delta\widehat{T} < 2\cdot 10^{-3}$, a moderate contribution to δg_{b_L} is found: g_{b_L}: $0.33\cdot 10^{-3} < \delta g_{b_L} < 0.66\cdot 10^{-3}$. As we already discussed (see fig. 4.6), the experimental measurements disfavor a positive contribution to the $Z\bar{b}_L b_L$ coupling. Thus the

[13] This relation was already noticed in Refs. [49, 68].

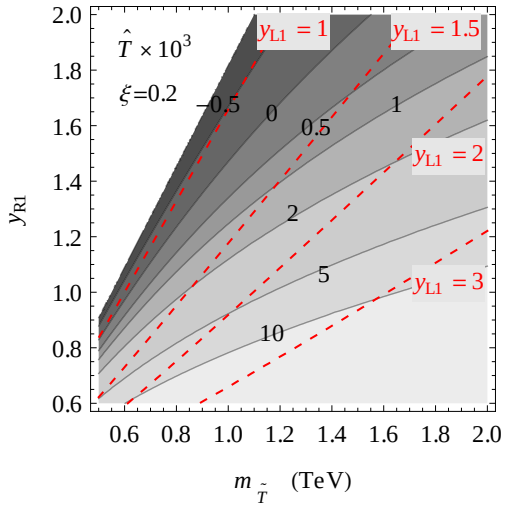

Figure 4.8: *Corrections to the $\widehat{T}$ parameter as a function of the singlet mass $m_{\widetilde{T}}$ and of the y_{R1} mixing. The result corresponds to the case with only a light singlet and includes the contribution due to the Higgs non-linear dynamics in eq. (4.2.7) and the exact fermion one-loop correction. The compositeness scale has been fixed to the value $\xi = 0.2$. The red dashed lines correspond to the contours with fixed y_{L1}.*

scenario with only a light singlet tends to be in worse agreement with the EW precision data than the SM.

On the other hand, if we neglect the constraints on δg_{b_L} and only consider the bounds on the oblique EW parameters, it is not hard to satisfy the experimental constraints even for sizable values of ξ.

4.3.2 The Case of a Light 4-plet

As a second simplified scenario we consider the case in which the resonance spectrum contains only a light 4-plet. The general analysis of section 4.2 showed that in this case only $\widehat{T}$ receives a finite contribution from fermion loops, whereas the corrections to the $\widehat{S}$ parameter and to the $Z\bar{b}_L b_L$ vertex are logarithmically divergent. [14]

Before discussing in details the contributions to the EW parameter, we analyze the spectrum of the resonances. The 4-plet gives rise to two $\mathrm{SU}(2)_L$ doublets with hypercharges 1/6 and 7/6. The $\mathbf{2}_{1/6}$ doublet contains a top partner T and a bottom partner B, while the $\mathbf{2}_{7/6}$ doublet contains an exotic state with charge 5/3 ($X_{5/3}$) and a top resonance ($X_{2/3}$). The mixing with the elementary states induces a mass splitting between the two doublets. The states inside each doublet, instead, receive only a small splitting due to EWSB effects and are nearly degenerate in mass. In particular the B and $X_{5/3}$ states are not coupled to the Higgs and their masses do not receive corrections after EWSB. The masses of the composite resonances are given by

$$m^2_{X_{2/3}} \simeq m^2_{X_{5/3}} = m_4^2 \qquad \text{and} \qquad m_T^2 \simeq m_B^2 = m_4^2 + y_{L4}^2 f^2 \,. \tag{4.3.7}$$

[14] The corrections to the $\widehat{T}$ parameter and to the $Z\bar{b}_L b_L$ vertex in this set-up have been studied also in Ref. [68]. The results for $\widehat{T}$ are similar to the ones we find. The results for the $Z\bar{b}_L b_L$ corrections are also in agreement with ours if we exclude the contributions from 4-fermion operators which are not included in the analysis of Ref. [68].

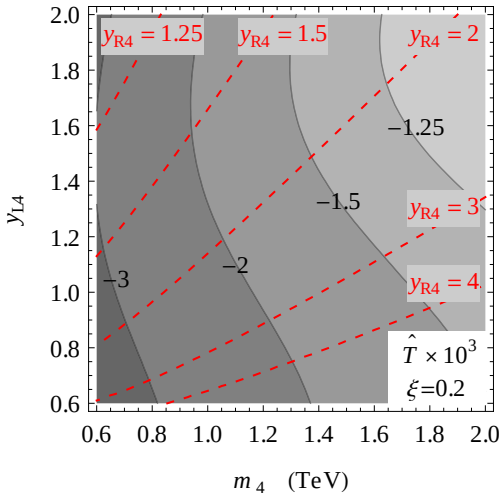

Figure 4.9: *Corrections to the $\widehat{T}$ parameter as a function of the mass parameter m_4 and of the y_{L4} mixing. The result corresponds to the case with only a light 4-plet and includes the contribution due to the Higgs non-linear dynamics in eq. (4.2.7) and the exact fermion one-loop correction. The compositeness scale has been fixed to the value $\xi = 0.2$. The red dashed lines correspond to the contours with fixed y_{R4}.*

The top mass at the leading order in v/f is given by

$$m_t^2 \simeq \frac{v^2\, y_{L4}^2 y_{R4}^2 f^2}{2(m_4^2 + y_{L4}^2 f^2)}\,. \tag{4.3.8}$$

The dominant contribution to the $\widehat{S}$ parameter comes from the logarithmically enhanced corrections due to loops of fermion resonances. The explicit result can be obtained from eq. (4.2.4) by setting $c = 0$: [15]

$$\Delta\widehat{S}_{ferm} = \frac{g^2}{8\pi^2}\xi \log\left(\frac{m_*^2}{m_4^2}\right) \simeq 1.6 \cdot 10^{-2}\,\xi\,, \tag{4.3.9}$$

where the numerical estimate has been obtained by setting $m_4 \simeq 700$ GeV and $m_* \simeq 3$ TeV. If the gauge resonances are heavy, $m_*/f = g_* \gtrsim 4$, the correction in eq. (4.3.9) is comparable or even larger than the tree-level one in eq. (4.2.1).

The sizable positive contribution to the $\widehat{S}$ parameter implies a quite stringent bound on the compositeness scale, $\xi \lesssim 0.1$ (see fig. 4.2). An even stronger constraint is obtained if we also consider the corrections to the $\widehat{T}$ parameter. The full expression of the fermion contributions at leading order in v/f is in this case too involved and does not give useful insights, so we only report here the leading term in the y expansion:

$$\Delta\widehat{T}_{ferm} = -\frac{\xi}{32\pi^2}\frac{y_{L4}^4 f^2}{m_4^2}\,. \tag{4.3.10}$$

[15] The same result can be obtained with the following equivalent procedure. We consider an effective theory containing a 4-plet and a singlet with $c^2 = 1/2$. In this case the fermion contribution to $\widehat{S}$ is finite and calculable. The explicit computation shows that a contribution of the form $g^2/(8\pi^2)\xi\log(m_1^2/m_4^2)$ is present. In the limit in which the singlet becomes heavy, $m_1 \to m_*$, we recover, as expected, the contribution in eq. (4.3.9).

The approximate result suggests that the shift in $\widehat{T}$ is negative. This conclusion is typically correct and has been explicitly verified with a numerical computation. The main contributions to $\widehat{T}$ coming from the non-linear Higgs dynamics (see eq. (4.2.7)) and from fermion loops are shown in fig. 4.9 for $\xi = 0.2$. Similar results are obtained for different values of ξ. Notice that the leading order expression in eq. (4.3.10) capture only the overall size of the fermion contributions. The exact result can deviate from the estimate at order one especially in the parameter space region in which y_{R4} becomes large.

The fact that the shift in $\widehat{T}$ is necessarily negative makes the constraints coming from the oblique parameters extremely severe. Using the results in fig. 4.2 an upper bound $\xi \lesssim 0.02$ at the 99% confidence level is obtained, which corresponds to a lower bound $f \gtrsim 1.7$ TeV.

Although the configuration with only a light 4-plet is strongly disfavored by the large corrections to the oblique parameters, it is still worth discussing the form of the corrections to the $Z\bar{b}_L b_L$ vertex. The explicit computation will be useful to verify the results obtained in our general analysis in section 4.2.

We start by considering the contributions related to the leading-order terms in the effective Lagrangian. If we neglect the effects coming from higher-dimensional operators and from 4-fermion contact interactions, we get the following corrections to the $Z\bar{b}_L b_L$ vertex at the leading order in the v/f expansion:

$$\begin{aligned}\delta g_{b_L}^{4-plet} \;=\; & -\frac{\xi}{32\pi^2}\frac{y_{L4}^2 y_{R4}^2 f^2}{m_4^2+y_{L4}^2 f^2}\left[\frac{y_{L4}^2 f^2}{m_4^2+y_{L4}^2 f^2}+\left(1-\frac{y_{R4}^2 f^2}{4m_4^2}\right)\log\left(1+\frac{y_{L4}^2 f^2}{m_4^2}\right)\right. \\ & \left. -y_{L4}^2 f^2\frac{4m_4^2(m_4^2+y_{L4}^2 f^2)-(2m_4^2+y_{L4}^2 f^2)y_{R4}^2 f^2}{4m_4^2(m_4^2+y_{L4}^2 f^2)^2}\log\left(\frac{2(m_4^2+y_{L4}^2 f^2)^2}{v^2 y_{L4}^2 y_{R4}^2 f^2}\right)\right] \end{aligned} \tag{4.3.11}$$

As expected, due to the selection rule discussed in subsection 4.2.2, the fermion contribution to the g_{b_L} coupling is finite.

If higher-order operators and in particular higher-order mixings between the elementary and the composite states are present in the effective Lagrangian, the selection rule can be violated and sizable corrections to the result in eq. (4.3.11) can arise. This is a signal of the fact that the $Z\bar{b}_L b_L$ vertex is sensitive to the UV dynamics of the theory. To explicitly verify this property we can use a procedure analogous to the one we adopted for the $\widehat{S}$ parameter in the case with only a light singlet. We consider a theory with a 4-plet as well as a singlet and then we recover the configuration with only a light 4-plet by taking the limit in which the singlet mass goes to the cut-off m_*. Using this procedure we find that the fermion correction to the $Z\bar{b}_L b_L$ vertex contains an additional contribution with respect to the result in eq. (4.3.11):

$$\delta g_{b_L} = \delta g_{b_L}^{4-plet} + \frac{\xi}{32\pi^2}\frac{y_{L4}^2 f^2}{m_4^2+y_{L4}^2 f^2} c^2 y_{L1}\left(y_{L1}-\sqrt{2}c y_{L4}\right) . \tag{4.3.12}$$

The additional contribution arises at leading order in the y expansion and is independent of the singlet mass, it only depends on the mixing of the singlet with the elementary states y_{L1}.

An equivalent way to understand the non-decoupling of the singlet is the following. In the limit in which the singlet becomes heavy we can integrate it out from the effective theory. This procedure generates a set of higher-order operators, in particular it gives rise to a term of the form $(y_{L1}c/m_*)(q_L^{\mathbf{5}}U)_5\gamma^\mu d_\mu^i\psi_4^i + \text{h.c.}$, where we replaced the singlet mass by the cut-off m_*. This higher-order mixing couples the q_L doublet with the left-handed component of the composite 4-plet and

induces a breaking of the $Z\bar{b}_L b_L$ selection rule, as can be easily inferred from the discussion in subsection 4.2.2.

Notice that in the case in which $c = 0$ the higher-dimension operators are not generated by integrating out the singlet, thus the selection rule is still unbroken and the additional correction to the $Z\bar{b}_L b_L$ vertex in eq. (4.3.12) vanishes. There is also a second case in which the additional corrections are not there. As we saw in subsection 4.2.3, if $c = \pm 1/\sqrt{2}$ and $y_{L1} = \pm y_{L4}$ the low-energy theory acquires an extra symmetry which protects the EW observables. In this case we expect the decoupling of the heavy dynamics to occur and, in fact, the extra correction in eq. (4.3.12) exactly cancels.

To conclude the analysis of the case with only a light 4-plet we now consider the effects due to the 4-fermion contact operators. As expected, vertices of the form given in eq. (4.2.17) induce a finite correction to the $Z\bar{b}_L b_L$ vertex:

$$\begin{aligned}\delta g_{b_L}^{4-ferm} &= \frac{3 e_{L4} \xi y_{L4}^2 f^2}{64\pi^2 (m_4^2 + y_{L4}^2 f^2)^3} \Bigg\{ m_4^2 y_{L4}^2 (m_4^2 + y_{L4}^2 f^2 - 4 y_{R4}^2 f^2) \\ &\quad + 2 y_{R4}^2 \left[(m_4^2 + y_{L4}^2 f^2)^2 \log\left(\frac{m_4^2 + y_{L4}^2 f^2}{m_4^2}\right) + y_{L4}^4 f^4 \log\left(\frac{v^2 y_{L4}^2 y_{R4}^2 f^2}{2(m_4^2 + y_{L4}^2 f^2)^2}\right) \right] \Bigg\} \end{aligned} \tag{4.3.13}$$

On the other hand, the vertex in eq. (4.2.18) induces a logarithmically divergent contribution:

$$\delta g_{b_L}^{4-ferm} = \frac{3\, e_{R4}}{32\pi^2} \xi \frac{y_{L4}^2 f^2}{m_4^2 + y_{L4}^2 f^2} y_{L4}^2 \log\left(\frac{m_*^2}{m_4^2}\right) . \tag{4.3.14}$$

Notice that the results in eqs. (4.3.13) and (4.3.14) correspond to the case in which the 4-fermion vertex has the structure $(\overline{B}_L^a \gamma^\mu B_L^a)(\overline{T}^b \gamma_\mu T^b + \overline{X}_{2/3}^b \gamma_\mu X_{2/3}^b)$, where a and b are color indices. Different color structures lead to results which only differ by group theory factors. [16]

The sign of the 4-fermion contribution crucially depends on the sign of the coefficients $e_{L,R}$. In our low-energy effective theory $e_{L,R}$ are completely free parameters, thus their sign is not fixed. From the UV perspective, instead, the operators in eqs. (4.2.17) and (4.2.18) arise from the exchange of heavy bosonic resonances and the sign of their coefficients is usually fixed by the quantum numbers of the resonances. It can be checked that the $e_{L,R}$ coefficients can be generated with arbitrary sign by considering resonances in different representations of SO(4).

4.3.3 Two Complete Models

In this subsection we finally consider two more complete models which include both a 4-plet and a singlet. In order to reduce the number of parameters we choose a common value for the left and right elementary mixings: $y_{L4} = y_{L1} = y_L$ and $y_{R4} = y_{R1} = y_R$. In this case the fermion Lagrangian (excluding the interactions with the gauge fields) becomes equal to the one of the 2-site model proposed in Refs. [6, 40].

An interesting byproduct of this choice is the fact that the fermion contribution, which dominates the Higgs potential, becomes only logarithmically divergent. One renormalization condition is enough to regulate the divergence and one can fix it by choosing the compositeness scale f. In this

[16] The combination of T and $X_{2/3}$ is dictated by the P_{LR} symmetry which is unbroken in the composite sector.

way the Higgs mass becomes calculable and an interesting relation between m_h and the masses of the top partners holds [6]:

$$\frac{m_h}{m_t} \simeq \frac{\sqrt{2N_c}}{\pi}\frac{m_T m_{\widetilde{T}}}{f}\sqrt{\frac{\log(m_T/m_{\widetilde{T}})}{m_T^2 - m_{\widetilde{T}}^2}}\,, \tag{4.3.15}$$

where m_T is the mass of the states in the $\mathbf{2}_{1/6}$ doublet coming from the 4-plet and $m_{\widetilde{T}}$ is the mass of the heavy singlet after the mixing with the elementary states. The complete spectrum of the composite resonances is a combination of the ones described in the cases with only one light multiplet considered in the previous subsections. The complete mass matrix for the charge 2/3 states is given by

$$M = \begin{pmatrix} 0 & -\frac{1}{2}y_{L4}f(c_h+1) & \frac{1}{2}y_{L4}f(c_h-1) & \frac{1}{\sqrt{2}}y_{L1}f s_h \\ -\frac{1}{\sqrt{2}}y_{R4}f s_h & m_4 & 0 & 0 \\ \frac{1}{\sqrt{2}}y_{R4}f s_h & 0 & m_4 & 0 \\ -y_{R1}f c_h & 0 & 0 & m_1 \end{pmatrix}, \tag{4.3.16}$$

where $c_h \equiv \cos(\langle h\rangle/f)$ and $s_h \equiv \sin(\langle h\rangle/f)$. The relation in eq. (4.3.15) allows us to fix the mass of one heavy multiplet as a function of the other parameters of the effective Lagrangian. Another mass parameter can be fixed by the requirement of reproducing the top mass. At the leading order in the v/f expansion we find that m_t is given by

$$m_t^2 = \frac{v^2(m_4 - m_1)^2 y_L^2 y_R^2 f^2}{2(m_4^2 + y_L^2 f^2)(m_1^2 + y_R^2 f^2)}\,. \tag{4.3.17}$$

Apart from the masses of the composite multiplets and the elementary mixings, only one free parameter appears in the effective Lagrangian: the coefficient of the d-symbol term, c. In the following we will analyze the models obtained for two particular choices of c. The first one is the case $c = 0$ which exactly corresponds to the 2-site model of Refs. [6,40]. The second case corresponds to the choice $c = 1/\sqrt{2}$ which, as explained in subsection 4.2.3, implies the presence of an additional protection for the EW parameters. This second choice reproduces the model studied in Ref. [69].

The Case $c = 0$

We start by considering the 2-site model ($c = 0$). In this case the leading corrections to the $\widehat{S}$ parameter are the same as in the case with only one light 4-plet. As shown in section 4.2, the constraints on $\widehat{S}$ alone are strong enough to put an absolute upper bound on the compositeness scale $\xi \lesssim 0.1$, as can be seen from fig. 4.3.

Let us now consider the $\widehat{T}$ parameter. We can reduce the number of free parameters by fixing the top and Higgs masses. The requirement of reproducing the correct Higgs mass gives a relation between m_T and $m_{\widetilde{T}}$ (see eq. (4.3.15)), while fixing the top mass allows us to determine the right mixing y_R as a function of the other parameters. With this procedure we are left with only two free parameters, which we choose to be m_T and the q_L compositeness angle ϕ_L defined as

$$\sin\phi_L \equiv \frac{y_L f}{\sqrt{m_4^2 + y_L^2 f^2}}\,. \tag{4.3.18}$$

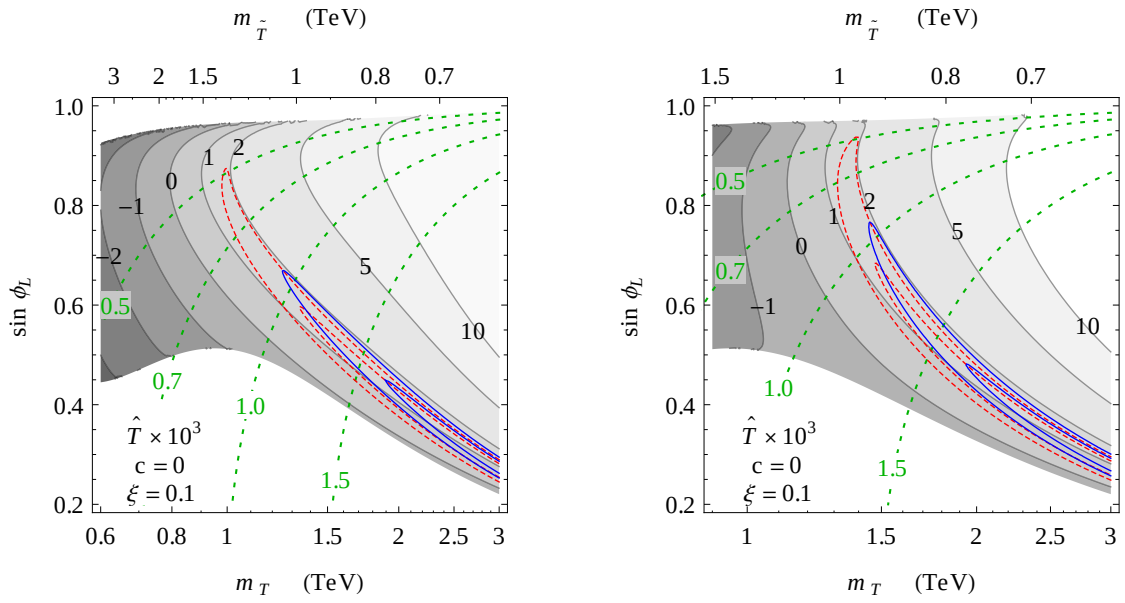

Figure 4.10: *Corrections to the $\widehat{T}$ parameter as a function of the mass of the top partners and of the q_L compositeness in the model with $c = 0$ for $\xi = 0.1$. The two plots correspond to the two different choices of y_R which allow to obtain the correct Higgs and top masses at fixed m_T and ϕ_L (see the main text for further details). In the white regions at the top and at the bottom of the plots the Higgs and top masses can not be reproduced. The dashed green contours show the mass (in TeV) of the exotic composite state $X_{5/3}$. The solid blue contours give the regions which pass the constraints on the oblique parameters at the 68% and 95% confidence level, while the dashed red lines show how the bounds are modified if we assume a 25% reduction of $\widehat{S}$.*

Notice that with this procedure the right mixing y_R is determined up to a twofold ambiguity. In the figures which show the numerical results we will thus include two plots that correspond to the two choices of y_R.

The corrections to the $\widehat{T}$ parameter are shown in fig. 4.10 for $\xi = 0.1$. To obtain the numerical results we fixed the Higgs mass to the value $m_h = 126$ GeV. [17] As expected from the results we discussed in the previous simplified cases, in the region in which the 4-plet is the lightest multiplet the corrections to $\widehat{T}$ are negative, whereas a light singlet typically implies a positive shift. The fit of the oblique parameters can put strong bounds on the parameter space of the model. In the plots we showed the allowed regions for 68% and 95% confidence level. To obtain the constraints we estimated $\widehat{S}$ by adding the leading corrections in eqs. (4.2.1), (4.2.2) and (4.2.4) for the choice $m_* = 3$ TeV.

The numerical results show that the oblique parameters can be used to set some lower bounds on the masses of the resonances coming from the composite 4-plet. At the 95% confidence level one finds $m_{X_{2/3}} \simeq m_{X_{5/3}} \gtrsim 0.95$ TeV for the masses of the exotic doublet $\mathbf{2}_{7/6}$ and $m_T \simeq m_B \gtrsim 1.2$ TeV for the $\mathbf{2}_{1/6}$ states. If we assume a 25% cancellation in the corrections to the $\widehat{S}$ parameter the bounds are significantly relaxed: $m_{X_{2/3}} \simeq m_{X_{5/3}} \gtrsim 0.5$ TeV and $m_T \simeq m_B \gtrsim 1$ TeV. Notice that these bounds are competitive or even stronger than the ones obtained from direct searches. For instance

[17] For simplicity we do not take into account the running of the Higgs mass.

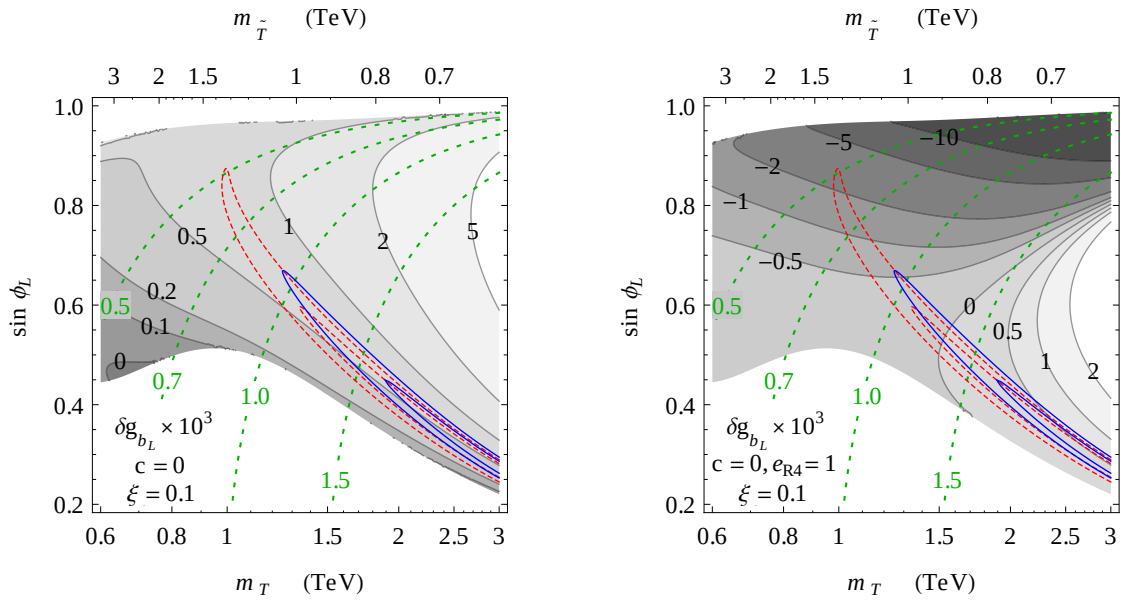

Figure 4.11: *Corrections to the $Z\bar{b}_L b_L$ vertex in the model with $c = 0$ for $\xi = 0.1$. The results on the left panel are obtained by neglecting the UV effects and the contributions from 4-fermion operators. On the right panel we added the logarithmically enhanced contribution induced by the operator in eq. (4.3.19) with $e_{R4} = 1$. The configurations correspond to the ones chosen for the left plot in fig. 4.10.*

the current bounds on the exotic top partners is $m_{X_{5/3}} \gtrsim 700$ GeV [110, 111].

Let us finally discuss the corrections to the $Z\bar{b}_L b_L$ vertex. The presence of a 4-plet in the low-energy spectrum makes this observable sensitive to the UV dynamics of the theory and to possible 4-fermion interactions present in the effective Lagrangian. In particular, as discussed in the general analysis of section 4.2, logarithmically divergent contributions can arise from a set of 4-fermion interactions.

If we neglect the UV contributions and set to zero the 4-fermion operators we find that the shift in the $Z\bar{b}_L b_L$ vertex is positive and somewhat correlated with the corrections to $\widehat{T}$. As an example we show in the left panel of fig. 4.11 the shift in g_{b_L} for the configurations corresponding to the left plot in fig. 4.10. One can see that the corrections become typically large and positive in the presence of a light singlet. The points which pass the constraints on the oblique parameters have a small positive shift in the $Z\bar{b}_L b_L$ vertex: $0.2 \cdot 10^{-3} \lesssim \delta g_{b_L} \lesssim 0.8 \cdot 10^{-3}$.

The UV contributions and the effects of 4-fermion operators can however drastically change the above result. In the right panel of fig. 4.11 we show how the previous result changes if we add to the low-energy Lagrangian the interaction

$$\frac{e_{R4}}{f^2}\left(\overline{B}^a_L \gamma^\mu B^a_L\right)\left(\overline{T}^b_R \gamma_\mu T^b_R + \overline{X}^b_{2/3R}\gamma_\mu X^b_{2/3R}\right), \tag{4.3.19}$$

with $e_{R4} = 1$. To obtain the numerical result we only included the leading logarithmically enhanced contribution to δg_{b_L} and we set the cut-off to the value $m_* = 3$ TeV. As expected, the new correction strongly changes the result in the configurations with large q_L compositeness, whereas the points with small ϕ_L are only marginally affected.

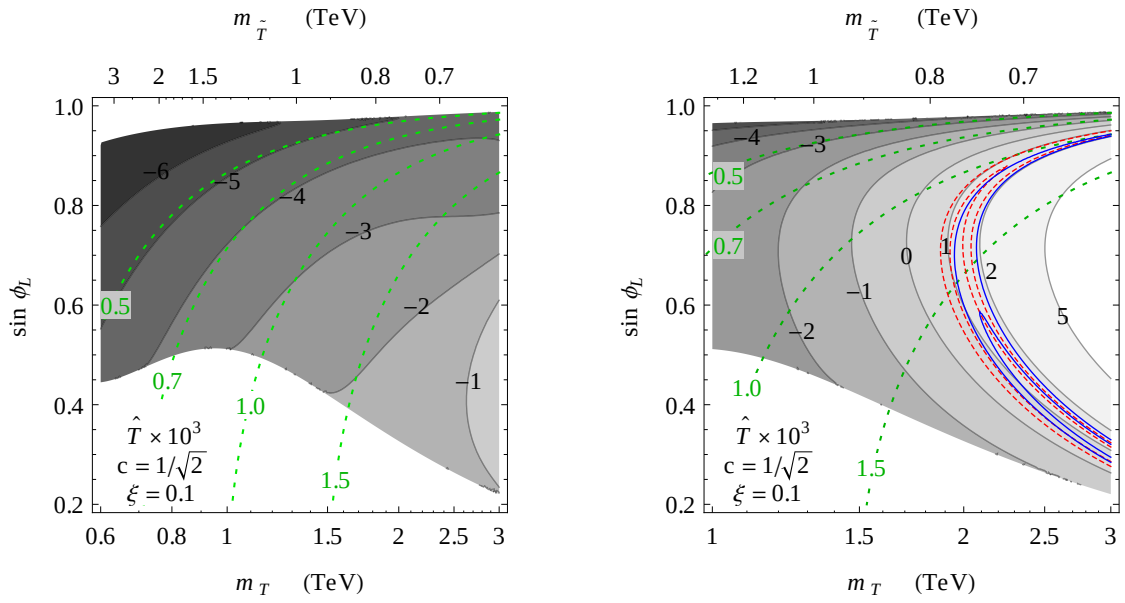

Figure 4.12: *Corrections to the $\widehat{T}$ parameter as a function of the mass of the top partners and of the q_L compositeness in the model with $c = 1/\sqrt{2}$ for $\xi = 0.1$.*

The Case $c = 1/\sqrt{2}$

The second complete model we consider corresponds to the case $c = 1/\sqrt{2}$. In this set-up the EW observables are finite. In particular the main corrections to the $\widehat{S}$ parameter are given by the tree-level UV contributions and by the logarithmically enhanced corrections due to the non-linear Higgs dynamics. These corrections, for a reasonably high cut-off ($m_* \gtrsim 3$ TeV) are well below the absolute upper bound on $\widehat{S}$.

The corrections to the $\widehat{T}$ parameter are shown in fig. 4.12. The configurations chosen for the plots correspond to the ones we used for the analogous plots in the case $c = 0$ (see fig. 4.10). The results, however, significantly differ in the two cases. In the case $c = 1/\sqrt{2}$ the corrections to $\widehat{T}$ tend to be more negative and a much lighter singlet is needed in order to pass the constraints on the oblique parameters ($m_{\widetilde{T}} \lesssim 0.8$ TeV). Notice that in this case the constraints are not significantly modified if we assume that some amount of cancellation in $\widehat{S}$ is present. Differently from the case $c = 0$, the corrections to $\widehat{S}$ are small and are typically much below the absolute upper bound $\widehat{S} \lesssim 2.5 \cdot 10^{-3}$.

As in the case $c = 0$, if we neglect the contributions from the UV dynamics and from the 4-fermion operators, the corrections to the $Z\bar{b}_L b_L$ parameter tend to be positive and correlated to the shift in $\widehat{T}$. The numerical results in the plane corresponding to the right plot in fig. 4.12 are shown in the left panel of fig. 4.13. Due to the protection of the EW observables, the presence of 4-fermion operators can not induce logarithmically divergent contributions to the $Z\bar{b}_L b_L$ vertex. However sizable finite corrections are still possible. In the right panel of fig. 4.13 we show how δg_{b_L} is modified if we add the contributions due to the vertex

$$\frac{e_{L4}}{f^2}\left(\overline{B}^a_L \gamma^\mu B^a_L\right)\left(\overline{T}^b_L \gamma_\mu T^b_L + \overline{X}^b_{2/3L} \gamma_\mu X^b_{2/3L}\right), \tag{4.3.20}$$

with $e_{L4} = -1$. As expected, the corrections are large only in the parameter space region in which the q_L has a large degree of compositeness. In this region the additional correction can easily induce

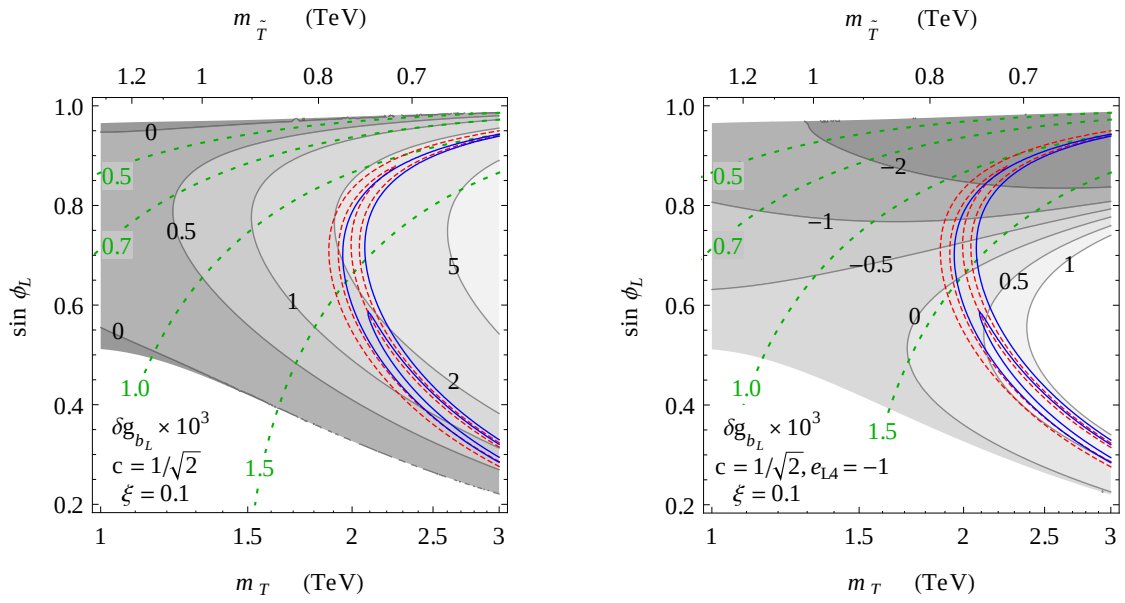

Figure 4.13: *Corrections to the $Z\bar{b}_L b_L$ vertex in the model with $c = 1/\sqrt{2}$ for $\xi = 0.1$. In the left plot we neglected the UV effects and the contributions from 4-fermion operators. On the right panel we added the shift induced by the operator in eq. (4.3.20) with $e_{L4} = -1$. The configurations correspond to the one chosen for the right plot in fig. 4.12.*

a negative value for δg_{b_L}. Notice however that the sign of the corrections crucially depends on the sign of the coefficient of the 4-fermion operators. In our effective approach this coefficient is a free parameter, but in a theory including a UV completion of our Lagrangian some constraints on the size and on the sign of the 4-fermion operators could be present.

4.4 The Case of a Totally Composite t_R

So far we analyzed a class of models based on the standard implementation of partial compositeness in which all the SM fermions have a corresponding elementary counterpart. Of course, due to the quantum numbers of the left-handed SM fermions, including them in the effective Lagrangian via some elementary fields is the only reasonable option if we want to preserve the global SO(5) invariance in the composite sector. The situation is different for the right-handed fermions. They are singlets under the SO(4) symmetry and can be embedded in the theory as elementary fields or, alternatively, as chiral fermions coming from the strong dynamics. In this case the right-handed fermions are part of the composite sector and are total singlets under the global SO(5) invariance.

This alternative implementation of partial compositeness is particularly appealing for the right-handed top component. As shown in Ref. [71] models with a totally composite t_R can lead to minimally tuned implementations of the composite Higgs idea and can give rise to an interesting collider phenomenology [7].

In this section we analyze the corrections to the EW observables which are present in this alternative scenario. Our strategy will be similar to the one followed in the previous sections. We will use an effective Lagrangian approach to parametrize the low-energy dynamics of the models and

we will analyze the EW parameters with particular attention to the corrections coming from the light composite fermions.

4.4.1 The Effective Lagrangian

As we did for the models in section 4.1, we will concentrate on a minimal scenario in which the elementary top component is mixed with a composite operator which transforms in the fundamental representation of the global SO(5) symmetry. For simplicity we only include one level of composite resonances which transform as a 4-plet (ψ_4) and a singlet (ψ_1) under the SO(4) subgroup. The elementary sector of the theory contains the left-handed doublet q_L, while the t_R is now an SO(5) chiral singlet belonging to the composite sector.

The effective Lagrangian for the composite states is given by [18]

$$\begin{aligned}\mathcal{L}_{comp} &= i\overline{\psi}_4 \not{D}\psi_4 + i\overline{\psi}_1 \not{D}\psi_1 + i\bar{t}_R \not{D} t_R - m_4\overline{\psi}_4\psi_4 - m_1\overline{\psi}_1\psi_1 \\ &+ \left(ic_L\overline{\psi}^i_{4L}\gamma^\mu d^i_\mu \psi_{1L} + ic_R\overline{\psi}^i_{4R}\gamma^\mu d^i_\mu \psi_{1R} + \text{h.c.}\right) + \left(ic_t\overline{\psi}^i_{4R}\gamma^\mu d^i_\mu t_R + \text{h.c.}\right) + \frac{1}{f^2}(\overline{\psi}\psi)^2 \,.\end{aligned} \tag{4.4.1}$$

As in eq. (4.1.5), the covariant derivative for the 4-plet ψ_4 contains the CCWZ e_μ symbol: $D_\mu\psi_4 = (\partial_\mu - 2/3ig'X_\mu + ie_\mu)\psi_4$. Notice that a mass term of the form $m_R\bar{t}_R\psi_{1L} + \text{h.c.}$ can be added to the effective Lagrangian in eq. (4.4.1). This term can however be removed by a redefinition of the ψ_{1R} and t_R fields. The Lagrangian containing the kinetic terms for the elementary fields and the mixings is

$$\mathcal{L}_{elem+mixing} = i\bar{q}_L \not{D} q_L + \left(y_{Lt} f \left(\overline{q}^{\mathbf{5}}_L\right)^I U_{I5} t_R + y_{L4} f \left(\overline{q}^{\mathbf{5}}_L\right)^I U_{Ii}\psi^i_4 + y_{L1} f \left(\overline{q}^{\mathbf{5}}_L\right)^I U_{I5}\psi_1 + \text{h.c.}\right) . \tag{4.4.2}$$

Differently from the case with an elementary right-handed top, in the present scenario a direct mass mixing between the q_L doublet and the t_R singlet appears in the effective Lagrangian. The parameters in our effective Lagrangian are in general complex and some of the complex phases can not be removed by field redefinitions. For simplicity we assume that our theory is invariant under CP, in this way all the parameters in eqs. (4.4.1) and (4.4.2) are real.

An interesting question is whether the scenarios with totally composite t_R can correspond to a particular limit of the case with an elementary t_R. To address this question we can notice that a property of the scenario with a totally composite right-handed top is the fact that the couplings and mixing of the t_R field with the other composite resonances respect the SO(5) symmetry. The only breaking of the global invariance in the fermion sector comes from the mixings of the elementary doublet q_L in eq. (4.4.2). In the case with an elementary t_R, instead, the y_R mixings induce an extra source of SO(5) breaking. The different symmetry structure of the two implementations of partial compositeness clearly points out that the two scenarios are independent and can not be simply connected by a limiting procedure.

4.4.2 Results

We can now discuss the explicit results for the scenarios with a totally composite t_R. The analysis presented in section 4.2 can be straightforwardly adapted to the present set-up, in particular all the

[18] The presence of chiral states coming from the strong dynamics does not allow us to impose a parity symmetry in the strong sector. For this reason in eq. (4.4.1) we wrote independent d-symbol interactions for the left- and right-handed chiralities.

general results are still valid. Before presenting the numerical results for some simplified models, we briefly summarize the main differences with respect to the results of section 4.2.

The contributions to the oblique parameters due to the non-linear Higgs dynamics (sse eqs .(4.2.2) and (4.2.7)) and the tree-level corrections to the $\widehat{S}$ parameter due to the gauge resonances (eq. (4.2.1)) are universal and do not depend on the assumptions on fermion compositeness. The presence of a light 4-plet of composite resonances still induces a logarithmically divergent contribution to the $\widehat{S}$ parameter, which is now given by

$$\Delta\widehat{S}^{div}_{ferm} = \frac{g^2}{8\pi^2}\left(1 - c_L^2 - c_R^2 - c_t^2\right)\xi \log\left(\frac{m_*^2}{m_4^2}\right) . \tag{4.4.3}$$

Notice that in this case the d-symbol involving the t_R and the 4-plet can lead to a cancellation of the divergent contributions even if no light singlet is present in the spectrum. This cancellation happens for $c_t = 1$.

As in the case with a partially composite t_R, the only couplings which break the custodial invariance and the P_{LR} symmetry are the mixings of the elementary q_L. In the present case, however, we can write three mixings of this kind, y_{L4}, y_{L1} and y_{Lt}. The fermion contribution to the $\widehat{T}$ parameter is generated at order y_L^4, thus it is finite and dominated by the contributions coming from the lightest resonances.

The corrections to the $Z\bar{b}_L b_L$ vertex are in general logarithmically divergent. We can extend to the present set-up the discussion of subsection 4.2.2 and show that a selection rule exists also in this case. In particular a logarithmically divergent correction can be generated only by specific 4-fermion operators and requires the presence of a light composite 4-plet. If the elementary q_L is significantly composite non-decoupling effects can arise and the contribution from the UV dynamics can be sizable making the corrections to g_{b_L} non predictable in the effective theory.

Notice that in the present set-up the top Yukawa is mainly determined by the y_{Lt} mixing. At the leading order in the v/f expansion we find

$$m_t^2 = \frac{m_4^2}{m_4^2 + y_{L4}^2 f^2}\frac{y_{Lt}^2 v^2}{2} . \tag{4.4.4}$$

The presence of a direct mixing between the elementary doublet q_L and the singlet t_R, allows to get the correct top mass even if we set to zero the y_{L4} and y_{L1} mixings. In this limit the composite 4-plet and singlet do not feel directly the breaking of the custodial and P_{LR} symmetries and their corrections to the $\widehat{T}$ parameter and to the $Z\bar{b}_L b_L$ vertex are totally negligible. The contributions to $\widehat{S}$, instead, can still be sizable.

In the following we will consider in details two simplified scenarios, namely the cases in which only a light composite singlet or a light composite 4-plet are present in the effective theory.

The Case of a Light Singlet

As a first simplified model we consider the case with only a light composite singlet. As we will see, in this limit the model with a totally composite t_R has many properties in common with the case of a partially composite t_R discussed in subsection 4.3.1.

The deviations in $\widehat{S}$ are dominated by the tree-level UV contribution and by the corrections due to the non-linear Higgs dynamics. For a high enough cut-off ($m_* \gtrsim 3$ TeV) the corrections to the $\widehat{S}$ parameter are well below the maximal value allowed by the EW precision tests.

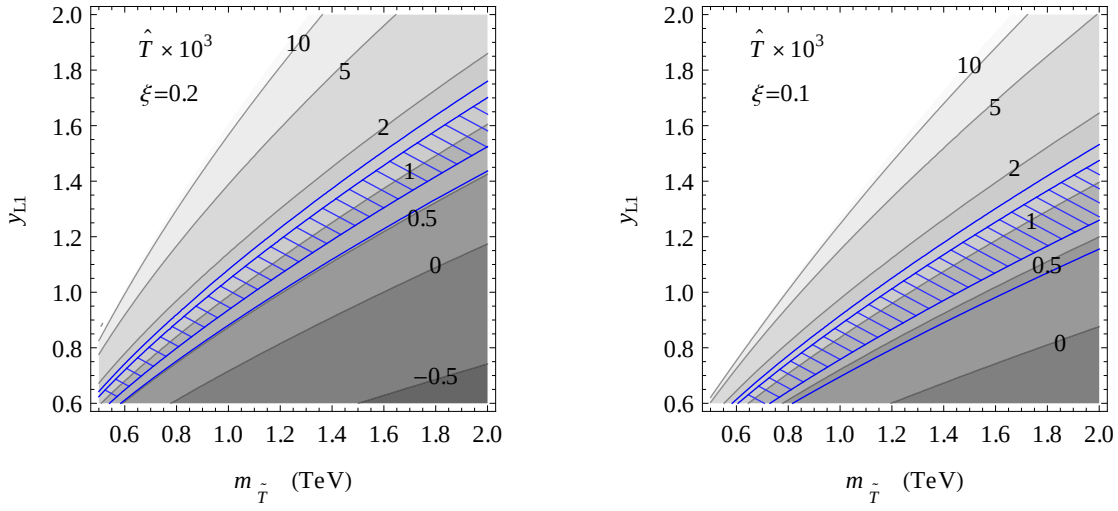

Figure 4.14: *Corrections to the $\widehat{T}$ parameter as a function of the mass of the top partners and of the q_L compositeness. The result corresponds to the scenario with a totally composite t_R with only a light singlet. The compositeness scale has been fixed to $\xi = 0.2$ in the left panel and $\xi = 0.1$ in the right one. The solid blue contours give the regions which pass the constraints on the oblique parameters at the 68% and 95% confidence level.*

The fermion contributions to the $\widehat{T}$ parameter can be sizable and are typically positive. At the leading order in v/f they are given by

$$\Delta\widehat{T}_{ferm} = \frac{3}{64\pi^2}\xi\frac{y_{L1}^2 f^2}{m_1^2}\left\{y_{L1}^2 + 2y_{Lt}^2\left[\log\left(\frac{2m_1^2}{v^2 y_{Lt}^2}\right) - 1\right]\right\} . \tag{4.4.5}$$

In fig. 4.14 we show the total correction to $\widehat{T}$ including the leading IR effects given in eq. (4.2.7).

As in the analogous case with a partially composite t_R, the fermion contributions to the $Z\bar{b}_L b_L$ vertex are strongly correlated with the corrections to $\widehat{T}$. At leading order in v/f we find

$$\delta g_{b_L} = \frac{1}{64\pi^2}\xi\frac{y_{L1}^2 f^2}{m_1^2}\left\{y_{L1}^2 + 2y_{Lt}^2\left[\log\left(\frac{2m_1^2}{v^2 y_{Lt}^2}\right) - 1\right]\right\} . \tag{4.4.6}$$

By comparing this expression with the result in eq. (4.4.5) we find the same relation we obtained in subsection 4.3.1: $\Delta\widehat{T}_{ferm} = 3\delta g_{b_L}$. The values of $\widehat{T}$ compatible with the bounds ($0 \lesssim \widehat{T} \lesssim 2\cdot 10^{-3}$) imply a moderate positive shift in δg_{b_L}. This shift slightly worsens the agreement with the experimental data with respect to the SM.

The Case of a Light 4-plet

The second simplified model we consider is the effective theory with only a light 4-plet. As can be seen from eqs. (4.4.1) and (4.4.2), in this case the low-energy Lagrangian contains 4 free parameters: the elementary–composite mixings, the 4-plet mass and the coefficient of the d-symbol term, c_t. As we will see, the d-symbol term can sizably affect the corrections to the EW observables. Its presence makes the properties of the model quite different from the ones found in the case with an elementary t_R (compare subsection 4.3.2). Moreover, as was pointed out in the analysis of Ref. [7], the d-symbol term can also play an important role for collider phenomenology.

In addition to the corrections from the Higgs non-linear dynamics and the UV tree-level shift, the $\widehat{S}$ parameter receives a logarithmically enhanced contributions from fermion loops:

$$\Delta\widehat{S}^{div}_{ferm} = \frac{g^2}{8\pi^2}\left(1-c_t^2\right)\xi\log\left(\frac{m_*^2}{m_4^2}\right) . \tag{4.4.7}$$

If c_t is not close to 1, this shift can be sizable and can induce stringent constraints on the compositeness scale ξ.

The contributions to the $\widehat{T}$ parameter coming from fermion loops at leading order in v/f are given by

$$\begin{aligned}\Delta\widehat{T}_{ferm} &= -\frac{\xi}{32\pi^2}\frac{y_{L4}f^2}{m_4^2}\Bigg\{3c_t^2 y_{L4}(y_{L4}^2-4y_{Lt}^2)+y_{L4}^2(y_{L4}-3\sqrt{2}c_t y_{Lt}) \\ &\quad -3y_{Lt}^2(y_{L4}-4\sqrt{2}c_t y_{Lt})\left[\log\left(\frac{2m_4^2}{v^2y_{Lt}^2}\right)-1\right]\Bigg\} .\end{aligned} \tag{4.4.8}$$

Notice that the terms related to the d-symbol operator come with accidentally large coefficients, thus even a relatively small value of c_t can drastically modify the result. In fig. 4.15 we show the total correction to $\widehat{T}$ as a function of y_{L4} and c_t for a fixed value of the 4-plet mass, $m_4 = 1$ TeV. One can see that a positive correction to the $\widehat{T}$ parameter is possible, but requires a sign correlation between y_{L4} and c_t. [19] In the plots we also show the regions compatible with the constraints on the oblique parameters. The parameter space regions with better agreement with the EW data are the ones with $c_t \sim -1$, in which the logarithmically enhanced shift in $\widehat{S}$ is partially cancelled.

The corrections to the $Z\bar{b}_L b_L$ vertex are given at the leading order in v/f by

$$\begin{aligned}\delta g_{b_L} &= -\frac{\xi}{64\pi^2}\frac{m_4^2 y_{L4}y_{Lt}^2 f^2}{(m_4^2+y_{L4}^2)^2}\Bigg[2y_{L4}-\sqrt{2}c_t y_{Lt} \\ &\quad +\left(2y_{L4}-\sqrt{2}c_t y_{Lt}+\frac{y_{L4}y_{Lt}^2 f^2}{2(m_4^2+y_{L4}^2 f^2)}\right)\log\left(\frac{v^2 m_4^2 y_{Lt}^2}{2(m_4^2+y_{L4}^2 f^2)^2}\right)\Bigg] .\end{aligned} \tag{4.4.9}$$

The above formula contains only the corrections coming from the lowest order terms in the effective Lagrangian without the contributions from 4-fermion operators. As can be seen from the numerical result in the left panel of fig. 4.16, the sign of δg_{b_L} has some correlation with the sign of $\widehat{T}$. The size of the corrections to the $Z\bar{b}_L b_L$ vertex is however typically one order of magnitude smaller than the one in $\widehat{T}$. The points compatible with the constraints on the oblique EW parameters have δg_{b_L} in the range $0 \lesssim \delta g_{b_L} \lesssim 0.5\cdot 10^{-3}$.

The corrections to the $Z\bar{b}_L b_L$ vertex can of course be modified if 4-fermion interactions are present in the effective Lagrangian. In particular logarithmically divergent contributions can be induced by operators of the form given in eq. (4.2.18). As an example we will show how the previous result for δg_{b_L} is modified by the operator given in eq. (4.3.19). In this case the following additional contribution arises:

$$\delta g_{b_L} = \frac{e_{R4}}{32\pi^2}\xi\frac{y_{L4}^2 f^2}{m_4^2+y_{L4}^2 f^2}y_{L4}\left(y_{L4}-\sqrt{2}c_t y_{Lt}\right)\log\left(\frac{m_*^2}{m_4^2}\right) , \tag{4.4.10}$$

[19] Notice that the Lagrangian is invariant under the transformation $y_{L4} \to -y_{L4}$ and $c_t \to -c_t$.

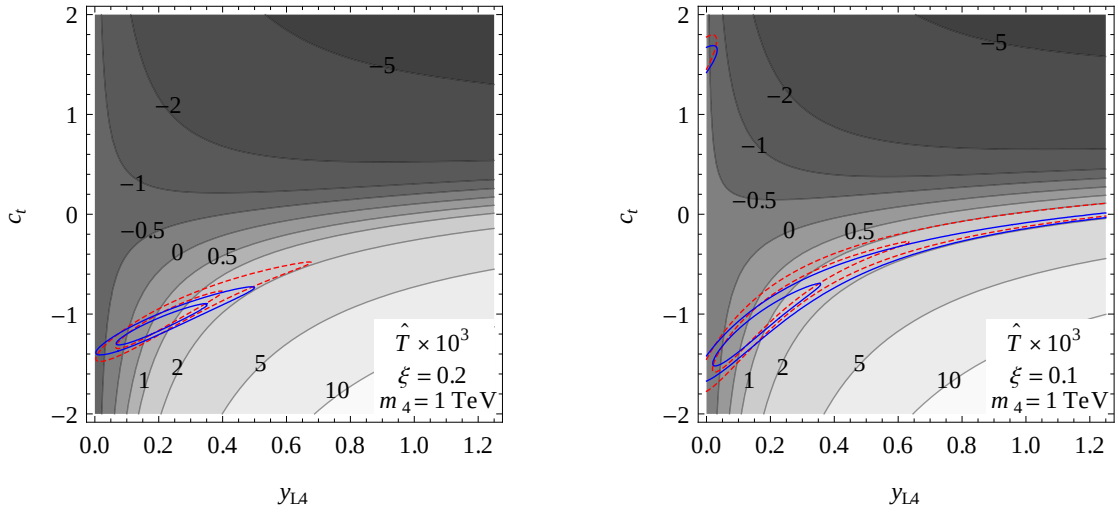

Figure 4.15: *Corrections to the $\widehat{T}$ parameter as a function of the y_{L4} mixing and of c_t. The result corresponds to the scenario with a totally composite t_R with only a light 4-plet with mass $m_4 = 1$ TeV. The compositeness scale has been fixed to $\xi = 0.2$ in the left panel and $\xi = 0.1$ in the right one. The solid blue contours give the regions which pass the constraints on the oblique parameters at the 68% and 95% confidence level. The dashed red lines show how the bounds are modified if we assume a 25% reduction in $\widehat{S}$.*

In the right panel of fig. 4.16 we show the numerical result for δg_{b_L} including the extra contribution in eq. (4.4.10) for $e_{R4} = -1$. In the region with sizable values for y_{L4} the new contribution dominates and can induce a negative shift in δg_{b_L}, which would improve the compatibility with the experimental measurements.

4.5 Corrections to the Top Couplings

So far we devoted our attention to the oblique EW parameters and the bottom couplings. The tight experimental bounds on these observables do not allow for large deviations from the SM predictions and lead to strong bounds on the new physics effects. Another class of observables, in particular the ones related to the top quark, are instead less constrained from the present data which allow sizable deviation from the SM. Large corrections to the top couplings are naturally predicted in the scenarios with partial compositeness due to the strong mixing of the third generation quarks with the composite dynamics. Notice that the P_{LR} invariance, which suppresses the corrections to the $Z\bar{b}_L b_L$ vertex, does not protect the couplings of the top quark. Thus big tree-level contributions can be generated which could be eventually tested at the LHC. The aim of this section is to determine the size of the distortion of the top couplings to the Z and to the W bosons.

The top coupling to the Z boson are described by the following effective Lagrangian

$$\mathcal{L}^Z = \frac{g}{c_w} Z_\mu \bar{t} \gamma^\mu \left[(g_{t_L}^{SM} + \delta g_{t_L}) P_L + (g_{t_R}^{SM} + \delta g_{t_R}) P_R \right] t \,, \tag{4.5.1}$$

where g^{SM} denote the SM couplings and δg correspond to the new physics contributions. In the above formula $P_{L,R}$ are the left and right chiral projectors. The tree-level values of the SM couplings

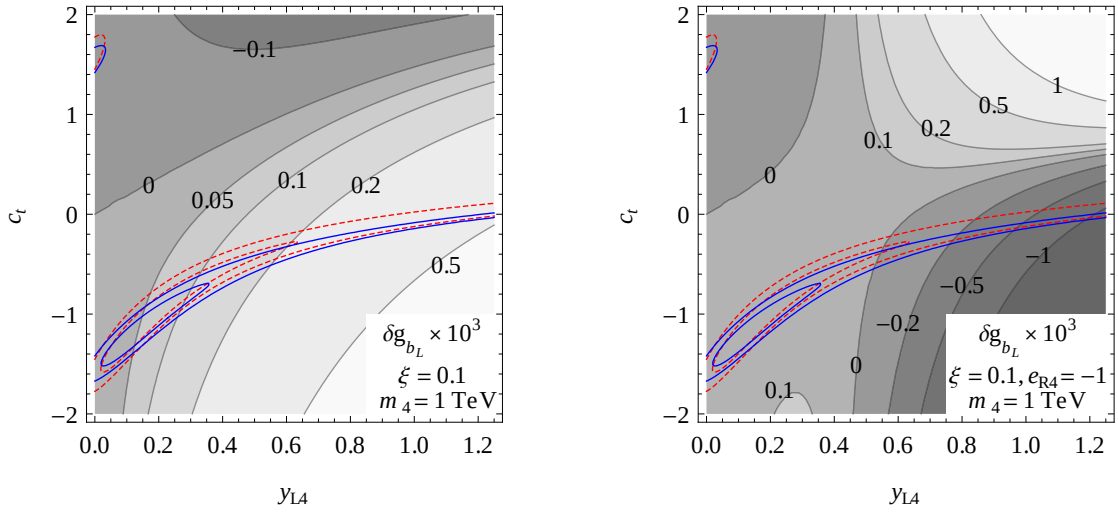

Figure 4.16: *Corrections to the $Z\bar{b}_L b_L$ vertex as a function of the y_{L4} mixing and of c_t. The results correspond to the scenario with a totally composite t_R with only a light 4-plet with mass $m_4 = 1$ TeV. The compositeness scale has been fixed by $\xi = 0.1$. In the left panel we neglected the contributions from 4-fermion operators, while in the right panel we included the corrections due to the operator in eq. (4.3.19) with $e_{R4} = -1$.*

are given by

$$g_{t_L}^{SM} = \frac{1}{2} - \frac{2}{3}s_w^2\,, \qquad g_{t_R}^{SM} = -\frac{2}{3}s_w^2\,. \tag{4.5.2}$$

The couplings of the left-handed top component with the charged W boson are related to the V_{tb} element of the CKM matrix. We will parametrize the new physics contributions as $V_{tb} = 1 + \delta V_{tb}$. The current LHC results already put a constraint on the new physics contribution at the 10% level: $V_{tb} = 1.020 \pm 0.046\,(\text{meas.}) \pm 0.017\,(\text{theor.})$ [133]. As we will see, the bounds on the models coming from this measurement are still weaker than the ones coming from the EW precision data.

4.5.1 A Relation Between δg_{t_L} and δV_{tb}

Before discussing the results in the explicit models we considered in this chapter, we rederive a general relation which links the deviations in the $Z\bar{t}_L t_L$ vertex to the corrections to V_{tb} as already noticed in Refs. [134–136]. In the effective Lagrangian describing the Higgs doublet and the SM fields only two dimension-six operators contribute to the corrections to the t_L couplings [20, 131, 134, 137]:

$$\mathcal{L} = i\frac{c_{Hq}}{f^2}(\bar{q}_L\gamma^\mu q_L)\left(H^\dagger \overleftrightarrow{D_\mu} H\right) + i\frac{c'_{Hq}}{f^2}(\bar{q}_L\sigma^i\gamma^\mu q_L)\left(H^\dagger\sigma^i \overleftrightarrow{D_\mu} H\right)\,. \tag{4.5.3}$$

A combination of the two operators in eq. (4.5.3) is strongly constrained by the experimental bound on the corrections to the $Z\bar{b}_L b_L$ vertex. Notice that, in the models we considered in our analysis, the corrections to g_{b_L} exactly vanish at tree level thanks to the P_{LR} symmetry. The condition of vanishing corrections to the $Z\bar{b}_L b_L$ coupling implies the relation $c'_{Hq} = -c_{Hq}$ [41, 138]. Using this relation we find that the operators in eq. (4.5.3) give rise to the following interactions of

the top quark with the EW gauge bosons:

$$\mathcal{L} \supset 2c_{Hq}\, v^2 \left[\frac{g}{c_w} \bar{t}_L Z^\mu \gamma_\mu t_L + \frac{g}{2} \left(\bar{t}_L \left(W^1_\mu - i W^2_\mu \right) \gamma^\mu b_L + \text{h.c.} \right) \right] . \tag{4.5.4}$$

From this equation we can easily conclude that the leading corrections to the $Z\bar{t}_L t_L$ vertex and to the V_{tb} matrix element satisfy the relation

$$\delta g_{t_L} = \delta V_{tb} \, . \tag{4.5.5}$$

Notice that the above result holds only at order v^2/f^2. The subleading terms, as for instance the dimension-eight operators, can generate independent corrections to g_{t_L} and V_{tb}.

It is important to stress that this analysis is valid as far as we can neglect the corrections to the $Z\bar{b}_L b_L$ vertex with respect to the corrections to the top couplings. Thus the result in eq. (4.5.5) is true in general and not only in the composite Higgs scenarios.

4.5.2 The Case of an Elementary t_R

As a first class of models we consider the scenarios with an elementary t_R. The corrections to the t_L couplings at leading order in v/f are given by

$$\delta g_{t_L} = \delta V_{tb} = -\frac{\xi}{4} \frac{f^2}{m_4^2 + y_{L4}^2 f^2} \left[\left(\frac{m_4 m_1 y_{L1} + y_{L4} y_{R4} y_{R1} f^2}{m_1^2 + y_{R1}^2 f^2} - \sqrt{2} c y_{L4} \right)^2 + (1 - 2c^2) y_{L4}^2 \right] . \tag{4.5.6}$$

This explicit result is in agreement with the relation derived in the previous subsection (see eq. (4.5.5)). We also verified that at order $(v/f)^4$ the corrections to g_{t_L} and V_{tb} do not coincide.

The coupling of the t_R with the Z boson is modified as well. The leading corrections take the form

$$\delta g_{t_R} = \frac{\xi}{4} \frac{f^2}{m_1^2 + y_{R1}^2 f^2} \left[\left(\frac{m_4 m_1 y_{R4} + y_{L4} y_{L1} y_{R1} f^2}{m_4^2 + y_{L4}^2 f^2} - \sqrt{2} c y_{R1} \right)^2 - \left(\frac{m_1 y_{R4}}{m_4} - \sqrt{2} c y_{R1} \right)^2 \right] . \tag{4.5.7}$$

As explicit numerical examples we show in fig. 4.17 the distortion of the V_{tb} matrix element in the complete models with $c = 0$ and $c = 1/\sqrt{2}$ (see subsection 4.3.3). In the case with $c = 0$, the configurations allowed by the constraints on the oblique EW parameters have small corrections to V_{tb}, $-0.03 \lesssim \delta V_{tb} \lesssim 0$, which are below the present experimental sensitivity. On the contrary, in the model with $c = 1/\sqrt{2}$, the corrections to V_{tb} can be sizable, $-0.12 \lesssim \delta V_{tb} \lesssim -0.03$, and the current bounds can already exclude a corner of the parameter space allowed by the EW precision data. In our numerical analysis we also found that, in the realistic regions of the parameter space, the deviations in the t_R couplings are always small, $\delta g_{t_R} \lesssim 0.01$. Moreover we checked numerically that the correlation between δg_{t_L} and δV_{tb} is always well verified and the deviations from eq. (4.5.5) are of order ξ as expected.

To conclude the analysis of the top couplings in the models with an elementary t_R, it is interesting to consider the simplified cases with only one light composite multiplet. In the limit with only a light singlet we find

$$\delta g_{t_L} = \delta V_{tb} = -\frac{\xi}{4} \frac{m_1^2 y_{L1}^2 f^2}{(m_1^2 + y_{R1}^2 f^2)^2} \, , \qquad \delta g_{t_R} = 0 \, . \tag{4.5.8}$$

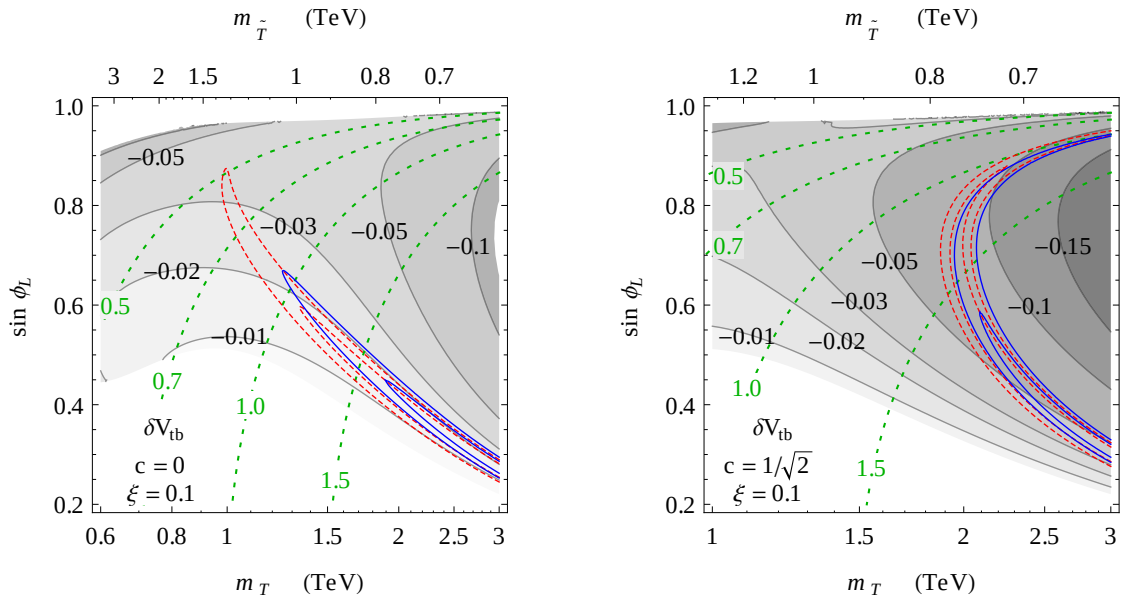

Figure 4.17: *Corrections to the V_{tb} matrix element in the complete models with $c = 0$ (left panel) and $c = 1/\sqrt{2}$ (right panel) for $\xi = 0.1$. The configurations correspond to the ones of the left plot of fig. 4.10 for the case $c = 0$ and of the right plot of fig. 4.12 for the case $c = 1/\sqrt{2}$.*

This shows that the corrections to the t_L couplings are suppressed in the parameter space region with a sizable t_R compositeness ($y_{R1} f > m_1$ and $y_{R1} > y_{L1}$). The corrections to g_{t_R} vanish in this case because the t_R can only mix with composite states with the same coupling to the Z boson.

In the case with only a light 4-plet we obtain the following results

$$\delta g_{t_L} = \delta V_{tb} = -\frac{\xi}{4}\frac{y_{L4}^2 f^2}{m_4^2 + y_{L4}^2 f^2}\,, \qquad \delta g_{t_R} = -\frac{\xi}{4}\frac{y_{L4}^2 y_{R4}^2 f^2}{m_4^2 + y_{L4}^2 f^2}\left(\frac{f^2}{m_4^2} + \frac{f^2}{m_4^2 + y_{L4}^2 f^2}\right)\,. \tag{4.5.9}$$

In this case the experimental bounds on V_{tb} can be used to put an upper bound on the t_L compositeness. Notice that the mixing of the t_R does not break the P_{LR} symmetry. The g_{t_R} coupling, however, can receive tree-level corrections through the mixing between the elementary t_R and composite resonances with different quantum numbers, which is induced by the non-zero top mass. This origin explains why the prefactor in the expression for δg_{t_R} is proportional to the square of the top Yukawa (see eq. (4.3.8)). The correction to g_{t_R} is enhanced if the top partners are light.

4.5.3 The Case of a Composite t_R

We now consider the scenarios with a totally composite t_R. The leading corrections to the V_{tb} matrix element and to the top couplings to the Z boson are given by

$$\delta g_{t_L} = \delta V_{tb} = -\frac{\xi}{4}\frac{f^2}{m_4^2 + y_{L4}^2 f^2}\left[\left(\frac{m_4 y_{L1}}{m_1} - \sqrt{2} c_L y_{L4}\right)^2 + (1 - 2c_L^2) y_{L4}^2\right]\,, \tag{4.5.10}$$

and

$$\delta g_{t_R} = \frac{\xi}{4}\frac{y_{L4} y_{Lt} f^2}{(m_4^2 + y_{L4}^2 f^2)^2}\left[y_{L4} y_{Lt} f^2 - 2\sqrt{2} c_t (m_4^2 + y_{L4}^2 f^2)\right]\,. \tag{4.5.11}$$

In the limits with only one light multiplet the expressions in eqs. (4.5.10) and (4.5.11) can be drastically simplified. If only a light singlet is present in the effective theory we find:

$$\delta g_{t_L} = \delta V_{tb} = -\frac{\xi}{4}\frac{y_{L1}^2 f^2}{m_1^2}\,, \qquad \delta g_{t_R} = 0\,. \tag{4.5.12}$$

In this case the corrections to the $Z\bar{t}_R t_R$ coupling are negligible, while the V_{tb} matrix element and the $Z\bar{t}_L t_L$ vertex can become large if the composite singlet is light.

In the model with only a light composite 4-plet the corrections to the top couplings become

$$\delta g_{t_L} = \delta V_{tb} = -\frac{\xi}{4}\frac{y_{L4}^2 f^2}{m_4^2 + y_{L4}^2 f^2}\,, \qquad \delta g_{t_R} = \frac{\xi}{4}\frac{y_{L4} y_{Lt} f^2}{(m_4^2 + y_{L4}^2 f^2)^2}\left[y_{L4} y_{Lt} f^2 - 2\sqrt{2} c_t (m_4^2 + y_{L4}^2 f^2)\right]\,. \tag{4.5.13}$$

Analogously to the case with an elementary t_R, the corrections to the V_{tb} matrix element can be used to put an upper bound on the degree of compositeness of the elementary doublet q_L.

4.6 Appendix

4.6.A Operator Analysis for the $Z\bar{b}_L b_L$ Vertex

In section 4.2 we presented a general analysis of the one-loop corrections to the $Z\bar{b}_L b_L$ vertex which are induced by the presence of composite fermion resonances. We found that logarithmically divergent contributions can be present if a light composite 4-plet is present in the spectrum. For simplicity in the main text we did not report rigorous proofs of our statements and we only gave some partial justifications. The aim of this appendix is to present a more rigorous and systematic study based on an operator analysis.

General Considerations

An important feature of our effective Lagrangian is the presence of a P_{LR} symmetry, which is exact in the composite sector and is only broken by the mixing with the elementary states (in particular with the doublet q_L). The P_{LR} symmetry plays an essential role in protecting the $Z\bar{b}_L b_L$ vertex from large tree-level corrections and it also leads to a reduction of the degree of divergence of the loop contributions. In the following we will take into account the consequences of the P_{LR} invariance through the method of spurions.

As a first step we need to formally restore the global SO(5) invariance in our effective Lagrangian. For this purpose we assume that the elementary fields transform only under an "elementary" $\mathrm{SU}(2)_L \times \mathrm{U}(1)_Y$ global group which is independent with respect to the global SO(5) invariance of the composite sector. In this picture the SM group corresponds to the diagonal combination of the "elementary" and the "composite" groups. The mixing between the elementary and the composite states clearly induces a breaking of the extended global invariance. We can however formally restore the complete global symmetry by promoting the couplings to spurions with non-trivial transformation properties under the "elementary" and the "composite" groups. In our set-up we need two spurions:

i) $(\tilde{y}_L)^\alpha_A$, which transforms as a doublet ($\overline{\mathbf{2}}_{-1/6}$) under the "elementary" symmetry (index α) and belongs to the fundamental representation of SO(5) with $U(1)_X$ charge 2/3 (index A). Its

physical value is given by

$$\langle \tilde{y}_L \rangle = \frac{1}{\sqrt{2}} \begin{pmatrix} 0 & i \\ 0 & 1 \\ i & 0 \\ -1 & 0 \\ 0 & 0 \end{pmatrix} . \tag{4.6.1}$$

ii) $(\tilde{y}_R)_A$, which is a singlet under the "elementary" group ($\mathbf{1}_{-2/3}$) and transforms in the fundamental representation of the "composite" group ($\mathbf{5}_{2/3}$). Its physical value is given by

$$\langle \tilde{y}_R \rangle = \begin{pmatrix} 0 \\ 0 \\ 0 \\ 0 \\ 1 \end{pmatrix} . \tag{4.6.2}$$

It is important to remark that in our definition the two spurions transform linearly under the SO(5) "composite" group.

Using the spurions we can rewrite the elementary–composite mixings in a fully invariant form

$$\begin{aligned} \mathcal{L}_{mix} \;=\; & y_{L4}\, \overline{q}_L^{\alpha} \big(\tilde{y}_L^{\dagger}\big)_A^{\alpha} U_{Ai} \psi_4^i + y_{L1}\, \overline{q}_L^{\alpha} \big(\tilde{y}_L^{\dagger}\big)_A^{\alpha} U_{A5} \psi_1 \\ & + y_{R4}\, \overline{t}_R \big(\tilde{y}_R^{\dagger}\big)_A U_{Ai} \psi_4^i + y_{R1}\, \overline{t}_R \big(\tilde{y}_R^{\dagger}\big)_A U_{A5} \psi_1 + \text{h.c.}\,. \end{aligned} \tag{4.6.3}$$

Notice that the two mixings of the q_L doublet are associated to the same spurion $\tilde{y}_L$ and analogously the t_R mixings correspond to the spurion $\tilde{y}_R$. From the Lagrangian in eq. (4.6.3) we can recover the original mixing terms in eq. (4.1.7) by replacing the spurions with their physical values $\langle \tilde{y}_{L,R} \rangle$.

We can now identify the building blocks which can be used to construct the operators in our effective theory. One key element is of course the Goldstone matrix U. Under the SO(5) group U transforms linearly on one side and non-linearly on the other. We can thus split the Goldstone matrix in two components: U_{Ai} whose index i transforms as a CCWZ 4-plet and U_{A5} which is a singlet. In both cases the index A corresponds to a linear realization of the fundamental representation of SO(5).

It is also useful to introduce a slight generalization of the covariant derivative. We define it in such a way that it acts on all the indices of a given object, for instance the covariant derivative of the 4-plet Goldstone component is

$$(D_\mu U)_{Ai} \equiv \partial_\mu U_{Ai} - i(A_\mu U)_{Ai} - i(U e_\mu)_{Ai}\,. \tag{4.6.4}$$

For the elementary fermions and the composite resonances the convariant derivative coincides with the one we used so far. It is useful to notice that the covariant derivative of the Goldstone matrix can always be expressed in terms of the d_μ symbol:

$$(D_\mu U)_{Ai} = -U_{A5} d_\mu^i \qquad \text{and} \qquad (D_\mu U)_{A5} = -U_{Ai} d_\mu^i\,. \tag{4.6.5}$$

Moreover it is easy to check that the covariant derivative of the spurions vanishes when it is computed on the spurion physical values, $\langle D_\mu y_{L,R} \rangle = 0$.

In our analysis, for simplicity, we will consider the limit in which the gauge couplings are sent to zero. This limit is justified by the fact that the largest corrections to the $Z\bar{b}_L b_L$ vertex come from loops containing the Goldstones and not the transverse gauge field components. Within this approximation, the elementary fermion interactions are necessarily mediated by the elementary–composite mixings. This implies that, in classifying the operators which contribute to the $Z\bar{b}_L b_L$ coupling, we can assume that the elementary fields are always contracted with the $\tilde{y}_{L,R}$ spurions.

To construct the operators which can appear in the effective Lagrangian we can use the following building blocks: [20]

$$\begin{aligned}
\text{elementary fields:} &\quad q_L^\alpha \text{ and } t_R \\
\text{composite fields:} &\quad \psi_4^i \text{ and } \psi_1 \\
\text{cov. der. of the fermions:} &\quad (D_\mu q_L)^\alpha,\ D_\mu t_R,\ (D_\mu \psi_4)^i \text{ and } D_\mu \psi_1 \\
d_\mu \text{ symbol:} &\quad d_\mu^i \\
\text{mixings:} &\quad (U^\dagger \tilde{y}_L)^\alpha_{i,5} \text{ and } (U^\dagger \tilde{y}_R)_{i,5}
\end{aligned}$$

Notice that, thanks to the unitarity of the Goldstone matrix, we can always write the spurions in the combinations $U^\dagger \tilde{y}_{L,R}$.

Classification of the Operators

We can now analyze the operators which can modify the coupling of the Z boson to the b_L with the aim of determining their degree of divergence. This can be easily achieved by classifying the operators in an expansion in the elementary–composite mixings.

To simplify the analysis it is more convenient to work in the basis of the elementary and composite fields and not in the one of the mass eigenstates. The mass eigenstate corresponding to the physical b_L, which we will denote here by $\widetilde{b}_L$, is given by a combination of the elementary b_L and of the composite state B contained in the 4-plet ψ_4:

$$b_L = \frac{m_4}{\sqrt{m_4^2 + y_{L4}^2 f^2}} \widetilde{b}_L - \frac{y_{L4} f}{\sqrt{m_4^2 + y_{L4}^2 f^2}} \widetilde{B}_L \,, \tag{4.6.6}$$

$$B_L = \frac{y_{L4} f}{\sqrt{m_4^2 + y_{L4}^2 f^2}} \widetilde{b}_L + \frac{m_4}{\sqrt{m_4^2 + y_{L4}^2 f^2}} \widetilde{B}_L \,, \tag{4.6.7}$$

where we denoted by $\widetilde{B}$ the heavy mass eigenstate. The operators which induce a distortion of the g_{b_L} coupling are trivially related to the ones which give the couplings of the Z boson to the elementary b_L and the composite B_L.

Notice that under the SM gauge group the b_L and the B_L fields have exactly the same charges as the physical $\widetilde{b}_L$, thus operators containing the covariant derivatives $D_\mu b_L$ and $D_\mu B_L$ do not give any distortion of the couplings. They only induce a rescaling of the canonical kinetic terms.

We start by analyzing the operators containing only q_L. As we said before, the elementary q_L must necessarily be contracted with the spurion $\tilde{y}_L$, thus the relevant operators contain at least two spurion insertions. The q_L field appears in the combination

$$(U^\dagger \tilde{y}_L q_L)_{i,5} \tag{4.6.8}$$

[20] Multiple covariant derivatives can be also used (*e.g.* $D_\mu D_\nu \psi$) but they are not relevant for our analysis.

where i and 5 denote the uncontracted index of $U^\dagger$. The singlet component (index 5) does not contain the b_L field, thus only the 4-plet part is relevant for our analysis. To get the Z boson we must use the covariant derivative or the d^i_μ symbol. The index structure, however, does not allow us to construct an operator with d^i_μ. The only possibility is

$$i\,\overline{q}_L \tilde{y}_L^\dagger \gamma^\mu \tilde{y}_L D_\mu q_L\,, \tag{4.6.9}$$

which gives a renormalization of the usual b_L kinetic term and does not induce a correction to the g_{b_L} coupling. At order y_L^4 we get one operator which contributes to the distortion of the $Z\bar{b}_L b_L$ vertex:

$$\mathcal{O} = i(\overline{q}_L y_L^\dagger \gamma^\mu y_L q_L)\left(U^\dagger_{5A}(y_L)^\alpha_A (y_L^\dagger)^\alpha_B U_{Bi} d^i_\mu\right) + \text{h.c.}\,. \tag{4.6.10}$$

In this case the 4 insertions of the $\tilde{y}_L$ spurion ensure that the corrections are finite at one loop.

We can now consider the operators containing only the composite 4-plet ψ_4. At least two spurion insertions are needed to generate an operator which breaks the P_{LR} symmetry and corrects the $Z\bar{b}_L b_L$ vertex. Notice that if more than two spurions are present the operator corresponds to a finite one-loop contribution. If we want to classify possible divergent corrections, we can focus on the case with only two $\tilde{y}_L$ insertions.

From the previous discussion it follows that the only way to contract the $\tilde{y}_L$ spurions is

$$U^\dagger_{*A}(y_L)^\alpha_A (y_L^\dagger)^\alpha_B U_{B*}\,, \tag{4.6.11}$$

where each $*$ denotes a free index which can correspond to a 4-plet or a singlet of SO(4). As we noticed before, operators containing $D_\mu\psi_4$ can only induce a rescaling of the canonical kinetic term for the B. Thus in order to obtain a distortion of the coupling with the Z boson we need to include the d^i_μ symbol. It is easy to show that the expression $d^i_\mu \psi^i_4$ does not contain a term of the form $Z_\mu B$. This term can only be generated if the d-symbol index is contracted with the Goldstone matrix U. We are left with only one possibility:

$$\mathcal{O} = i(\overline{\psi}_4 \gamma^\mu \psi_4)\left(U^\dagger_{5A}(y_L)^\alpha_A (y_L^\dagger)^\alpha_B U_{Bi} d^i_\mu\right) + \text{h.c.}\,. \tag{4.6.12}$$

With an explicit computation we find that this operator contains a coupling of the B with the Z boson:

$$\mathcal{O} \supset \left(\sqrt{2}\sin^2\left(\frac{\langle h\rangle}{f}\right)\right)\frac{g}{c_w} Z_\mu \overline{B}\gamma^\mu B\,. \tag{4.6.13}$$

The operator in eq. (4.6.12) contains only two spurion insertions and corresponds to a logarithmically divergent contribution at one loop. After the rotation to the mass eigenstates a correction to the $Z\bar{b}_L b_L$ vertex is induced. Using eq. (4.6.7) we find that this correction arises at order y_L^4, as expected.

Finally we can consider the mixed operators containing one elementary and one composite field. The elementary b_L must necessarily be contracted with a $\tilde{y}_L$ spurion. It is straightforward to show that at least two other spurion insertions are needed to construct an operator which can contribute to δg_{b_L} and the associated one-loop corrections are finite.

To conclude we summarize the results of this section. We found that the one-loop corrections to the $Z\bar{b}_L b_L$ can be logarithmically divergent. Moreover we showed that the divergence can only come from diagrams with two composite B's as external states. The contributions related to the elementary b_L fields are instead always finite.

4.6.B Computation of the Loop Corrections to the $Z\bar{b}_L b_L$ Vertex

In this appendix we compute the one-loop corrections to the $Z\bar{b}_L b_L$ vertex. For simplicity we consider the limit in which the gauge couplings are sent to zero. This approximation is justified by the fact that, as in the SM, the most relevant contributions are related to the Yukawa interactions and not to the gauge couplings. [21]

The computation can be significantly simplified by using a consequence of the operator analysis presented in appendix 4.6.A. We saw that, an operator can contribute to the distortion of the $Z\bar{b}_L b_L$ interaction only if it contains the CCWZ d^i_μ symbol. Moreover we found that the 4-plet index of d_μ must be necessarily contracted with the Goldstone matrix. By an explicit computation one easily finds that the combination $U_{Ai}d^i_\mu$ contains the Z boson always in association with the neutral Goldstone ϕ^0:

$$U_{Ai}d^i_\mu \supset -\frac{1}{\sqrt{2}}\left(\frac{g}{c_w}\sin\left(\frac{\langle h\rangle}{f}\right)Z_\mu + 2\partial_\mu\phi^0\right)\,, \tag{4.6.14}$$

where ϕ^0 denotes the canonically normalized neutral Goldstone, $\phi^0 = -(f/\langle h\rangle)\sin(\langle h\rangle/f)\Pi_3$. It is also straightforward to check that the covariant derivatives $D_\mu b_L$ and $D_\mu\psi_4$ do not contain any term of the form $(\partial_\mu\phi^0)b_L$. From these results it follows that we can extract the corrections to the g_{b_L} coupling by computing the one loop contributions to the $(\partial_\mu\phi^0)\bar{b}_L\gamma^\mu b_L$ interaction. [22]

Notice that, thanks to the P_{LR} symmetry under which ϕ^0 is odd, the vertex $(\partial_\mu\phi^0)\bar{b}_L\gamma^\mu b_L$ is not present at tree level and this makes the computation of the $(\partial_\mu\phi^0)\bar{b}_L\gamma^\mu b_L$ one-loop corrections even simpler. Due to the presence of a tree-level $Z\bar{b}_L b_L$ vertex, the one loop renormalization of the b_L must be taken into account to compute δg_{b_L} in the standard way. In the case of the $(\partial_\mu\phi^0)\bar{b}_L\gamma^\mu b_L$ interaction, instead, the wave function renormalization does not induce a one-loop contribution, thus we only need to compute the vertex correction.

We parametrize the relevant Goldstone couplings in the following way:

$$\begin{aligned}\mathcal{L} \;=\;& \overline{T}_i(A_i\,\phi^+ + i\,B_i\,\not\partial\,\phi^+)b_L + \text{h.c.}\\ &+ \left(i\,C_{ij}\,\phi^0\,\overline{T}_i P_L T_j + \text{h.c.}\right) + \partial_\mu\phi^0\,\overline{T}_i\gamma^\mu\left(D^L_{ij}P_L + D^R_{ij}P_R\right)T_j\\ &+ \overline{T}_i\left(iE_i\phi^+\phi^0 + F^+_i\phi^0\,\not\partial\,\phi^+ + F^0_i\phi^+\,\not\partial\,\phi^0\right)b_L + \text{h.c.}\,,\end{aligned} \tag{4.6.15}$$

where we denoted by T_i the charge 2/3 states in the mass eigenbasis and $P_{L,R}$ are the left and right projectors. ϕ^+ and ϕ^0 are the canonically normalized Goldstone fields, in particular the charged Goldstone is given by $\phi^+ = (f/\langle h\rangle)\sin(\langle h\rangle/f)h_u$. Notice that, in the effective theory we considered, the ϕ^0 Goldstone has no vertex which involves only charge $-1/3$ states. As a consequence the diagrams which give a correction to the $Z\bar{b}_L b_L$ vertex only contain charge 2/3 fermions inside the loop.

As we discussed in the main text, corrections to the g_{b_L} coupling can also be induced by 4-fermion effective interactions. We parametrized them by the Lagrangian:

$$\mathcal{L}^{4-ferm.} = G^L_{ij}[\bar{b}^a_L\gamma_\mu b^a_L][\overline{T}^b_i\gamma^\mu P_L T^b_j] + G^R_{ij}[\bar{b}^a_L\gamma_\mu b^a_L][\overline{T}^b_i\gamma^\mu P_R T^b_j]\,, \tag{4.6.16}$$

[21] We verified numerically in the model of Ref. [69] that the corrections due to non-vanishing gauge couplings are small and can be safely neglected.

[22] Another proof of the correctness of this procedure was given in Ref. [139], in which the two loop corrections to the $Z\bar{b}_L b_L$ vertex in the SM are computed.

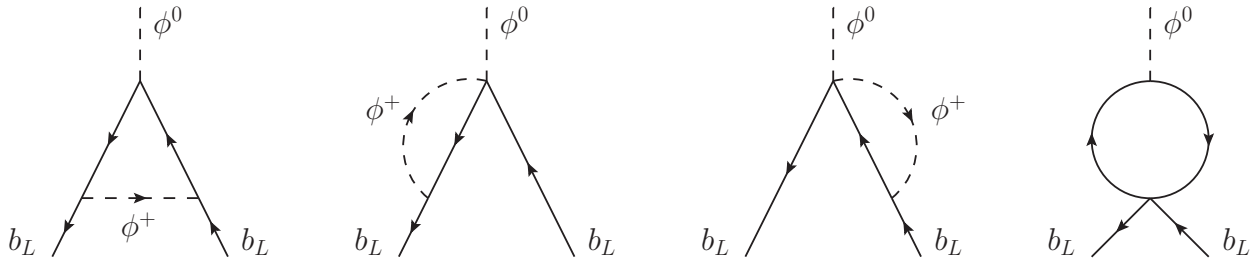

Figure 4.18: *Topologies of the diagrams contributing to the* $(\partial_\mu \phi^0)\bar{b}_L \gamma^\mu b_L$ *interaction. The internal fermion lines are fields with electric charge* $2/3$.

where a and b are color indices. For simplicity we consider only the color structure given in the previous formula. The results for different color structures only differ by an overall group theory factor.

The topologies of the diagrams which contribute to the $(\partial_\mu \phi^0)\bar{b}_L \gamma^\mu b_L$ interaction are shown in fig. 4.18. The "triangle" topology and the diagrams with a loop on the external legs arise from the leading order terms in the composite Higgs effective Lagrangian. The 4-fermion interactions, instead, generate the diagrams with a "bubble" topology. For our explicit computation we use dimensional regularization and we encode the divergent part in the parameter $\Delta \equiv 1/\epsilon - \gamma + \log(4\pi)$, where ϵ is defined by $d = 4 - 2\epsilon$. We denote the renormalization scale by μ.

The correction to the $Z\bar{b}_L b_L$ vertex coming from the "triangle" diagrams is given by

$$\begin{aligned}
\delta g_{b_L}^{\text{triangle}} \;=\; & \frac{f\sin(\langle h\rangle/f)}{64\pi^2}\sum_{i,j}\Bigg\{ A_j A_i^* \left[D^R_{ij} I_1^{ij} + 2D^L_{ij} m_i m_j I_2^{ij} - C_{ij} m_j (I_2^{ij} - I_4^{ij}) - C^\dagger_{ij} m_i (I_2^{ij} + I_4^{ij}) \right] \\
& + B_j B_i^* \left[D^R_{ij} m_i m_j I_1^{ij} - 2D^L_{ij} I_3^{ij} + \frac{1}{2} C_{ij} m_i (I_1^{ij} + I_5^{ij}) + \frac{1}{2} C^\dagger_{ij} m_j (I_1^{ij} - I_5^{ij}) \right] \qquad (4.6.17) \\
& + \text{Re}\left[A_j B_i^* \left(C^\dagger_{ij} (3I_1^{ij} - I_5^{ij} + 1) + 2C_{ij} m_i m_j I_4^{ij} + 2D^R_{ij} m_i I_1^{ij} - 2D^L_{ij} m_j (2I_1^{ij} + 1) \right) \right] \Bigg\},
\end{aligned}$$

where we defined the $I_{1,\dots,5}$ functions as

$$\begin{aligned}
I_1^{ij} &= \Delta + \frac{1}{2} - \frac{1}{m_i^2 - m_j^2}\left[m_i^2 \log\left(\frac{m_i^2}{\mu^2}\right) - m_j^2 \log\left(\frac{m_j^2}{\mu^2}\right) \right], \\
I_2^{ij} &= \frac{1}{m_i^2 - m_j^2} \log\left(\frac{m_i^2}{m_j^2}\right), \\
I_3^{ij} &= (m_i^2 + m_j^2)(\Delta + 1) - \frac{1}{m_i^2 - m_j^2}\left[m_i^4 \log\left(\frac{m_i^2}{\mu^2}\right) - m_j^4 \log\left(\frac{m_j^2}{\mu^2}\right) \right], \qquad (4.6.18) \\
I_4^{ij} &= \frac{1}{m_i^2 - m_j^2} - \frac{m_i^2 + m_j^2}{2(m_i^2 - m_j^2)^2} \log\left(\frac{m_i^2}{m_j^2}\right), \\
I_5^{ij} &= \frac{m_i^2 + m_j^2}{m_i^2 - m_j^2} - \frac{2m_i^2 m_j^2}{(m_i^2 - m_j^2)^2} \log\left(\frac{m_i^2}{m_j^2}\right).
\end{aligned}$$

The contribution from the diagrams with loops on the external legs is given by

$$\delta g_{b_L}^{\rm legs} = \frac{f\sin(\langle h\rangle/f)}{128\pi^2}\sum_i {\rm Re}\Bigg[4F_i^0 m_i\left(A_i^* + B_i^* m_i\right) I_6^i - E_i\left(A_i^*(I_6^i+1) - B_i^* m_i(I_6^i-1)\right) - F_i^+ m_i\left(A_i^*(I_6^i-1) + B_i^* m_i(3I_6^i-1)\right)\Bigg], \quad (4.6.19)$$

where I_6 is given by

$$I_6^i = 2\Delta + 2 - 2\log\left(\frac{m_i^2}{\mu^2}\right). \quad (4.6.20)$$

Notice that in the effective theory we considered, the two contributions $\delta g_{b_L}^{\rm triangle}$ and $\delta b_{b_L}^{\rm legs}$ are always finite.

Finally the contribution induced by the 4-fermion interactions is given by

$$\delta g_{b_L}^{\rm bubble} = N_c\frac{f\sin(\langle h\rangle/f)}{32\pi^2}\sum_{i,j}\Bigg\{\left(D_{ij}^L G_{ji}^L + D_{ij}^R G_{ji}^R\right)\left(I_3^{ij} - (m_i^2+m_j^2)/2\right) - \left(D_{ij}^R G_{ji}^L + D_{ij}^L G_{ji}^R\right) m_i m_j\left(2I_1^{ij}+1\right) + {\rm Re}\left[C_{ij}G_{ji}^L - C_{ij}^\dagger G_{ji}^R\right] m_i I_7^{ij}\Bigg\}, \quad (4.6.21)$$

where

$$I_7^{ij} = 2\Delta + 3 - 2\frac{m_i^2}{m_i^2-m_j^2} - 2\frac{1}{(m_i^2-m_j^2)^2}\left[(m_i^4 - 2m_i^2 m_j^2)\log\left(\frac{m_i^2}{\mu^2}\right) + m_j^4\log\left(\frac{m_j^2}{\mu^2}\right)\right]. \quad (4.6.22)$$

Differently from the first two classes of diagrams, in our effective theory the "bubble" diagrams can give a divergent contribution. This can happen if the G_{ij}^R couplings are non-vanishing. The G_{ij}^L couplings, instead, give rise only to finite corrections.

Chapter 5

Summary

The Standard Model of particles physics demonstrated an ability to describe the collider experiments with an incredible accuracy apart from few not dramatic deviations. The first run of the LHC seems to point at the continuation of its glory – the properties of the observed new scalar resonance so far are in a good agreement with the SM predictions. There are however strong reasons to expect that further stages of data taking will show us the tracks of new physics beyond the Standard Model. These expectations are based on our vision of the SM as an effective description of a more fundamental theory, in which case the mass of the Higgs can not be much below the scale of new physics unless a significant accidental tuning of the theory parameters takes place.

One of the motivated scenarios for a new physics beyond the Standard Model is a scenario with a new strongly coupled dynamics. It not only adds the new states at scales above the electroweak scale but also assumes a modification of the nature of the SM particles – some of them, in particular the Higgs boson, are bound states of more fundamental degrees of freedom. Description of such theories represents a challenge related to a failure of a usual perturbative approach.

There are still ways to obtain a useful information about effective theories describing bound states of the strong dynamics. The Goldstone nature of the Higgs, the knowledge about a behaviour of confining $SU(N)$ gauge theories allow to draw a general framework for the exploration of the Composite Higgs idea. However its general features are not sufficient to predict such important parameters of the theory as the Higgs mass or a vacuum expectation value of the Higgs field. To make these quantities computable one needs to add more states and constraints on their couplings which can be done in different ways thus introducing some model dependence compared to a general effective field theory approach. The two approaches – using general effective field theory or invoking specific models – have their advantages and we used both of them to address different questions related to the CH phenomenology.

In our analysis we focused on the minimal coset $SO(5)/SO(4)$ allowing to realize the Higgs doublet as a Goldstone field while maintaining a weak breaking of the SM custodial symmetry. Our CH constructions are also based on the partial compositeness mechanism allowing for the Goldstone symmetry breaking and the SM fermion mass generation. Under this basic assumptions we considered different possibilities to embed the SM fermions into the global symmetry group $SO(5)$, couplings with different composite $SO(4)$-multiplets and also considered the case in which the t_R is a member of the composite sector. The composite fermions coupled to the top quark, the top partners, were the main object of our studies.

The starting point of our analysis was a demonstration of the structural correlation between the mass of the Higgs boson and the masses of the top partners. The source of this correlation is in the twofold role of the linear mixings of the elementary top quark with top partners. Since the mixings break the Goldstone symmetry, the quartic term of the Higgs potential and consequently the Higgs mass are proportional to the mixing strength. The lighter the Higgs is, the smaller these mixings should be. The top mass is also proportional to these mixings and if they are small, the only way to obtain the observed top mass is to make the top partners light since the top mass is inversely proportional to partners masses. Quantitatively, assuming a moderate tuning, we found that in a model with SM quarks embedded into **5** of $SO(5)$ a Higgs mass $m_h \simeq 125$ GeV requires at least one top partner with a mass of the order or below the TeV. This correlation can already be observed in a general EFT but the robust results can only be obtained in the specific models allowing for computable Higgs mass, therefore we use the DCHM_3 and DCHM_2 to confirm the validity of our conclusions.

The presence of the anomalously light partners has important implications for the CH phenomenology. First of all, the LHC experiments must be sensitive to their direct production. For the sake of comparison with the experimental bounds there is no need for example to carefully take into account all the structures needed to provide a calculability of the Higgs potential. Therefore we adapted a general CCWZ parametrization of CH model for the case when only one composite multiplet is sufficiently light to be observed. This approach allows for a small number of relevant parameters but at the same time reflects the implications of the Goldstone nature of the Higgs boson. Furthermore we focussed on the possibility where the right-handed top quark t_R is itself a composite fermion. We considered the two possible embeddings of the elementary left-handed fermions into $SO(5)$: as a 5- and 14-dimensional representations. Associated top partners can therefore form a singlet, four-plet and a nine-plet of the $SO(4)$.

To constrain our models we recast the available LHC searches for the top partners, fourth generation quarks and quantum balckholes. Our results show that available experimental analyses have already started excluding the region of the parameter space favoured by naturalness considerations. We also identified possible interesting channels for the top partners searches and made an estimate of the LHC potential reach in the next run for one of the channels.

Another possible effect of the light top partners can take place in the EWPT parameters of the composite Higgs models. The contributions to the EWPT parameters related to the composite Higgs alone and the heavy vectorial resonances are known to lead the models away from the experimentally allowed regions. The contribution of the light fermions therefore is welcomed to improve the compatibility of the CH models with EWPT. In order to consider the effect of the composite fermions we again adopted the general model-independent EFT approach which allowed us to obtain results valid for a broad class of specific realizations of the CH idea.

We identified a new and potentially large logarithmically divergent contribution to the S-parameter, which comes purely from the strong dynamics, and can have a negative sign which allows to cancel the unwanted deviations of the S. As expected, the corrections to the T-parameter coming from fermion loops are finite and dominated by the contributions of the lightest composite states and are also capable to cancel the large unwanted negative shift in T induced by other sectors of the theory. In addition, we point out that contact 4-fermion interactions can remove the correlation between the correction to the Zb_Lb_L vertex and a T parameter, which can also relax the constraints on the CH scenarios. Still, a general fit of the oblique parameters suggests a rather stringent lower bound

on the σ-model scale $f \simeq 750$ GeV.

Summarizing stated above, we can conclude that Composite Higgs scenarios with a partial compositeness represent a viable possible description of the physics underlying the Standard Model and require a tolerable amount of tuning. Their robust prediction, the light top partners, are one of the most accessible experimental manifestations of the Higgs compositeness, and will play a central role for the validation of this scenarios in the upcoming LHC run.

Bibliography

[1] G. Aad *et al.* [ATLAS Collaboration], Phys. Lett. B **710** (2012) 49 [arXiv:1202.1408 [hep-ex]].

[2] S. Chatrchyan *et al.* [CMS Collaboration], arXiv:1202.1488 [hep-ex].

[3] F. Englert and R. Brout, Phys. Rev. Lett. 13 (1964) 321. P. W. Higgs, Phys. Rev. Lett. 13 (1964) 508.

[4] Riccardo Barbieri, Alessandro Strumia [arXiv:hep-ph/0007265v2]

[5] S. Dimopoulos, J. Preskill, Nucl. Phys. **B199** (1982) 206. D. B. Kaplan, H. Georgi, Phys. Lett. **B136** (1984) 183. D. B. Kaplan, H. Georgi, S. Dimopoulos, Phys. Lett. **B136** (1984) 187. H. Georgi, D. B. Kaplan, P. Galison, Phys. Lett. **B143** (1984) 152. T. Banks, Nucl. Phys. **B243** (1984) 125. H. Georgi, D. B. Kaplan, Phys. Lett. **B145** (1984) 216. M. J. Dugan, H. Georgi, D. B. Kaplan, Nucl. Phys. **B254** (1985) 299.

[6] O. Matsedonskyi, G. Panico and A. Wulzer, JHEP **1301** (2013) 164 [arXiv:1204.6333 [hep-ph]].

[7] A. De Simone, O. Matsedonskyi, R. Rattazzi and A. Wulzer, arXiv:1211.5663 [hep-ph].

[8] C. Grojean, O. Matsedonskyi and G. Panico, [arXiv:1306.4655 [hep-ph]]

[9] O. Matsedonskyi, F. Riva, T. Vantalon, [arXiv:1401.3740 [hep-ph]]

[10] G. F. Giudice [arXiv:hep-ph/1307.7879v1]

[11] L. J. Hall, D. Pinner and J. T. Ruderman, JHEP **1204** (2012) 131 [arXiv:1112.2703 [hep-ph]].

[12] M. Shaposhnikov [arXiv:hep-th/0708.3550]

[13] M. Farina, D. Pappadopulo and A. Strumia [arXiv:hep-ph/1303.7244v1]

[14] V. Agrawal, S. M. Barr, J. F. Donoghue and D. Seckel, Phys. Rev. D 57 (1998) 5480 [arXiv:hep-ph/9707380]

[15] K. Agashe, R. Contino and A. Pomarol, Nucl. Phys. B **719**, 165 (2005) [hep-ph/0412089]. R. Contino, T. Kramer, M. Son and R. Sundrum, JHEP **0705** (2007) 074 [hep-ph/0612180].

[16] F. Caracciolo, A. Parolini, M. Serone JHEP **1302** (2013) 066 [arXiv:1211.7290 [hep-ph]]

[17] J. Barnard, T. Gherghetta and T. S. Ray, arXiv:1311.6562 [hep-ph].

[18] R. Foadi, M.T. Frandsen, F. Sannino Phys.Rev. **D87** (2013) 095001 arXiv:1211.1083 [hep-ph]

[19] J. Mrazek, A. Pomarol, R. Rattazzi, M. Redi, J. Serra and A. Wulzer, Nucl. Phys. B **853** (2011) 1 [arXiv:1105.5403 [hep-ph]].

[20] G. F. Giudice, C. Grojean, A. Pomarol, R. Rattazzi, JHEP **0706** (2007) 045. [hep-ph/0703164].

[21] E. Witten, Phys. Rev. Lett. 51, 2351 (1983)

[22] S. R. Coleman, J. Wess and B. Zumino, Phys. Rev. **177** (1969) 2239. C. G. Callan, Jr., S. R. Coleman, J. Wess and B. Zumino, Phys. Rev. **177** (1969) 2247.

[23] Adam Falkowski, Slava Rychkov, Alfredo Urbano arXiv:1202.1532v3 [hep-ph]

[24] E. Witten, Nucl. Phys. B160 (1979) 57;

[25] *Aspects of Symmetry. Selected Erice Lectures*, Sidney Coleman

[26] H. Georgi, Phys. Lett. B **298**, 187 (1993) [hep-ph/9207278].

[27] H. Georgi and A. Manohar, Nucl. Phys. 234B, 189 (1984).

[28] R. Rattazzi, A. Zaffaroni, Comments on the holographic picture of the Randall-Sundrum model, JHEP 0104, 021 (2001). [hep-th/0012248]

[29] "A Combination of Preliminary Electroweak Measurements and Constraints on the Standard Model" The LEP Collaborations and the LEP Electroweak Working Group [arXiv:hep-ex/0612034v2], Particle Data Group, http://pdg.lbl.gov/2011/listings/rpp2011-list-quark-lepton-compositeness.pdf

[30] M. Bona et al. [UTfit Collaboration], JHEP 0803, 049 (2008) [arXiv:0707.0636 [hep-ph]]

[31] Savas Dimopoulos and Leonard Susskind (1979). "Mass without scalars". Nuclear Physics B155 (1): 237252

[32] J. Galloway, J. A. Evans, M. A. Luty and R. A. Tacchi, JHEP **1010** (2010) 086 [arXiv:1001.1361 [hep-ph]].

[33] D. B. Kaplan. Nucl. Phys., B365:259278, 1991.

[34] H. Georgi, D. B. Kaplan and P. Galison, Phys. Lett. B 143, 152 (1984). H. Georgi and D. B. Kaplan, Phys. Lett. B 145, 216 (1984). M. J. Dugan, H. Georgi and D. B. Kaplan, Nucl. Phys. B 254, 299 (1985)

[35] M. Redi and A. Weiler, Flavor and CP Invariant Composite Higgs Models, JHEP 1111, 108 (2011) [arXiv:1106.6357 [hep-ph]]

[36] "Flavour physics from an approximate $U(2)^3$ symmetry" Riccardo Barbieri, Dario Buttazzo, Filippo Sala, David M. Straub [arXiv:1203.4218v1 [hep-ph]]

[37] S. Weinberg, Phys. Rev. Lett. 18 (1967) 507

[38] R. Contino, Y. Nomura, A. Pomarol, Nucl. Phys. **B671** (2003) 148-174. [hep-ph/0306259].

[39] N. Arkani-Hamed, A. G. Cohen, H. Georgi, Phys. Lett. B513 (2001) 232-240. Phys.Lett.B513:232-240,2001. [hep-ph/0105239] N. Arkani-Hamed, A. G. Cohen, H. Georgi, Phys. Rev. Lett. **86** (2001) 4757-4761. [hep-th/0104005].

[40] G. Panico, A. Wulzer, JHEP **1109** (2011) 135. [arXiv:1106.2719 [hep-ph]].

[41] K. Agashe, R. Contino, L. Da Rold and A. Pomarol, Phys. Lett. B **641**, 62 (2006) [hep-ph/0605341]. J. Mrazek, A. Pomarol, R. Rattazzi, M. Redi, J. Serra and A. Wulzer, Nucl. Phys. B **853** (2011) 1 [arXiv:1105.5403 [hep-ph]].

[42] M. Montull, F. Riva, E. Salvioni and R. Torre, arXiv:1308.0559 [hep-ph]

[43] Aleksandr Azatov, Roberto Contino, Andrea Di Iura, Jamison Galloway arXiv:1308.2676v1 [hep-ph]

[44] The CMS Collaboration, arXiv:1307.5515v2 [hep-ex]

[45] A. Azatov, J. Galloway PhysRevD.85.055013 (2012) arXiv:1110.5646 [hep-ph]

[46] Roberto Contino, Christophe Grojean, Mauro Moretti, Fulvio Piccinini, Riccardo Rattazzi, arXiv:1002.1011v2 [hep-ph]

[47] R. Contino, C. Grojean, D. Pappadopulo, R. Rattazzi, A. Thamm, arXiv:1309.7038v1 [hep-ph]

[48] Adrian Carmona, Mikael Chala and Jose Santiago arXiv:1205.2378v2 [hep-ph]

[49] R. Barbieri, B. Bellazzini, V. S. Rychkov and A. Varagnolo, Phys. Rev. D **76** (2007) 115008 [arXiv:0706.0432 [hep-ph]].

[50] M. Ciuchini, E. Franco, S. Mishima, L. Silvestrini. [arXiv:1306.4644 [hep-ph]]

[51] CMS Collaboration, 2013, CMS PAS EXO-12-060. ATLAS Collaboration, 2013, ATLAS-CONF-2013-017.

[52] R. Contino and G. Servant, JHEP **0806** (2008) 026 [arXiv:0801.1679 [hep-ph]].

[53] J. Mrazek and A. Wulzer, Phys. Rev. D **81** (2010) 075006 [arXiv:0909.3977 [hep-ph]].

[54] O. Domenech, A. Pomarol and J. Serra, [arXiv:1201.6510]

[55] C. Delaunay, T. Flacke, J. GonzalezFrailed, S. J. Lee, G. Panico, G. Perez [1311.2072 [hep-ph]]

[56] W. Altmannshofer, D.M. Straub arXiv:1308.1501 [hep-ph]

[57] R. Contino, L. Da Rold and A. Pomarol, Phys. Rev. D **75**, 055014 (2007) [hep-ph/0612048].

[58] R. Contino, T. Kramer, M. Son, R. Sundrum, JHEP **0705** (2007) 074. [hep-ph/0612180].

[59] G. Panico, M. Serone, A. Wulzer, Nucl. Phys. **B762** (2007) 189-211. [hep-ph/0605292].

[60] S. De Curtis, M. Redi and A. Tesi, JHEP **1204** (2012) 042 [arXiv:1110.1613 [hep-ph]].

[61] H.-C. Cheng, J. Thaler, L.-T. Wang, JHEP **0609** (2006) 003. [hep-ph/0607205]. R. Foadi, J. T. Laverty, C. R. Schmidt, J.-H. Yu, JHEP **1006** (2010) 026. [arXiv:1001.0584 [hep-ph]]. M. Baumgart, [arXiv:0706.1380 [hep-ph]].

[62] G. Panico, A. Wulzer, JHEP **0705** (2007) 060. [hep-th/0703287].

[63] J. R. Espinosa, C. Grojean and M. Muhlleitner, JHEP **1005** (2010) 065 [arXiv:1003.3251 [hep-ph]]; A. Azatov, R. Contino and J. Galloway, arXiv:1202.3415 [hep-ph].

[64] Leandro Da Rold, Cedric Delaunay, Christophe Grojean, Gilad Perez arXiv:1208.1499v1 [hep-ph]

[65] C. Csaki, A. Falkowski and A. Weiler, JHEP **0809**, 008 (2008) [arXiv:0804.1954 [hep-ph]].

[66] B. Keren-Zur, P. Lodone, M. Nardecchia, D. Pappadopulo, R. Rattazzi and L. Vecchi, Nucl. Phys. B **867**, 429 (2013) [arXiv:1205.5803 [hep-ph]].

[67] R. Contino, D. Marzocca, D. Pappadopulo and R. Rattazzi, JHEP **1110**, 081 (2011) [arXiv:1109.1570 [hep-ph]].

[68] M. Gillioz, Phys. Rev. D **80** (2009) 055003 [arXiv:0806.3450 [hep-ph]].

[69] C. Anastasiou, E. Furlan and J. Santiago, Phys. Rev. D **79** (2009) 075003 [arXiv:0901.2117 [hep-ph]].

[70] G. Dissertori, E. Furlan, F. Moortgat and P. Nef, JHEP **1009** (2010) 019 [arXiv:1005.4414 [hep-ph]].

[71] G. Panico, M. Redi, A. Tesi and A. Wulzer, arXiv:1210.7114 [hep-ph].

[72] [ATLAS Collaboration], ATLAS-CONF-2012-130

[73] [CMS Collaboration], CMS-PAS-B2G-12-003.

[74] J. A. Aguilar-Saavedra, JHEP **0911**, 030 (2009) [arXiv:0907.3155 [hep-ph]].

[75] M. Perelstein, M. E. Peskin and A. Pierce, Phys. Rev. D **69**, 075002 (2004) [hep-ph/0310039]. T. Han, H. E. Logan, B. McElrath and L. -T. Wang, Phys. Rev. D **67**, 095004 (2003) [hep-ph/0301040]. N. Vignaroli, Phys. Rev. D **86**, 075017 (2012) [arXiv:1207.0830 [hep-ph]].

[76] A. Azatov, O. Bondu, A. Falkowski, M. Felcini, S. Gascon-Shotkin, D. K. Ghosh, G. Moreau and S. Sekmen, Phys. Rev. D **85**, 115022 (2012) [arXiv:1204.0455 [hep-ph]]; K. Harigaya, S. Matsumoto, M. M. Nojiri and K. Tobioka, Phys. Rev. D **86**, 015005 (2012) [arXiv:1204.2317 [hep-ph]].

[77] J. M. Cornwall, D. N. Levin and G. Tiktopoulos, Phys. Rev. D 10, 1145 (1974) [Erratum-ibid. D 11, 972 (1975)]; C. E. Vayonakis, Lett. Nuovo Cim. 17, 383 (1976); M. S. Chanowitz and M. K. Gaillard, Nucl. Phys. B 261, 379 (1985).

[78] S. S. D. Willenbrock and D. A. Dicus, Phys. Rev. D **34**, 155 (1986).

[79] S. Godfrey, T. Gregoire, P. Kalyniak, T. A. W. Martin and K. Moats, JHEP **1204**, 032 (2012) [arXiv:1201.1951 [hep-ph]].

[80] E. L. Berger and Q. -H. Cao, Phys. Rev. D **81**, 035006 (2010) [arXiv:0909.3555 [hep-ph]].

[81] M. Aliev, H. Lacker, U. Langenfeld, S. Moch, P. Uwer and M. Wiedermann, Comput. Phys. Commun. **182**, 1034 (2011) [arXiv:1007.1327 [hep-ph]].

[82] A. D. Martin, W. J. Stirling, R. S. Thorne and G. Watt, Eur. Phys. J. C **63**, 189 (2009) [arXiv:0901.0002 [hep-ph]].

[83] J. M. Campbell and R. K. Ellis, Phys. Rev. D **62**, 114012 (2000) [hep-ph/0006304]; J. M. Campbell, R. K. Ellis and F. Tramontano, Phys. Rev. D **70**, 094012 (2004) [hep-ph/0408158]; J. M. Campbell, R. Frederix, F. Maltoni and F. Tramontano, Phys. Rev. Lett. **102**, 182003 (2009) [arXiv:0903.0005 [hep-ph]]; J. M. Campbell, R. Frederix, F. Maltoni and F. Tramontano, JHEP **0910**, 042 (2009) [arXiv:0907.3933 [hep-ph]].

[84] J. Alwall, M. Herquet, F. Maltoni, O. Mattelaer and T. Stelzer, JHEP **1106**, 128 (2011) [arXiv:1106.0522 [hep-ph]].

[85] N.D. Christensen, C. Duhr, Comput. Phys. Commun.180 (2009) 1614-1641 [arXiv:0806.4194 [hep-ph]]

[86] The ATLAS Collaboration, ATLAS-CONF-2013-051.

[87] The CMS collaboration, CMS PAS B2G-12-012.

[88] A. Azatov, M. Salvarezza, M. Son and M. Spannowsky, arXiv:1308.6601 [hep-ph].

[89] The CMS Collaboration, CMS-PAS-B2G-12-015, [hep-ex:1311.7667].

[90] A. Avetisyan and T. Bose, [arXiv:1309.2234v1 [hep-ex]]

[91] M. Wobisch and T. Wengler, arXiv:hep-ph/9907280; Y. L. Dokshitzer et al., JHEP 9708 (1997) 001, [arXiv:hep-ph/9707323]

[92] M. Cacciari, G. P. Salam, and G. Soyez, JHEP **04** (2008) 063 [arXiv:0802.1189].

[93] A. L. Read, J. Phys. G **28**, 2693 (2002).

[94] J. Berger, J. Hubisz and M. Perelstein, JHEP **1207**, 016 (2012) [arXiv:1205.0013 [hep-ph]].

[95] D. Marzocca, M. Serone and J. Shu, JHEP **1208** (2012) 013 [arXiv:1205.0770 [hep-ph]].

[96] M. Redi and A. Tesi, JHEP **1210** (2012) 166 [arXiv:1205.0232 [hep-ph]].

[97] A. Pomarol and F. Riva, JHEP **1208** (2012) 135 [arXiv:1205.6434 [hep-ph]].

[98] D. Pappadopulo, A. Thamm and R. Torre, arXiv:1303.3062 [hep-ph].

[99] A. Atre, M. Carena, T. Han and J. Santiago, Phys. Rev. D **79** (2009) 054018 [arXiv:0806.3966 [hep-ph]]. R. Barcelo, A. Carmona, M. Chala, M. Masip and J. Santiago, Nucl. Phys. B **857** (2012) 172 [arXiv:1110.5914 [hep-ph]]. A. Atre, G. Azuelos, M. Carena, T. Han, E. Ozcan, J. Santiago and G. Unel, JHEP **1108** (2011) 080 [arXiv:1102.1987 [hep-ph]]. A. Atre, M. Chala and J. Santiago, JHEP **1305** (2013) 099 [arXiv:1302.0270 [hep-ph]].

[100] G. Brooijmans *et al.* [New Physics Working Group Collaboration], arXiv:1005.1229 [hep-ph].

[101] T. Han, I. Lewis and Z. Liu, JHEP **1012** (2010) 085 [arXiv:1010.4309 [hep-ph]].

[102] C. Bini, R. Contino and N. Vignaroli, JHEP **1201** (2012) 157 [arXiv:1110.6058 [hep-ph]]. N. Vignaroli, JHEP **1207** (2012) 158 [arXiv:1204.0468 [hep-ph]].

[103] K. Harigaya, S. Matsumoto, M. M. Nojiri and K. Tobioka, Phys. Rev. D **86** (2012) 015005 [arXiv:1204.2317 [hep-ph]].

[104] J. Berger, J. Hubisz and M. Perelstein, JHEP **1207** (2012) 016 [arXiv:1205.0013 [hep-ph]].

[105] S. Dawson and E. Furlan, Phys. Rev. D **86** (2012) 015021 [arXiv:1205.4733 [hep-ph]].

[106] Y. Okada and L. Panizzi, Adv. High Energy Phys. **2013** (2013) 364936 [arXiv:1207.5607 [hep-ph]]. G. Cacciapaglia, A. Deandrea, L. Panizzi, S. Perries and V. Sordini, JHEP **1303** (2013) 004 [arXiv:1211.4034 [hep-ph]]. M. Buchkremer, G. Cacciapaglia, A. Deandrea and L. Panizzi, arXiv:1305.4172 [hep-ph].

[107] J. A. Aguilar-Saavedra, R. Benbrik, S. Heinemeyer and M. Perez-Victoria, arXiv:1306.0572 [hep-ph].

[108] S. Gopalakrishna, T. Mandal, S. Mitra and G. Moreau, arXiv:1306.2656 [hep-ph].

[109] The CMS Collaboration, CMS-PAS-B2G-12-003.

[110] The CMS Collaboration, "Search for T5/3 top partners in same-sign dilepton final state", CMS-PAS-B2G-12-012.

[111] The ATLAS Collaboration, "Search for exotic same-sign dilepton signatures (b' quark, $T_{5/3}$ and four top quarks production) in 4.7/fb of pp collisions at $\sqrt{s} = 7$ TeV with the ATLAS detector", ATLAS-CONF-2012-130; "Search for anomalous production of events with same-sign dileptons and b jets in 14.3/fb of pp collisions at $\sqrt{s} = 8$ TeV with the ATLAS detector", ATLAS-CONF-2013-051.

[112] R. Contino, arXiv:1005.4269 [hep-ph].

[113] J. R. Espinosa, C. Grojean, M. Muhlleitner and M. Trott, JHEP **1212** (2012) 045 [arXiv:1207.1717 [hep-ph]].

[114] A. Falkowski, F. Riva and A. Urbano, arXiv:1303.1812 [hep-ph].

[115] M. Ciuchini, E. Franco, S. Mishima, L. Silvestrini, to appear.

[116] K. Agashe, A. Delgado, M. J. May and R. Sundrum, JHEP **0308** (2003) 050 [hep-ph/0308036].

[117] K. Agashe and R. Contino, Nucl. Phys. B **742** (2006) 59 [hep-ph/0510164].

[118] P. Lodone, JHEP **0812** (2008) 029 [arXiv:0806.1472 [hep-ph]].

[119] A. Pomarol and J. Serra, Phys. Rev. D **78** (2008) 074026 [arXiv:0806.3247 [hep-ph]].

[120] M. Gillioz, R. Grober, C. Grojean, M. Muhlleitner and E. Salvioni, JHEP **1210** (2012) 004 [arXiv:1206.7120 [hep-ph]].

[121] R. Barbieri, D. Buttazzo, F. Sala, D. M. Straub and A. Tesi, JHEP **1305** (2013) 069 [arXiv:1211.5085 [hep-ph]].

[122] G. Panico, E. Ponton, J. Santiago and M. Serone, Phys. Rev. D **77** (2008) 115012 [arXiv:0801.1645 [hep-ph]].

[123] G. Panico, M. Safari and M. Serone, JHEP **1102** (2011) 103 [arXiv:1012.2875 [hep-ph]].

[124] M. E. Peskin and T. Takeuchi, Phys. Rev. D **46** (1992) 381.

[125] R. Barbieri, A. Pomarol, R. Rattazzi, A. Strumia, Nucl. Phys. **B703** (2004) 127-146. [hep-ph/0405040].

[126] M. Baak, M. Goebel, J. Haller, A. Hoecker, D. Kennedy, R. Kogler, K. Moenig and M. Schott *et al.*, Eur. Phys. J. C **72** (2012) 2205 [arXiv:1209.2716 [hep-ph]].

[127] A. Orgogozo and S. Rychkov, arXiv:1211.5543 [hep-ph].

[128] L. Lavoura and J. P. Silva, Phys. Rev. D **47** (1993) 2046.

[129] M. S. Carena, E. Ponton, J. Santiago and C. E. M. Wagner, Nucl. Phys. B **759** (2006) 202 [hep-ph/0607106]; Phys. Rev. D **76** (2007) 035006 [hep-ph/0701055].

[130] J. Elias-Miro, J. R. Espinosa, E. Masso and A. Pomarol, arXiv:1302.5661 [hep-ph].

[131] R. Contino, M. Ghezzi, C. Grojean, M. Muhlleitner and M. Spira, arXiv:1303.3876 [hep-ph].

[132] B. Batell, S. Gori and L.-T. Wang, JHEP **1301** (2013) 139 [arXiv:1209.6382 [hep-ph]]. D. Guadagnoli and G. Isidori, arXiv:1302.3909 [hep-ph].

[133] S. Chatrchyan *et al.* [CMS Collaboration], JHEP **1212** (2012) 035 [arXiv:1209.4533 [hep-ex]].

[134] F. del Aguila, M. Perez-Victoria and J. Santiago, Phys. Lett. B **492** (2000) 98 [hep-ph/0007160].

[135] F. del Aguila, M. Perez-Victoria and J. Santiago, JHEP **0009** (2000) 011 [hep-ph/0007316].

[136] J. A. Aguilar-Saavedra and M. Perez-Victoria, arXiv:1302.5634 [hep-ph].

[137] B. Grzadkowski, M. Iskrzynski, M. Misiak and J. Rosiek, JHEP **1010** (2010) 085 [arXiv:1008.4884 [hep-ph]].

[138] J. A. Aguilar-Saavedra, M. C. N. Fiolhais and A. Onofre, JHEP **1207** (2012) 180 [arXiv:1206.1033 [hep-ph]].

[139] R. Barbieri, M. Beccaria, P. Ciafaloni, G. Curci and A. Vicere, Nucl. Phys. B **409** (1993) 105.